Investigation of Coal Dust Remediation using a Surfactant in an Aqueous Solution

Connor Burton Brown

Thesis submitted to the faculty of the Virginia Polytechnic Institute and State University in fulfillment of the requirements for the degree of

Master of Science
In
Mining and Mineral Engineering

Kramer Luxbacher, Chairman
Gerald Luttrell
Emily Sarver

August 10, 2016
Blacksburg, VA

Keywords: Coal Dust, Surfactant, Black Lung, Scrubber

Investigation of Coal Dust Remediation using a Surfactant in an Aqueous Solution

Connor Brown

ABSTRACT

In addition to ventilation practices, the application of water via sprays is the most economical and popular means of combating respirable dust in an underground coal mine. Due to a noticeable increase in black lung among coal miners and new dust regulations, surfactants or wetting agents have been used to aid in dust suppression. The surfactant facilitates the wetting process by lowering the surface tension and allowing the hydrophobic coal dust to come into contact with the water.

One of the most straightforward and effective benchtop tests is a simple wetting test. Although there are variations of this type of test, principle and technique remain the same. A known amount of dust was placed on the surface of a solution and the time it takes for all the dust to fall through the interface would be the wetting rate. This investigation examined the specific density of the bulk dust and concentration of a surfactant in solution and their effects on the wetting rate. It was found that both factors were significant in determining the wetting rate. It was seen that the surfactant had a more significant effect on the dust which consisted mostly of coal particle when compared to a dust with a higher non-coal mineral content.

Additionally, full-scale tests were conducted to determine the effect of the surfactant at a constant concentration. During the field implementation, the

surfactant was pumped through the mines spray water to the cutter heads of the continuous miner. A large number of uncontrollable variables present during the implementation, made determining the effects difficult, and the resulting impact from the surfactant inconclusive. Further long-term testing would be needed while accounting for all of the identified variables. Significantly higher concentration was however found when using the continuous personal dust monitor as opposed to the older personal dust samples when left in the same environment. Additionally, a very significant drop in dust concentrations was observed when the miner operators were allowed to activate the scrubbers.

Investigation of Coal Dust Remediation using a Surfactant in an Aqueous Solution

Connor Brown

General Audience Abstract

People who work in mines are exposed to many dangers and illnesses. One of the illnesses, which has in recent history resurged, is black lung. Black lung is a disease caused by coal dust entering the lungs. The body's reaction to it is to build scar tissue around the piece of dust. If this happens enough times over the miner's career, then it becomes nearly impossible to breath. Normally, to prevent this from happening, water is sprayed in the coal before it is chipped off by the machine. Since this appears to no longer be effective, soapy chemicals are added to the water, which helps to keep the dust from lifting into the air in the first place.

One of the easiest ways to test whether the chemicals are working well or not is to conduct a wetting test. When conducting a wetting test, a known about of dust is placed on top of the water and chemical mixture, and the time it takes for all of the dust to be wet is call the wetting rate. To get better results in an actual mine, faster wetting rates were sought after. The wetting test showed that the two main factors which determine the wetting were how much coal is in the coal and rock dust mixture and how much chemical is used. It was seen that the chemical had a more significant effect on the dust which had mostly of coal particle when compared to dust with more rock dust.

Another study was conducted at a mine with only one mixture of water and chemical. During the study, the chemical was pumped through the mine and to the cutter heads of the continuous miner. A continuous miner is the name of the equipment used to mine coal and other soft material. The cutter head is the piece of the equipment which actually makes contact with coal. Since the conditions at the mine were not ideal and not enough data was taken, the resulting effect of the chemical could not be certain. More long-term studies need to be done in the future to help account for the less than ideal conditions. There were, however, larger amounts of dust when using new sampling equipment as opposed to the older equipment given the same conditions. Also, smaller amounts of dust were seen when the miner operators were allowed to activate the air cleaning attachments on the continuous miner. These issues should be revisited in the future.

ACKNOWLEDGEMENTS

I would like to thank my advisor, Dr. Kray Luxbacher, for her support and direction as well as her continuous encouragement throughout this projects. Dr. Luxbacher's advice and understanding were essential in the success of this project. I also greatly appreciate the support of my committee members, Dr. Emily Sarver, and Dr. Gerald Luttrell. These two were an irreplaceable resource, providing me with insight and perspective. Also, I would like to thank the whole Department of Mining and Minerals Engineering at Virginia Tech for the opportunity to pursue this research; and to thank everyone, fellow students and faculty alike, for their excitement and willingness to provide feedback making my time here a gratifying experience.

TABLE OF CONTENTS

List of Figures

LIST OF TABLES

1 INTRODUCTION

There has been a recent surge of concern in the mining community on the topic of occupational health. One of the areas of intrigue and interest revolves around exposure of mine workers to respirable dust. Specifically, the exposure of coal workers to respirable dust, coal, and silica-based dust. Respirable dust in coal mines has been an issue for a number of years. Efforts throughout the last half-century have greatly decreased the number of cases of black lung to record lows in the early 2000's. That being the case, a recent uptick in the number of cases has been noticed. There are many efforts under way to both identify the source or sources of the recent increase and to regulate its influence on the health of coal workers. The regulations which will be instated puts more pressure on the producers to prevent and control hazards through better safe work practices or administrative and engineering controls. A possible use of an engineering control will be investigated in this paper. One of the more popular engineering controls for abating respirable dust is the use of sprays during the production and transport of ores. The continuous demand for energy, driven by the rising populations, has forced mining companies to produce in more difficult and thinner seams. The thinning of the seam has led to the coal producers mining more rock than in previous operations. These pressures on the industry have not only changed the mineralogy of the dust, but the tonnages and raw production rates necessary have stretched the effectiveness of sprays to their limits. There have been many attempts to enlist the aid of surfactant in mitigating the exposure of underground coal miners to respirable dust, and there have been mixed results both from lab and field testing. The surfactant or wetting agent reduces the surface tension of the water and accelerates the wetting process. This thesis assesses a surfactant in an aqueous solution for the purpose of mitigating airborne coal dust.

A variation of a simple wetting test was used as benchtop test. Wetting rates were found by dividing a known amount of material over the wetting time. In addition to the surfactant concertation, the gravity class of the dust was examined. After it had been determined that the surfactant was effective, full-scale tests were run in a room and pillar underground coal mine. Dust concentrations were compared with regards to different experimental variables.

2 LITERATURE REVIEW

Increasing population leads to increased demand for natural resources. The demand leads to increased mining activity. Coupled with the decreasing quality of ores and thinning of seams, increasing tonnages of excess rock becomes an inescapable part of the mining process. For the employees working in the mines, the dust becomes more difficult to control, resulting in increased exposure. Specifically, this paper will discuss what Progressive Massive Fibrosis (PMF), silicosis, and black lung are and how exposure to coal and silica dust causes the diseases. This thesis will also examine methods used to mitigate exposure to the dust, such as water sprays, as well as test a surfactant in both a laboratory and a field environment.

This research was spurred by a noticeable uptick in the number of cases of lung diseases among coal miners. Underground coal miners' occupational hazards, as they relate to mortality, have been extensively studied. Coal mine dust has been found to be one of the most dangerous of these occupational hazards due in part to its ability to cause "Miners' Black Lung", or Coal Worker's Pneumoconiosis (CWP) and silicosis. CWP and silicosis are chronic occupational lung diseases caused by long-term exposure to respirable dust (particles with 100% passing through a 10-micron screen). After coming in contact with the alveoli, the dust triggers inflammation, eventually resulting in fibrosis and irreversible lung damage. (Laney et al., 2012) It has been found that the particles in the two to six-micron range can be most damaging (Méndez-Vargas et al., 2013). CWP and silicosis are both diagnosed by examining a chest X-ray. The radiographic test will show opacities and will be classified by the size, shape, and extent. The two diseases are only differentiated by the individual's work history (Neimeier, 1993).

2.1 COAL WORKERS PNEUMOCONIOSIS

Some of the earliest references and investigations, including post-mortem examinations, into what we know now as black lung took place in the early 1800's. The term pneumoconiosis or "dusty lung" was not used until 1874 During this time, the tools used to study the disease were an examination of the lung tissue and societal correlations (Meiklejohn, 1951). Around 1907, an etiological investigation into the disease began in earnest with the use of chest x-rays. The x-rays at this time, however, lacked the resolution for early detection and could only be used for detection of very significant pathological differences (Neimeier, 1993). It was not until the 1930's-1950 that the investigators studying the disease had a wider range of tools and innovative techniques including radiology, biochemistry pathology, and dust sampling and analysis (Meiklejohn, 1952). In addition, for a number of years, the causative agent was thought to be solely silica exposure. This assumption, however, was brought into question after investigations found pneumoconiosis among coal trimmers in the United Kingdom. The occupational responsibility of the coal trimmer was to load and distribute coal, which had been previously washed and separated from rock, into the hold of ships (Collis & Gilchrist, 1928). Although the conclusions were contested in the 1930's, additional support was received in 1940 (Gough, 1940). Also, around this time, a technique of preemptive diagnosis, and assessment of the disease were attempted, but the accuracy remained low (Gough et al., 1949). Correlation between the total dust and the severity of the pneumoconiosis was later found by analyzing radiographic and pathologic data (King et al., 1956). There were some investigations conducted in the US in the earlier part of the 20th century which also mirrored the sentiments of British researchers, and brought forth evidence that the lung disease among coal miners must be differentiated from the broad label of silicosis (Dreessen & Jones, 1936). It was not until around the late 1950's, and 1960's that more emphasis was placed on studying the disease and finding an adequate method of reporting its incidence (Doyle et al., 1958). In the US, a number of studies were conducted in Pennsylvania, a region with a higher reported frequency of the disease (Baier & Diakun, 1961; Lieben & McBride, 1963; Mc Bride et al., 1963; McBride et al., 1966; Tokuhata et al., 1970). Later studies looked at the larger Appalachian region and other coal fields throughout the US (Lainhart, 1969; Morgan et al., 1973; R. L. Naeye & Dellinger, 1970). Experts in the earlier part of the 1970's began proposing that black lung was an agglomeration of complex disorders differing in severity and frequency, all of which depended on aggregate exposure, and individual predisposition based on personal habits and exposure to pollutants in their respective communities (R. Naeye & Dellinger, 1972).

The medical definition of CWP is a parenchymal lung disease resulting from the body's response to the deposited and retained coal dust in the lung (Weeks & Wagner, 1986). The current legal definition of pneumoconiosis is "a chronic dust disease of the lung and its sequelae, including respiratory and pulmonary impairments, arising out of coal mine employment." From 20 CFR 718.201. While the coal dust is predominately comprised of carbon, the dust also has trace metals and inorganic minerals in its composition which can be cytotoxic (Castranova & Vallyathan, 2000; Huang et al., 2006). It has also been found and confirmed over the years that there is an increased risk of contracting CWP with an increase in coal rank (M. D. Attfield & Kuempel, 2008; M. Attfield & Morring, 1992; Morgan et al., 1973). Additionally, the large surface area of the coal dust resulting from the small size has the ability to absorb aromatic compounds such as benzene and phenol present in the mine atmosphere. These compounds may have an adverse effect on the lung tissue (Castranova & Vallyathan, 2000). In order to start developing CWP an individual could normally have ten or more years of exposure to respirable coal dust. The radiographic test will show opacities <10mm (Neimeier, 1993) normally in the upper chest area (Castranova & Vallyathan, 2000). An example of one of these x-rays can be seen in Figure 1 below. Although the x-ray may show these opacities, the individual may not be suffering from any symptoms (Neimeier, 1993; Colinet et al., 2010). Once diagnosed, the individual is at a greater risk for complicated CWP or PMF. When the opacities found on the x-ray combine to cover an area greater than 1 cm then, the disease has progressed to the point of complicated CWP. This can be seen in Figure 2 below. It is not necessary for the individual to be diagnosed with simple CWP prior to this diagnosis (Neimeier, 1993).

Figure 1: Simple CWP (Colinet, 2010)

Figure 2: Complicated CWP (Colinet, 2010)

2.2 SILICOSIS

When respirable crystalline silica is deposited in the alveoli, it is possible for silicosis to develop. This is due to the high reactivity of the cell membranes and the surface of the crystalline silica. The silicon dioxides (SiO_2) come in contact with water and form silanol (-SiOH) which are hydrogen donors (Castranova & Vallyathan, 2000). Hydrogen bonds are then formed due to lone pair electrons on the oxygen and nitrogen that make up many biological macromolecules. These bonds can lead to unfavorable interactions and cell damage, ultimately developing into silicosis (Castranova & Vallyathan, 2000). This disease has four categories, chronic, complicated, accelerated, or acute (Neimeier, 1993). Exposure to the respirable crystalline silica for 15 for more years can result in the contraction of chronic silicosis. The silicotic nodule is the telltale feature. It is made up of an amorphous center of a fibrous tissue surrounded by systematic hyalinized collagen fibers, sometimes referred to as onion skinning (Castranova & Vallyathan, 2000; Neimeier, 1993). An example of this can be seen in Figure 3. As with the case of simple CWP, the individuals does not need to show any symptoms, and the nodules will show up on the x-ray as opacities covering an area of less than 1 cm (Neimeier, 1993). As the area of the opacities increases to greater than 1 cm, the diagnosis is changed to complicated silicosis. At this stage, the individual would be experiencing impaired respiratory function. The accelerated form of the disease is similar to the chronic form, except the exposure to the dust is normally five to ten years (Neimeier, 1993). The acute form of silicosis is developed when the individual is exposed to virtually pure silica for intense and short periods of time (Castranova & Vallyathan, 2000). The disease can develop within six months to two years of exposure and is characterized by granular eosinophilic material in the alveoli (Neimeier, 1993). An example can be seen in Figure 4. Other sources submit the symptoms can develop over a period of a few weeks (Colinet et al., 2010).

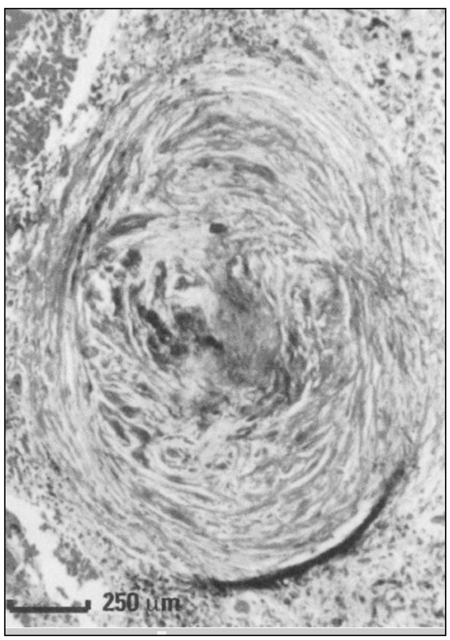

Figure 3: Chronic silicotic nodule (Castranova & Vallyathan, 2000)

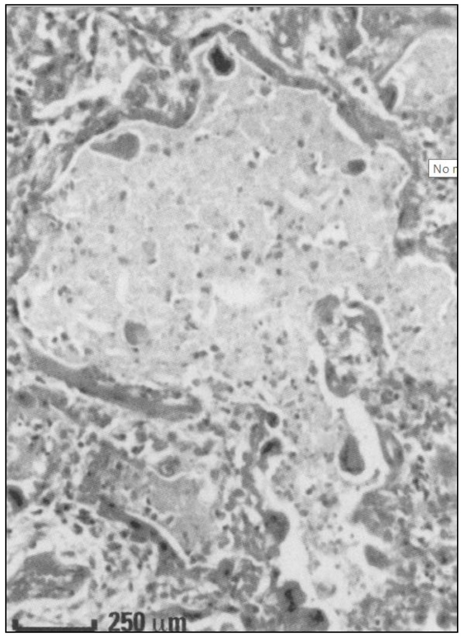

Figure 4: Acute silicosis (Scarisbrick, 2002)

2.3 PROGRESSIVE MASSIVE FIBROSIS

Progressive massive fibrosis is a generic term used for a multitude of pneumoconiosis comprising both the complicated CWP and complicated silicosis (Castranova & Vallyathan, 2000). PMF is accompanied by breathlessness while resting or exercise due to greatly impaired lung function and oxygen diffusion (Neimeier, 1993). Other complications associated with these diseases include chronic bronchitis, chronic obstructive pulmonary disease (COPD), cor pulmonale, and respiratory failure (Hadjiliadis, 2015).

2.4 REGULATIONS

In order to lessen the impact of CWP and silicosis, provisional mandatory standards were put in place by the Federal Mine Safety and Health Act of 1977, section 202. Later the standards were superseded by amended permanent standards under Section 101. Section 202(b)(2) of the Act required each operator in a coal mine to continuously maintain the average concentration of respirable dust in the mine atmosphere during each shift to which each miner in the active workings of such mine is exposed at or below 2.0 milligrams of respirable dust per cubic meter of air (Congress, 1977). Proclamation of the Mine Act occurred on April 8, 1980, and is currently implemented under 30 CFR § 70.100, Respirable dust standards. In the case where more than 5 percent silica is found in the respirable dust, then the limit is determined using the following formula from 30 CFR § 71.101:

$$\Phi = \frac{10}{\%\, silica} \tag{1.1}$$

Where Φ = respirable dust limit (mg/m^3)

% Silica = percent silica found in dust as a fraction

Since 1980, average coal dust exposures and incidence of CWP have declined under the existing standards (National Mining Association, 2013), but recently, “CWP has increased among experienced miners, and in some cases, CWP has progressed rapidly to PMF” (Department of Labor - Mine Safety and Health Administration, 2010). Additionally, it was found that there is a geographic concentration of CWP cases in central Appalachia as shown in Figure 5.

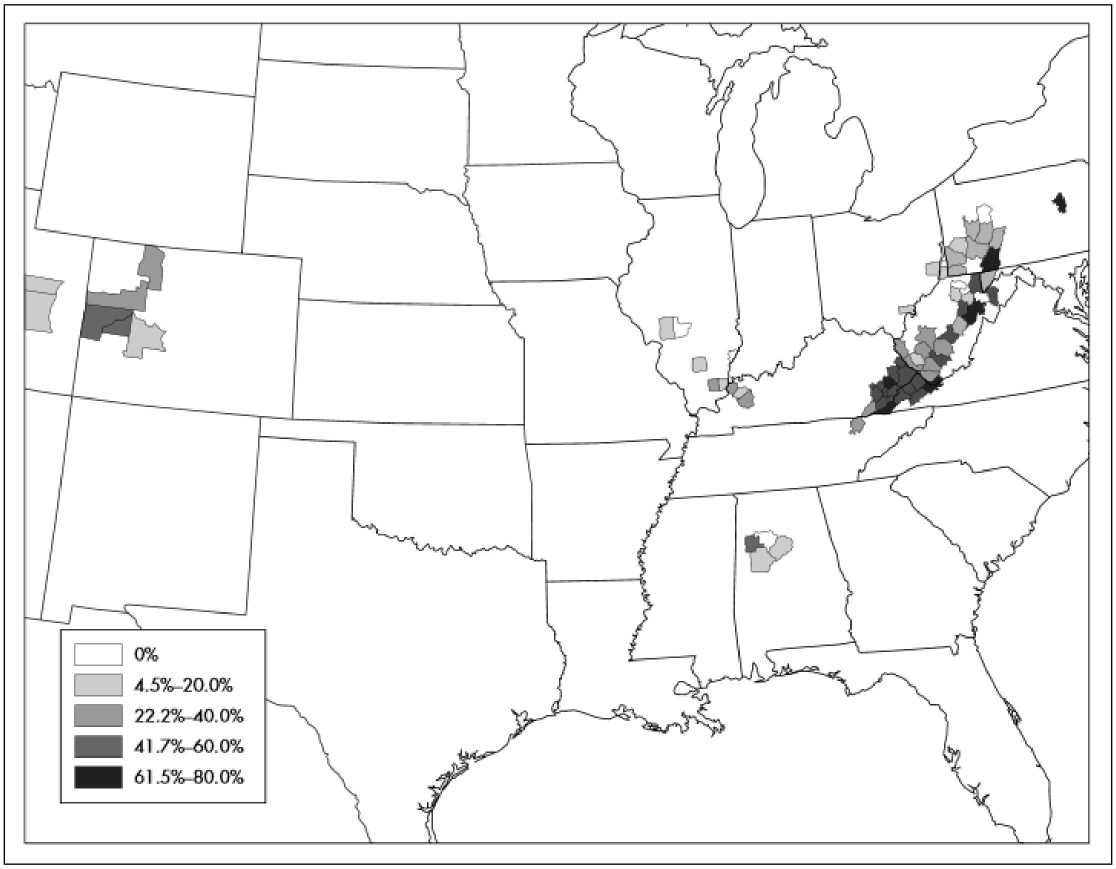

Figure 5: Proportion of evaluated miners with rapidly progressive coal workers' pneumoconiosis by county (Antao et al., 2005)

In other studies, higher concentrations of CWP and PMF cases took place in West Virginia, Virginia and Kentucky (Laney et al., 2012). Additional studies have shown that the prevalence of CWP and PMF is more closely tied to mine size rather than the geographic location or coal rank. A study conducted by Laney and others found that the individuals working in a mine with less than 50 miners were at a risk for increased frequency and severity of CWP and PMF (Laney & Attfield, 2010; Suarthana et al., 2011). The level of exposure to crystalline silica is another factor that deserves consideration. A study found that through careful examination of chest x-rays for abnormalities and documentation of rapid disease progression, coal miners may be exposed to more toxic levels of respirable silica than in previous years due to more difficult geology (Laney et al., 2010).

For this reason, in October of 2010, the Mine Safety and Health Administration (MSHA) put forth a proposal to limit exposure further, changing the limit from 2.0 mg/m^3 1.0 mg/m^3. Grounds for the proposal were primarily based on a National Institute for Occupational Safety and Health (NIOSH) report submitted to the Secretary of Labor Lynn Martin, on November 7, 1995. The NIOSH report recommended that "exposures to respirable coal mine dust be limited to 1.0 milligrams per cubic meter as a time-weighted average" (NIOSH, 1995). The final ruling is a comprehensive method which utilizes new continuous personal dust monitor (CPDM) technology to display real-time dust concentrations, as well as increased sampling and stricter standards. The final rule has gone into effect as of August 1, 2014, with sections being introduced during the following two years (Department of Labor - Mine Safty and Health Administration, 2014).

2.5 SPRAYS

Most of the coal dust production in a mine occurs at the face during cutting and has the potential to produce up to 8600 grams of respirable dust per ton of coal (Tien & Kim, 1997). In order to meet the new standards and be proactive in the protection of miners from respirable dust, there are a number of methods that can be implemented. The most predominate methods include are the introduction of engineering controls. The engineering controls used to limit the miners' exposure to dust can vary from improved ventilation controls to the introduction of scrubbers and collectors. One of the most popular engineering controls used to curb the dust problem has been the application of water via sprays in areas where there is significant dust production.

There are three functions sprays play in limiting the exposure of a coal miner to coal dust particulates. There are also a few factors regarding the effectiveness of water spray systems depending in the function of the sprays; including the nozzle type, pattern, flow, location, and pressure (Colinet et al., 2010). The first function, redirection, can aid in separating the miner from the primary source of the dust, by moving the direction of air flow (Pollock & Organiscak, 2007). The key characteristics for these sprays are high pressure and strategic location. The second function is capture of dust particles, which has been demonstrated (Cheng, 1973; Goodman et al., 2006). When capturing airborne dust with sprays, water droplet size and velocity are the most influential parameters. Lastly is suppression and wetting where low pressure high flowrates are the most advantageous characteristics. The function of wetting coal is also thought to be the primary mechanism for dust suppression, while capture and redirection are secondary effects (Kissell, 2003).

There are a number of spray designs, each of which has a specific application. Figure 6 shows the types of sprays using in mines to control and mitigate dust.

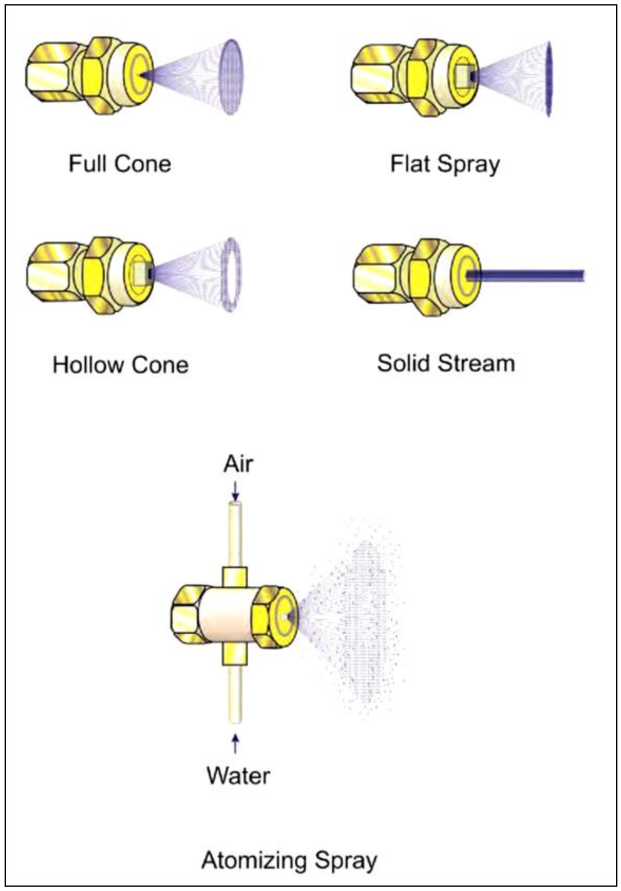

Figure 6: Spray nozzle types used for controlling dust in mines (Colinet et al., 2010)

The smaller the water droplets produced by the hollow cone and atomizing spray, the faster the initial speed when it is propelled out of the spray nozzle. However, the small droplets are quickly slowed due to the effects of air resistance. Even so, these sprays are more commonly used for capturing purposes. The larger droplets are less affected by air resistance and maintain their momentum over larger distances. The variability of the spray droplet characteristics accounts for the variety of spray nozzle types.

The full cone sprays are most commonly used at belt transfer points because they offer a uniform wetting pattern and can be placed farther way from the dust source. The flat fan nozzles are used for dust containment, normally located on the sides of cutter heads and before stockpile transfer points (Co.

Spraying Systems, 2013; Colinet et al., 2010). Hollow cone nozzles are primarily used for combating the entrainment of dust and redirection of air flow. These are also the most common type of spray placed behind the cutting head on the boom of a continuous miner. In addition, the large openings help to keep the nozzle from clogging and allow for higher flow rates needed for wetting the host rock. The atomizing and fine spray nozzles are used less in the industry due to their higher price and high maintenance requirements (Colinet et al., 2010). The effectiveness of each type of spray nozzle in capturing airborne dust can be seen in Figure 7.

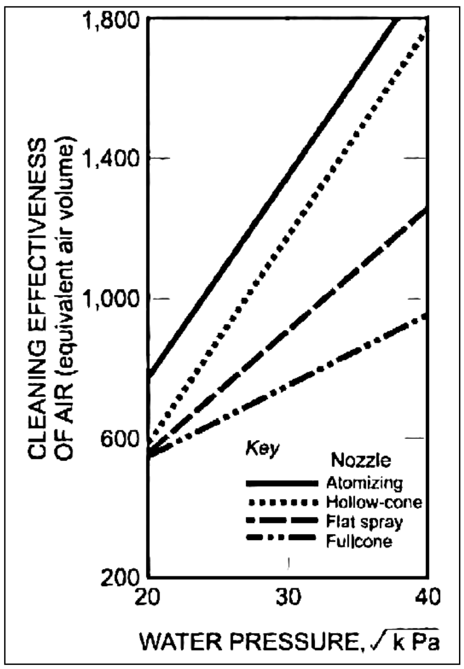

Figure 7: Relative spray nozzle effectiveness (J Colinet et al., 2010)

2.6 SURFACE TENSION

Simple water sprays have now reached their useful limits in suppressing respirable dust due to the physical parameters, and new effective suppression aids are needed. The wettability of coal is limited due to its hydrophobic nature and ultimately the surface tension of the water.

Surface tension is the phenomenon which results due to the cohesive force between the water molecules. The cohesion arises from the hydrogen bonds which are due to the polar nature of water molecules (Figure 8). The cohesive forces within the bulk of the liquid are essentially uniform and shared by all neighboring molecules. The exceptions are the molecules on the surface. On the surface, since there are no molecules above, a film of stronger attractive forces are formed.

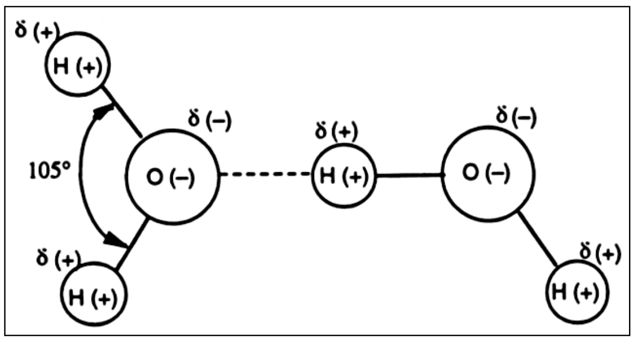

Figure 8: Cohesion due to polarity (Tien & Kim, 1997)

These stronger attractive forces resist any distortion or increase of surface area and act as an elastic membrane. This is the reason for the round shape of water droplets or of air bubbles (Silberberg & Weberg, 2009). The round shape allows for the least amount of surface area per volume and is the most stable arrangement. Any distortion or increase in surface area will take energy. The higher the surface tension, the more energy it takes to create a new surface. The units of measurement are N/m, which is a force per unit length. The factor with the largest effect on the amount of surface tension is the difference in composition between the bulk and the surface. This relationship is explained extensively in the work produced by J. W Gibbs. A portion of that work is shown in the equation below (Gibbs, 1878).

$$-d\gamma = \Gamma_1 d\mu_1 + \Gamma_2 d\mu_2 \quad (1.2)$$

Where γ is the surface tension in newton per meter, Γ is the surface excess of a given component in mole per meter squared and μ is the chemical potential of a given component in joules per mole. An example of this can be found by examining the surface tensions of fresh water and salt water. The freshwater will typically have a surface tension of around 73 dynes/cm while the saltwater will be around 78 dynes/cm (Stewart, 2009). The increase in surface tension occurs because on average the surface of the water is less salty than the bulk, or in other words, the salt has a negative surface excess. In this case, if a new surface is to be created, the molecules of salt within the new surface layer must be forced back into the bulk (Chaplin, 2009). If more salt is added to the solution and the potential is raised, it becomes harder to push the molecules back into the bulk. As a result, the surface tension is increased. In this case, the surface excess of the salt component is negative, and any increase in the potential of the salt component leads to the increase in the surface tension of that solution (Nalwa, 2001). The inverse is also true. If a solution of soap and water were to be examined there would be an excess of soap molecules on the surface of the solution and a lesser concentration of soap in the bulk. In this case, the soap has a positive surface excess, so when a new surface is formed soap molecules must be taken from the bulk and placed in the new surface layer. If more soap is added to the solution, increasing the potential, then the abundance of molecules in the bulk are easily transferred to the surface. The fact that the soap molecules are readily available makes the process easier and less energy intensive, resulting in a lower surface tension. In this case, the surface excess of the soap component is positive, and any increase in the potential of the soap component leads to the decrease in the surface tension of that solution (Nalwa, 2001).

2.7 SURFACTANTS

In the last case discussed the soap is acting as a surface active agent or a surfactant. Surface active chemicals, also known as surfactants or wetting agents, can be added to the water, and enhance the effective capture and suppression of the dust particles. Surfactants all have a similar structure with a nonpolar hydrophobic tail and a polar hydrophilic head group. Examples can be seen below in Figure 9.

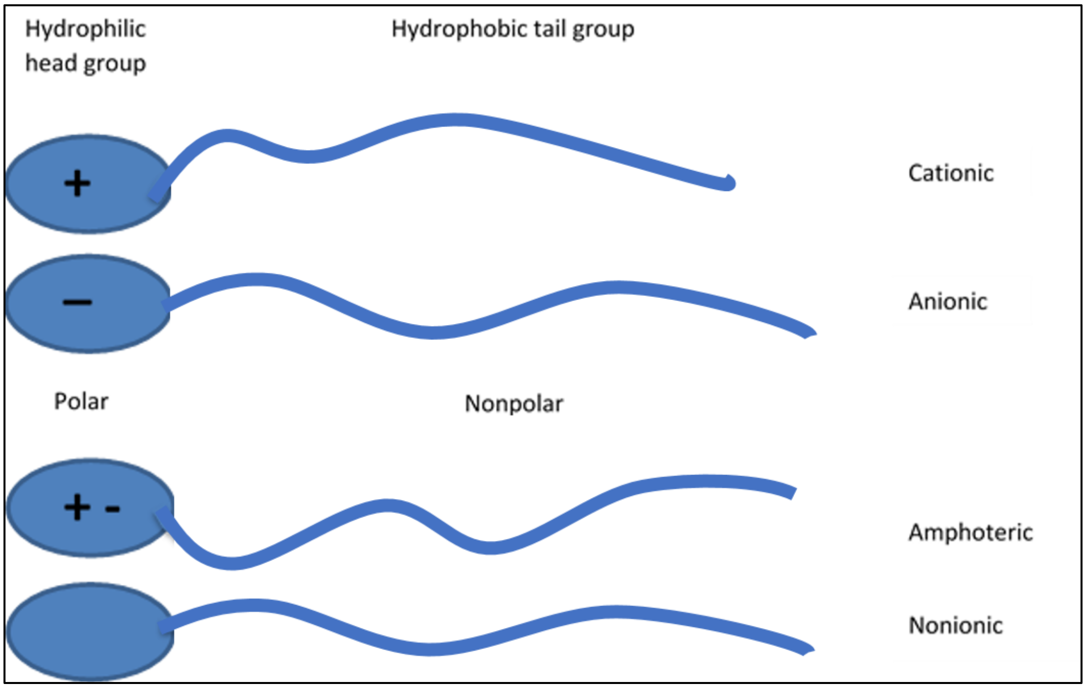

Figure 9: Subgroups of surfactant molecules; cationic/anionic/amphoteric/nonionic

The polar nature of water is ideal for adsorbing the surfactants.

An additional benefit of surfactants is that they allow for improved adhesion, engulfment, and agglomeration. These three steps can be summarized as the wettability of coal. The wetting is improved by converting the hydrophobic sites on the coal surface into hydrophilic site through the process of adsorption of surfactants. The tail group of the surfactant comes in contact with the hydrophobic sites, and the hydrophilic head group will be at the interface with the water. This arrangement allows the coal surface to have peso-hydrophilic properties.

2.7.1 Past Work

There have been many studies which have not reached a consensus on how well surfactants improve dust capture or by what mechanism. In one study conducted by Goldshmid and Calvert, the conclusion was that the interfacial tension was the primary mechanism by which the collection efficiency of water droplet could be greatly increased (Goldshmid & Calvert, 1963). On the other hand, findings from Brauer and Varma suggested that the wetting characteristics rather than interfacial tension, were the primary mechanism (Brauer & Varma, 1981). There have also been observations where the results were inconclusive, and the use of surfactants for the purpose of dust control are not justified (Hargraves & McKinnon, 1961). Another study found that surfactants are useful or effective in high dust concentration areas, such as the face while cutting (Chander et al., 1991). Additionally, this study by Chandler et al. found that the decrease in droplet diameter increased collection efficacy. A study done by Tien and Kim found that it was better wettability and not droplet parameters which lead to higher collection efficiencies (Tien & Kim, 1997), and they also determined that nonionic surfactants were found to have best collection efficiency (Tien & Kim, 1997). Conversely, a study by Hu, Polat and Chandler observed that a nonionic surfactant had a narrow maximum peak, and that cationic surfactant had both a broad operating range and the highest collection efficiency (Hu et al., 1992).

With so many varying results and contradicting conclusions, additional studies should be conducted in order to tip the balance of results and shed light on areas of dispute. The purpose of the paper is to investigate the effectiveness of a surfactant in an aqueous solution to aid in coal dust remediation by reducing the surface tension of the mine water and allow for increased wetting of coal dust. This would aid in the implementation of an engineering control to combat a preventable occupational disease in the coal mining industry.

3 ASSESSMENT OF SURFACTANT VIABILITY FOR DUST WETTING VIA SINK TEST

3.1 ABSTRACT

In addition to ventilation practices, the application of water via sprays is the most economical and popular means of combating respirable dust in an underground coal mine. Due to a noticeable increase in black lung among coal miners and new dust regulations, the use of surfactants or wetting agents have been to aid in dust suppression. The surfactant facilitates the wetting process by lowering the surface tension and allowing the hydrophobic coal dust to come into contact with the water. One of the most straightforward and effective benchtop tests is a simple wetting test. Although there are variations of this type of test, principle and technique remain the same. In this study, a known amount of dust was placed on the surface of a solution and the time it takes for all the dust to fall through the interface was determined as the wetting rate. This investigation examined the specific density of the bulk dust and concentration of a surfactant in solution and their effects on the wetting rate. It was found that both factors were significant in determining the wetting rate. It was seen that the surfactant had a more significant effect on the dust, which consisted mostly of coal particle when compared to a dust with a higher non-coal mineral content.

3.2 INTRODUCTION

There has been a recent surge of concern in the mining community on the topic of occupational health, specifically, the exposure of coal workers to the respirable dust, including coal, and silica-based dust. Respirable dust in coal mines has been seen as an issue for a number of years. Efforts throughout the last half-century have greatly decreased the number of cases of black lung to record lows in the early 2000, however, a recent uptick in the number of cases has been noticed (Blackley et al. 2014). There are many efforts under way to both identify the source or sources of the recent increase and to regulate its influence on the health of coal workers. The regulations instated put more pressure on coal producers to prevent and control hazards, whether that be through better safe work practices or administrative and engineering control. Advances in engineering controls such as ventilation practices, remote control equipment, dust scrubbers, and water spray systems have reduced the exposure of miners to respirable dust. The use of water sprays as an engineering control for abating respirable dust is common during the production and transport of ores. The mechanism for abating dust is twofold; the airborne dust capture and the preemptive wetting of the coal or rock, the latter of which is the primary means (Kissel, 2003). The continuous demand for energy, driven by the rising populations, has forced mining companies to produce in more difficult and thinner seams. The thinning of the seam has led to the coal producers mining more of the host strata than in previous operations. These pressures on the industry have not only changed the mineralogy of the dust, but the sheer tonnages and rate of raw material being moved have stretched the effectiveness of water sprays to their limits. There been many attempts to enlist the aid of surfactants to mitigate the exposure to respirable dust, with mixed results (Copeland, 2007; Hu et al., 1992; Kost et al., 1980; Organiscak, 2014; Zeller, 1983). This paper will consider the practicality of using a surfactant to aid in wetting coal dust with differing mineral content using a variation of the Walker Sink

Test to gather preliminary data. Wetting rates have been used numerous times in investigations to examine surfactant effectiveness to wet dust (Chander et al., 2007; Copeland & Eisele, 2008; Copeland, 2007; Feldstein, 1981; Glanville & Haley, 1983; Glanville & Wightman, 1979; Kawatra, 2006; Kim & Tien, 1993; Tien & Kim, 1997; Zeller, 1983).

3.3 MATERIALS & METHOD

3.3.1 Description of study

The following sink test was conducted to determine the effectiveness of a surfactant to improve the wettability of coal dust. Additionally, the study seeks to determine how the mineral content affects the wettability of the dust. Due to the occupational hazards of respirable dust when coupled with the recent increase in the number of cases of lung disease among mine employees, a practical surfactant which reduces the amount of respirable dust which a mine employee is exposed to is needed.

The laboratory test is first needed in order to determine the viability for the surfactant before running any experiment in the field. For this purpose, the sink test was used. The following sink test experiment uses an analytical balance to find the apparent weight of the wetted dust at predetermined time intervals. By examining the changes in weight of the wetted dust over time, a wetting rate can be ascertained. The subsequent section will describe in detail the initial efforts to observe the effects of varying concentrations of a surfactant, and the impact of mineral content on the wetting rates.

3.3.2 Experimental design

3.3.2.1 Equipment

For this experiment, the most important piece of equipment was the analytical balance. The analytical balance used was an Ohaus Pioneer PA214. This scale was chosen because it had the necessary capacity to hang weights from the underside of the scale. It also had the added benefit of being able to link to a laptop via a USB2.0/RS232 serial cable. With these attributes, the scale could be programmed to send a measurement at predetermined time intervals. A computer was used as the data storage and data acquisition unit. The software used to control and manage the scale's output was WinWedge. A wire cable was used to connect a plastic platform and counterweights to the underside of the analytical balance, and a small glass basin was used to hold the solution.

3.3.2.2 Equipment setup

The analytical balance was set and suspended above a glass basin. Tied to the underside of the analytical balance, via a wire, were the platform and the counter weights. When the basin is filled with water or the solution, the platform is submerged. The platform was cut to fit the basin with about one to two millimeters of space along the edge. The RS232 end of the cable was connected to the analytical balance, and the USB end was connected to a computer. The computer had previously been loaded with WinWedge software for data acquisition. The basic equipment setup can be seen in Figure 10 below.

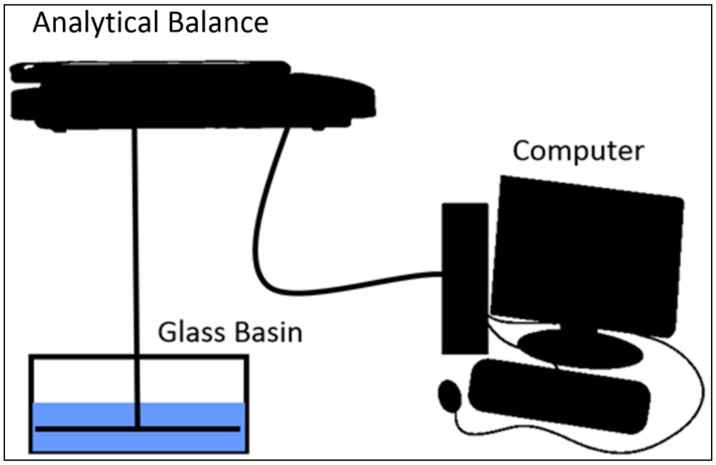

Figure 10: Schematic of experimental setup

3.3.2.3 Sample

The laboratory testing was conducted with a single type of bituminous coal. The coal being used for this experiment was anonymously donated. The samples used had previously been gravity separated into nine gravity classes via submersion into baths with varying specific gravities. The heavy material would sink, and the lighter material would float and was used as the feed for the next lower gravity bath. This process is shown in Figure 11 below.

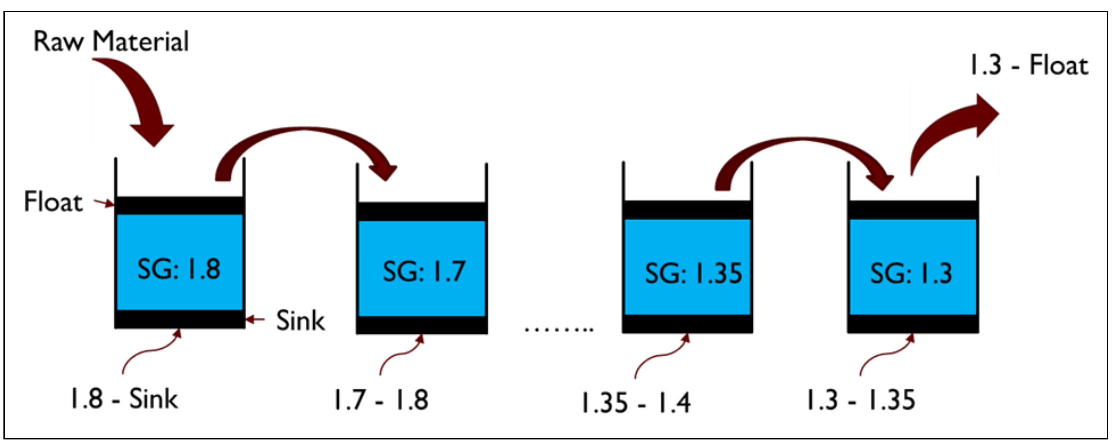

Figure 11: Method of gravity separation

These coal samples were ground and then pulverized. The pulverized coal samples were then run through a wet screen of 400 mesh. This was done to help limit the amount of larger particles which would fall through the surface interface due simply to their individual weight. It is important to note that the top sizes of the dust fraction will be larger than what is defined as respirable. The size distribution of each gravity class can be seen in Appendix A. An example of a typical size distribution plot and tabulation can be seen respectively in Figure 12 and Table 1 below.

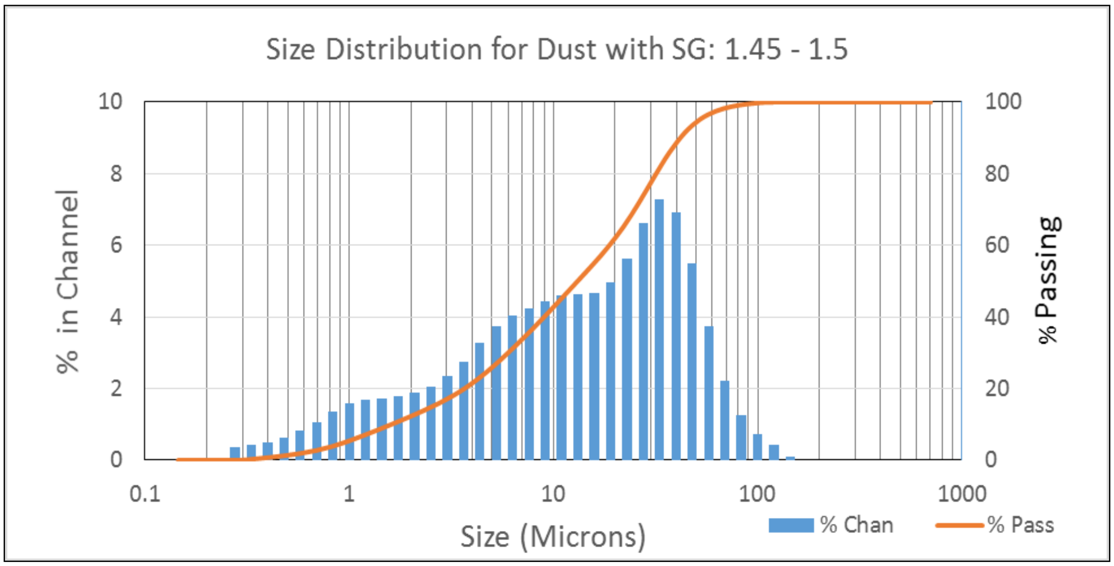

Figure 12: Example of a size distribution plot for gravity class 1.45-1.5

Table 1: Tabulated size distribution for gravity class 1.45-1.5

Size (µm)	Pass %	Change %	Size (µm)	Pass %	Change %	Size (µm)	Pass %	Change %
352.0	100.0	0.0000	26.16	71.83	6.630	1.945	11.97	1.790
296.0	100.0	0.0000	22.00	65.20	5.640	1.635	10.18	1.730
248.9	100.0	0.0000	18.50	59.56	4.950	1.375	8.450	1.690
209.3	100.0	0.0000	15.56	54.61	4.660	1.156	6.760	1.590
176.0	100.0	0.0000	13.08	49.95	4.630	0.972	5.170	1.370
148.0	100.0	0.0000	11.00	45.32	4.590	0.818	3.800	1.070
124.5	100.0	0.1100	9.250	40.73	4.440	0.688	2.730	0.8100
104.7	99.89	0.4400	7.778	36.29	4.240	0.578	1.920	0.6200
88.00	99.45	0.7200	6.541	32.05	4.030	0.486	1.300	0.5000

74.00	98.73	1.260	5.500	28.02	3.730	0.409	0.8000	0.4300
62.23	97.47	2.230	4.625	24.29	3.270	0.344	0.370	0.3700
52.33	95.24	3.730	3.889	21.02	2.760	0.289	0.0000	0.0000
44.00	91.51	5.490	3.270	18.26	2.340	0.243	0.0000	0.0000
37.00	86.02	6.910	2.750	15.92	2.060	0.204	0.0000	0.0000
31.11	79.11	7.280	2.312	13.86	1.890			

After the screening, these samples were then oven-dried and collected in plastic sample bags. Table 2 below shows the different gravity classes that would be tested and the estimations for their respective mineral content.

Table 2: Tabulation of gravity class and estimated mineral content

Gravity class	*Mineral content*
1.3 Float	0%
1.3 - 1.35	0 - 4%
1.35 - 1.4	4 - 7%
1.4 - 1.45	7 - 11%
1.45 - 1.5	11 - 15%
1.5 - 1.6	15 - 22%
1.6 - 1.7	22 - 30%
1.7 - 1.8	30 - 37%
1.8 Sink	> 37 %

The mineral content was estimated by assuming the specific gravity of coal and non-coal or mineral were 1.3 and 2.65 respectively.

The surfactant being used was initially found to be too viscous to be drawn with a micropipette. For this reason, the concentration was diluted mixing equal parts by volume of deionized water and surfactant. The surfactant was measured via a 100 ml syringe. A large syringe was used because of its large ratio of volume to surface area. There was concern that the viscosity of the surfactant may lead to an excess of material adhering to the inside of the nozzle of the measuring device. The surfactant was added to the container first. Next, the then the deionized water was added with a separate 100 ml syringe. Using the solution, the syringe that was used to measure the surfactant was then rinsed to free any surfactant that was still adhering to the inner surface of the syringe. The tested ratios are tabulated in Table 3 below along with their respective volumetric percent of the solution.

Table 3: Tabulation of tested surfactant to DI water ratios

Ratio of surfactant to DI water	*Surfactant as a percent of solution*
0	0.000%
1:7000	0.014%
1:6000	0.017%
1:5000	0.020%
1:4000	0.025%
1:3000	0.033%
1:2000	0.050%
1:1000	0.100%
1:500	0.200%

3.3.3 Procedure

Initially, the suspended analytical balance was leveled. After randomizing the order of sample combinations to be tested, the concentration of the solution to be tested was prepared. This was accomplished by mixing 300 ml of deionized water with the appropriate amount of diluted surfactant. The deionized water was measured 50 ml at a time with a 60 ml syringe and place in a 500 ml beaker. The surfactant was measured with a micropipette. The prepared solution or unaltered deionized water was then poured into the basin. Next, the platform and weights were placed in the solution and the basin centered beneath the analytical balance. Due to the movement involved, the system was allowed to settle before taring the analytical balance. In this time, the dust sample was prepared. The dust sample to be tested was weighed in a separate analytical balance. A dust sample of at least 500 mg, but no greater than 510 mg was taken from the sample bags. Due to the drying process, some of the dust formed cakes which were broken up. After breaking up the cakes, the dust was placed on a spatula, which would be used to place the dust on the surface of the liquid. In combination with the spatula, a sieve was used in order to disperse the dust evenly on the surface of the solution. After the analytical balance had settled, it was zeroed, and the software was set to record the incoming data. After the first entry in excel appeared, the dust was distributed on the surface of the liquid. The data were recorded as long as the dust continued to settle on the submerged platform. The test was halted only when the recorded data appeared to reach steady state, and it was observed that the dust would no longer wet. After the test was halted the platform and the counter weights were removed from the wire. Lastly, the platform, basin, and beaker were all washed and rinsed thoroughly with deionized water a total of three times and then allowed to dry.

3.4 RESULTS AND ANALYSIS

3.4.1 Analysis

The results that were recorded yielded some formatting errors. Before the results could be analyzed the errors had to be removed. In some cases, a negative sign would be incorporated into the data, not representative of any physical phenomena, and some entries had a misplaced decimal point or had multiple decimal points with the entry. Finally, the data that were used had to be corrected due to displacement to depict the actual weight of the dust. In its recorded form, the data were showing the apparent weight of the dust in the solution. The first steps began with correcting the apparent weight to reflect the actual weight of the dust. This was achieved for each gravity class by using Archimedes' principle to find a correction factor. The correction factor was found, assuming the gravity of the dust in each gravity class was the arithmetic mean of the limits for each class. Next, the problem of negative entries and misplaced decimals, which led to entries having values an order of magnitude larger than they should have been, were corrected. This was done by setting limits of zero and 500 mg around the recorded data set. It is important to note that errors remained in the data in some cases. (An entry of 320 milligrams when it should have been 32 mg or vice versa would remain unaffected.) When the corrections were made the data entries were replaced with blanks as placeholders in order to not skew the data and to ensure the data points remained at the right time tag.

After the data were refined, a model was selected. The initial form of the data has two parts. The first is the settling of the majority of the dust, approximately 0 to 4000 seconds in Figure 13. The shallower incline of the second section of the plot describes the slower settling times of the very small particle and may be due to the mixing effect caused by the settling of the larger particles of dust, approximately 4000 to 30000 seconds in Figure 13. In order to find the wetting rate, the model used a piecewise function with the first part being a linear function and the second part being a power function. Although there were models that fit the data better, this one was chosen because the wetting rates could be determined directly from the model. The slope of the first part of the piecewise function is considered the wetting rate of the sample. The model was initially rough fitted by manually altering the constants in the model. On a point to point basis, the model was compared to the recorded data. The difference from each point was squared, and these values were then summed. It was this sum which was minimized by fine tuning the constants of the model. An example of the result is shown in Figure 13.

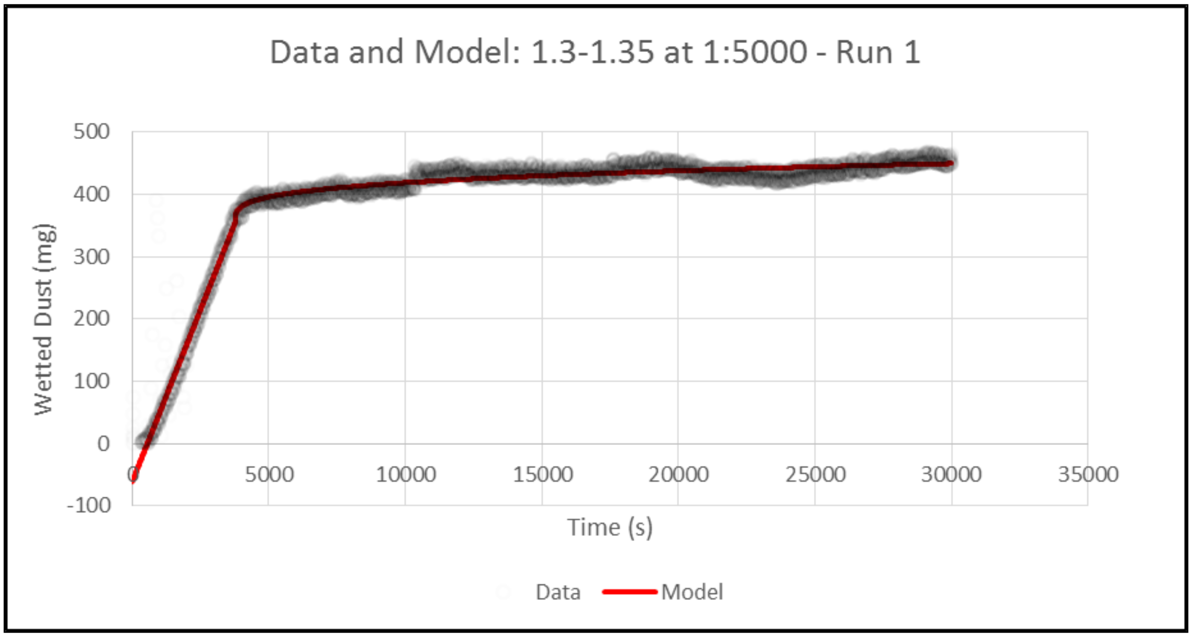

Figure 13: Recorded data and fitted model for gravity class 1.3 - 1.35 with a surfactant ratio of 1:5000

After the initial models were completed, it became obvious that the shallower slopes in some of the models had too much influence over the first section of the model. The model is fit by minimizing the difference between the observed data and what would be predicted by the model. Since each point of data is equally weighted, more significance was being placed on readings which occurred after the vast majority of the dust had settled through the solution. It would be safe to assume the slower settling particles were ultrafine and simply took much longer to settle on the platform after wetting. For this reason, the tail ends of data were trimmed to allow the wetting rates to be more accurately represented. An example of the altered model is shown in Figure 14.

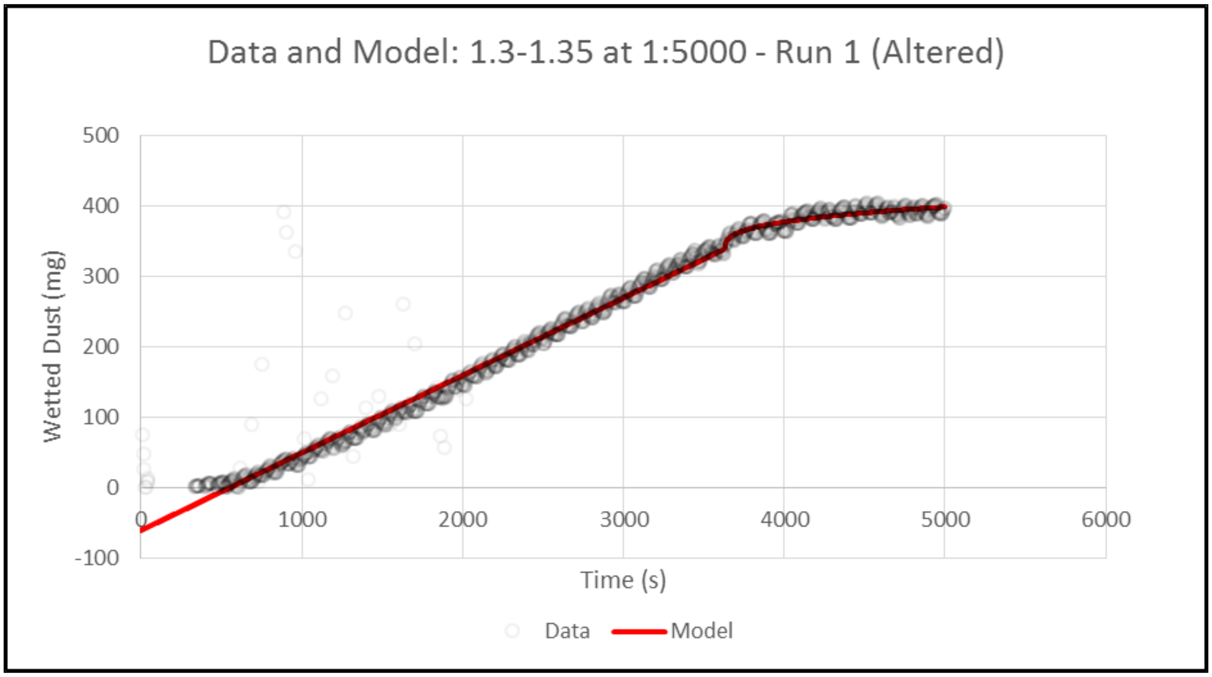

Figure 14: Recorded data and fitted model for gravity class 1.3 - 1.35 with a surfactant ratio of 1:5000 after alteration

The most common problem in all models was accurately depicting the beginning of the experiment, possibly due to the manual deposition of dust onto the surface of the solution. The wetting rates of some dust might appear higher in the beginning if the particles were agglomerated or released from a higher position than other samples. Additionally, the higher wetting rates may be a result of higher than normal deposition of dust directly on the connecting wire or hook of the experimental setup. In other cases, the initial measurements are lower than expected or negative, shifting the y-intercept of the model below zero. This may be a result of the data transfer or interpretation between the analytical balance and the computer. These depiction problems can be seen very well in the Observation versus Predicted (OvP) plots for each model. Examples of these OvP plots for both the higher and lower than expected wetting rates can be seen in Figure 15 and Figure 16 respectively.

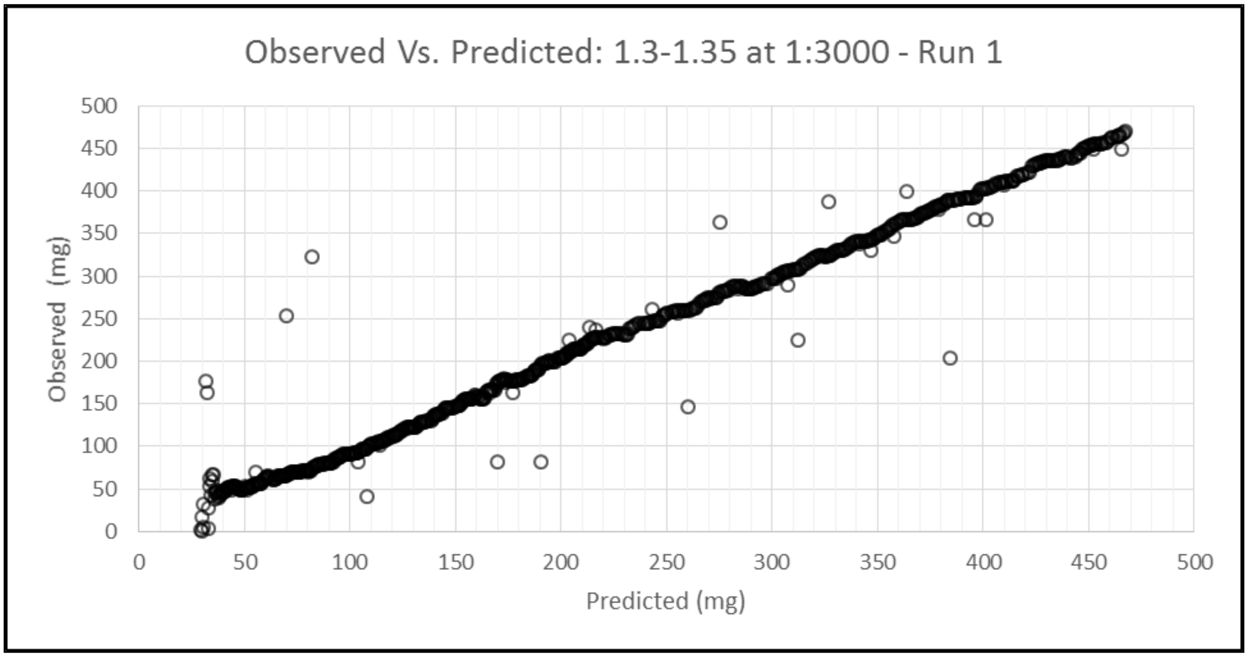

Figure 15: Observed vs. predicted plot with initially higher than expected wetting rates

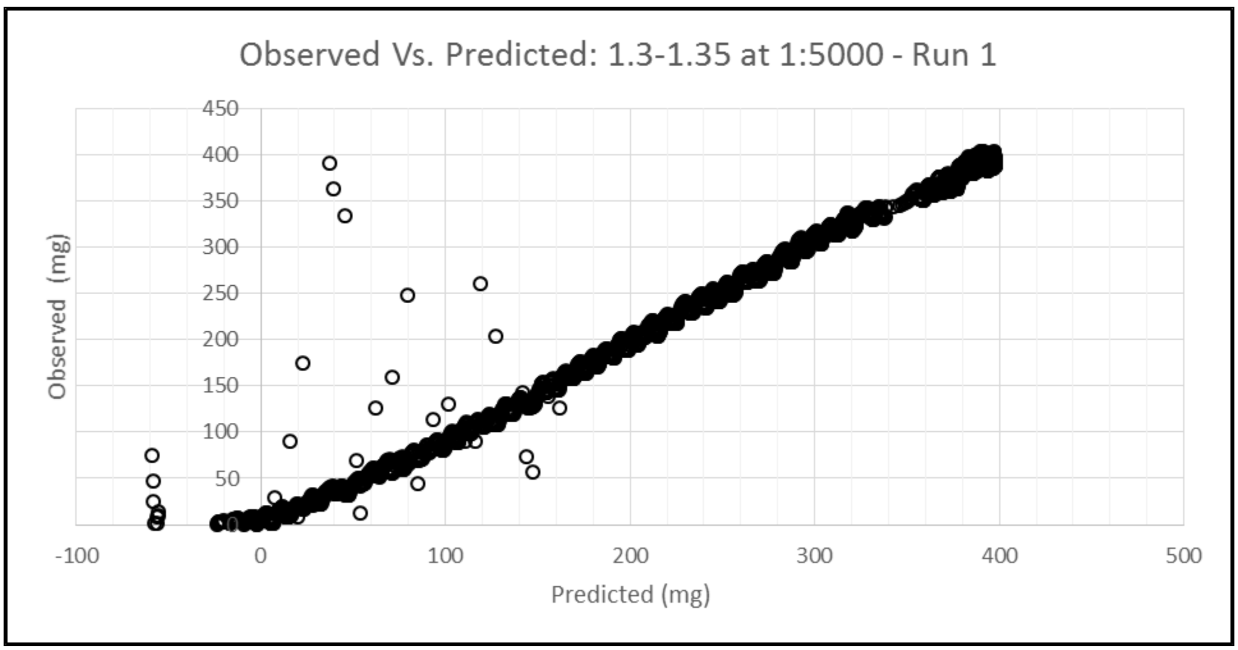

Figure 16: Observed vs. predicted plot with initially lower than expected wetting rates

These OvP plots were also used to confirm whether the model was a good fit to the data or not. A coefficient of determination was used to determine if the model was a good fit. A limit of 0.95 was used to assess when the model did not fit the data sufficiently. Most of the OvP plots displayed bunching or curving of the end around 400 mg and above, as well as a scattered and curved section at the beginning, normally around 150 mg and below. The residuals of the model were of less concern since the model was simply used to get a quick understanding of the relationship, and relative rates. If the models were going to be used for more predictive purposes, then a more accurate nonlinear model would be needed. All of the OvP plots, as well as the Residuals plots for each run, are tabulated in Appendix A.

In addition to the typical cases, there were also typical shapes for the case where no surfactant was used. With the lower gravity class, there was no perceived wetting of the dust. Any increase in weight was presumed to be due to evaporation, and the increased exposure of the previously submerged connecting cable. In some cases, the experiment was allowed to run until the counter weights were exposed. This resulted in the typical shape shown in Figure 17 below.

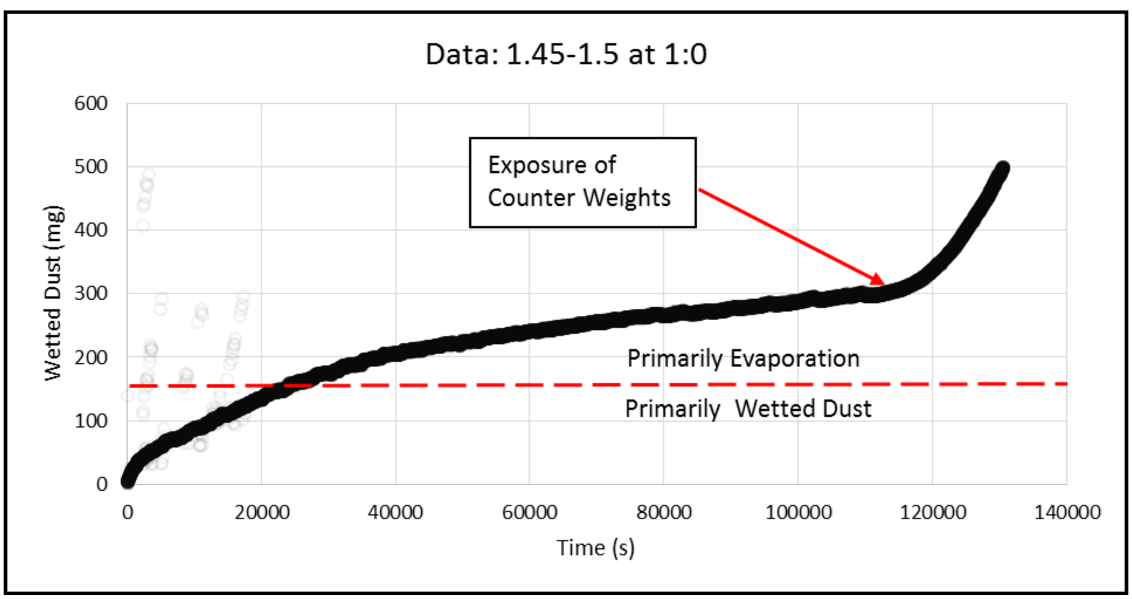

Figure 17: Evaporation as primary means of recorded increase in mass

When testing the higher gravity classes with no surfactant, there is a slight weight gain from wetted dust, but this was only a portion of the total dust. It is suspected the slight weight gain is due to the high liberation of the material. The hydrophobic particles of coal and hydrophilic mineral particles are separated which may lead to the hydrophilic minerals settling onto the submerged plate.

During some runs, regular oscillations were noticed in the data. In all cases, the oscillations lead to less than significant variation in the data due to a large amount of data collected. In a few, very pronounced cases, the oscillations could be clearly seen. These regular oscillations can be seen in Figure 18 and Figure 19 below.

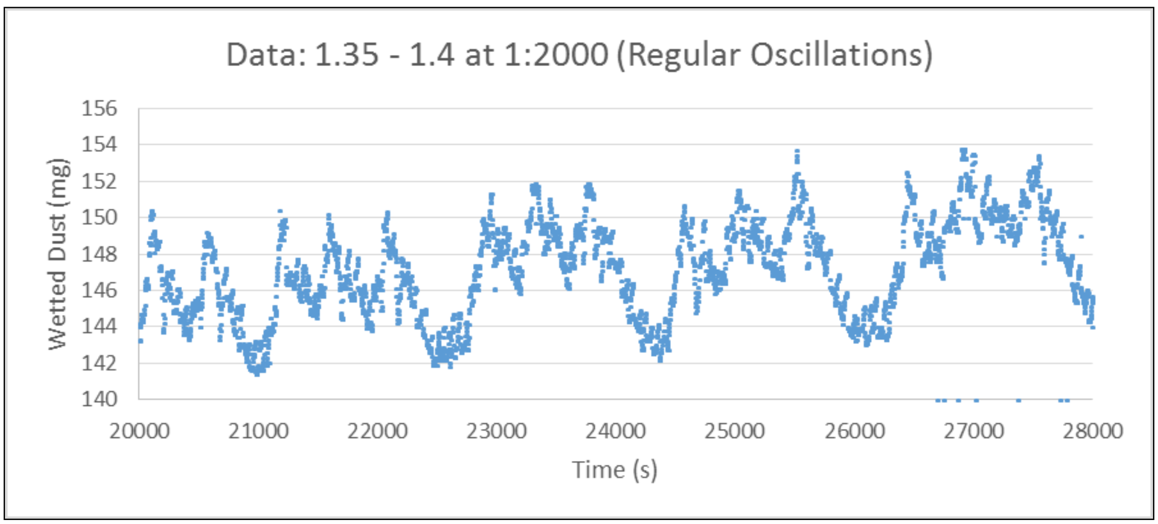

Figure 18: Example 1 of regular oscillations

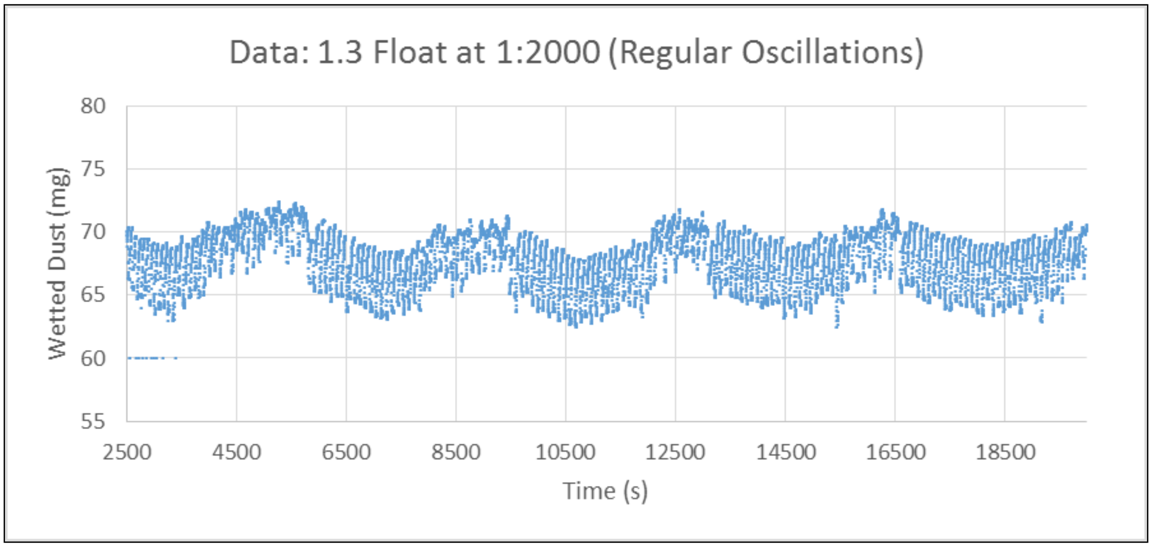

Figure 19: Example 2 of regular oscillations

In Figure 18 and Figure 19 above, the period for the oscillations ranged from 1 minute to 1 hour. No known source of the noise was ever identified.

3.4.2 Results

The initial testing consisted of triplicates of three gravity classes and three dosage levels. The three gravity classes examined were 1.3-1.35, 1.4-1.45, and 1.5-1.6. The three dosage ratio used were 1:5000, 1:3000 and 1:1000. After the data were cleaned, the wetting rates were collected and compared. The examination of the OvP plots, as well as a coefficient of determination of 0.95, was used as a minimum to remove any model which did not sufficiently represent the data. Weighted means of the wetting rates were then prepared. A summary of the results for the triplicates can be seen in Figure 20 below.

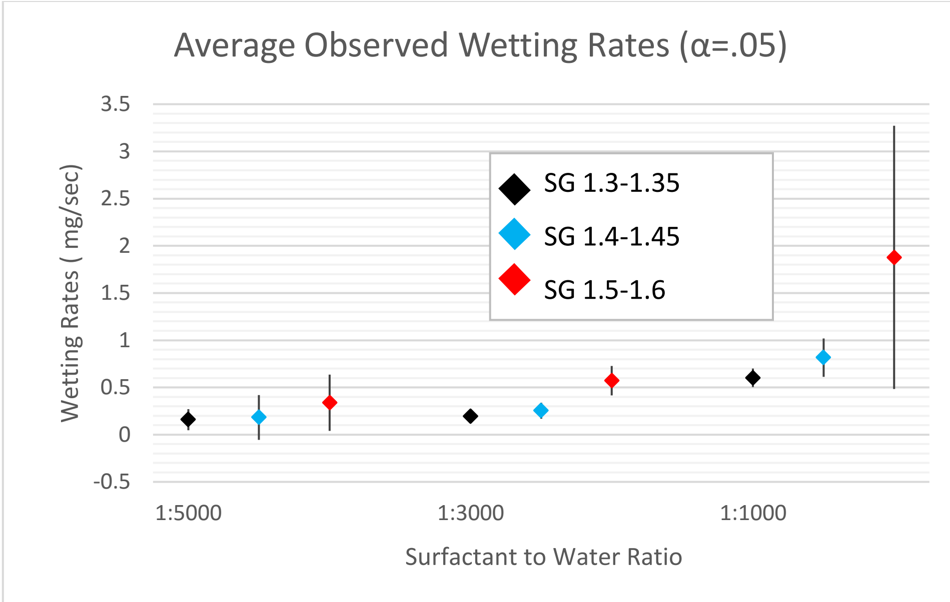

Figure 20: Average wetting rates resulting from changes in gravity and surfactant ratios

In Figure 20 above, it can be seen that the increase in surfactant concentration significantly increases the rate of wetting. Even more evident is the wetting rates for the dust with a higher mineral content increase at faster rates than those with primarily coal dust. An ANOVA two factor with replication test was conducted to confirm the observed influence of the gravity classes and the surfactant ratios. The null hypotheses tested were as follows.

- H_{0a}: There is no significant difference in the wetting rates correlated to the surfactant dosage ratio.
- H_{0b}: There is no significant difference in the wetting rates correlated to the gravity class.
- H_{0c}: There is no interaction between the variables mention in H_{0a} and H_{0b}.

The resulting analysis, detailed in Appendix A, Table 28, rejected all three null hypotheses. Therefore, the conclusion is drawn that there is a significant difference in the wetting rates which correlate with both the surfactant dosage and the gravity class. There is also a less considerable, but still significant, interaction between the two variables.

After conducting the initial experiments, additional data points were sought. In order to get a better picture of the correlation between the wetting rates to the gravity class and surfactant, additional parameters were tested. The same procedures were followed. The Observed vs. Predicted plots were also used to aid in the decision process of removing anomalous data. In addition, the coefficients of determination had to be greater than 0.95. The results are shown in Figure 21.

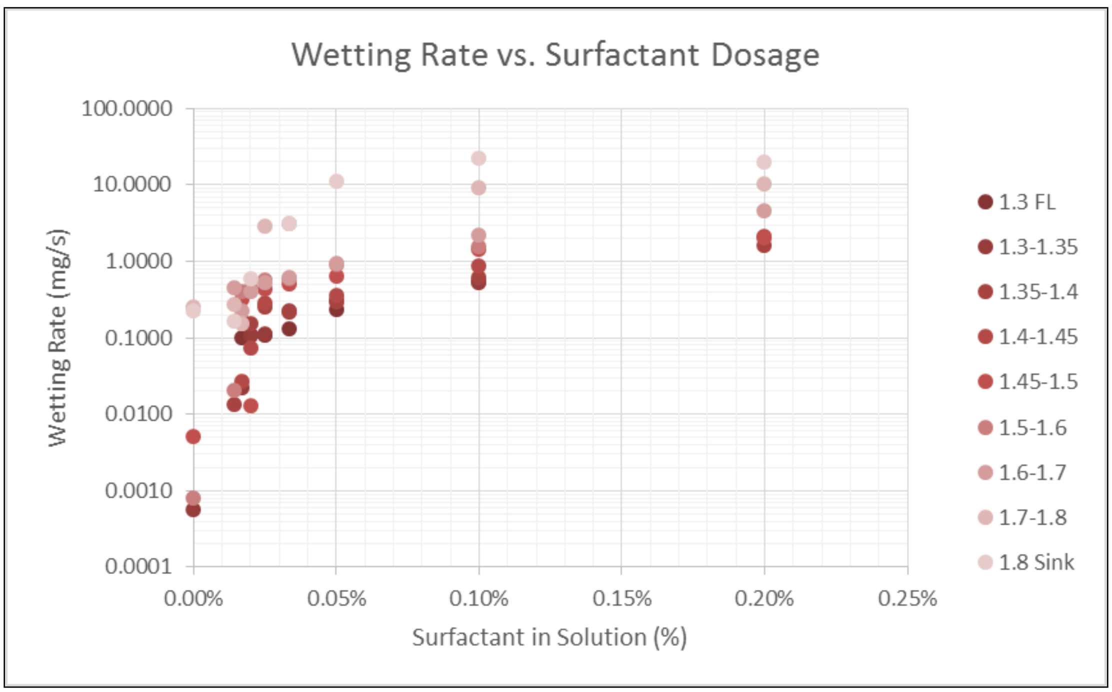

Figure 21: Wetting rates resulting from dosage ratio

Figure 21 shows a general trend of increased wetting rates with increased silica content and dosage ratio. Wetting rates are also seen to increase at a slower rate at the higher concentrations of 1:500 and 1:1000. At the high dosage ratios and high gravity, the dust applied to the surface of the water immediately fell through, leading to the wetting rates which are highly dependent on application time. When examining dosage ratios, the largest increases are seen when a small amount of surfactant was added and compared to the runs with no surfactant at all. Also, the effect of the surfactant on the different gravity classes is evident. Figure 22 below compares the wetting rates of two high gravity dusts and two low gravity dusts.

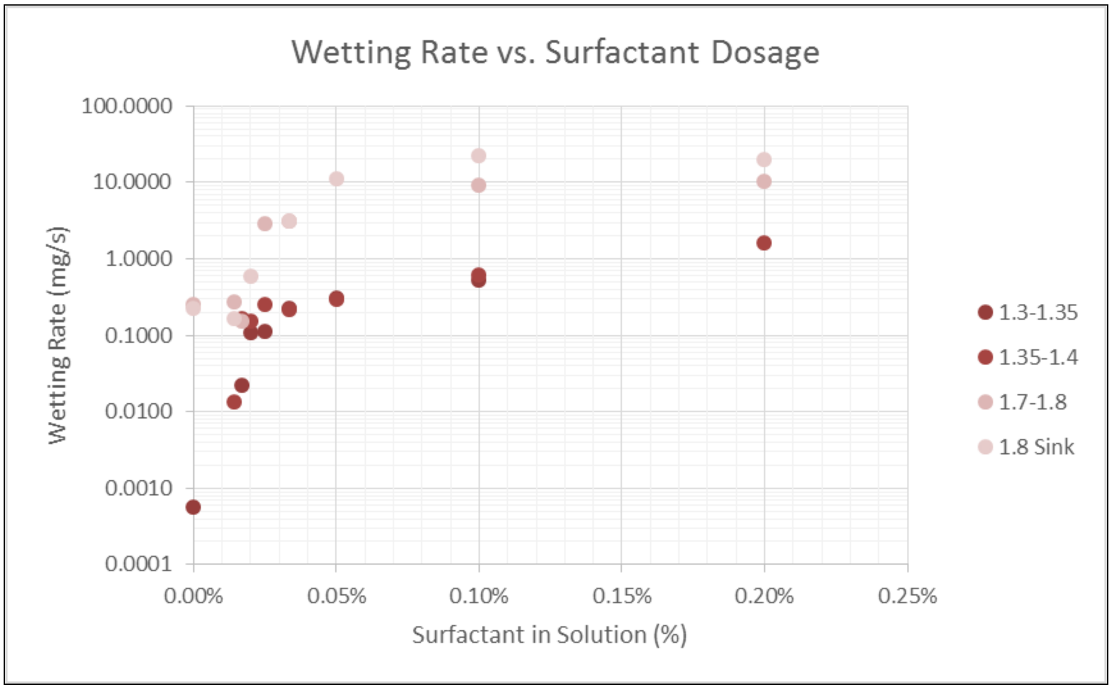

Figure 22: Wetting rates of high and low gravity dust

It can be seen in Figure 22 that the wetting rates from the high gravity dust increase about an order of magnitude from no surfactant to a 0.03% surfactant solution. At the same time, the lower gravity dust increases almost three orders of magnitude. This noticeable difference may be due to the high gravity coal already being close to a maximum wetting rate as a result of being more hydrophilic. The hydrophilic characteristic of the dust does not allow for a significant improvements to be made.

ANOVA tests were conducted, and detailed in Appendix A, Table 38, Table 39, and Table 40. The results show that there is a significant difference in the wetting rates correlated with the different dosage ratios of the surfactant as well as the different gravity classes of the dust.

3.5 DISCUSSION

Figure 20 and Figure 21 show the results of a dust wettability experiment in a static environment. A hanging submerged platform was used to measure the amount of wetted dust placed on the surface of the water and surfactant solution. As the measurements were taken at known time intervals, a wetting rate was derived. The results gathered from settling tests conducted using the method described shows evidence of a correlation between the dosage level and the wetting rates. The data presented in Figure 20 also shows the significant interaction between the dosage level and the gravity class with the assumed mineral content. These series of experiments were successful in demonstrating the correlations between the increased wetting rates and the increased dosage level and gravity class. In order to gain a more detailed representation of the correlation, additional experiments were conducted, and the results are displayed in Figure 21 above. These experiments were successful in reinforcing the previous findings.

In addition, it could be seen that improvements to the experimental methodology would be needed when expecting higher wetting rates due to the combination of high dosage ratios and high gravity classes. Due to the extremely rapid wetting rates, the manual dust deposition on the surface of the surfactant could be deemed inadequate and may have introduced bias. This problem may be alleviated with an automatic, single burst of dust deposition via compressed air or the like. Such a device should also bring about more consistency and even surface coverage with less agglomeration of the dust particles. This burst mechanism along with tests run in triplicate would also aid to make sure the regular oscillations were not skewing the results. On the same note, additional improvements could be made to the test apparatus with regards to isolation. Due to the longer period of the regular oscillations, the source is most likely mechanical or environmental. Additional support under the analytical balance would help in removing some of the higher frequency oscillations. The very low-frequency oscillations may be due to some environmental interference. A small enclosure around the apparatus would aid to isolate the tests from these interferences.

Additionally, scanning electron microscopy (SEM) analysis of the dust would also be beneficial in determining the true mineral content. The use of SEM in determining the mineral content of the wetted dust would also be very informative. Taking samples at various points during the wetting process would also help to determine whether the non-coal fraction is wetting before the coal fraction due to the high degree of liberation.

Under laboratory conditions, it has been shown that the surfactant is an effective additive for wetting dust. Until this point, no studies have been conducted in order to test the effectiveness of the surfactant at reducing the amount of airborne dust. As a result, the potential to take the surfactant to a more dynamic environment to examine the effects of a sprayer type application, either in a lab on in the field, does exist.

REFERENCES

Blackley, D. J., Halldin, C. N., & Laney, A. S. (2014). Resurgence of a debilitating and entirely preventable respiratory disease among working coal miners. American journal of respiratory and critical care medicine, 190(6), 708-709.

Chander, S., Hogg, R., & Fuerstenau, D. W. (2007). Characterization of the wetting and dewetting behavior of powders. KONA Powder and Particle Journal, 25, 56-75.

Copeland, C. R. (2007). Suppression and dispersion of airborne dust and nanoparticulates (Doctoral dissertation, Michigan Technological University).

Copeland, C., & Eisele, T. (2008). Factors influencing dust suppressant effectiveness. Minerals & …, 25(4), 215–222. Retrieved from http://www.smenet.org/minerals-and-metallurgical-processing-journal/abstract.cfm?aid=2855

Feldstein, N. (1981). Surface Chemical Technology for Improved Wetting of Coal Dust, (February). Retrieved from http://scholar.google.com/scholar?hl=en&btnG=Search&q=intitle:Surface+Chemical+Technology+For+Improved+Wetting+Of+Coal+Dust#0

Glanville, J., & Haley, L. (1983). The Wetting of “Nusance” Dust By Surfactant Solutions. Colloids and Surfaces, 8, 93–97.

Hu, Q., Polat, H., & Chander, S. (1992). Effect of surfactants in dust control by water sprays. Proceedings of the Emerging Process Technologies for a Cleaner Environment. SME, 269-276.

Kawatra, S. K. (2006). Dust in Mineral Processing. In Proceedings of the International Seminar on Mineral Processing Technology and Indo-Korean Workshop on Resource Recycling (Vol. 1, pp. 51-56). Allied Publishers.

Kissel, F. N. (2003). Handbook for Dust Control in Mining (IC 9465), 1–131. Retrieved from http://www.cdc.gov/niosh/mining/UserFiles/works/pdfs/2003-147.pdf

Kost, J. a, Shirey, G. a, & Ford, C. T. (1980). In-mine Tests for Wetting Agent Effectiveness. USBM Contract Final Report, Contract J0295041.

Organiscak, J. A. (2014). Examination of water spray airborne coal dust capture with three wetting agents, 334(October 2012), 427–434.

Tien, J., & Kim, J. (1997). Respirable coal dust control using surfactants. Applied Occupational and Environmental Hygiene, (May 2013), 37–41. Retrieved from http://www.tandfonline.com/doi/abs/10.1080/1047322X.1997.10390635

Zeller, H. W. (1983). Laboratory tests for selecting wetting agents for coal dust control. US Department of the Interior, Bureau of Mines.

4 Evaluation of Spray Water with the Addition of Surfactant for the Purpose of Respirable Coal Dust Suppression

4.1 Abstract

The application of water sprays is one of the most popular means of suppressing respirable dust in an underground coal mine. Due to a recent spike in the number of cases of black lung among coal miners, the use of surfactants has been investigated to aid in dust wetting. The surfactant lowers the surface tension thereby allowing the hydrophobic coal dust to come into contact with the water more easily. Full-scale field testing is needed to assess the effectiveness of surfactant in an underground coal environment. During the field implementation, the surfactant was pumped into the section mine water to the cutter heads of the continuous miner. The study implemented continuous personal dust monitors and personal dust samplers, which were placed in the mine environment to monitor the dust concentrations. Measurements were taken when the surfactant was off and on. When comparing the level of dust concentrations, no significant differences were found. There was, however, a significant difference as a result of location or distance from the face. Additionally, the volumetric air flow showed significant impact reinforcing the use of ventilation as a primary engineering control. Interestingly, the dust measurement between the two devices and activation of scrubbers were significantly impactful.

4.2 INTRODUCTION

The continuous demand for energy, driven by a rising population and subsequent increased demand for energy has forced many coal mines to produce in thinner and more difficult seams. These difficult conditions have led to an increase of host rock being mined in the process. In addition, several stakeholders have pointed out the increase of occupational lung disease among coal miners in recent years (Blackley et al., 2014). Some effort seeks to lessen the impact of these diseases through regulation. These new regulations, along with market pressure have placed more onus on the coal producers to implement better engineering controls. The most popular method is the better implementation of ventilation which dilutes and removes the dust from the mine atmosphere. The next most cost effective and popular method is the use of water sprays for preemptive wetting of the coal before cutting and removal of dust from air near the source. The pressures felt by the mining community have stretched the practical application of water sprays to their limit. The method which is investigated in this paper is the addition of a surfactant into the spray water. The surfactant lowers the surface tension of water allowing for easier wetting of coal at the interface. The aid of surfactants to mitigating the exposure to respirable dust has been investigated in the past, but with mixed results for both laboratory and field testing (Copeland, 2007; Hargraves & McKinnon, 1961; Hu et al., 1992; Kost et al., 1980; Organiscak, 2014; Zeller, 1983). This paper will consider the practicality of using a surfactant to aid in suppressing respirable coal dust in a mine environment.

4.3 MATERIALS & METHOD

4.3.1 Description of study

The field test described in this chapter was conducted to determine the effectiveness of a surfactant to improve the wettability of coal dust, and subsequently, decrease the dust concentrations to which miners would be exposed. Additionally, the study seeks to determine how well the surfactant mitigates the silica concentration of the dust. Due to the known occupational hazards of respirable dust and the recent increase in the number of cases of lung disease among mine employees, new and practical engineering controls which reduce the amount of respirable dust to which a mine employee is exposed to are urgently needed. This is even more important when it comes to suppressing the more toxic silica portion of the airborne dust in the mine atmosphere, since crystalline silica is a classified carcinogen. The wettability rates resulting from previous laboratory sink tests suggest the surfactant plays a vital role in the wettability of dust particulate. In addition, it was observed that dust with higher concentrations of silica was more easily wetted. The following field testing used a number of CPDM's and personal dust monitors to determine the dust concentrations experienced at locations near the face as well as locations further outby and inby active continuous mining operations. The measurements were taken during active cutting, with and without the surfactant addition. These measurements collected during the test will be subjected to a number of analyses to determine the total dust concentrations and the silica content. By examining the differences between the measurements, this study hopes to determine the effectiveness of the surfactant. The subsequent sections will describe in detail how the testing was conducted as well as the significance of the resulting measurements.

4.3.2 Experiment Location

The experiment was conducted in West Virginia, in an underground bituminous coal mine, utilizing room and pillar mining technique. Seam thickness at this mine is about nine feet. The mine had two supersections in operation. A split-type ventilation on each supersection was used with an exhausting fan. For this study, a single supersection with two continuous miner production units was monitored. The two continuous mining units alternated production and included three shuttle cars for haulage. Budgeted production was 300 ft of advance per shift using 40 ft deep cuts.

4.3.3 Equipment

For this testing, two pieces of equipment were used to gather the data. The first of which was Thermo Scientific PDM3600, which acted as the continuous personal dust monitor (CPDM). The CPDM is a respirable personal dust monitor designed for US-based mining applications and provides real-time measurements. Battery powered pumps draw a continuous sample, the respirable portion of which is collected and measured on an exchangeable filter. The PC-based software allows for the recorded data to be downloaded and reviewed. This piece of equipment can be seen in Figure 23.

Figure 23:CPDM with filter casing removed (J Colinet et al., 2010)

The second piece of equipment was the Zefon Escort ELF Personal air sampling pump, which will be referred to as the personal dust monitoring pump for the rest of this paper. This pump is also battery powered and designed for US-based mining applications. Dust samples can be collected with an attached Dorr-Oliver cyclone and filter. A depiction of the personal dust monitor can be found in Figure 24.

Figure 24: Personal dust sampler - Escort EFL pump with cyclone and filter (J Colinet et al., 2010)

4.3.4 Equipment Setup

In order to have each pump subjected to relatively consistent exposure, they were placed in a metal cage. The PDM3600 were placed in the center of the cage with the pump and battery pack placed on the inside. The inlet to the PDM3600 was clipped onto the front of the cage. Two personal dust monitoring pumps were attached to the side of the cage and had the Dorr-Oliver cyclones clipped onto the front of the cage. An example of the instrument setup can be seen in Figure 25.

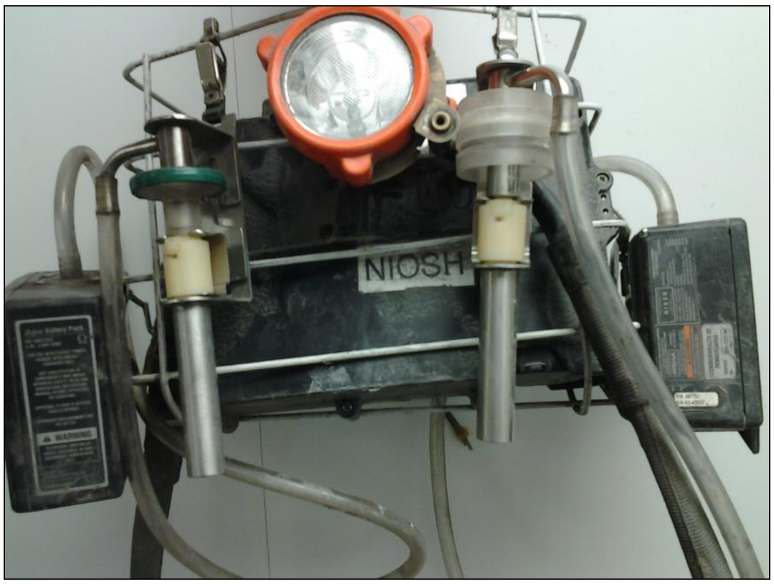

Figure 25: Example of equipment setup utilizing a CPDM and two personal dust samplers

In total, four of these cages were made. These pumps were hung from hooks at varying locations throughout the mine.

4.3.5 Equipment Location

Two of the sampling units were placed in the returns halfway back the last pillar after the last sealed crosscut. Figure 26 shows the locations of the sampling units in the returns represented by a red diamond. Data from these locations are referred to as left return (LR) and right return (RR).

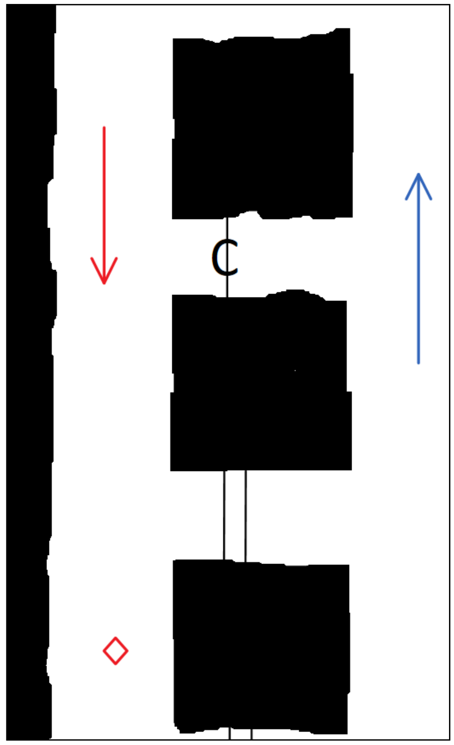

Figure 26: Location of sampling units in the returns

Two more of the sampling units were hung near the face, behind the line curtain. These sampling units gathered the respirable content immediately after being cut from the face. Data from these locations are referred to as left curtain (LC) and right curtain (RC). Figure 27, Figure 28 and Figure 29 show the locations of the pumps with varying continuous miner orientations.

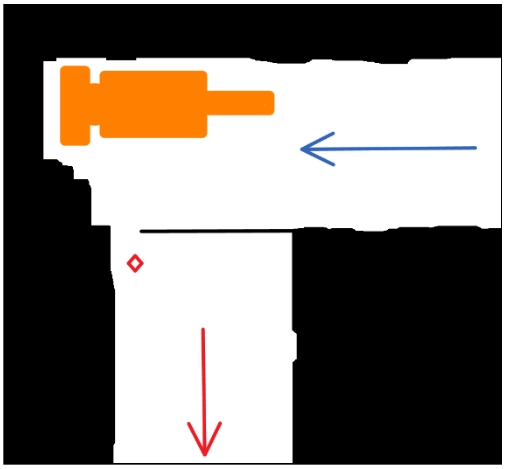

Figure 27: Location of sampling units placed behind the curtain - orientation 1

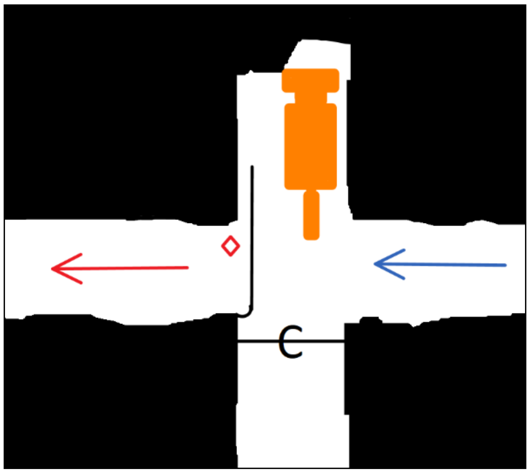

Figure 28: Location of sampling units placed behind the curtain - orientation 2

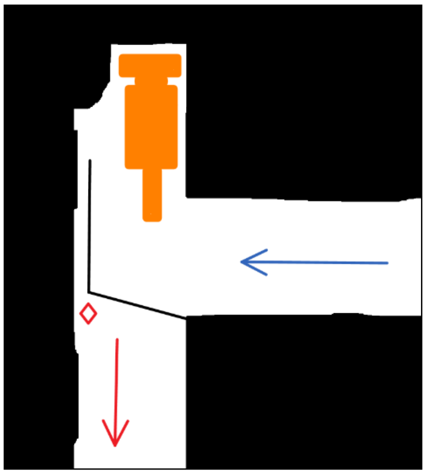

Figure 29: Location of sampling units placed behind the curtain - orientation 3

In addition, a fifth CPDM and cage sampling apparatus was constructed. This would have been used as a reserve if one of the other CPDM's failed. The reserve CPMD started at the same time as all of the others and was hung in the intake measuring incoming air as a secondary objective.

4.3.6 Experimental schedule

The experiment was run within a two week time period. The mine operated with three shifts. The first two, morning and evening shifts, were normally for production and the third, night shift, is for maintenance. Prior to the study beginning, pipes to the continuous miner were flushed with regular mine water. This was done since the mine was, at the time, using the surfactant in their water. The intent of running normal water before the study was to make sure the pipes were swept of any surfactant before the study began. The study began on Monday, July 14th, 2014 with the surfactant turned off. Sampling was conducted during the evening shift. Sampling with the surfactant turned off was repeated during the evening shift on the 15th. At the end of the second run, the surfactant was turned on, and the surfactant was allowed to flow through the system. This was done to ensure that the sampling conducted on the 16th was measuring a thoroughly mixed solution. Sampling was conducted on the evening shifts of the 16th and 17th with the surfactant turned on. After sampling on the 17th, the surfactant was turned off. This was done to make sure any surfactant in the pipe would be washed out by the beginning of the following week. The entire process was repeated the following week beginning on the 21st of July and ending on the 24th. Table 4 below shows the experimental schedule in detail with each week, the three shifts and dates. The red cells denotes when the surfactant was off, and blue denotes when the surfactant was on.

Table 4: Testing schedule

Week	Shift	Mon.	Tue.	Wed.	Thur.	Fri.	Sat.	Sun.
		7/14/2014	7/15/2014	7/16/2014	7/17/2014	7/18/2014	7/19/2014	7/20/2014
1	morning							
	evening	sampled	sampled	sampled	sampled			
	night							
		7/21/2014	7/22/2014	7/23/2014	7/24/2014	7/25/2014	7/26/2014	7/27/2014
2	morning							
	evening	sampled	sampled	sampled	sampled			
	night							

Due to changes in the availability of personnel and environmental conditions the procedure was altered. The new procedures only had one team for both continuous miners. This change may have led to less detailed observations during the cut because the researcher had to leave before the cut of the first continuous miner was finished. It was necessary, due to the need to remove the other sampling unit from behind the curtain, to allow for tramming of the second continuous miner as well as placement behind the line curtain at the new location of the second continuous miner. In addition, the total number of feet of advance had to be reduced due to the presence of poor roof conditions. The instability of the roof restricted the amount of advance per cut (normally 40 ft) to 10-20 ft per cut, depending on location. The increased frequency and less productive characteristics of the cuts increased the relative amount of time used for tramming of equipment. Since it became clear that 100 ft would not be achievable for each CM, for every shift, the target feet of linear advance was decreased to 60 ft. It is important to note that the initial plan was followed for the first shift, as it pertains to personnel. Due to the roof conditions the targeted 100 ft of advance was never attained.

4.3.7 Pre-test

A day prior to the testing the CPDMs were cleaned and programmed. The mass transducer and the grit pot were removed, and compressed air was used to clear the sample line and the grit pot. In addition, the surfaces were wiped down. While the mass transducers were disconnected, the filters were carefully replaced using the designated filter replacement tool. Then, the mass transducers were placed back into the CPDM units and secured. The software WinPDM v7.20, provided by Thermo Fisher Scientific, was used to program the PDMs to startup and stop times in accordance with shift's scheduled start and stop times. After the units had been programmed, they were charged overnight.

The Zefon gravimetric samplers were also broken down and cleaned. All of the components of the cyclone including the fittings and holding apparatus were washed with water and a detergent. Extra attention and care were taken not to scratch the cyclones surfaces. After washing, the components were allowed to dry overnight, and the pumps were charged.

Before testing began, the dried components for the Zefon gravimetric samplers were inspected and assembled. The CPDM units were be placed in the cages along with the two Zefon gravimetric samplers. When the CPDMs began to warm up, the cassettes containing the filters were be attached to the Zefon gravimetric samplers.

4.3.8 Test

Before the production shifts began, the flow data from the main water pump which fed the mine were gathered. In addition, the tote which contained the surfactant was examined, and the level marked with a date and time examined. After arrival to the mining section, the team would hang the cages and record the location during which the mining crew conducted the pre-shift checklist. In the pre-shift checklist the mining crew would measure the water pressure on the continuous miner. This data was relayed by the mine foreman and recorded. Prior to each cut, a water sample was taken from each CM's wash-down hose; in addition to the volumetric flow of air behind the curtain with an anemometer by the mine personnel. After the cages had been hung, the personal sampling pumps were turned on as the CM made its first cut, and time was recorded. After each cut was completed, the feet of advance were recorded in addition to the number of bits changed. Cuts were directly observed and any changes in the environment were recorded. The instability of the roof restricted the amount of advance per cut (normally 40 ft) to 10-20 ft per cut, depending on location. The increased frequency and less productive characteristics of the cuts increased the relative amount of time used for tramming of equipment. During each shift, a target of 60 ft of liner advance was for each CM was set. Recording continued until a total of approximately 60 ft of advance were logged from each CM. After the predetermined amount of material was mined, the Zefon gravimetric samplers were turned off and the time was recorded. The sampling units were then collected, and the flow was recorded at the main pump. Finally, the chemical level was inspected and marked along with date and time. Depending on the day, the surfactant pump may also be turned on or off.

4.3.9 Post-test

After exiting the mine, the CPDM and gravimetric samplers were removed from the cages. The cassettes were collected and recorded, and the data from the CPDM was extracted. Afterward, the pretest procedures were repeated for the following run.

4.4 RESULTS AND ANALYSIS

This section will detail and analyze the results including the surface tension measurements from water samples, the gravimetric measurements from the personal dust samplers, including the estimated silica content, and the gravimetric measurements from the CPDM units.

4.4.1 Water samples

The water samples that were collected before each cut were sent to be analyzed by NALCO. The surface tension of the water was analyzed in triplicate for each of the water samples taken. This was done to ensure the surfactant was consistent in lowering the surface tension of the spray water. A complete index of the measurements can be found in Appendix B, Table 41. The summarized results from week one and two are shown in **Error! Reference source not found.** and Figure 31.

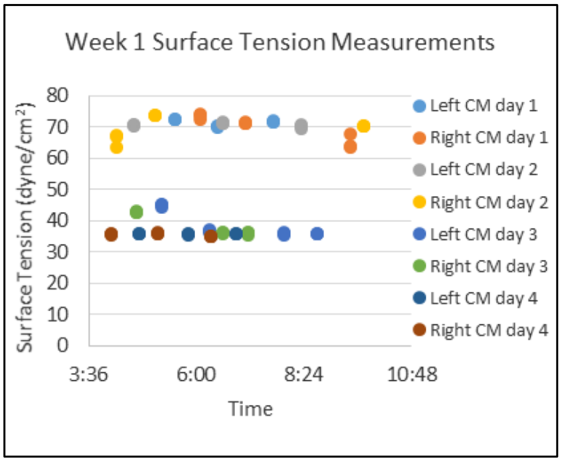

Figure 30: Summarized surface tensions measurement for week one

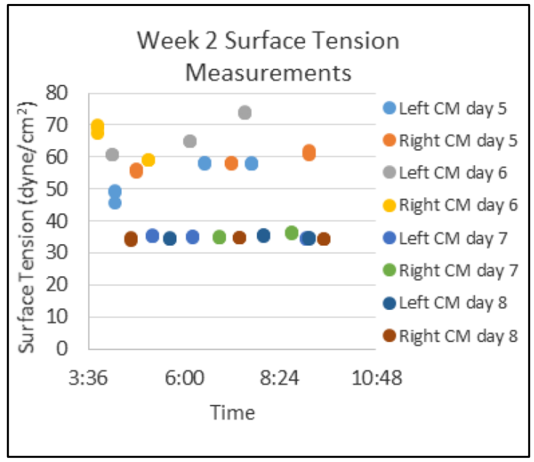

Figure 31: Summarized surface tensions measurement for week two

It can be seen from the plots in Figure 30 and Figure 31, that when the surfactant was added to the spray water, the surface tension was consistently reduced to approximately 36 N/m^2. The erratic nature seen in at the beginning of the second week, with the surface tension ranging from 46 to 74 N/m^2 may be due to a lack of flow running through the wash-down hose. If the wash down hose was not utilized enough between the first and second week of testing, then the insufficient flow through the hose may have led to some of the surfactant remaining in the hose at the beginning of the second week. The flow running through to the sprayer heads of the continuous miners were as assumed to be ample to clear out the surfactant from the week before.

4.4.2 Silica Analysis

After the field testing had been conducted, the sealed gravimetric samples were sent to NIOSH for silica analysis. The silica analysis conducted by NIOSH used an experimental non-destructive method. The results of the silica analysis at tabulated in Table 5.

.

Table 5: Resulting silica analysis from NIOSH

	Location	*Respirable dust (mg)*	*Sampling time (min)*	*Respirable dust concentration (mg/m^3)*	*Silica mass estimation (µg)*	*Silica concentration estimation (µg/m3)*	*% Silica estimation*
Day 1	LC	0.641	161	1.99	62.9	195	9.80%
	RC	0.767	179	2.14	70.6	197	9.20%
	LR	0.295	180	0.820	31.4	87.2	10.6%
	RR	0.381	184	1.04	39.0	106	10.2%
Day 2	LC	1.11	340	1.64	163	240	14.7%
	RC	1.32	301	2.19	256	425	19.4%
	LR	0.848	409	1.04	136	166	16.0%
	RR	0.217	52.0	2.09	39.1	376	18.0%
Day 3	LC	0.954	270	1.77	94.5	175	9.90%
	RC	0.755	221	1.71	84.1	190	11.1%
	LR	0.712	271	1.31	65.4	121	9.20%
	RR	0.260	227	0.570	29.9	65.9	11.5%
Day 4	LC	1.31	197	3.34	136	345	10.4%
	RC	0.937	175	2.68	88.5	253	9.40%
	LR	0.556	194	1.43	45.9	118	8.30%
	RR	0.206	180	0.570	44.8	124	21.7%
Day 5	LC	1.39	204	3.41	226	553	16.2%
	RC	1.31	165	3.97	149	452	11.4%
	LR	0.324	205	0.790	106	259	32.7%
	RR	0.390	165	1.18	45.7	139	11.7%
Day 6	LC	1.21	198	3.06	166	420	13.7%
	RC	0.419	161	1.30	31.8	98.6	7.60%
	LR	0.725	214	1.69	98.8	231	13.6%
	RR	0.213	157	0.68	9.7	30.7	4.50%
Day 7	LC	1.15	222	2.60	119	268	10.3%
	RC	1.49	198	3.77	140	352	9.4%
	LR	0.738	222	1.66	119	268	16.1%
	RR	0.239	193	0.62	20.5	53.1	8.6%
Day 8	LC	1.77	309	2.86	255	412	14.4%
	RC	1.18	228	2.58	118	259	10.0%
	LR	0.414	311	0.670	69.7	112	16.8%
	RR	0.416	230	0.900	51.2	111	12.3%

The limit of detection (LOD) of the nondestructive method is five micrograms. Using the silica mass of each sample and the total time that the samples were taken, the concentrations of each sample were calculated. When compared to the total dust concentration, a silica content could be derived. Multivariate regression was conducted to determine the variables which significantly affected the silica content. The analysis looked at the presence of the surfactant, which CM operator, left or right, and the location, behind the curtain or in the returns. None of the variables were deemed significant.

When comparing the average levels of silica, it could be seen that the silica percentage dropped about 2% when the surfactant was turned on. The drop in average levels of silica content can be seen below in Figure 32.

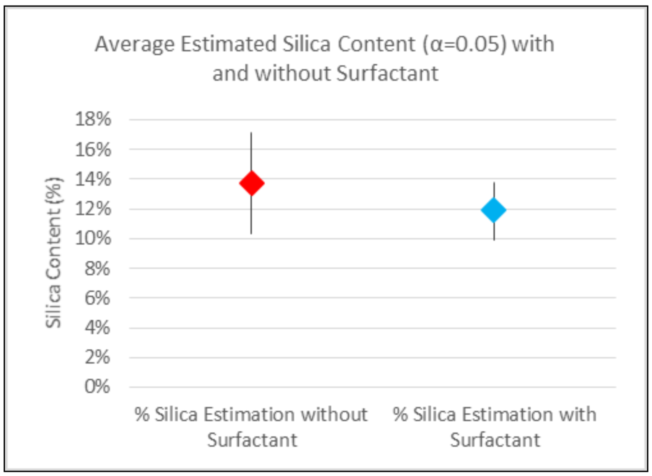

Figure 32: Comparison of silica content before and after the addition of surfactant

It can be seen in Figure 32 that the data also had a slightly more narrow distribution when the surfactant was turn on. Although a drop in silica content can be observed, it is not statistically significant.

Comparing the influence of sampling location in the airway showed an increase in the average silica content when moving from behind the curtain into the returns. The increase in average silica content can be seen in Figure 33.

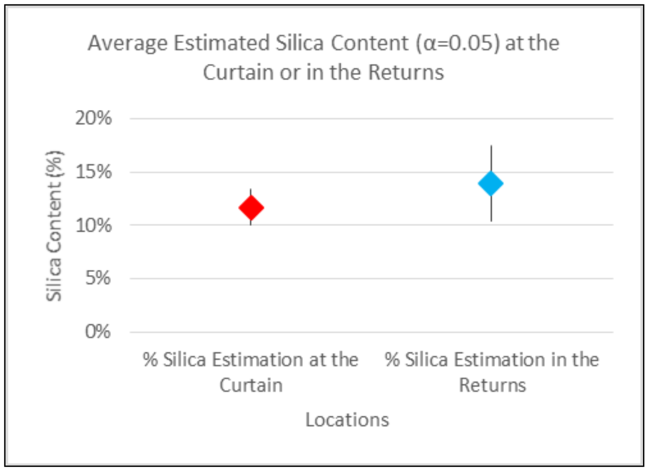

Figure 33: Comparison of silica content behind the curtain and in the returns

Figure 33 also depicts the wider distribution of data found in the returns. The actual cause of this increase may be due to the addition of silica from rock dust in the returns. Although the increase is noticeable, it was not found to be statistically significant.

The influence of the CM's operating conditions was also examined. During the study, a slightly larger amount of silica was produced on the left CM when compared to the right CM. The difference of 2% can be seen in Figure 34 below.

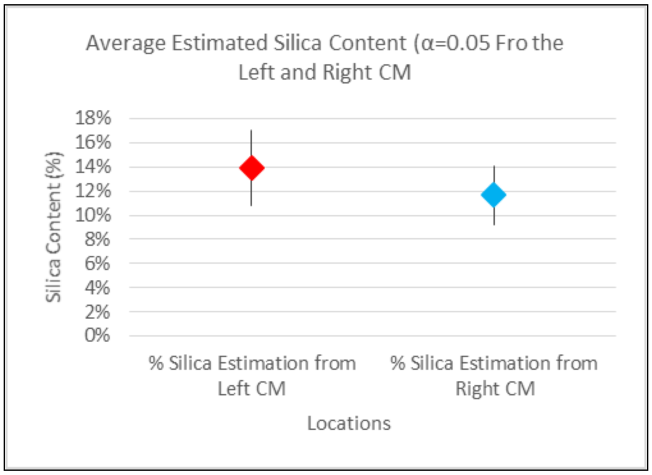

Figure 34: Comparison of silica content between the left and right CM operators

The slight increase in silica content shown in Figure 34 may be due to the geology. The left CM had a tendency to take slightly smaller cuts due to unfavorable geology. The smaller and more frequent spalling of the roof material may have led to this increase, even though it is not statistically significant.

4.4.3 Dust Concentration during Shift

After each day of testing the data saved on the CPDMs were extracted and exported to excel. Using the total dust that was measured on the filter every minute dust accumulation can be observed. A complete index of the total dust values collected from the CPDM's can be found in Appendix B. An example of the total dust plots collected for a CM, and sampled at both the returns and curtain locations, can be seen below in Figure 35.

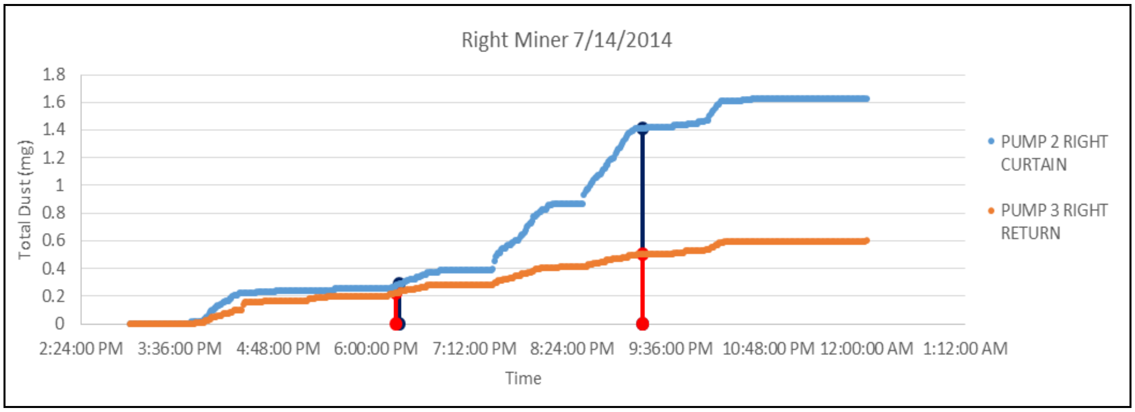

Figure 35: Example of a typical total dust plot collected from a continuous miner

In order to extract the average concentrations during testing, the start and stop time of the CM ripper motors were used. The total dust for the entire test was found using the total dust levels at each start and stop time. The sampling rates of 2.2 l/min and the total time of sampling allows the one to calculate the average concentrations. After the field testing was completed, the sealed gravimetric samples from the PDS were sent to NIOSH for analysis. The sampling rate for the PDS pumps was 2.0 l/min. The resulting dust concentrations from the two devices are shown below in Table 6.

Table 6: Resulting dust concentration from PDS and CPDM

		PDS			CPDM		
	Location	*Respirable dust (mg)*	*Sampling time (min)*	*Respirable dust concentration (mg/m³)*	*Respirable dust (mg)*	*Sampling time (min)*	*Respirable dust concentration (mg/m³)*
Day 1	LC	0.641	161	1.99	0.62	161	1.75
	RC	0.767	179	2.14	1.12	179	2.84
	LR	0.295	180	0.82	0.32	180	0.81
	RR	0.381	184	1.04	0.28	184	0.69
Day 2	LC	1.112	340	1.64	1.79	340	2.39
	RC	1.317	301	2.19	2.38	301	3.59
	LR	0.848	409	1.04	1.74	409	1.93
	RR	0.217	52	2.09	0.3	51	2.67
Day 3	LC	0.954	270	1.77	2.35	270	3.96
	RC	0.755	221	1.71	1.3	221	2.67
	LR	0.712	271	1.31	0.86	271	1.44
	RR	0.26	227	0.57	0.4	227	0.80
Day 4	LC	1.314	197	3.34	2.06	197	4.75
	RC	0.937	175	2.68	1.2	175	3.12

	LR	0.556	194	1.43	0.91	194	2.13
	RR	0.206	180	0.57	0.33	180	0.83
Day 5	LC	1.39	204	3.41	2.18	204	4.86
	RC	1.309	165	3.97	2.61	165	7.19
	LR	0.324	205	0.79	1.36	205	3.02
	RR	0.39	165	1.18	0.72	165	1.98
Day 6	LC	1.211	198	3.06	1.84	198	4.22
	RC	0.419	161	1.3	0.69	161	1.95
	LR	0.725	214	1.69	0.99	214	2.10
	RR	0.213	157	0.68	0.31	157	0.90
Day 7	LC	1.154	222	2.6	2.52	222	5.16
	RC	1.491	198	3.77	2.94	198	6.75
	LR	0.738	222	1.66	1.14	222	2.33
	RR	0.239	193	0.62	0.45	193	1.06
Day 8	LC	1.768	309	2.86	2.5	309	3.68
	RC	1.178	228	2.58	1.92	228	3.83
	LR	0.414	311	0.67	0.68	311	0.99
	RR	0.416	230	0.9	1.07	230	2.11

With the pre and post test weights, the total dust was determined for each sample. Using the net gains of each sample and the total time that the samples were taken, the concentrations of each sample were calculated. Multivariate regression was conducted to determine the variables which significantly affected the dust concentration. The analysis examined the impacts of the measuring device themselves, the location in the airway, the CM operator, and the addition of surfactant. The variables which were found to have a significant impact were the sample location in the airway and the measuring devices.

4.4.3.1 PDS vs. CPDM

When examining the influence of the two devices, the average level of dust concentration was higher for the CPDM when compared to the PDS. The difference between the two devices can be seen in Figure 36 below.

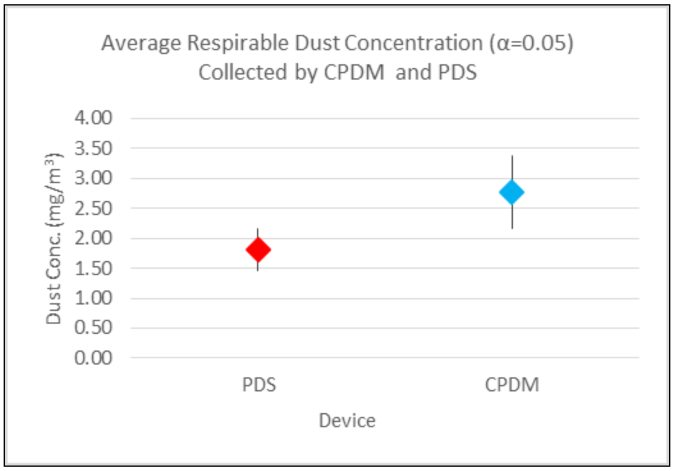

Figure 36: Comparison of dust concentration between PDS and CPDM

The very notable increase of measured dust concentration from the CPDM amounted to just under 1 mg/m^3 and was found to be statistically significant. The cause of this increase is unknown since both devices were left to measure the same environment. The different flow rates for the devices, 2.0 l/min for the PDS and 2.2 l/min for CPD, were taken into account.

In some cases, the individual dust concentrations for a shift significantly higher than regulatory limits, but these are not compliance samples and only concentration during mining is calculated rather than an 8-hour time-weighted average.

4.4.3.2 Left vs. Right CM

Additionally, the study examined the impact of the CM operator on the respirable dust level. The results are shown in Figure 37 below.

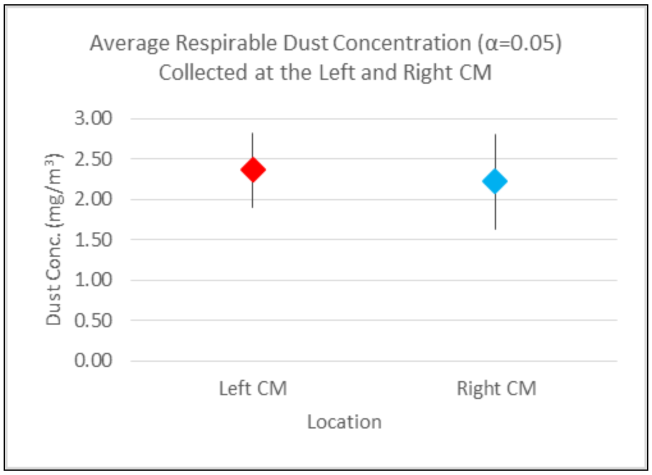

Figure 37: Comparison of dust concentrations between the left and right CM

Figure 37 does not show any notable difference between the two CM operators, and no statistical significance was found.

4.4.3.3 Curtain vs. Returns

When discerning between the sampling locations in the air way, a very noticeable difference was seen. The resulting comparison of dust concentration levels at the curtain and in the returns are shown in Figure 38.

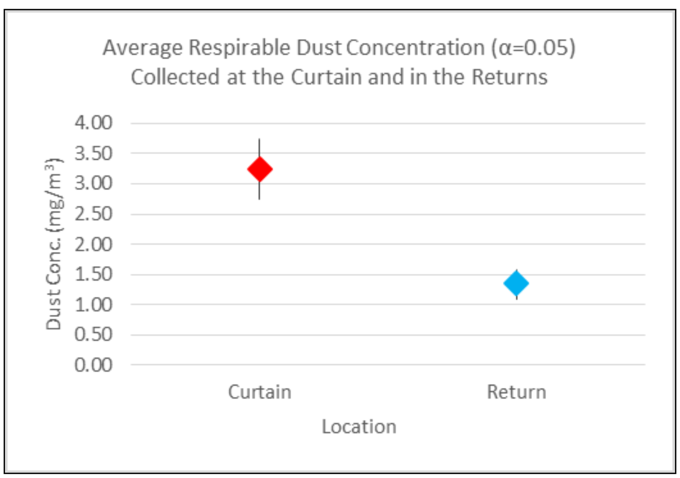

Figure 38: Comparison of dust concentrations at the curtain and in the returns

Figure 38 shows more than a 50% reduction of the dust concentration when moving into the returns. The difference of 1.9 mg/m^3 was found to be statistically significant. The drop in concentration is most likely due to the settling of the respirable content by agglomerations.

4.4.3.4 Surfactant

Lastly, the average dust concentrations were compared for when the surfactant was off and on. The results are shown in Figure 39.

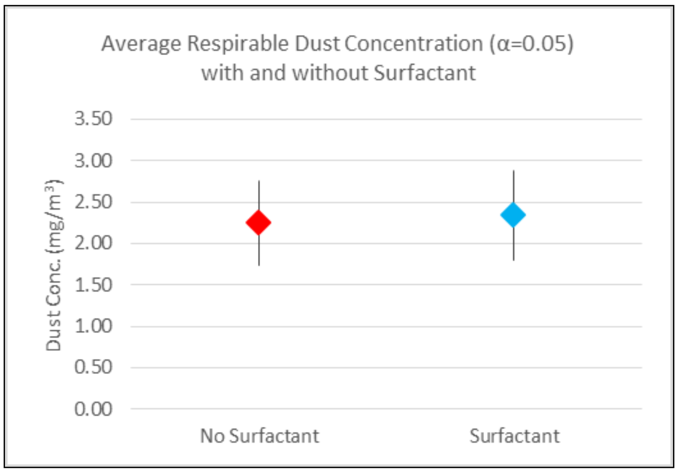

Figure 39: Comparison of dust concentrations with and without surfactant

In Figure 39, no significant differences in the respirable dust were seen with the addition of surfactant.

4.4.4 Dust Concentration during Cut

In addition to the average concentration during testing, the cut by cut concentrations could be found from the CPDM data. Using the known start and stop times of each cut, and the total dust, the dust concentration for each cut could be found. The results of the dust concentrations collected cut by cut are shown in Table 7.

Table 7: Tabulation of cut by cut dust concentrations

Cut depth (ft.)	Starting depth (ft.)	Surfactant	Left/right CM	Curtain/ return	Number of bits changed (#)	Air flow (CFM)	Dust conc. for cut (mg/m^3)
20	20	w/o	L	L	12	14,904	2.88
20	20	w/o	L	R	12	14,904	0.44
20	28	w/o	R	L	11	12,690	1.60
20	28	w/o	R	R	11	12,690	1.07
20	32	w/o	L	L	10	10,458	3.23
20	32	w/o	L	R	10	10,458	0.31
20	10	w/o	R	L	10	11,088	3.63
20	10	w/o	R	R	10	11,088	1.02
20	40	w/o	L	L	10	9,261	4.51
20	40	w/o	L	R	10	9,261	0.28
25	0	w/o	R	L	9	11,016	5.29
25	0	w/o	R	R	9	11,016	0.85
20	0	w/o	L	L	12	11,795	5.04
20	0	w/o	L	R	12	11,795	1.89
25	0	w/o	R	L	19	12,587	8.77
25	0	w/o	L	R	10	13,680	8.44
25	0	w/o	L	L	10	13,680	6.76
25	33	w/o	R	R	0	11,875	2.25
25	33	w/o	R	L	0	11,875	1.07
15	0	w/o	R	R	18	12,300	8.56
15	0	w/o	R	L	18	12,300	2.76
15	20	w/o	L	R	12	9,980	1.50
15	20	w/o	L	L	12	9,980	5.90
20	20	w/	R	R	15	9,643	2.72
20	20	w/	R	L	15	9,643	0.61
20	0	w/	R	R	23	12,690	5.67
20	0	w/	R	L	23	12,690	1.40
25	55	w/	R	R	14	13,797	4.82
25	55	w/	R	L	14	13,797	2.63
25	0	w/	L	R	21	14,960	13.63
25	0	w/	L	L	21	14,960	5.62
20	46	w/	R	R	11	10,260	4.03
20	46	w/	R	R	11	10,260	1.62
20	25	w/	L	L	13	9,010	3.52
20	25	w/	L	R	13	9,010	1.41
30	54	w/	R	L	10	9,324	7.19
30	54	w/	R	R	10	9,324	0.14
10	25	w/	L	L	0	11,178	4.89
10	25	w/	L	R	0	11,178	1.92
20	0	w/o	L	L	24	18,080	10.24
20	0	w/o	L	R	24	18,080	7.14
15	20	w/o	R	L	11	9,207	5.82
15	20	w/o	R	R	11	9,207	4.33
20	30	w/o	L	L	4	11,560	3.82
20	30	w/o	L	R	4	11,560	1.61
15	50	w/o	R	L	6	10,044	6.64
15	50	w/o	R	R	6	10,044	0.69
15	20	w/o	L	L	9	11,760	1.60
15	20	w/o	L	R	9	11,760	7.26
30	20	w/o	R	L	12	9,820	7.88
30	20	w/o	R	R	12	9,820	2.85
10	0	w/o	L	L	9	15,066	6.72
10	0	w/o	L	R	9	15,066	1.71
30	65	w/o	R	L	20	12,690	3.18
30	65	w/o	R	R	20	12,690	1.66
35	0	w/o	L	L	18	14,784	13.14

Cut depth (ft.)	Starting depth (ft.)	Surfactant	Left/right CM	Curtain/ return	Number of bits changed (#)	Air flow (CFM)	Dust conc. for cut (mg/m^3)
20	20	w/o	L	L	12	14,904	2.88
35	0	w/o	L	R	18	14,784	4.70
30	87	w/o	R	L	7	11,088	2.29
30	87	w/o	R	R	7	11,088	1.31
15	36	w/o	L	L	0	15,620	10.38
15	36	w/o	L	R	0	15,620	2.09
30	0	w/	R	L	6	17,388	7.21
30	0	w/	R	R	6	17,388	1.64
30	0	w/	L	L	19	15,302	9.35
30	0	w/	L	R	19	15,302	1.90
10	0	w/	L	L	6	16,855	21.38
10	0	w/	L	R	6	16,855	6.39
35	0	w/	R	L	10	12,852	10.14
35	0	w/	R	R	10	12,852	0.56
35	0	w/	R	L	17	10,792	5.47
35	0	w/	R	R	17	10,792	3.39
10	30	w/	L	L	5	13,008	4.71
10	30	w/	L	R	5	13,008	1.58
20	37	w/	L	L	25	14,769	11.97
20	37	w/	L	R	25	14,769	1.97
10	0	w/	L	L	8	12,600	7.19
10	0	w/	L	R	8	12,600	3.16
25	20	w/	R	L	7	16,870	9.03
25	20	w/	R	R	7	16,870	3.86
10	40	w/	L	L	9	11,576	3.10
10	40	w/	L	R	9	11,576	1.19
10	47	w/	L	L	8	10,240	3.86
10	47	w/	L	R	8	10,240	1.94

During the testing, unfavorable roof conditions restricted the CM operators from taking normal deep cuts of 40 ft. In a few cases, roof falls were experienced. A number or variables were recorded for each cut and examined to determine their significance. The first and most obvious variables were the locations of the monitors: ventilation curtain versus in the returns. The results are shown in Figure 40.

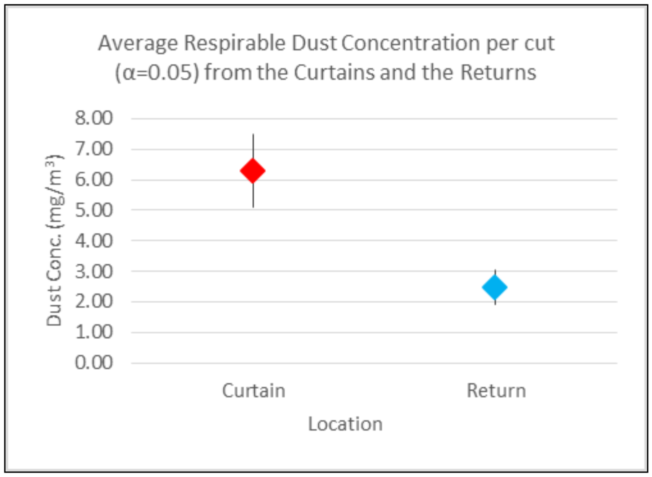

Figure 40: Comparison of dust concentrations between the curtain and the return locations on a cut by cut basis

As expected, Figure 40 shows a significant drop in the concentration when moving into the returns. As seen before in the comparison of the average shift concentrations, the drop is most likely due to the settling of the respirable dust as agglomerations. Next, the difference between the left and right CM was examined and plotted in Figure 41.

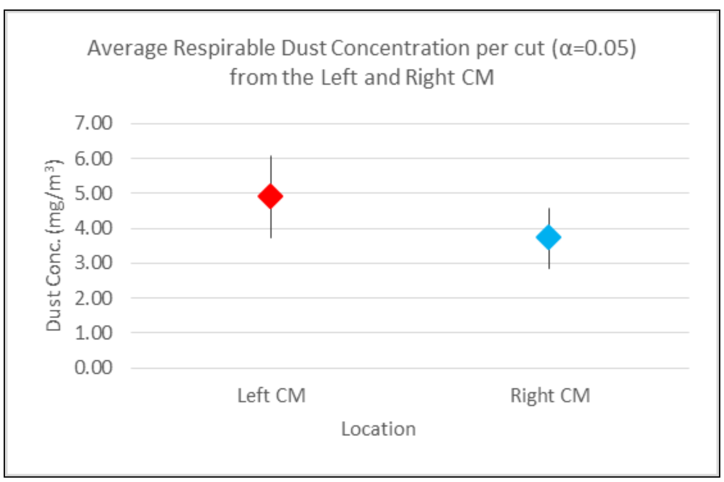

Figure 41: Comparison of dust concentration between the left and right CM on a cut by cut basis

The analysis found no significant impact due to the CM locations, although a slightly higher dust concentration is seen from the left CM. This slight difference may have been a result of the atypical cutting schedule caused by the unfavorable roof conditions. The lack of productivity on the left caused the right CM to move further away from the right returns in some cases. This atypical cut schedule and the inability to keep the measurement apparatuses at a constant distance from the active face may be the cause of some of the variability seen in the data. Next, the influence of the surfactants on the levels of dust concentration on a percent basis were examined. The resulting average dust concentrations are shown in Figure 42.

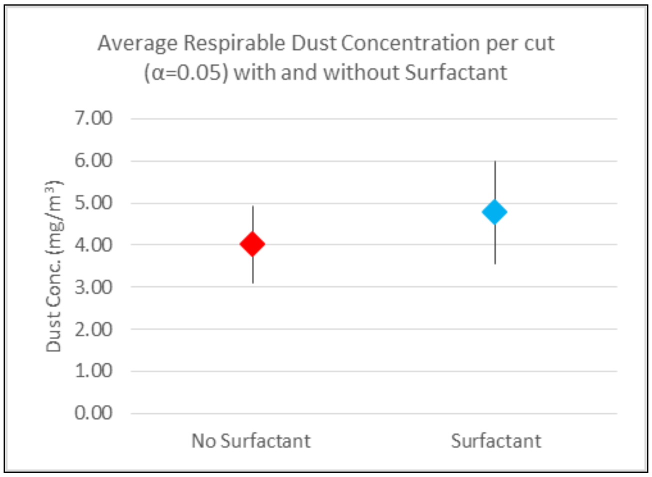

Figure 42: Comparison of dust concentration with and without surfactant on a cut by cut basis

A slight increase in the average dust concentration can be seen when the surfactant was added, but this difference was found to be insignificant. In addition, other variables that could impact dustiness were examined. The first of these variables were the number of bits changes after the cut. Figure 43 below shows a plot of the average dust concentration versus the number of bits changed in three groups. The groups chosen for the study were 0-9, 10-19, and 20+ bits changed.

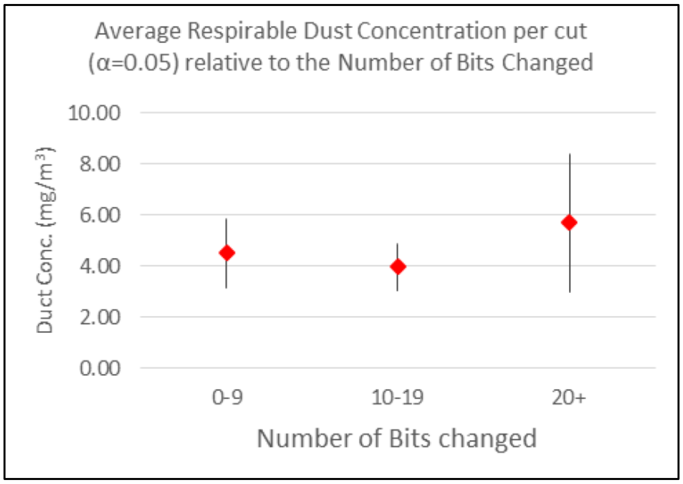

Figure 43: Average dust concentration per cut relative to the number of bits changed

The resulting analysis yielded no significant difference in the dust concentration of a cut when examining the number of bits changed. Some number of bits may be a bit subjective to the continuous miner operator in some cases, while in other cases productivity was suffering and the time was not taken to examine or change the bits. Next, the volumetric air flow behind the curtain was examined. Figure 44 below is a plot depicting the average dust concentration versus the groups of volumetric airflow behind the curtain.

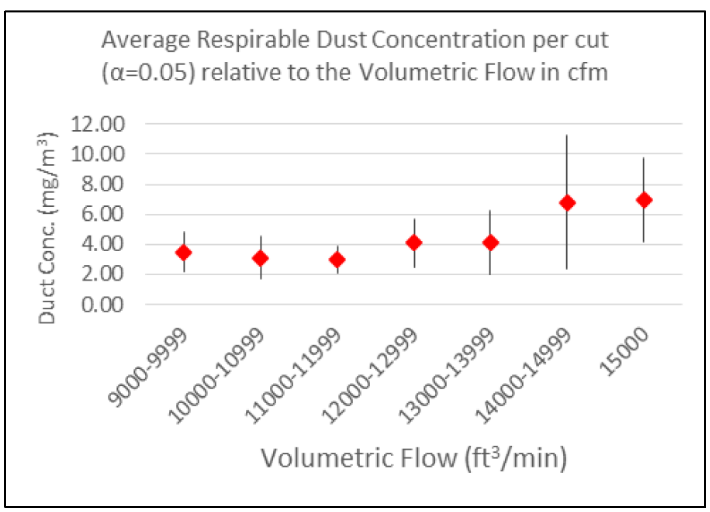

Figure 44: Average dust concentration per cut relative to the volumetric flow in cfm

The results show that there was a significant difference in the observed dust concentrations correlating with changes in the volumetric airflow behind the curtain. The general trend shows that an increase in the volumetric flow behind lead to higher dust concentrations behind the curtain. The differences were statistically significant which shows the effectiveness of ventilation as a primary engineering control which, when used correctly, can limit the miners exposure by sweeping more dust away from their location at the face. Lastly, an analysis was conducted with regards to the starting cut depth. The starting cut depth describes how many feet of coal were previously cut relative to the beginning of the pillar. The starting cut depth data was split into five groups; ≤10 ft, 11-20 ft., 21-30 ft., 31-40 ft. and greater than 40 ft. The analysis shows that the differences between the dust concentrations of the different groups are significant, but the only group which stood out was the starting depth of less than or equal to 10 ft. This can be seen in Figure 45.

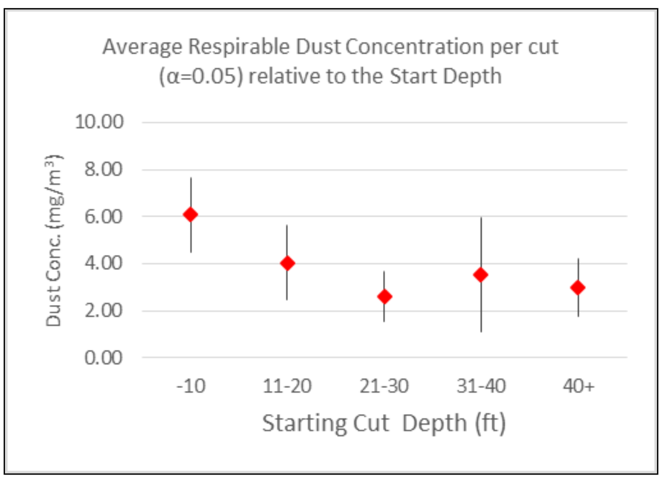

Figure 45: Dust concentration per cut against the starting cut depth

In an effort to understand the possible cause of the significant difference, total dust plots were inspected. The primary difference noted was the use of scrubbers.

4.4.5 Influence of Scrubbers

4.4.5.1 Scrubbers

While examining the total dust, discernable spikes were noticed. A correlation was evident between the large spikes and the starting cut depth. When the starting cut depth was flush with the pillars, the dust concentrations were much higher. According to the dust control plan of the mine, the scrubbers were only to be activated after the CM had reached a cutting depth of 20 ft. An example of the spike in total dust can be seen in Figure 46 below.

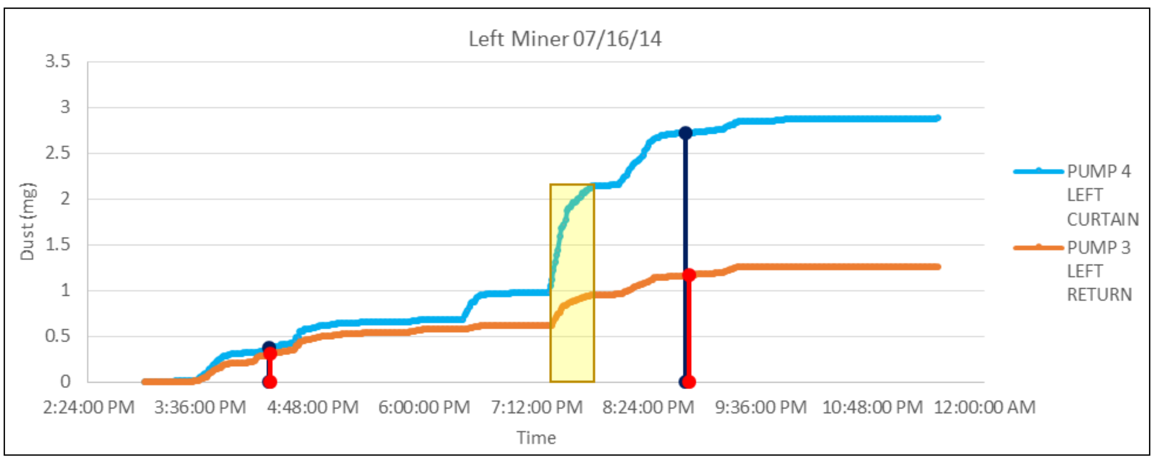

Figure 46: Example of a typical total dust plot collected from a continuous miner including a highlighted spike

Due to the irregularity of the spikes from test to test, it was decided that each of the spikes would be isolated, and their characteristics examined. The criteria for determining whether the cut was identified as "scrubber off" were as followed. The cut had to start below 20 ft or flush with the pillars, and the ending depth could not be more than 20 ft. Cuts which were identified as "scrubber on" cuts had an initial starting depth greater than 20 ft. This ensured that the scrubbers would always be on, as detailed in the mine ventilation plan. In some cases, the starting depth was at 10 or 15 ft, and then 20 ft of advance would be made. In this case, the scrubber would be off at the beginning and on at the end. These "hybrid cuts" were not included in the analysis. This is clarified with the examples below in Figure 47, Figure 48 and Figure 49.

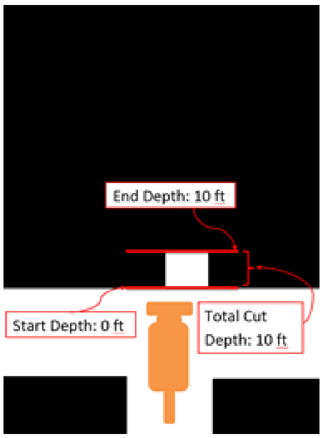

Figure 47. Environmental setup of when scrubber was off during the cut.

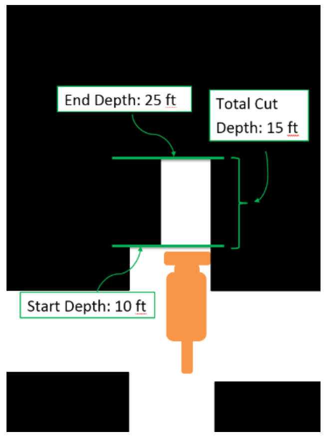

Figure 48. Environmental setup of when scrubber was both on and off during cut.

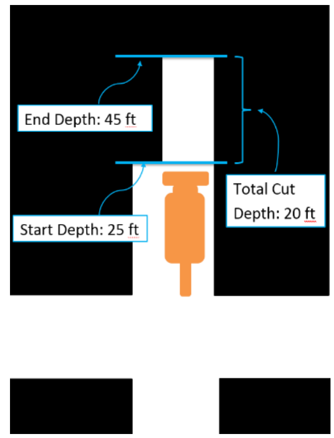

Figure 49. Environmental setup of when scrubber was on during cut.

The following figures show the isolated cuts as total dust plots. In addition, the series of figures are split into the subgroups with and without the surfactant addition. Figure 50 shows the isolated cuts with the surfactant off and scrubbers off. Figure 51 shows the cuts with the surfactant on and scrubbers off. Figure 52 show the cuts with the surfactant off and scrubbers on. Lastly, Figure 53 shows the cuts with surfactant added and the scrubbers on.

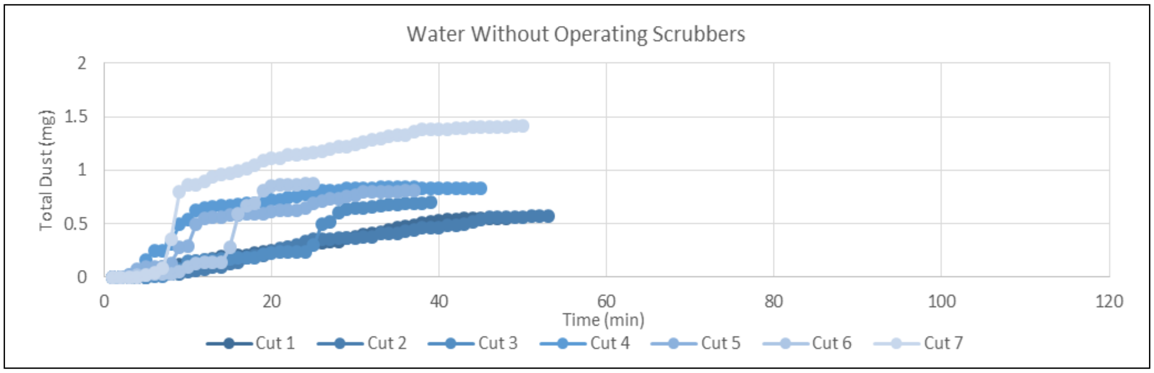

Figure 50: Collection of isolated cuts which used no surfactant and no operating scrubber

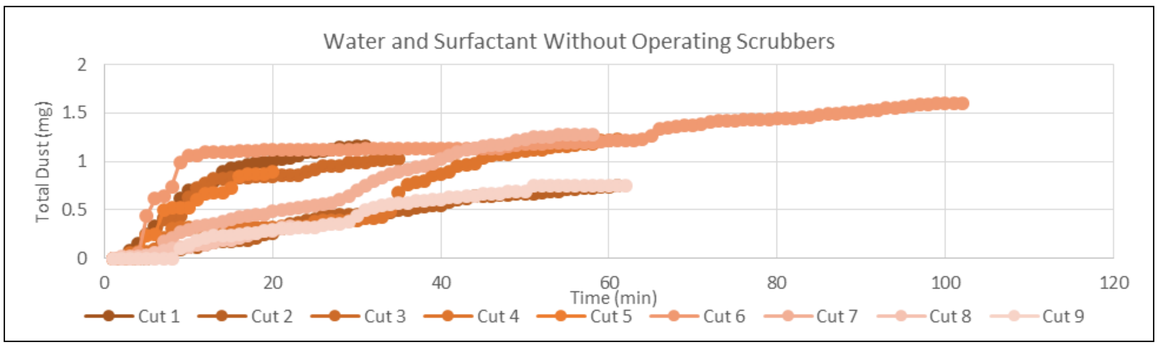

Figure 51: Collection of isolated cuts which used surfactant but no operated scrubber

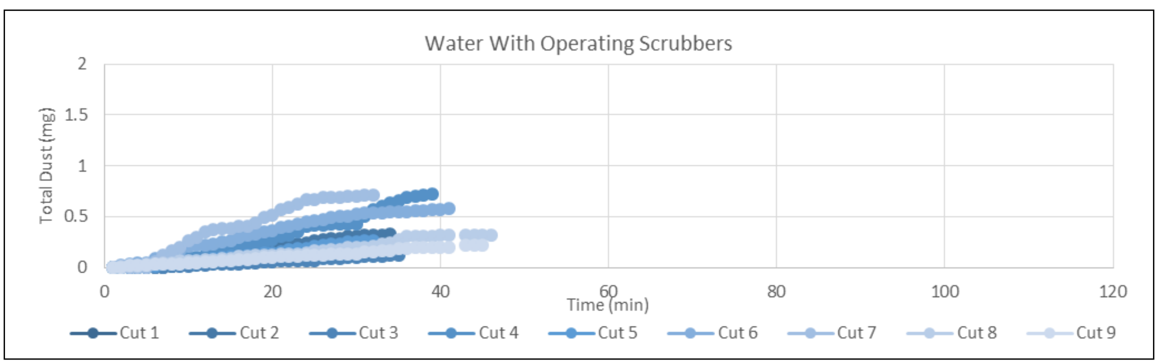

Figure 52: Collection of isolated cuts which used no surfactant but operated scrubber

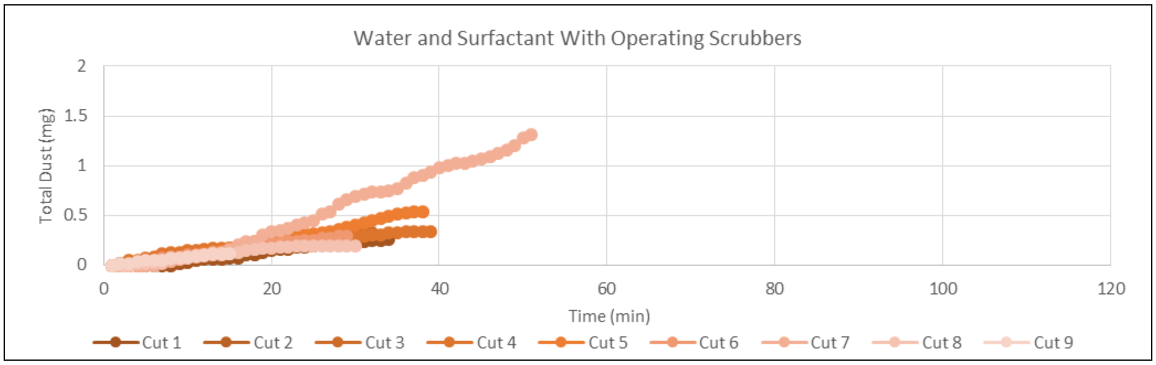

Figure 53: Collection of isolated cuts which used the surfactant and operated scrubber

From the series of figures (Figure 50, Figure 51, Figure 52 and Figure 53) it can be seen that the plots depicting the lack of scrubber activation are much more varied and have a step-like feature.

From these cuts, specific cuts were examined which had similarly recorded characteristics. The recorded characteristics used to determine the specific cuts were the number of new bits after the cut, cut depth, and starting depth. The cuts have been stacked to avoid clutter at the origin. The cuts are also stacked chronologically, with the first cut starting at the origin. The second cut starts at the same time and total dust level as the end of the first cut. The same procedure was followed for the third cut. The basic statistics for the cuts characteristics are shown in Table 8 below, followed by the cuts plotted in Figure 54.

Table 8: Statistics of cut characteristics with inactive scrubbers

	Water w/o scrubbers			Water and surfactant w/o scrubbers		
	Total	$\bar{X}$	σ	Total	$\bar{X}$	σ
New bits	54	18	6	53	18	8
Cut depth (ft)	55	18	3	65	22	3
Starting depth (ft)	0	0	-	0	0	-

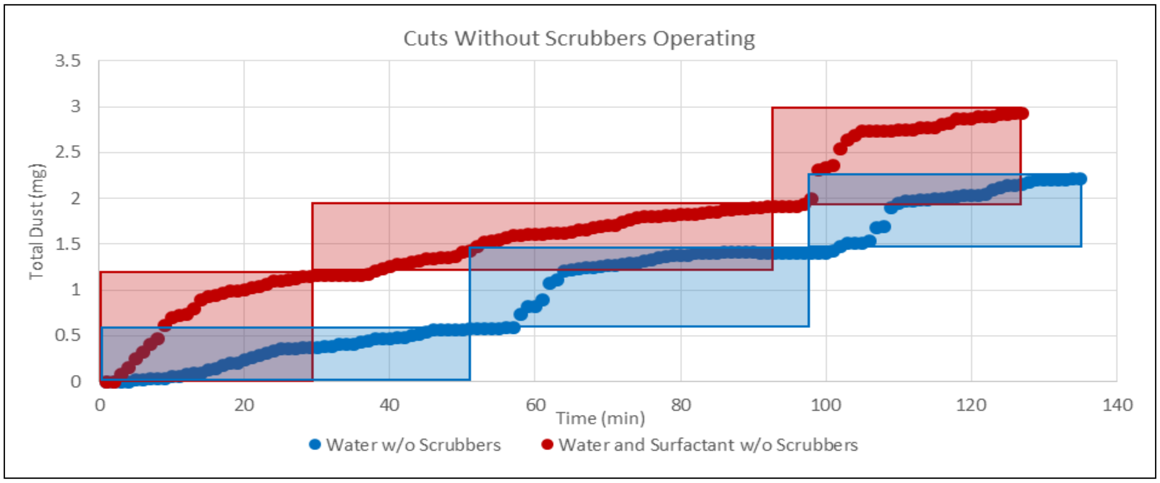

Figure 54: Depiction of selected isolated cuts which did not implement scrubbers

In Figure 54 it can be seen that the cuts are quite variable again, and the step form is evident. The same process was carried out on cuts with the scrubbers activated. Table 8 shows the statistics of the characteristics, and Figure 55 shows the cuts stacked chronologically.

Table 9: Statistics of cut characteristics with active scrubbers

	water w/ scrubbers			water and surfactant w/ scrubbers		
	Total	$\bar{X}$	σ	Total	$\bar{X}$	σ
New bits	31	10	1	38	13	2
Cut depth (ft)	60	20	0	65	22	3
Starting depth (ft)	-	33	6	-	42	15

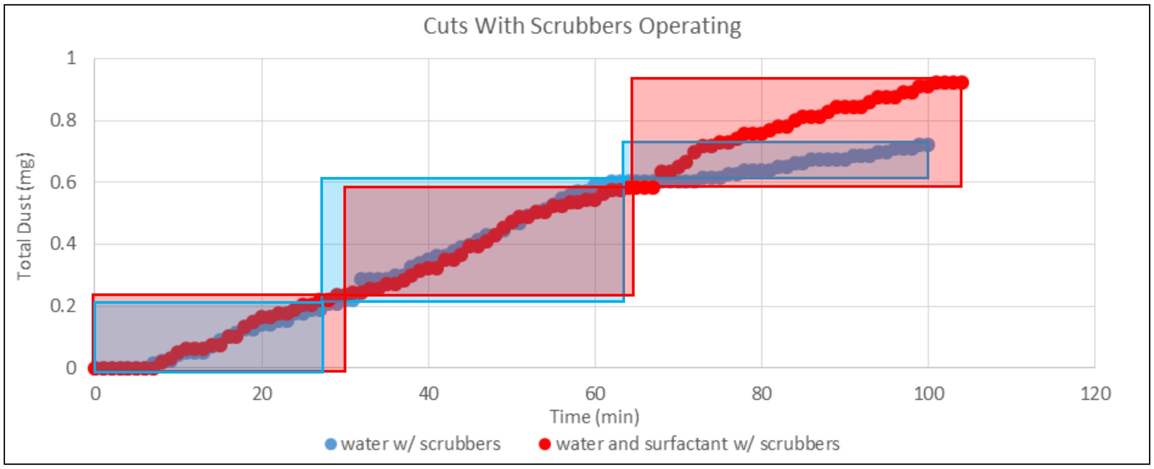

Figure 55: Depiction of selected isolated cuts which implemented scrubbers

In Figure 55 above it can be seen that the cuts have more consistent dust production. To compare the cuts with and without the scrubber turned on Figure 54 and Figure 55 were combined. This combination is shown in Figure 56 below.

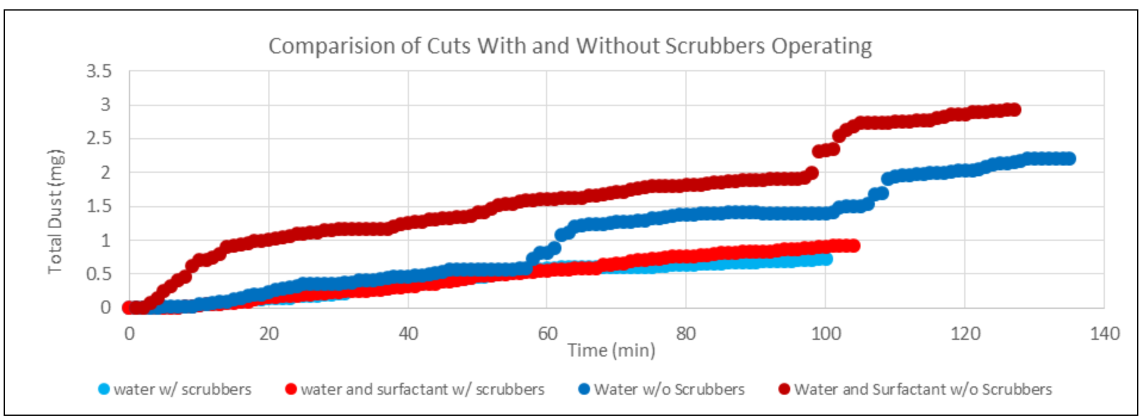

Figure 56: Plot comparing the total dust from selected isolated cuts with and without scrubbers operating

In Figure 56 it can be seen that the total dust production is approximately twice as much when the scrubbers are not on. It can also be seen that this increased production is due primarily to the step form seen in the plots. The total respirable dust during each cut was plotted. The significant drop in total dust can be seen in Figure 57.

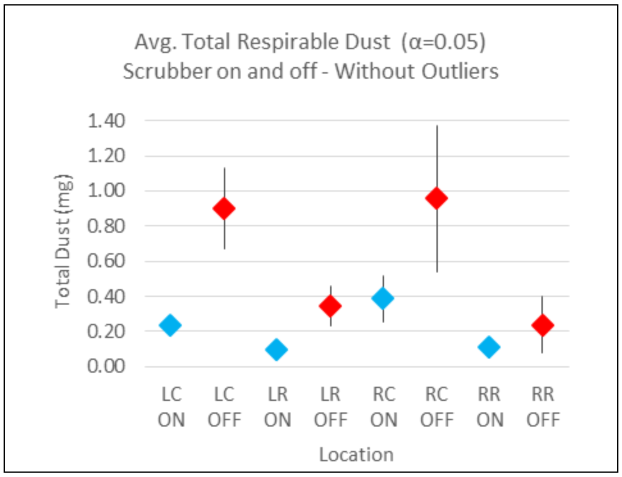

Figure 57: Plot of average total respirable dust from isolated cuts with and without operating scrubber

In Figure 57 a very clear and consistent lowering of the average total dust can be seen when the scrubbers are activated.

4.5 Discussion

The data gathered during the field test which was presented in Figure 34 and Figure 35 demonstrates the effectiveness of the surfactant in successfully and consistently lowering the surface tension of the mine spray water. There was a perceived issue of the surfactant being left in the washed down hose water after the first week of testing. Since the hose was not in significant use and the hose not being left to run for a sufficient amount of time, the surface tension was not able to return to its normal level of about 72 N/m^2 at the beginning of the second week. Regardless of the still substantial difference in the surface tension, no significant difference in the dust concentration was observed with the monitoring instrumentation.

A significant difference was observed, however, between the two pieces of instrumentation, the CPDM, and the PDS. The CPDM measured a higher concentration when compared to the PDS. Although this may be an important distinction for the required implementation the CPDM, it has no important impacts with regards to the aims of the study via relative dust levels. Additional work, however, should be done to confirm the deviation between the two devices. This does have much larger implication with regards to enforcement of the new dust standards, but was not explored with vigor in this study.

Additionally, a significant difference was observed between the testing locations, in the returns and directly behind the curtain. This difference was revealed in the analysis shown in Figure 38. This would be expected, since given enough time, some amount of the dust will fall to a lower position in the entry or settle out completely by agglomerating together and acting as a large sized particle. Additionally, the respirable particle could be attached to the larger particle and then fall out of suspension.

Some additional factors examined were the number of bits changed and the quantity of air flow. The number of bits changed was initially thought to be an influencing factor, but the resulting data collection and analysis showed otherwise. Airflow, however, was a considerable factor. The data showed that the higher volumetric flows were sweeping larger amounts of dust from the working face. This reinforces the use of ventilation as a primary engineering control for diluting and transporting dust out of the immediate mine atmosphere.

The changing distances from the face and other environmental conditions lead to an almost impossible comparison of data (need multiple samples with the same start and stop depths as well as air velocities). Ideally, a study on the order of months is required to look at these parameters in depth.

However, the nature of mining assures us that more variables, particularly geologic, would likely be introduced.

Although not initially taken into account, the pronounced effect of scrubbers on concentrations was clearly observed. An argument for the continuous use of the scrubbers could be made, but not without first studying the effects of dust concentration around the CM operator, as well as potential methane concentrations. To get a complete picture of the effectiveness of the scrubber, additional work should be done which places a dust measuring a device by the CM operator. In the past, there were concerns that the scrubbers would cause recirculation at the face resulting in a pocket of methane developing (Kissell & Bielicki, 1975). Past studies have shown that the recirculation of methane at the face will occur when the scrubber is moving more air than the ventilation (Divers et al., 1981). No deterioration of ventilation performances was observed in one study, but these were at curtain setbacks of 25 ft or more with a blowing system (Halfinger, 1984). Recently, a study in three mines using exhausting ventilation found that there was an improvement in the respirable content of dust outby the CM, but not by the CM operator for cuts within 20 ft of the face. Interestingly, there was also no significant difference in the dust level at the CM operator location when the scrubber was off or on (Colinet et al., 2013). A strong case could be made to investigate the role of scrubbers further with conditions that elevate concerns of methane buildup and negative alterations to the vent controls.   In addition, this preliminary study indicates that dust exposure may be high for operators when starting a new cut and that studying the use of specialized engineering controls for this scenario could prove meaningful in reducing exposure.

Through all of the analysis, no significant impact from the surfactant was observed due to many significant variables. However, the high degree of variation from cut to cut and a limited number of samples does not allow for meaningful conclusions to be drawn with regards to the ultimate effectiveness.

REFERENCE

Blackley, D. J., Halldin, C. N., & Laney, A. S. (2014). Resurgence of a debilitating and entirely preventable respiratory disease among working coal miners. American journal of respiratory and critical care medicine, 190(6), 708-709.

Colinet, J. F., Reed, W., & Potts, J. D. (2013). Impact on Respirable Dust Levels When Operating a Flooded-bed Scrubber in 20-foot Cuts. Niosh RI 9693.

Colinet, J., Listak, J. M., Organiscak, J. A., Rider, J. P., & Wolfe, A. L. (2010). Best practices for dust control in coal mining. Department of Health and Human Services, Centers for Disease Control and Prevention, National Institute for Occupational Safety and Health, Office of Mine Safety and Health Research.

Copeland, C. R. (2007). Suppression and dispersion of airborne dust and nanoparticulates (Doctoral dissertation, Michigan Technological University).

Divers, E. F., LaScola, J. C., & Hundman, G. J. (1981). New twin scrubber installation for continuous mining machines.

Halfinger, G. (1984). Feasibility of a machine-mounted scrubber system for ventilating coal-mine working faces. Open File report (No. PB-85-185742/XAB). Ingersoll-Rand Research, Inc., Princeton, NJ (USA).

Hargraves, A. J., & McKinnon, R. L. (1961). Wetting Agents in Colliery Dust Suppression. Proc. Australian IMM, (200), 37-46.

Hu, Q., Polat, H., & Chander, S. (1992). Effect of surfactants in dust control by water sprays. Proceedings of the Emerging Process Technologies for a Cleaner Environment. SME, 269-276.

Kissell, F. N., & Bielicki, R. J. (1975). Methane Buildup Hazards Caused by Dust Scrubber Recirculation at Coal Mine Working Faces, A Preliminary Estimate. Bureau of Mines Report of Investigations.

Organiscak, J. A. (2014). Examination of water spray airborne coal dust capture with three wetting agents, 334(October 2012), 427–434.

Zeller, H. W. (1983). Laboratory tests for selecting wetting agents for coal dust control. US Department of the Interior, Bureau of Mines.

5 CONCLUSION

This study evaluated the potential of using a surfactant to aid in coal dust remediation to lower the risk of coal miner developing coal workers pneumoconiosis. This study specifically examined the effects of adding a surfactant to water at varying concentrations and varying the specific gravity of the exposed dust in a static environment. The testing method used in this instance was a particle wetting test. More detail on the testing procedure can be found in Section 3.3.3. Additionally, full-scale testing of the surfactant described in Section 4.4, was as also implemented. A number other investigations have been conducted in the past with other surfactants. Due to the lack of a consensus, these investigations were undertaken to shed more light on the issue.

To evaluate the additive, the concentration of the surfactant in the aqueous solution was varied in conjunction with a varying specific gravity of the coal dust. The current mineral content of the coal dust, to which coal workers are exposed, is of concern since it is known that silica dust is more harmful to human health than coal dust alone. For this reason, the assumed mineral content of the coal dust was studied using the specific gravity of the coal dust as a proxy. It should be noted that the mineral content of the coal dust tested was not however confirmed. The first battery of tests conducted looked at three specific gravities and three surfactant concentrations with each cell of the 3x3 test matrix tested in triplicate. Both of the variables were found to be significant. The wetting rates of the dust increased with increasing specific gravity and surfactant concentration. There was also significant, albeit to a lesser extent, interactions between the two variables.

The second battery of wetting test extended the boundaries of the initial study by including more surfactant concentrations and more classes of specific gravity. The test matrix included nine surfactant concentrations and nine gravity classes. The results of the tests showed that both variables again were significant, and the increase in either one was correlated with an increase in the wetting rate. A stronger effect from the surfactant was observed on dust with a smaller specific gravity or a larger coal fraction in the dust. This may be due to the non-coal fraction, which is already hydrophilic, being close to its fastest wetting rate with little room for improvement.

The second effort in this investigation was geared towards a full-scale study. The surfactant which was being examined was kept at a constant concentration of 1:5000. This solution was pumped through the mine to the continuous miner. The solution was then used in the CM's sprays during production. A control of no surfactant was also used. Dust concentration measurements were collected outby the working face both behind the curtain and further in the returns. Two different types of samples were collected, the continuous personal dust monitor (CPDM), and the personal dust sampler (PDS). Both devices were placed in the same location, and the data was aggregated and examined to see if there was a significant change in the dust concertation when the surfactant was being used. No significant changes in the dust levels were observed. However, in the CPDM data there were distinctive spikes in some places of the data which correlated to the depth of the cut. The mine ventilation plan did not allow for the scrubbers to be turned on until a cut depth of 20 ft was reached. The significant decreases in the dust concentrations from the activation of scrubbers are grounds for continued work on the topic. This area of future study should be focused on the scrubber usage and procedure. It is unclear whether the continuous activation of scrubber would be beneficial to CM operators and other personnel in the mine. This being the case, an additionally identified area of study would focus on potential controls aimed at reducing the risk of expose at the beginning of a pillar line of a crosscut. With so many variables and relativly short experimental window, there were not enough cuts taken to gather enough similar cut to make meaning conclusions about the surfactant. For this reason, further investigation with longer term studies is suggested. Even with the limited number of consistent samples, a significant increase in the dust concentration was observed from the CPDM when compared to the PDS. The larger implication of this finding should be examined in future studies.

6 FUTURE WORK

There are noticeable critiques and further assessment which should be added as addenda to these two main studies. With regards to the first study of the wetting rates, analysis of the dust contained in the material should be conducted. The analysis should be conducted on the dust before and after the wetting test. This will both confirm the actual silica content and allow the investigator to determine whether the higher gravity class material is selectively wetting the most hydrophilic components of the dust. The additional knowledge will also shift the correction factor used to derive the wetting rate.

It has also been noted that the manual method for applying the dust on the surface of the solution became inadequate when testing high gravity class material or greater concentrations of the surfactant in solution. If these are areas of future interest, the concern may be alleviated by introducing an automated mechanism for the application of dust. The automation should allow for the rapid and even application of the dust onto the solution surface. Some populations of the apparatus may include a very tight enclosure with compressed air as a dispersing mechanism.

One of the more justifiable critiques for future studies was the lack of testing of the dynamic capability of the surfactant to strip the dust from the air. All of the benchtop work executed dealt with the wetting rates in a static environment. Although wetting rates have been successfully used to some extent in the past for the preselection of surfactants, the abilities of the additive should still be scrutinized within a controllable mock setup. A number of tests could be run including particle sizing of the water droplet from sprays and airborne dust alike using laser diffraction. Relative concentrations of dust could be assessed immediately downwind of the area of application with an obscuration meter, which actual concentration could be measured further down a mock entry. This would also allow investigators to quickly change a variable like pressure, orientation, and sprayer type in addition to the variable examined in this first study.

The second study is also not without its own areas of improvement. The principal amendment to the full-scale study is simply further investigation for the purpose of controlling for a large amount of environmental variation and atypical mining condition within which the study took place. Due to unforeseen circumstance, the study was adapted to gather as much data as possible, even if the conditions and production cycles were not the norm.

Through the data analysis, however, intriguing trends were observed with the operation of scrubbers. Another engineering control used mine to diminish the dust exposure. Further investigations should also place measurement devices on or near the CM operator at the working face. Measuring the CM operators immediate environment would aid investigators in confirming the observed improvement in the mine environment. This is not just the case for examining surfactant or scrubbers, but also substantiating the assertions made with regards to the high airflow rates.

The deviation of the CPDM and PDS from each other is also of interest. The deviations seen should be reexamined by exposing both instruments to similar conditions with the aim of repeating the findings. The implications of this difference in measurement are far reaching with regards to the new dust regulations.

BIBLIOGRAPHY

dos S Antao, V. C., Petsonk, E. L., Sokolow, L. Z., Wolfe, A. L., Pinheiro, G. A., Hale, J. M., & Attfield, M. D. (2005). Rapidly progressive coal workers' pneumoconiosis in the United States: geographic clustering and other factors. Occupational and environmental medicine, 62(10), 670-674.

Attfield, M. D., & Kuempel, E. D. (2008). Mortality among US underground coal miners: A 23-year follow-up. American journal of industrial medicine, 51(4), 231-245.

Attfield, M. D., & Morring, K. (1992). AN INVESTIGATION INTO THE RELATIONSHIP BETWEEN COAL WORKERS'PNEUMOCONIOSIS AND DUST EXPOSURE IN US COAL MINERS. The American Industrial Hygiene Association Journal, 53(8), 486-492.

Baier, E. J., & Diakun, R. (1961). Pneumoconiosis Study in Central Pennsylvania Coal Mines: II. ENVIRONMENTAL PHASE. Journal of Occupational and Environmental Medicine, 3(11), 507-521.

Blackley, D. J., Halldin, C. N., & Laney, A. S. (2014). Resurgence of a debilitating and entirely preventable respiratory disease among working coal miners. American journal of respiratory and critical care medicine, 190(6), 708-709.

Brauer, H., & Varma, Y. B. . (1981). Chemie-Ingenieur-Technik, Air pollution control equipment, 54. Retrieved from http://search.informit.com.au/fullText;dn=987449606786534;res=IELENG

Castranova, V., & Vallyathan, V. (2000). Silicosis and coal workers' pneumoconiosis. Environmental health perspectives, 108(Suppl 4), 675.

Chander, S., Alaboyun, A. R., & Aplan, F. F. (1990, October). On the mechanism of capture of coal dust particles by sprays. In Proceedings of the Third Symposium on Respirable Dust in the Mineral Industries (pp. 193-202).

Chander, S., Hogg, R., & Fuerstenau, D. W. (2007). Characterization of the wetting and dewetting behavior of powders. KONA Powder and Particle Journal, 25, 56-75.

Chaplin, M. (2009). Theory vs experiment: what is the surface charge of water. Water, (July), 1–28. Retrieved from http://www.waterjournal.org/uploads/vol1/chaplin/WATER-Vol1-Chaplin.pdf

Cheng, L. (1973). Collection of airborne dust by water sprays. Industrial & Engineering Chemistry Process Design and Development, 12(3), 221-225.

Co. Spraying Systems. (2013). A Guide to Spray Technology for Dust Control Efficient , Effective Solutions for Dust Prevention and Suppression. Retrieved from http://www.spray.com/literature_pdfs/German/B652-EN-D_Dust_Control.pdf

Colinet, J. (2010). Health Consequences of Overexposure to Respirable Coal and Silica Dust - Public Health Advisor.

Colinet, J. F., Reed, W., & Potts, J. D. (2013). Impact on Respirable Dust Levels When Operating a Flooded-bed Scrubber in 20-foot Cuts. Niosh RI 9693.

Colinet, J., Listak, J. M., Organiscak, J. A., Rider, J. P., & Wolfe, A. L. (2010). Best practices for dust control in coal mining. Department of Health and Human Services, Centers for Disease Control and Prevention, National Institute for Occupational Safety and Health, Office of Mine Safety and Health Research.

Collis, E. L. ., & Gilchrist, J. C. (1928). Effects of dust upon coal trimmers. Journal of Chemical Information and Modeling, 53, 160. http://doi.org/10.1017/CBO9781107415324.004

Congress, U. (1977). Federal Mine Safety and Health Act of 1977. Public Law. Retrieved from http://scholar.google.com/scholar?hl=en&btnG=Search&q=intitle:Federal+Mine+Safety+&+Health+Act+of+1977#3

Copeland, C. R. (2007). Suppression and dispersion of airborne dust and nanoparticulates (Doctoral dissertation, Michigan Technological University).

Copeland, C., & Eisele, T. (2008). Factors influencing dust suppressant effectiveness. Minerals & …, 25(4), 215–222. Retrieved from http://www.smenet.org/minerals-and-metallurgical-processing-journal/abstract.cfm?aid=2855

Department of Labor - Mine Safety and Health Administration, M. (2010). Lowering Miners' Exposure to Respirable Coal Mine Dust, Including Continuous Personal Dust Monitors; Proposed Rule. Federal Register, 75(201). Retrieved from http://www.oig.dol.gov/public/reports/oa/2002/04-02-003-03-315x.pdf

Department of Labor - Mine Safety and Health Administration, M. (2014). Lowering Miners' Exposure to Respirable Coal Mine Dust, Including Continuous Personal Dust Monitors; Proposed Rule. Federal Register, 79(84). Retrieved from http://www.oig.dol.gov/public/reports/oa/2002/04-02-003-03-315x.pdf

Divers, E. F., LaScola, J. C., & Hundman, G. J. (1981). New twin scrubber installation for continuous mining machines.

Doyle, H. N., Funs, R. H., & Dreessen, W. C. (1958). A Review of the Pneumoconiosis Problem in the United States A Review of the. American Industrianl Hygiene Association. http://doi.org/10.1080/00028895809343597

Dreessen, W., & Jones, R. (1936). Anthracosilicosis. The Jounal of the American Medical Association, 107(15).

Feldstein, N. (1981). Surface Chemical Technology for Improved Wetting of Coal Dust, (February). Retrieved from http://scholar.google.com/scholar?hl=en&btnG=Search&q=intitle:Surface+Chemical+Technology+For+Improved+Wetting+Of+Coal+Dust#0

Gibbs, J. (1878). On the equilibrium of heterogeneous substances. American Journal of Science. Retrieved from http://www.ajsonline.org/content/s3-16/96/441.short

Glanville, J., & Haley, L. (1983). The Wetting of “Nusance” Dust By Surfactant Solutions. Colloids and Surfaces, 8, 93–97.

Glanville, J., & Wightman, J. (1979). Actions of wetting agents on coal dust. Fuel, 58, 819–822. Retrieved from http://www.sciencedirect.com/science/article/pii/0016236179901893

Goldshmid, Y., & Calvert, S. (1963). Small particle collection by supported liquid drops. AIChE Journal, 352–358. Retrieved from http://onlinelibrary.wiley.com/doi/10.1002/aic.690090315/abstract

Goodman, G. V. R., Beck, T. W., Pollock, D. E., Colinet, J. F., & Organiscak, J. A. (2006). Emerging technologies control respirable dust exposures for continuous mining and roof bolting personnel. In Proceedings of the 11th U.S./North American Mine Ventilation Symposium (pp. 211–216).

Gough, J. (1940). Pneumonoconiosis in coal trimmers. The Journal of Pathology and Bacteriology, 51, 277–285. Retrieved from http://onlinelibrary.wiley.com/doi/10.1002/path.1700510213/abstract

Gough, J., James, W. R. L., & Wentworth, J. E. (1949). a Comparison of the radiological and pathological changes in coalworkers’ pneumoconiosis. JOURNAL OF THE FACULTY OF RADIOLOGISTS, 1(1), 28–39. Retrieved from http://www.sciencedirect.com/science/article/pii/S0368224249800170

Hadjiliadis, Denis. (2015) "Coal Worker's Pneumoconiosis – Penn Medicine." – Penn Medicine. N.p., 22 June 2015. Retrieved from https://www.pennmedicine.org/for-patients-and-visitors/patient-information/conditions-treated-a-to-z/coal-workers-pneumoconiosis

Halfinger, G. (1984). Feasibility of a machine-mounted scrubber system for ventilating coal-mine working faces. Open File report (No. PB-85-185742/XAB). Ingersoll-Rand Research, Inc., Princeton, NJ (USA).

Hargraves, A. J., & McKinnon, R. L. (1961). Wetting Agents in Colliery Dust Suppression. Proc. Australian IMM, (200), 37-46.

Hu, Q., Polat, H., & Chander, S. (1992). Effect of surfactants in dust control by water sprays. Proceedings of the Emerging Process Technologies for a Cleaner Environment. SME, 269-276.

Huang, X., Gordon, T., Rom, W. N., & Finkelman, R. B. (2006). Interaction of Iron and Calcium Minerals in Coals and their Roles in Coal Dust-Induced Health and Environmental Problems. Reviews in Mineralogy and Geochemistry, 64(1), 153–178. http://doi.org/10.2138/rmg.2006.64.6

Kawatra, S. K. (2006). Dust in Mineral Processing. In Proceedings of the International Seminar on Mineral Processing Technology and Indo-Korean Workshop on Resource Recycling (Vol. 1, pp. 51-56). Allied Publishers.

Kim, J., & Tien, J. (1993). Enhanced dust suppression using surfactants. SME, LITTLETON, CO(USA). 1993. Retrieved from http://scholar.google.com/scholar?hl=en&btnG=Search&q=intitle:Enhanced+Dust+suppression+Using+Surfactants#0

King, E. J., Maguire, B. A., & Nagelschmidt, G. (1956). Further studies of the dust in lungs of coal-miners. British journal of industrial medicine, 13(1), 9.

Kissel, F. N. (2003). Handbook for Dust Control in Mining (IC 9465), 1–131. Retrieved from http://www.cdc.gov/niosh/mining/UserFiles/works/pdfs/2003-147.pdf

Kissell, F. N., & Bielicki, R. J. (1975). Methane Buildup Hazards Caused by Dust Scrubber Recirculation at Coal Mine Working Faces, A Preliminary Estimate. Bureau of Mines Report of Investigations.

Kost, J. a, Shirey, G. a, & Ford, C. T. (1980). In-mine Tests for Wetting Agent Effectiveness. USBM Contract Final Report, Contract J0295041.

Lainhart, W. S. (1969). Roentgenographic evidence of coal workers' pneumoconiosis in three geographic areas in the United States. Journal of Occupational and Environmental Medicine, 11(8), 399-408.

Laney, A. S., & Attfield, M. D. (2010). Coal workers' pneumoconiosis and progressive massive fibrosis are increasingly more prevalent among workers in small underground coal mines in the United States. Occupational and environmental medicine, 67(6), 428-431.

Laney, A. S., Petsonk, E. L., & Attfield, M. D. (2009). Pneumoconiosis among underground bituminous coal miners in the United States: is silicosis becoming more frequent?. Occupational and environmental medicine.

Laney, A. S., Petsonk, E. L., Hale, J. M., Wolfe, A. L., & Attfield, M. D. (2012). Potential determinants of coal workers' pneumoconiosis, advanced pneumoconiosis, and progressive massive fibrosis among underground coal miners in the United States, 2005–2009. American journal of public health, 102(S2), S279-S283.

Lieben, J., & McBride, W. (1963). Pneumoconiosis in Pennsylvania 's Bituminous Mining Industry. JAMA, 183(3), 176–179.

Mc Bride, W., Pendergrass, E., & Lieben, J. (1963). Pneumoconiosis study of western Pennsylvania bituminous coal miners. Journal of Occupational Medicine, 5(8), 376–388.

McBride, W. W., Pendergrass, E. G., & Lieben, J. (1966). Pneumoconiosis study of Pennsylvania anthracite miners. J Occup Med, 8(7), 365–376.

Meiklejohn, A. (1951). HISTORY OF LUNG DISEASES OF COAL MINERS IN GREAT BRITAIN : PART I , 1800-1875.

Meiklejohn, A. (1952). History of Lung Diseases of Coal Miners in Great BritainPART III, 1920-1952. British Journal of Industrial Medicine, 9(3), 208–220.

Méndez-Vargas, M. M., Báez-Revueltas, F. B., López-Rojas, P., HoracioTovalín-Ahumada, J., Zamudio-Lara, J. O., Marín-Cotoñieto, I. A., & Villedaf, F. (2013). Silicosis and industrial bronchitis by exposure to silica powders and cement. Rev Med Inst Mex Seguro Soc, 51(4), 384-9.

Morgan, W. K. C., Burgess, D. B., Jacobson, G., O'Brien, R. J., Pendergrass, E. P., Reger, R. B., & Shoub, E. P. (1973). The prevalence of coal workers' pneumoconiosis in US coal miners. Archives of Environmental Health: An International Journal, 27(4), 221-226.

Naeye, R., & Dellinger, W. (1972). Coal Workers ' Pneumoconiosis Correlation of Roentgenographic and Postmortem Findings. JAMA, 220(2).

Naeye, R. L., & Dellinger, W. S. (1970). Lung disease in Appalachian soft-coal miners. American Journal of Pathology, 58(3), 557–564.

Nalwa, H. S. (2001). Handbook of Surfaces and Interfaces of Materials. Elsevier.

National Mining Association (2013). MSHA's Proposed Coal Mine Dust Rule.

Neimeier, R. (1993). Occupational Exposure to Respirable Coal Mine Dust. Retrieved from http://www.cabusinessdirectory.info/niosh/docket/archive/pdfs/NIOSH-242/0242-091393-strickland.pdf

NIOSH. (1995). Coal Mine Dust Exposures and Associated Health Outcomes.

Organiscak, J. A. (2014). Examination of water spray airborne coal dust capture with three wetting agents, 334(October 2012), 427–434.

Pollock, D., & Organiscak, J. (2007). Airborne dust capture and induced airflow of various spray nozzle designs. Aerosol Science and Technology. Retrieved from http://www.tandfonline.com/doi/abs/10.1080/02786820701408517

Silberberg, M., & Weberg, E. (2009). Student Study Guide to accompany Chemistry: The Molecular Nature of Matter and Change. Retrieved from http://scholar.google.com/scholar?hl=en&btnG=Search&q=intitle:Student+Study+Guide+to+accompany+Chemistry:+The+Molecular+Nature+of+Matter+and+Change#0

Stewart, K. M. (2009). Physical Properties of Water. http://doi.org/10.1016/B978-012370626-3.00007-7

Suarthana, E., Laney, A. S., Storey, E., Hale, J. M., & Attfield, M. D. (2011). Coal workers' pneumoconiosis in the United States: regional differences 40 years after implementation of the 1969 Federal Coal Mine Health and Safety Act. Occupational and environmental medicine, oem-2010.

Tien, J., & Kim, J. (1997). Respirable coal dust control using surfactants. Applied Occupational and Environmental Hygiene, (May 2013), 37–41. Retrieved from http://www.tandfonline.com/doi/abs/10.1080/1047322X.1997.10390635

Tokuhata, G. K., Dessauer, P., Pendergrass, E. P., Hartman, T., Digon, E., & Miller, W. (1970). Pneumoconiosis among anthracite coal miners in Pennsylvania. American Journal of Public Health and the Nations Health, 60(3), 441-451.

Weeks, J. L., & Wagner, G. R. (1986). Compensation for occupational disease with multiple causes: The case of coal miners’ respiratory diseases. American Journal of Public Health, 76(1), 58–61. http://doi.org/10.2105/AJPH.76.1.58

Zeller, H. W. (1983). Laboratory tests for selecting wetting agents for coal dust control. US Department of the Interior, Bureau of Mines.

APPENDIX A

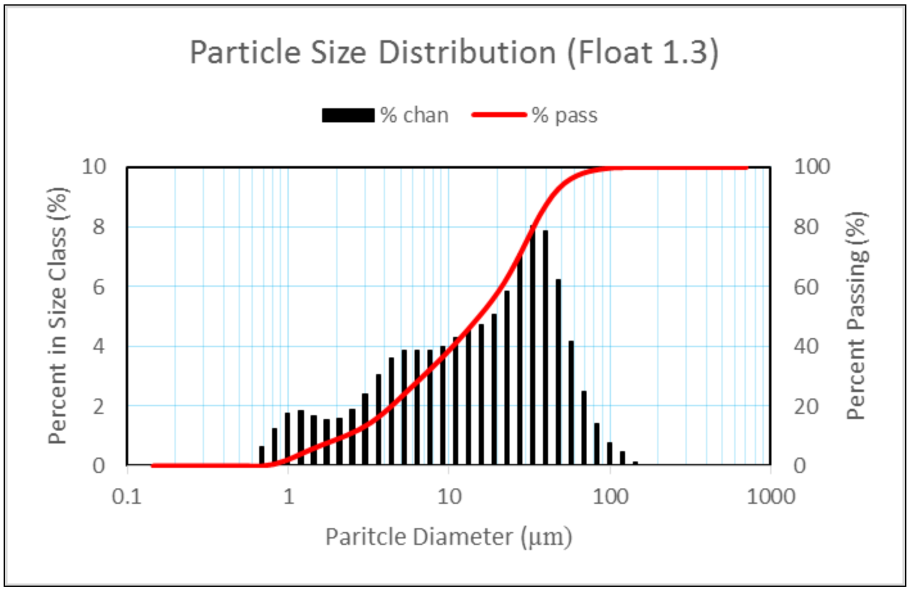

Figure 58:A1 - Particle size distribution for gravity class float 1.3

Table 10:A2 - Tabulated size distribution for gravity class float 1.3

Size (µm)	Pass %	Chan %	Size (µm)	Pass %	Chan %	Size (µm)	Pass %	Chan %	Size (µm)	Pass %	Chan %
352.0	100.0	0.0000	52.33	94.73	4.180	7.778	32.76	3.850	1.156	3.640	1.750
296.0	100.0	0.0000	44.00	90.55	6.240	6.541	28.91	3.850	0.972	1.890	1.250
248.9	100.0	0.0000	37.00	84.31	7.850	5.500	25.06	3.850	0.818	0.640	0.640
209.3	100.0	0.0000	31.11	76.46	8.050	4.625	21.21	3.600	0.688	0.000	0.0000
176.0	100.0	0.0000	26.16	68.41	7.090	3.889	17.61	3.050	0.578	0.000	0.0000
148.0	100.0	0.0000	22.00	61.32	5.860	3.270	14.56	2.400	0.486	0.000	0.0000
124.5	100.0	0.1200	18.50	55.46	5.080	2.750	12.16	1.890	0.409	0.0000	0.0000
104.7	99.88	0.4600	15.56	50.38	4.730	2.312	10.27	1.600	0.344	0.0000	0.0000
88.00	99.42	0.7900	13.08	45.65	4.560	1.945	8.670	1.540	0.289	0.0000	0.0000
74.00	98.63	1.410	11.00	41.09	4.310	1.635	7.130	1.660	0.243	0.0000	0.0000
62.23	97.22	2.490	9.250	36.78	4.020	1.375	5.470	1.830	0.204	0.0000	0.0000

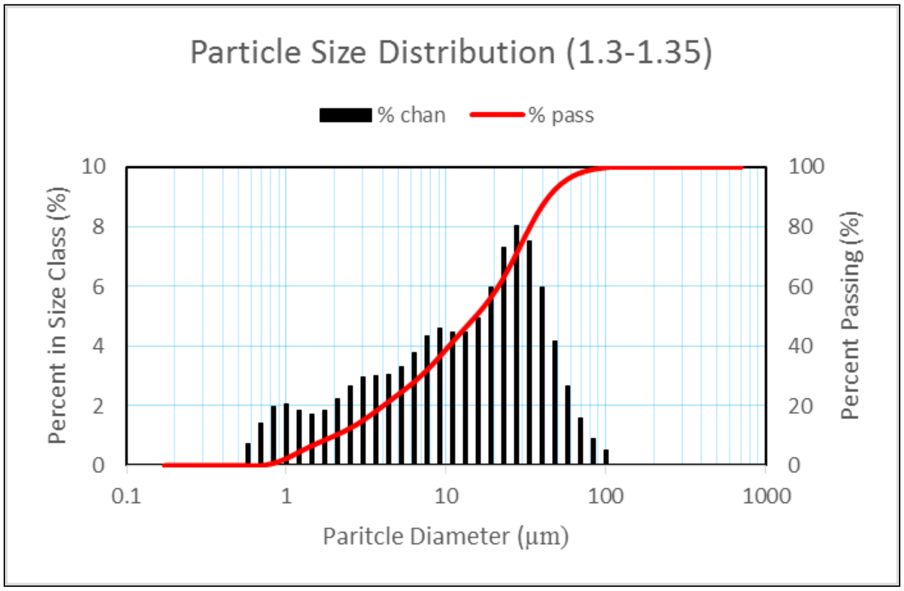

Figure 59:A3 - Particle size distribution for gravity class 1.3-1.35

Table 11:A4 - Tabulated size distribution for gravity class 1.3-1.35

Size (µm)	Pass %	Chan %	Size (µm)	Pass %	Chan %	Size (µm)	Pass %	Chan %	Size (µm)	Pass %	Chan %
352.0	100.0	0.0000	52.33	94.39	4.180	7.778	32.59	3.800	1.156	4.120	1.980
296.0	100.0	0.0000	44.00	90.21	5.980	6.541	28.79	3.290	0.972	2.140	1.410
248.9	100.0	0.0000	37.00	84.23	7.520	5.500	25.50	3.050	0.818	0.730	0.730
209.3	100.0	0.0000	31.11	76.71	8.030	4.625	22.45	3.020	0.688	0.000	0.0000
176.0	100.0	0.0000	26.16	68.68	7.290	3.889	19.43	2.970	0.578	0.000	0.0000
148.0	100.0	0.0000	22.00	61.39	5.970	3.270	16.46	2.680	0.486	0.000	0.0000
124.5	100.0	0.0000	18.50	55.42	4.940	2.750	13.78	2.220	0.409	0.0000	0.0000
104.7	100.0	0.5000	15.56	50.48	4.470	2.312	11.56	1.850	0.344	0.0000	0.0000
88.00	99.50	0.8900	13.08	46.01	4.490	1.945	9.71	1.710	0.289	0.0000	0.0000
74.00	98.61	1.570	11.00	41.52	4.580	1.635	8.00	1.830	0.243	0.0000	0.0000
62.23	97.04	2.650	9.250	36.94	4.350	1.375	6.170	2.050	0.204	0.0000	0.0000

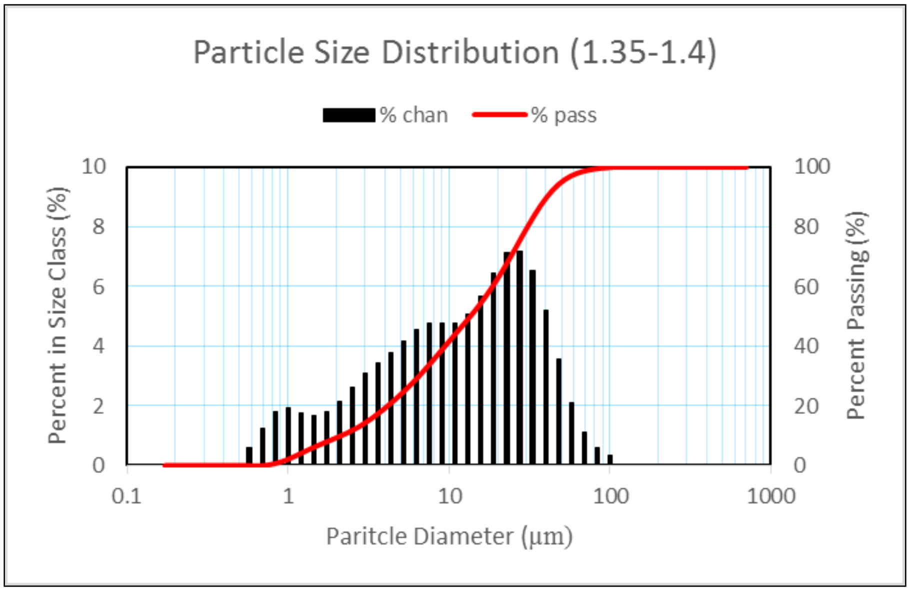

Figure 60:A5 - Particle size distribution for gravity class 1.35-1.4

Table 12:A6 - Tabulated size distribution for gravity class 1.35-1.4

Size (µm)	Pass %	Chan %	Size (µm)	Pass %	Chan %	Size (µm)	Pass %	Chan %	Size (µm)	Pass %	Chan %
352.0	100.0	0.0000	52.33	95.86	3.550	7.778	34.67	4.570	1.156	3.680	1.810
296.0	100.0	0.0000	44.00	92.31	5.200	6.541	30.10	4.170	0.972	1.870	1.250
248.9	100.0	0.0000	37.00	87.11	6.550	5.500	25.93	3.770	0.818	0.6200	0.6200
209.3	100.0	0.0000	31.11	80.56	7.200	4.625	22.16	3.450	0.688	0.0000	0.0000
176.0	100.0	0.0000	26.16	73.36	7.120	3.889	18.71	3.090	0.578	0.0000	0.0000
148.0	100.0	0.0000	22.00	66.24	6.470	3.270	15.62	2.620	0.486	0.0000	0.0000
124.5	100.0	0.0000	18.50	59.77	5.680	2.750	13.00	2.130	0.409	0.0000	0.0000
104.7	100.0	0.3400	15.56	54.09	5.060	2.312	10.87	1.790	0.344	0.0000	0.0000
88.00	99.66	0.5900	13.08	49.03	4.790	1.945	9.080	1.680	0.289	0.0000	0.0000
74.00	99.07	1.120	11.00	44.24	4.790	1.635	7.400	1.780	0.243	0.0000	0.0000
62.23	97.95	2.090	9.250	39.45	4.780	1.375	5.620	1.940	0.204	0.0000	0.0000

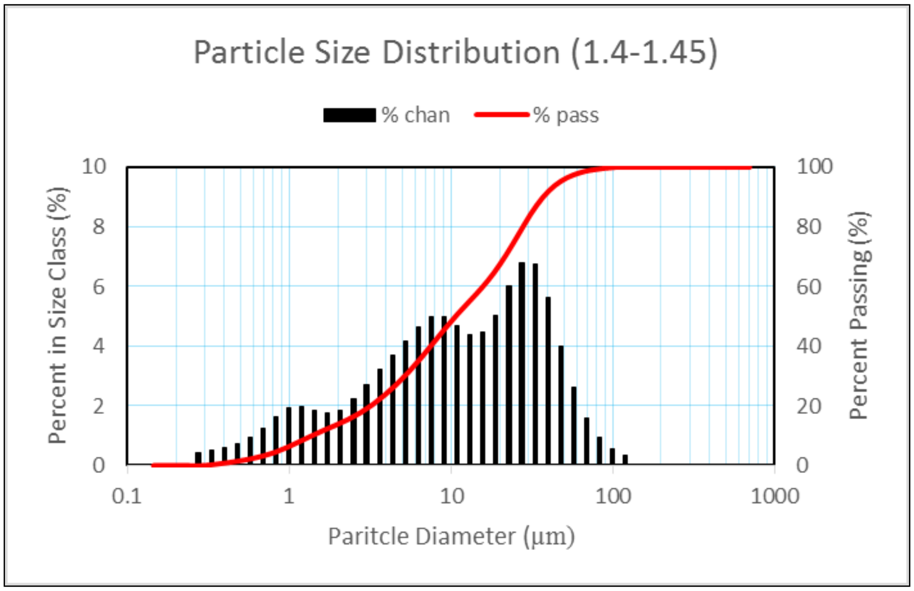

Figure 61:A7 - Particle size distribution for gravity class 1.4-1.45

Table 13:A8 - Tabulated size distribution for gravity class 1.4-1.45

Size (µm)	Pass %	Chan %	Size (µm)	Pass %	Chan %	Size (µm)	Pass %	Chan %	Size (µm)	Pass %	Chan %
352.0	100.0	0.0000	52.33	96.51	2.610	7.778	41.08	5.000	1.156	8.030	1.920
296.0	100.0	0.0000	44.00	93.90	4.020	6.541	36.08	4.640	0.972	6.110	1.630
248.9	100.0	0.0000	37.00	89.88	5.640	5.500	31.44	4.150	0.818	4.480	1.250
209.3	100.0	0.0000	31.11	84.24	6.770	4.625	27.29	3.680	0.688	3.230	0.9500
176.0	100.0	0.0000	26.16	77.47	6.790	3.889	23.61	3.220	0.578	2.280	0.7500
148.0	100.0	0.0000	22.00	70.68	6.000	3.270	20.39	2.710	0.486	1.530	0.6100
124.5	100.0	0.0000	18.50	64.68	5.040	2.750	17.68	2.220	0.409	0.9200	0.5100
104.7	100.0	0.3600	15.56	59.64	4.470	2.312	15.46	1.870	0.344	0.4100	0.4100
88.00	99.64	0.5700	13.08	55.17	4.400	1.945	13.59	1.760	0.289	0.0000	0.0000
74.00	99.07	0.960	11.00	50.77	4.690	1.635	11.83	1.840	0.243	0.0000	0.0000
62.23	98.11	1.600	9.250	46.08	5.000	1.375	9.990	1.960	0.204	0.0000	0.0000

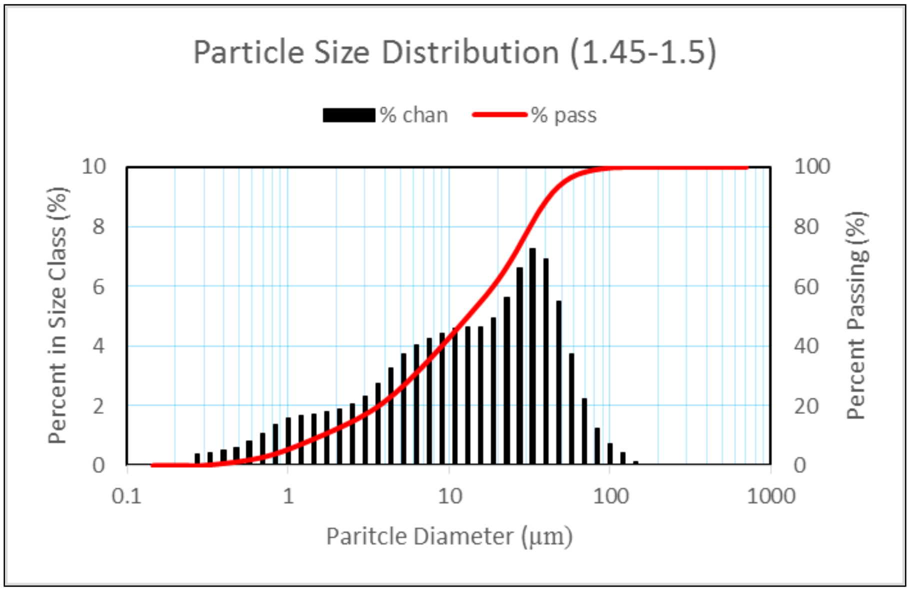

Figure 62:A9 - Particle size distribution for gravity class 1.45-1.5

Table 14:A10 - Tabulated size distribution for gravity class 1.45-1.5

Size (µm)	Pass %	Chan %	Size (µm)	Pass %	Chan %	Size (µm)	Pass %	Chan %	Size (µm)	Pass %	Chan %
352.0	100.0	0.0000	52.33	95.24	3.730	7.778	36.29	4.240	1.156	6.760	1.590
296.0	100.0	0.0000	44.00	91.51	5.490	6.541	32.05	4.030	0.972	5.170	1.370
248.9	100.0	0.0000	37.00	86.02	6.910	5.500	28.02	3.730	0.818	3.800	1.070
209.3	100.0	0.0000	31.11	79.11	7.280	4.625	24.29	3.270	0.688	2.730	0.8100
176.0	100.0	0.0000	26.16	71.83	6.630	3.889	21.02	2.760	0.578	1.920	0.6200
148.0	100.0	0.0000	22.00	65.20	5.640	3.270	18.26	2.340	0.486	1.300	0.5000
124.5	100.0	0.1100	18.50	59.56	4.950	2.750	15.92	2.060	0.409	0.8000	0.4300
104.7	99.89	0.4400	15.56	54.61	4.660	2.312	13.86	1.890	0.344	0.3700	0.3700
88.00	99.45	0.7200	13.08	49.95	4.630	1.945	11.97	1.790	0.289	0.0000	0.0000
74.00	98.73	1.260	11.00	45.32	4.590	1.635	10.18	1.730	0.243	0.0000	0.0000
62.23	97.47	2.230	9.250	40.73	4.440	1.375	8.450	1.690	0.204	0.0000	0.0000

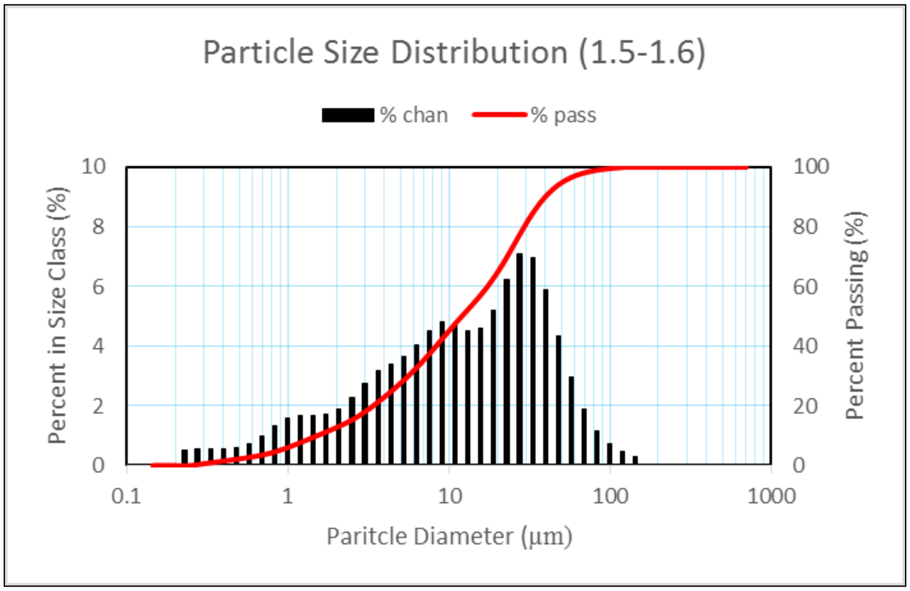

Figure 63:A11 - Particle size distribution for gravity class 1.5-1.6

Table 15:A12 - Tabulated size distribution for gravity class 1.5-1.6

Size (µm)	Pass %	Chan %	Size (µm)	Pass %	Chan %	Size (µm)	Pass %	Chan %	Size (µm)	Pass %	Chan %
352.0	100.0	0.0000	52.33	95.46	2.950	7.778	38.18	4.530	1.156	7.390	1.580
296.0	100.0	0.0000	44.00	92.51	4.340	6.541	33.65	4.040	0.972	5.810	1.320
248.9	100.0	0.0000	37.00	88.17	5.870	5.500	29.61	3.650	0.818	4.490	0.9900
209.3	100.0	0.0000	31.11	82.30	6.970	4.625	25.96	3.410	0.688	3.500	0.7300
176.0	100.0	0.0000	26.16	75.33	7.110	3.889	22.55	3.170	0.578	2.770	0.5900
148.0	100.0	0.0000	22.00	68.22	6.220	3.270	19.38	2.770	0.486	2.180	0.5400
124.5	100.0	0.3200	18.50	62.00	5.210	2.750	16.61	2.280	0.409	1.640	0.5500
104.7	99.68	0.4600	15.56	56.79	4.590	2.312	14.33	1.890	0.344	1.090	0.5800
88.00	99.22	0.7100	13.08	52.20	4.500	1.945	12.44	1.700	0.289	0.5100	0.5100
74.00	98.51	1.170	11.00	47.70	4.710	1.635	10.74	1.670	0.243	0.0000	0.0000
62.23	97.34	1.880	9.250	42.99	4.810	1.375	9.070	1.680	0.204	0.0000	0.0000

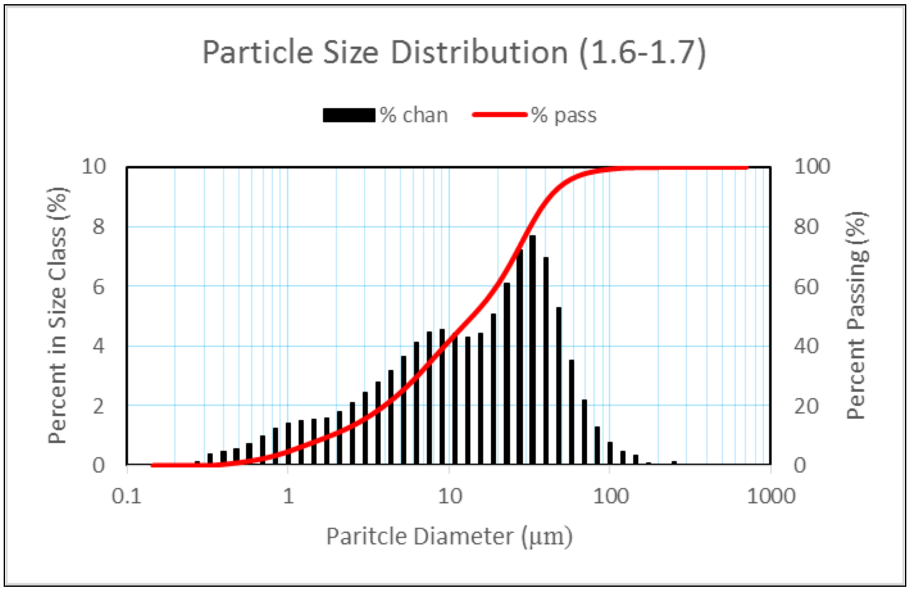

Figure 64:A13 - Particle size distribution for gravity class 1.6-1.7

Table 16:A14 - Tabulated size distribution for gravity class 1.6-1.7

Size (µm)	Pass %	Chan %	Size (µm)	Pass %	Chan %	Size (µm)	Pass %	Chan %	Size (µm)	Pass %	Chan %
352.0	100.0	0.0000	52.33	94.73	3.540	7.778	35.18	4.470	1.156	5.910	1.440
296.0	100.0	0.0000	44.00	91.19	5.280	6.541	30.71	4.130	0.972	4.470	1.240
248.9	100.0	0.0000	37.00	85.91	6.960	5.500	26.58	3.660	0.818	3.230	0.9700
209.3	100.0	0.1100	31.11	78.95	7.680	4.625	22.92	3.200	0.688	2.260	0.7300
176.0	99.89	0.0000	26.16	71.27	7.240	3.889	19.72	2.810	0.578	1.530	0.5700
148.0	99.89	0.1000	22.00	64.03	6.090	3.270	16.91	2.450	0.486	0.9600	0.4600
124.5	99.79	0.3300	18.50	57.94	5.060	2.750	14.46	2.100	0.409	0.5000	0.3800
104.7	99.46	0.4800	15.56	52.88	4.450	2.312	12.36	1.800	0.344	0.1200	0.1200
88.00	98.98	0.7700	13.08	48.43	4.300	1.945	10.56	1.600	0.289	0.0000	0.0000
74.00	98.21	1.300	11.00	44.13	4.410	1.635	8.960	1.530	0.243	0.0000	0.0000
62.23	96.91	2.180	9.250	39.72	4.540	1.375	7.430	1.520	0.204	0.0000	0.0000

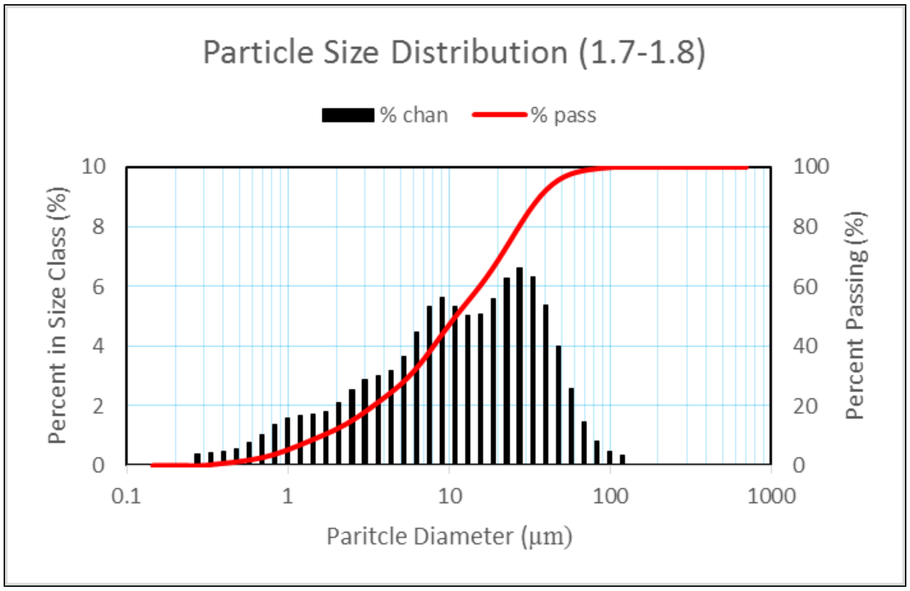

Figure 65:A15 - Particle size distribution for gravity class 1.7-1.8

Table 17:A16 - Tabulated size distribution for gravity class 1.7-1.8

Size (µm)	Pass %	Chan %	Size (µm)	Pass %	Chan %	Size (µm)	Pass %	Chan %	Size (µm)	Pass %	Chan %
352.0	100.0	0.0000	52.33	96.87	2.580	7.778	39.01	5.320	1.156	6.660	1.610
296.0	100.0	0.0000	44.00	94.29	4.000	6.541	33.69	4.460	0.972	5.050	1.360
248.9	100.0	0.0000	37.00	90.29	5.390	5.500	29.23	3.640	0.818	3.690	1.040
209.3	100.0	0.0000	31.11	84.90	6.320	4.625	25.59	3.190	0.688	2.650	0.7600
176.0	100.0	0.0000	26.16	78.58	6.620	3.889	22.40	3.020	0.578	1.890	0.5800
148.0	100.0	0.0000	22.00	71.96	6.270	3.270	19.38	2.860	0.486	1.310	0.4800
124.5	100.0	0.0000	18.50	65.69	5.600	2.750	16.52	2.540	0.409	0.8300	0.4300
104.7	100.0	0.3300	15.56	60.09	5.080	2.312	13.98	2.120	0.344	0.4000	0.4000
88.00	99.67	0.4900	13.08	55.01	5.020	1.945	11.86	1.810	0.289	0.0000	0.0000
74.00	99.18	0.8300	11.00	49.99	5.350	1.635	10.05	1.700	0.243	0.0000	0.0000
62.23	98.35	1.480	9.250	44.64	5.630	1.375	8.350	1.690	0.204	0.0000	0.0000

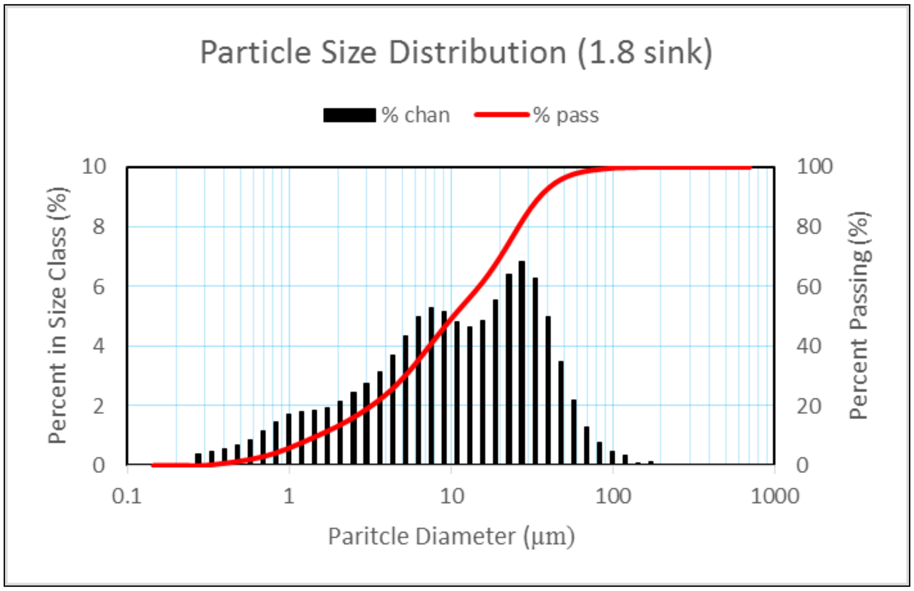

Figure 66:A17 - Particle size distribution for gravity class 1.8 Sink

Table 18:A18 - Tabulated size distribution for gravity class 1.8 Sink

Size (µm)	Pass %	Chan %	Size (µm)	Pass %	Chan %	Size (µm)	Pass %	Chan %	Size (µm)	Pass %	Chan %
352.0	100.0	0.0000	52.33	96.89	2.210	7.778	41.73	5.290	1.156	7.330	1.710
296.0	100.0	0.0000	44.00	94.68	3.480	6.541	36.44	4.990	0.972	5.620	1.480
248.9	100.0	0.0000	37.00	91.20	4.980	5.500	31.45	4.360	0.818	4.140	1.160
209.3	100.0	0.0000	31.11	86.22	6.260	4.625	27.09	3.680	0.688	2.980	0.8700
176.0	100.0	0.0000	26.16	79.96	6.830	3.889	23.41	3.140	0.578	2.110	0.6800
148.0	100.0	0.1100	22.00	73.13	6.400	3.270	20.27	2.770	0.486	1.430	0.5600
124.5	99.89	0.1000	18.50	66.73	5.550	2.750	17.50	2.450	0.409	0.8700	0.4800
104.7	99.79	0.3500	15.56	61.18	4.860	2.312	15.05	2.160	0.344	0.3900	0.3900
88.00	99.44	0.4800	13.08	56.32	4.630	1.945	12.89	1.940	0.289	0.0000	0.0000
74.00	98.96	0.760	11.00	51.69	4.810	1.635	10.95	1.830	0.243	0.0000	0.0000
62.23	98.20	1.310	9.250	46.88	5.150	1.375	9.120	1.790	0.204	0.0000	0.0000

Table 19:A19 - Tabulated sink test using dust with gravity 1.3-1.35 and surfactant concentration 1:5000 in triplicate

<table>
<tr><th>Data and Model</th><th>Residuals</th><th>Observed Vs. Predicted</th></tr>
<tr>
<td>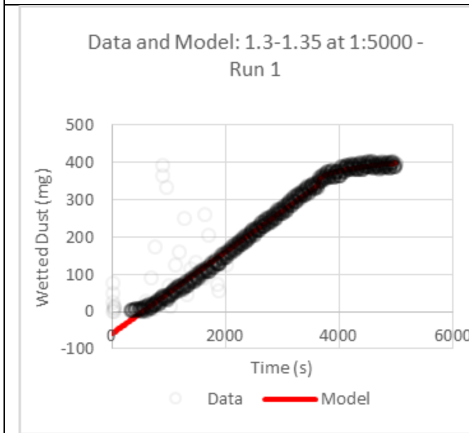
</td>
<td>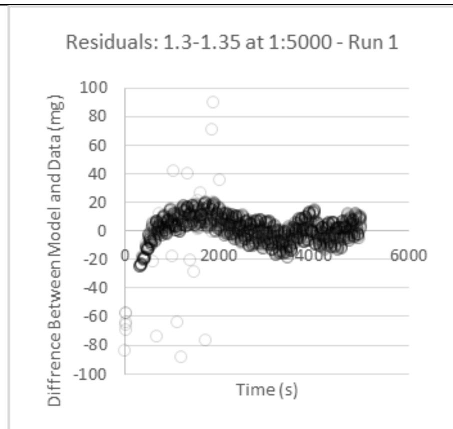
</td>
<td>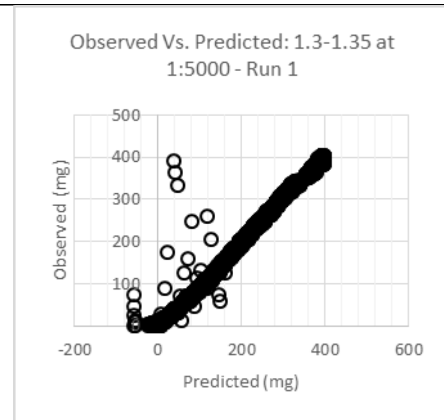
</td>
</tr>
<tr>
<td>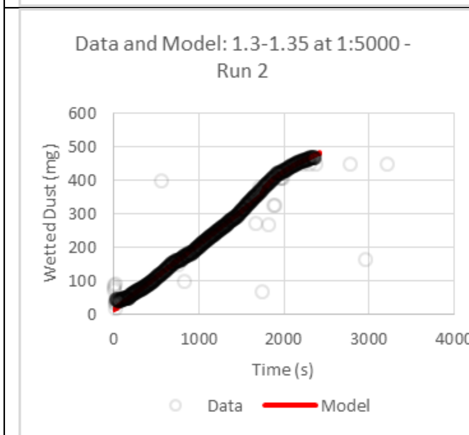
</td>
<td>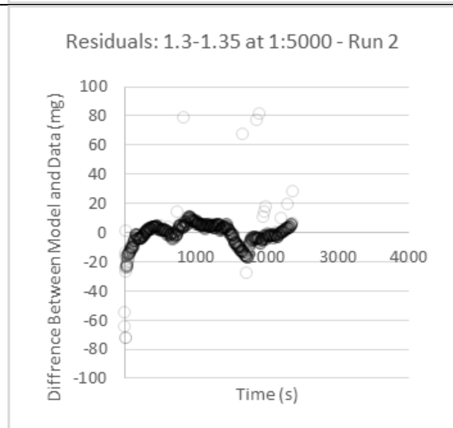
</td>
<td>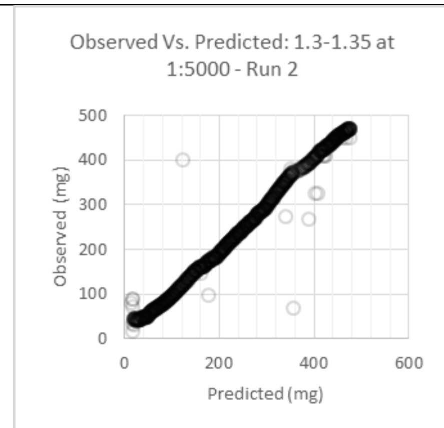
</td>
</tr>
<tr>
<td>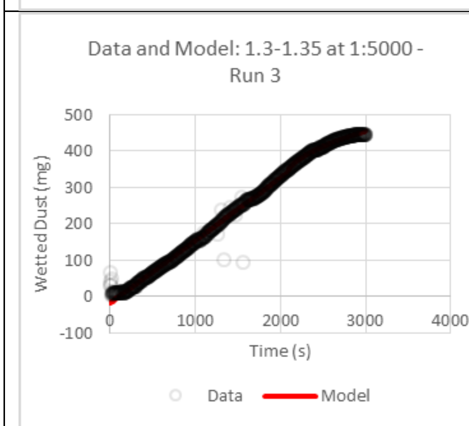
</td>
<td>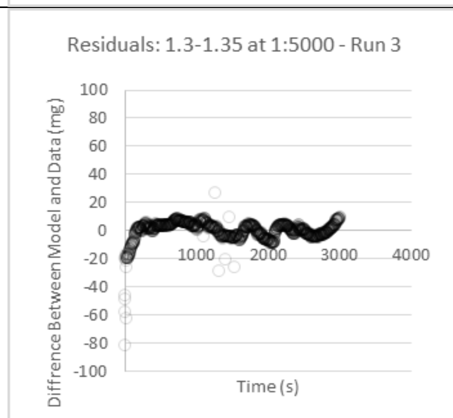
</td>
<td>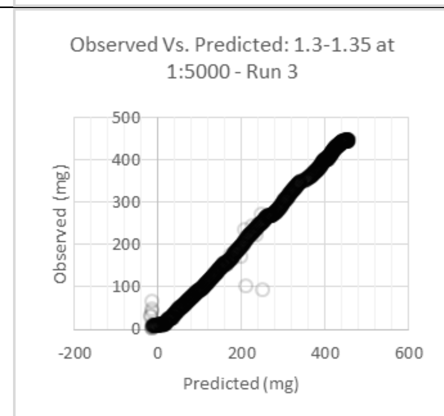
</td>
</tr>
</table>

Table 20:A20 - Tabulated sink test using dust with gravity 1.3-1.35 and surfactant concentration 1:3000 in triplicate

<table>
<tr><th>Data and Model</th><th>Residuals</th><th>Observed Vs. Predicted</th></tr>
<tr>
<td>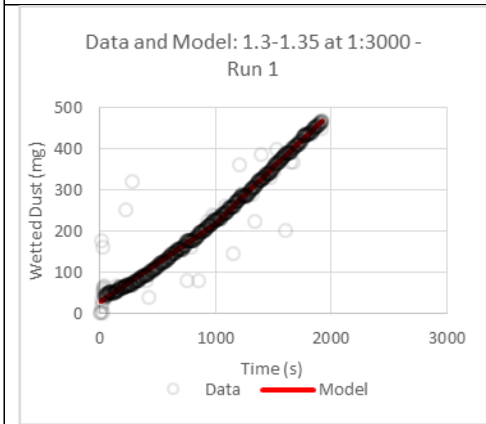
</td>
<td>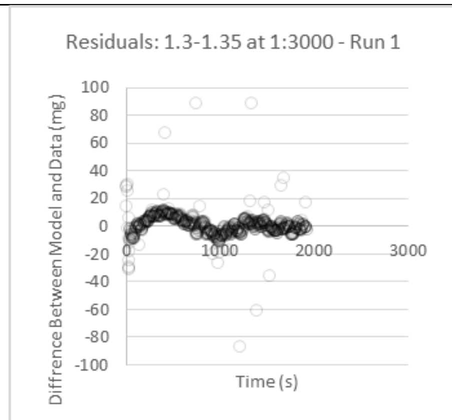
</td>
<td>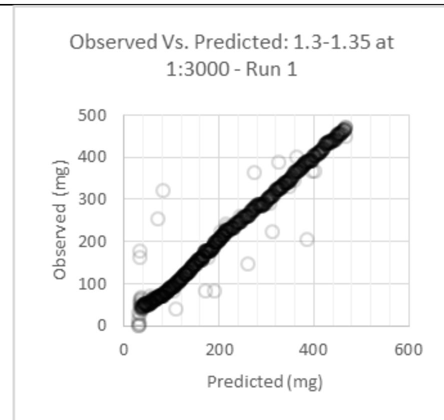
</td>
</tr>
<tr>
<td>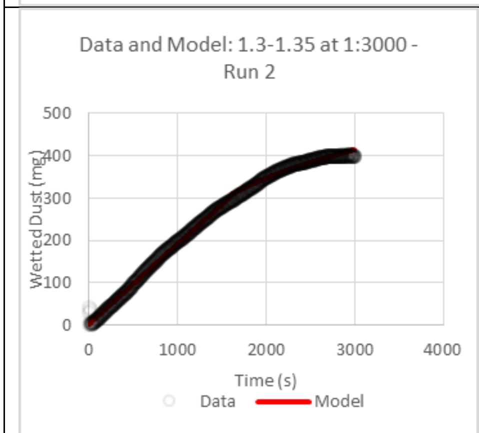
</td>
<td>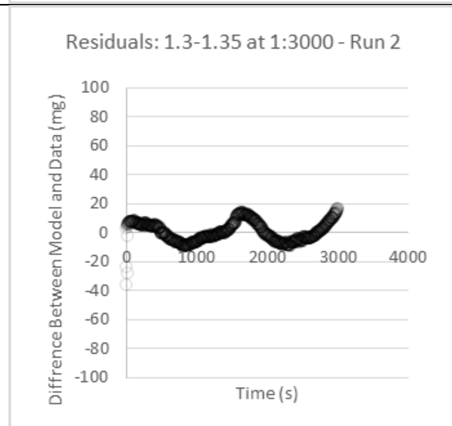
</td>
<td>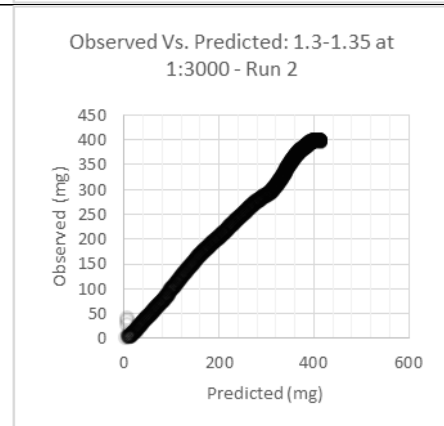
</td>
</tr>
<tr>
<td>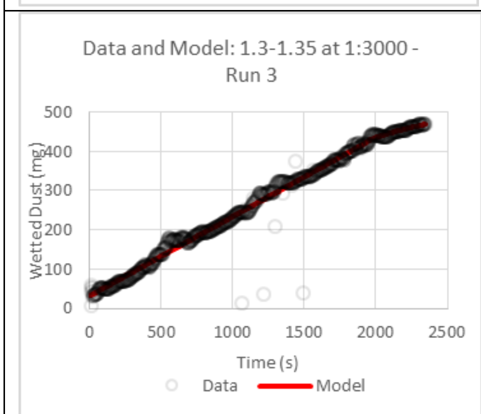
</td>
<td>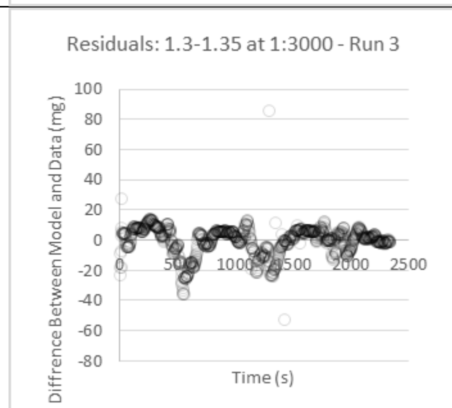
</td>
<td>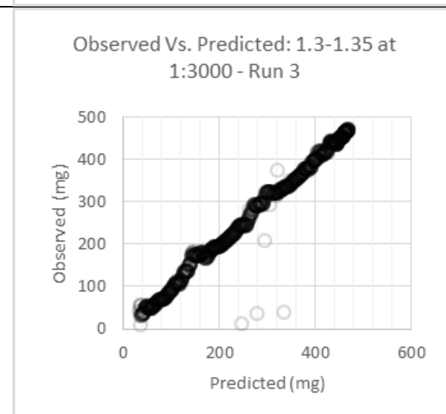
</td>
</tr>
</table>

Table 21:A21 - Tabulated sink test using dust with gravity 1.3-1.35 and surfactant concentration 1:1000 in triplicate

Data and Model	Residuals	Observed Vs. Predicted

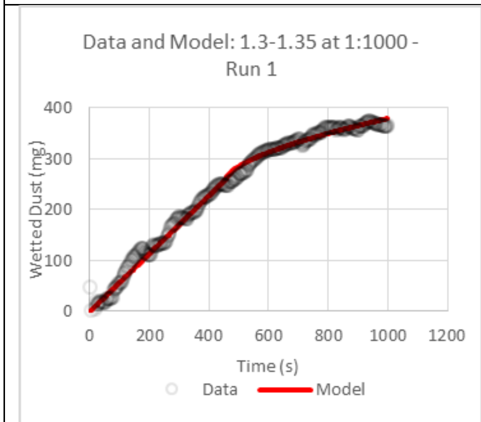

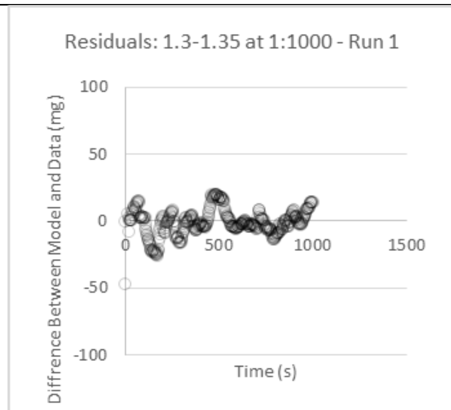

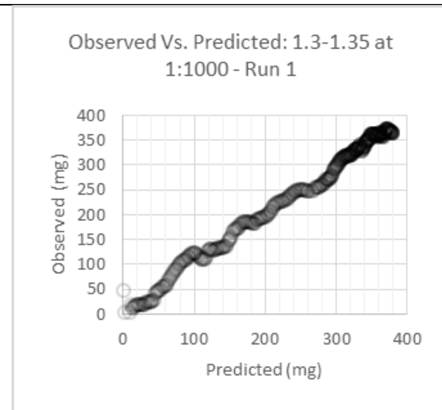

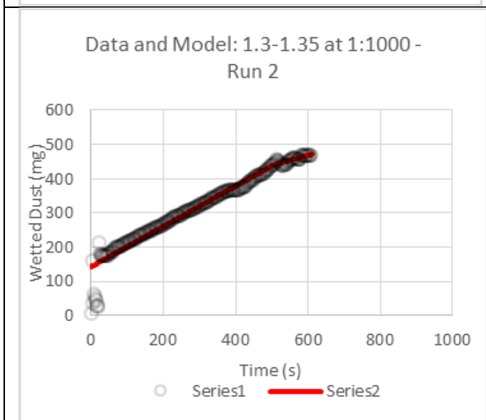

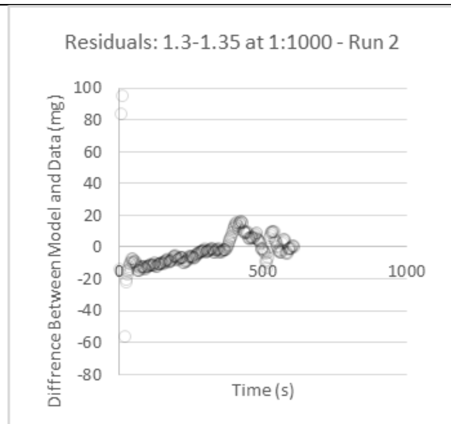

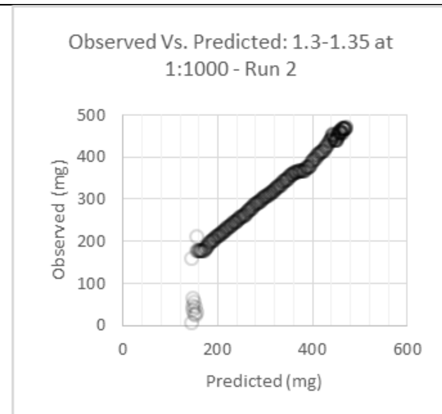

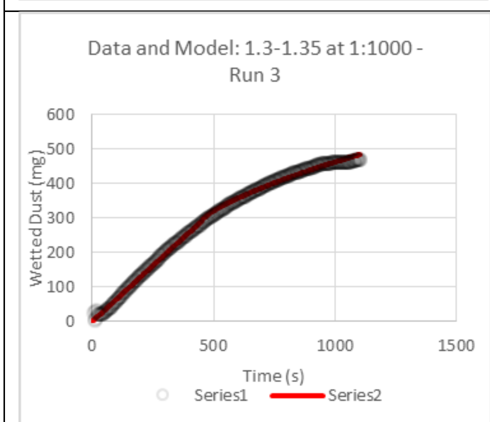

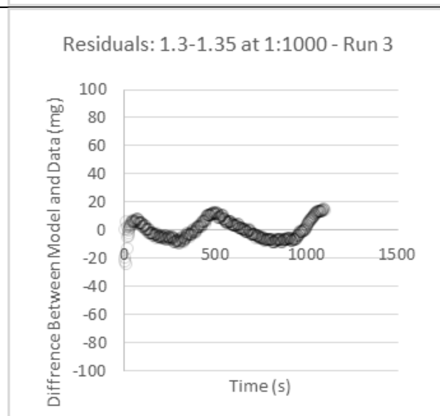

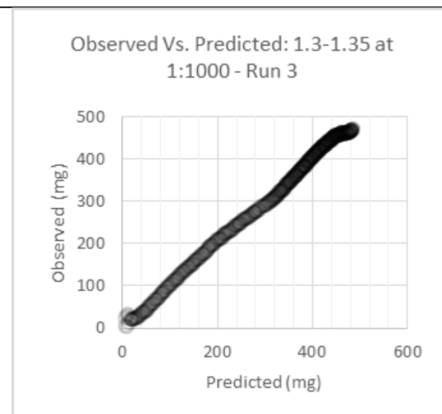

Table 22:A22 - Tabulated sink test using dust with gravity 1.4-1.45 and surfactant concentration 1:5000 in triplicate

Data and Model	Residuals	Observed Vs. Predicted
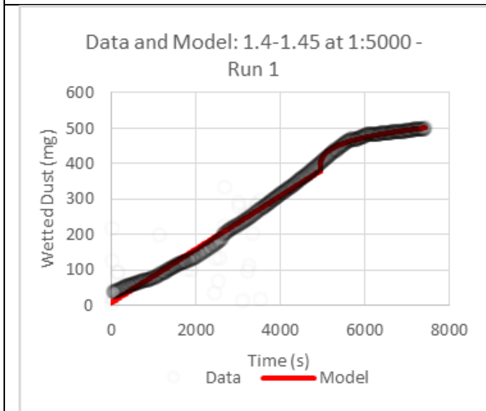	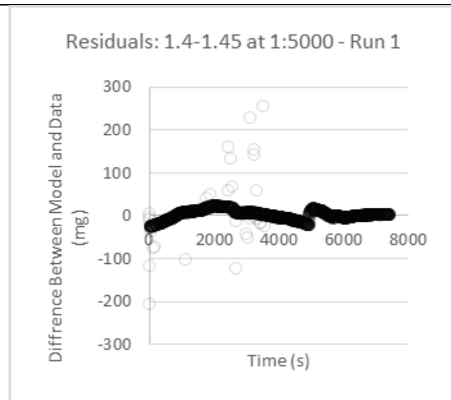	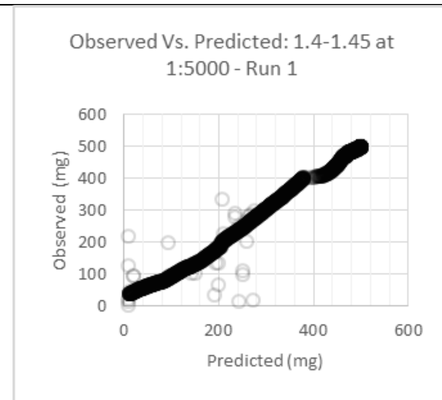
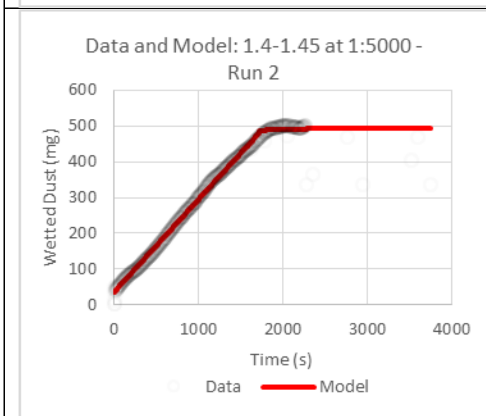	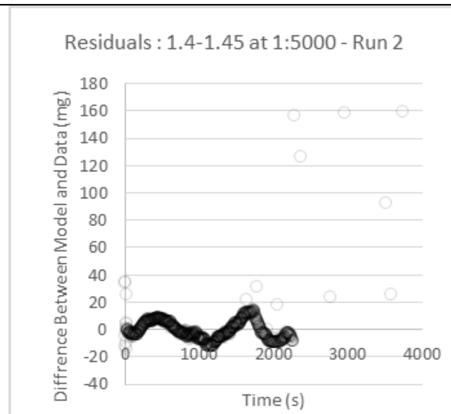	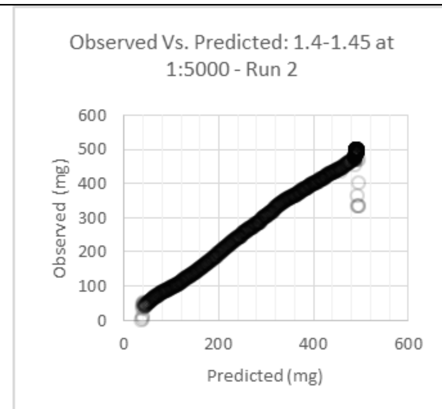
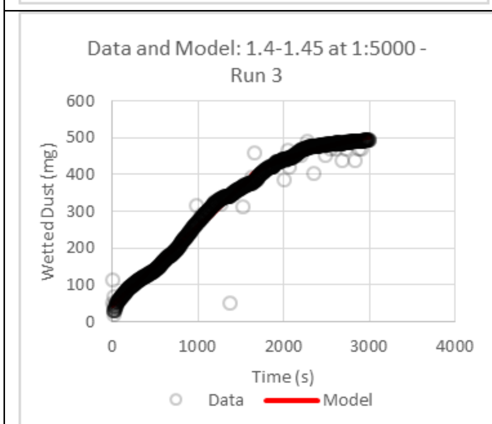	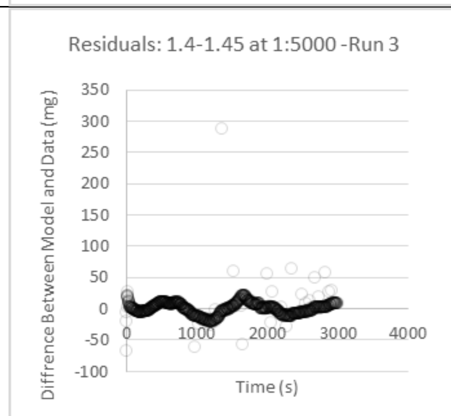	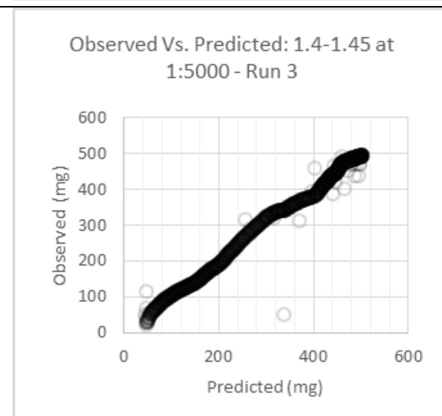

Table 23:A23 - Tabulated sink test using dust with gravity 1.4-1.45 and surfactant concentration 1:3000 in triplicate

<table>
<tr><th>Data and Model</th><th>Residuals</th><th>Observed Vs. Predicted</th></tr>
<tr>
<td>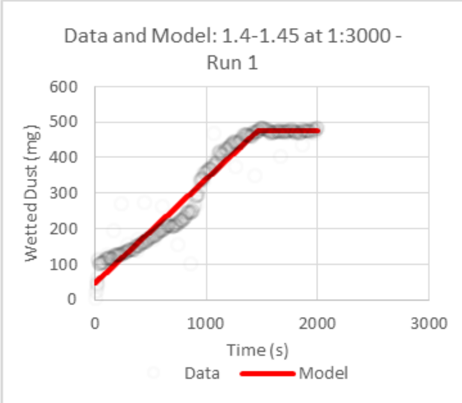
</td>
<td>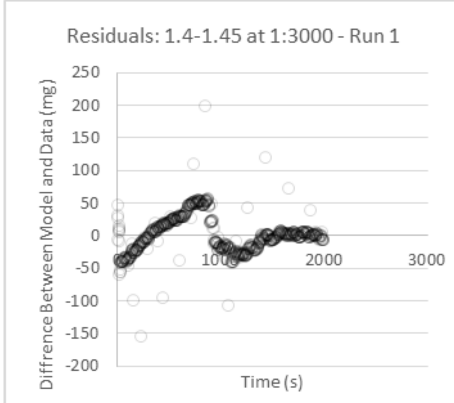
</td>
<td>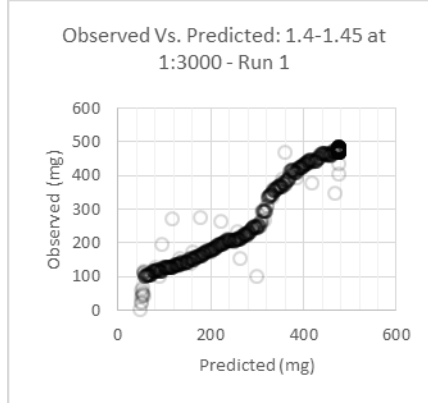
</td>
</tr>
<tr>
<td>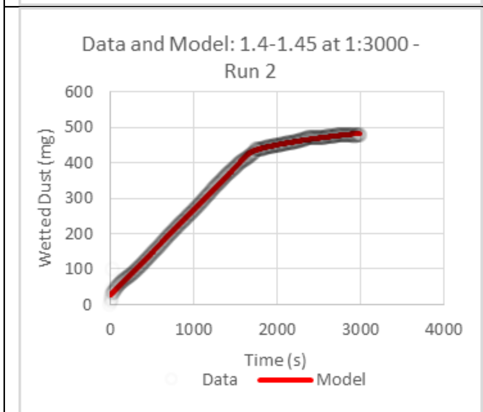
</td>
<td>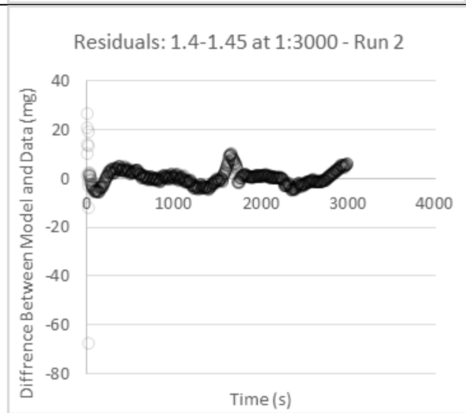
</td>
<td>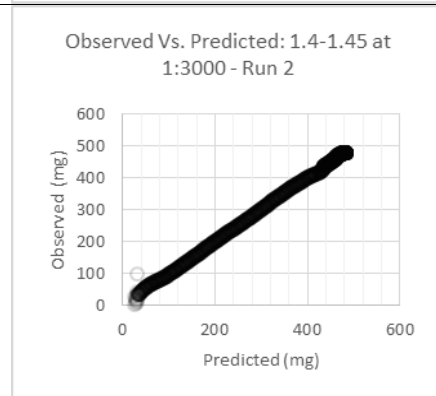
</td>
</tr>
<tr>
<td>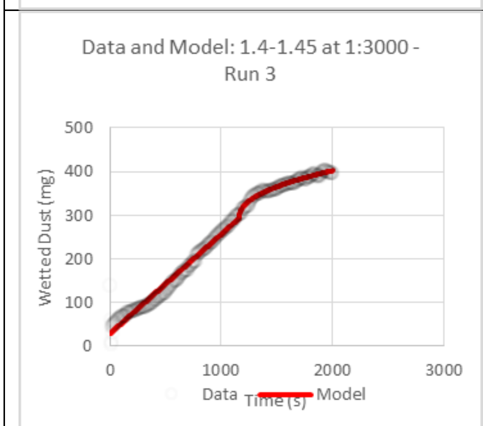
</td>
<td>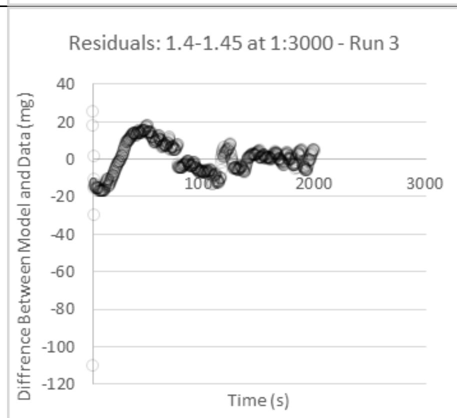
</td>
<td>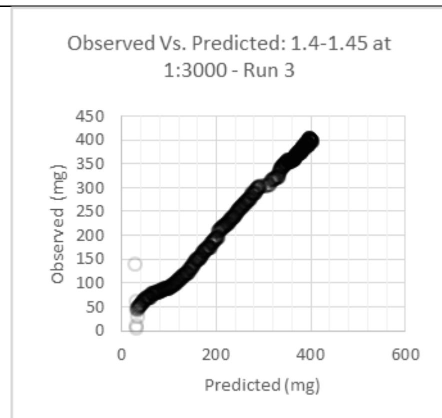
</td>
</tr>
</table>

Table 24:A24 - Tabulated sink test using dust with gravity 1.4-1.45 and surfactant concentration 1:1000 in triplicate

Data and Model	Residuals	Observed Vs. Predicted

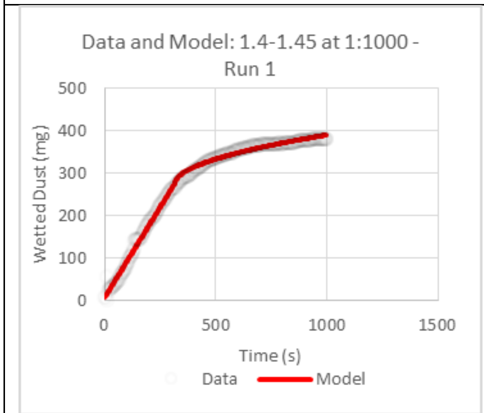

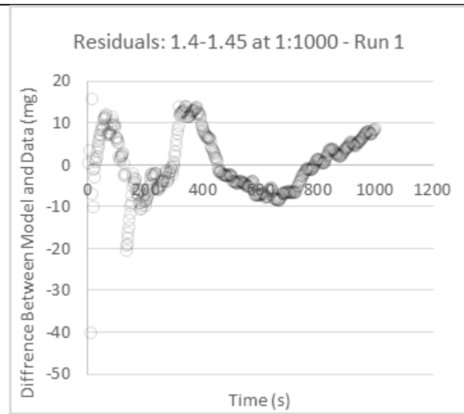

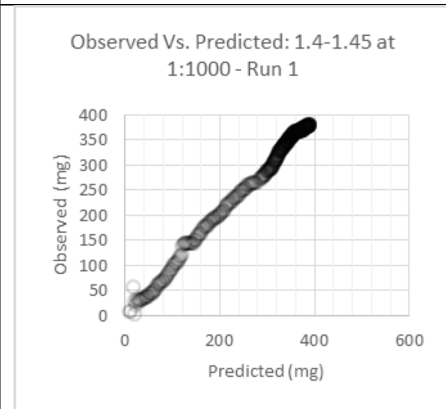

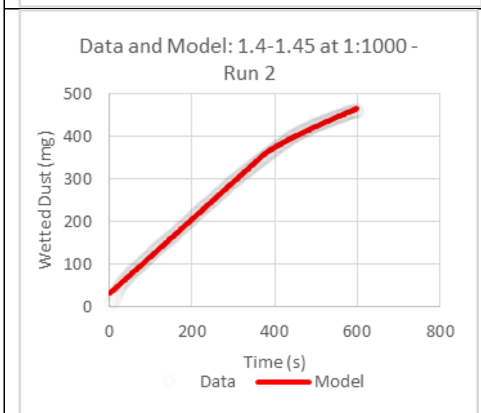

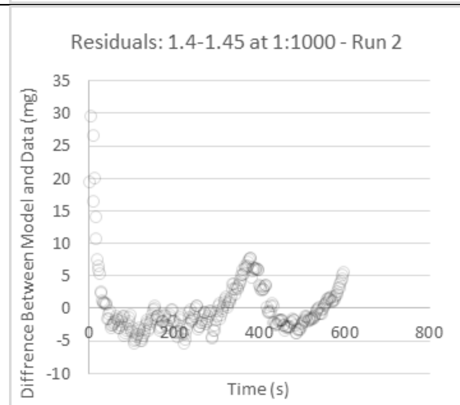

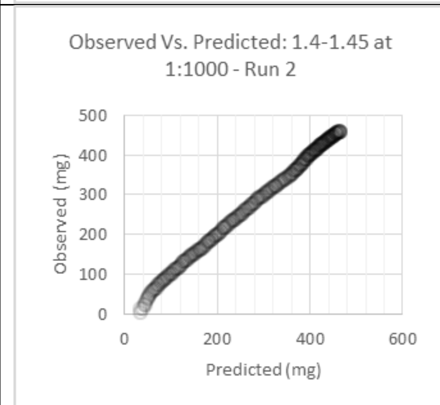

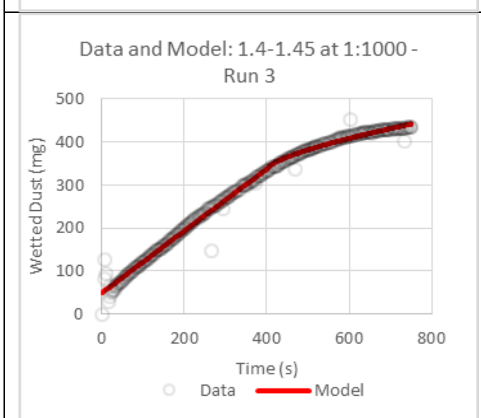

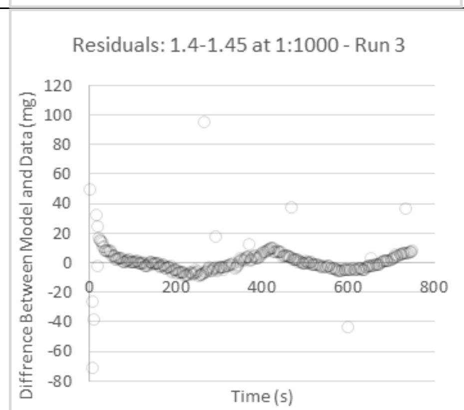

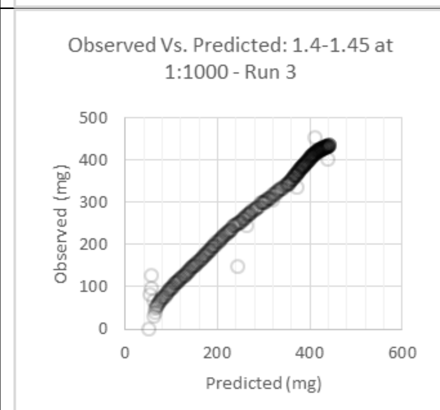

Table 25:A25 - Tabulated sink test using dust with gravity 1.5-1.6 and surfactant concentration 1:5000 in triplicate

Data and Model	Residuals	Observed Vs. Predicted
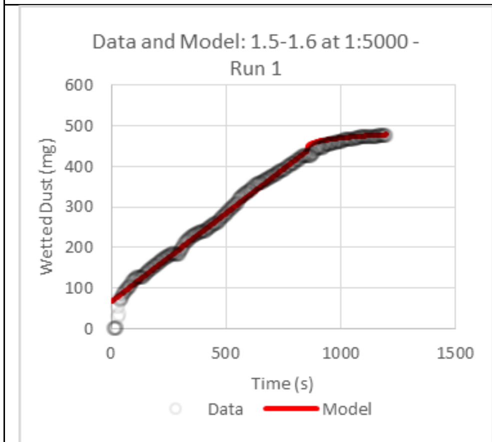	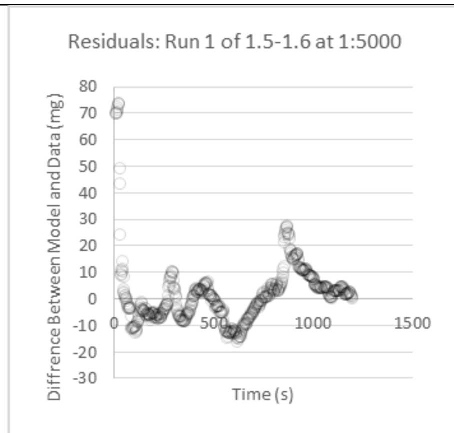	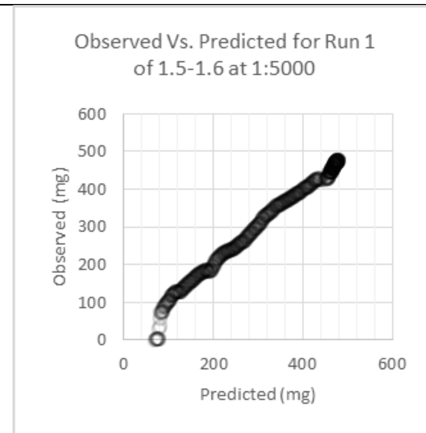
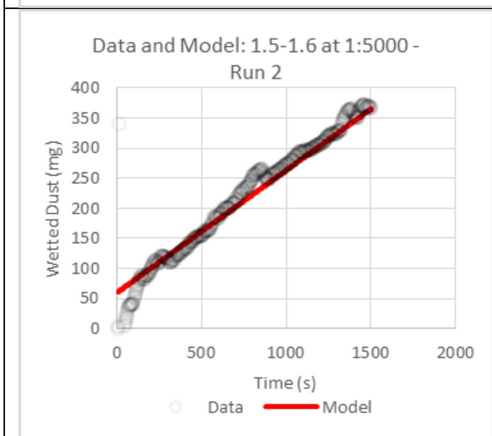	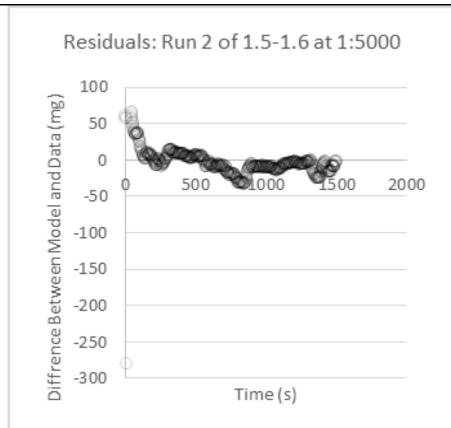	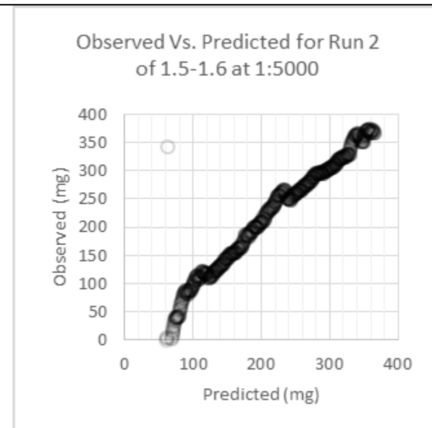
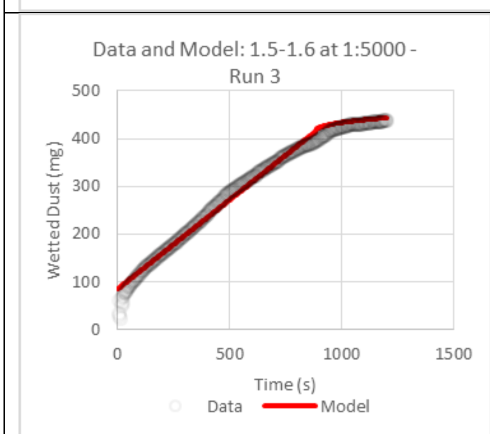	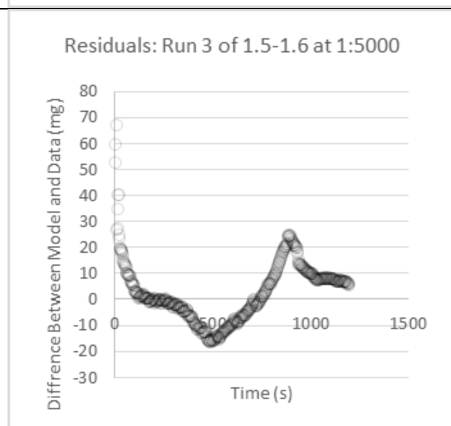	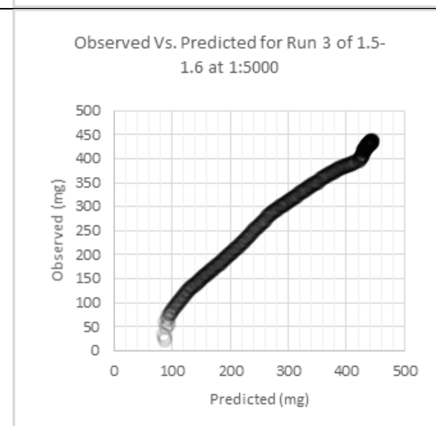

Table 26:A26 - Tabulated sink test using dust with gravity 1.5-1.6 and surfactant concentration 1:3000 in triplicate

Data and Model	Residuals	Observed Vs. Predicted

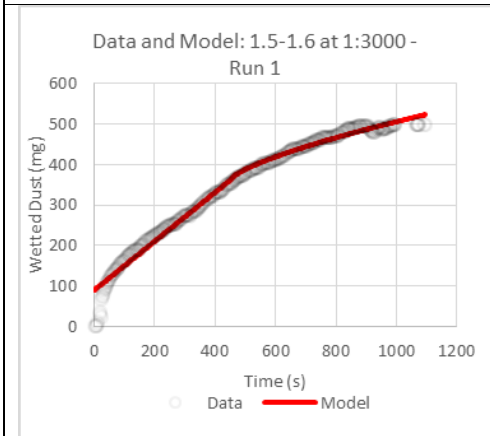

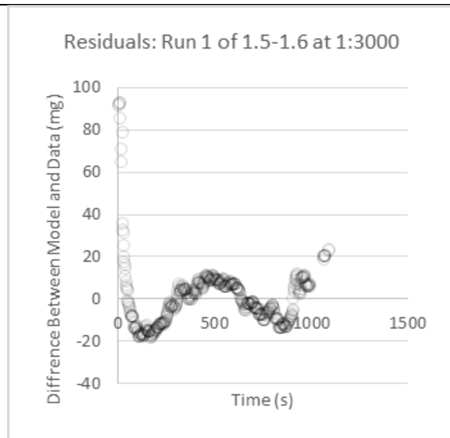

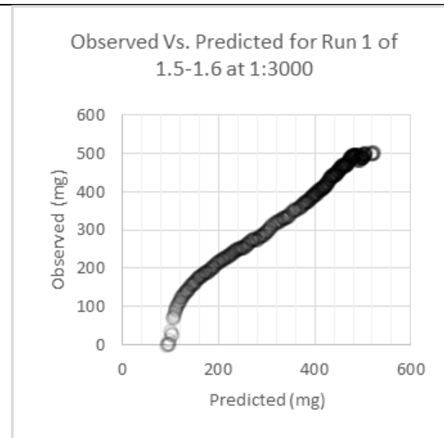

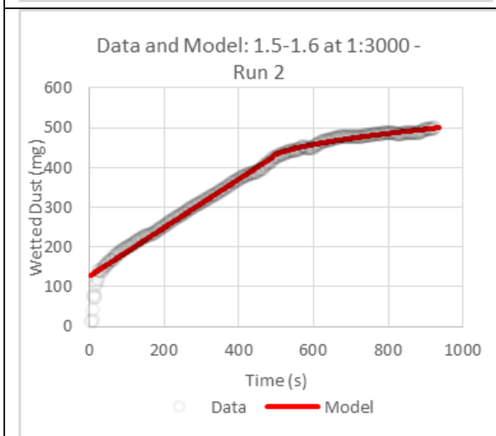

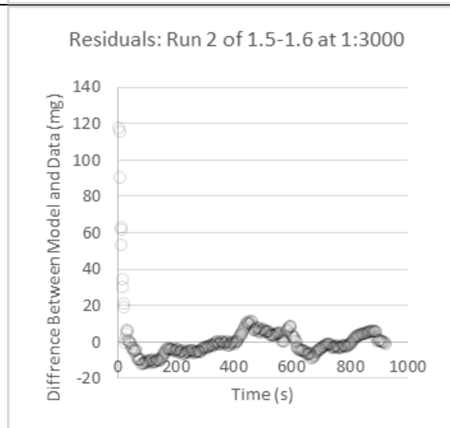

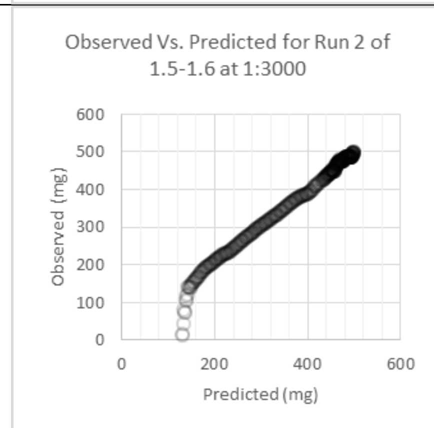

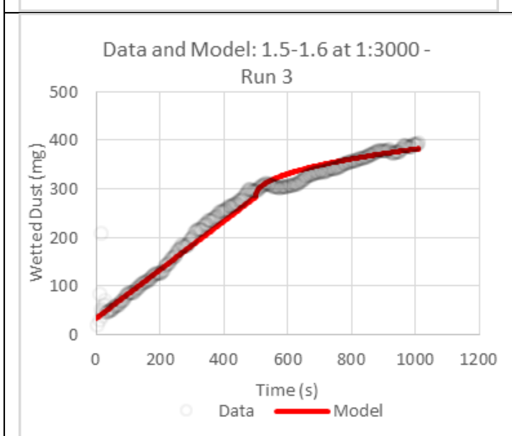

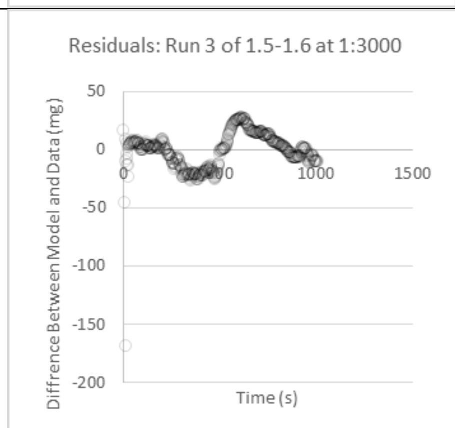

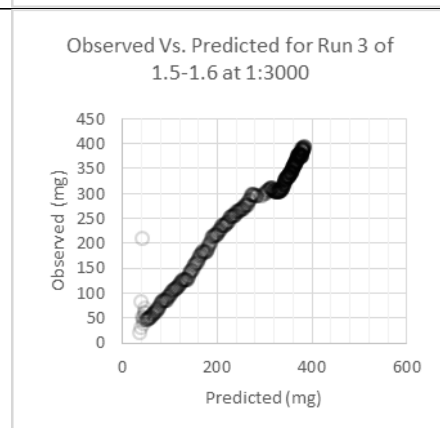

Table 27:A27 - Tabulated sink test using dust with gravity 1.5-1.6 and surfactant concentration 1:1000 in triplicate

Data and Model	Residuals	Observed Vs. Predicted
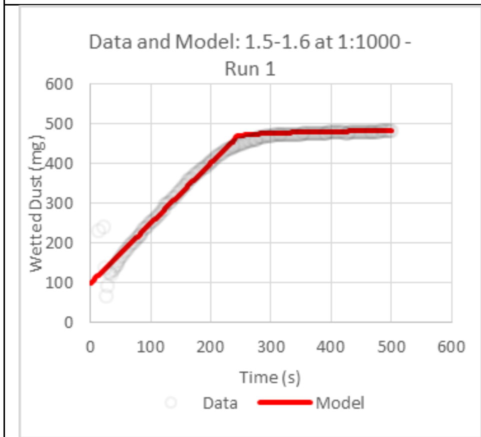	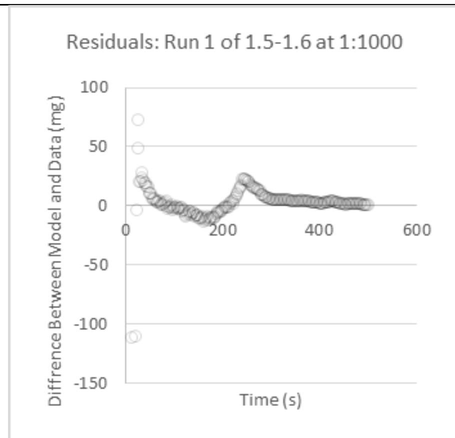	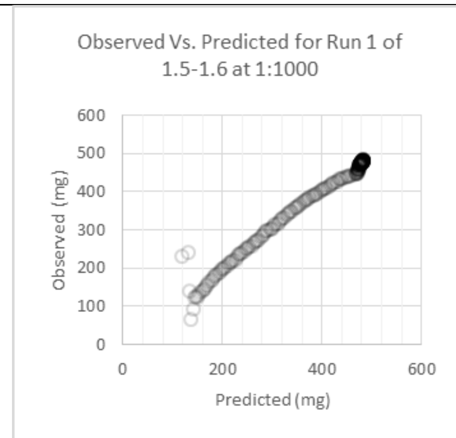
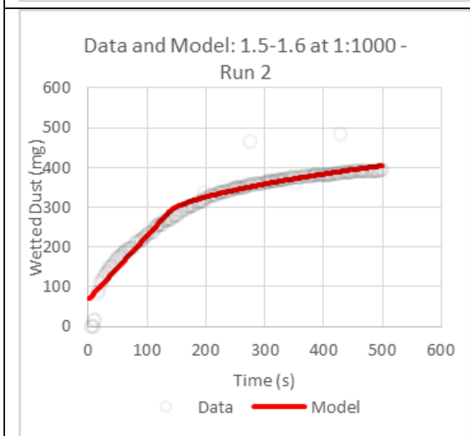	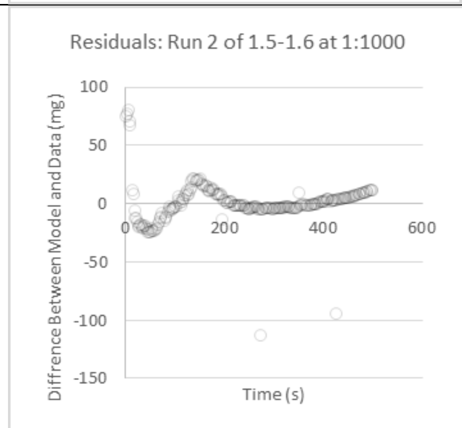	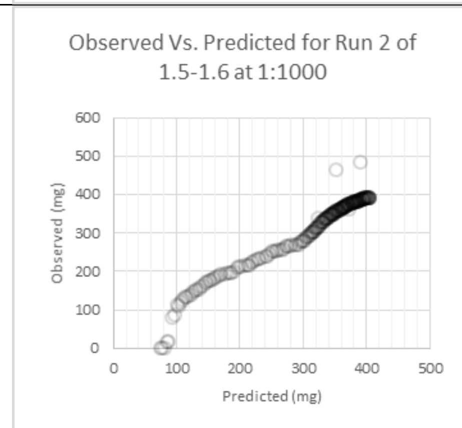
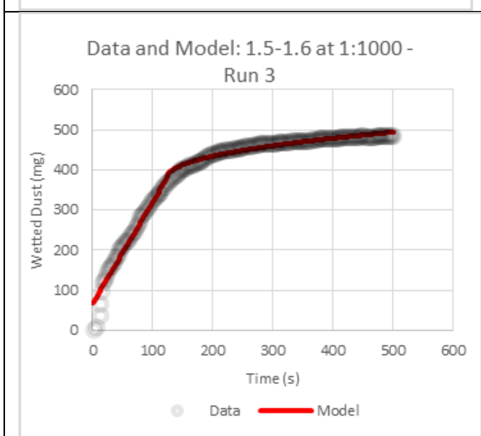	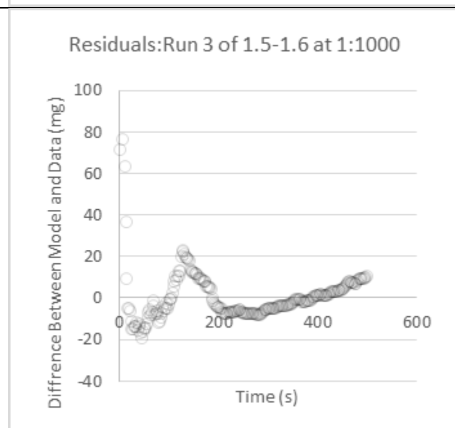	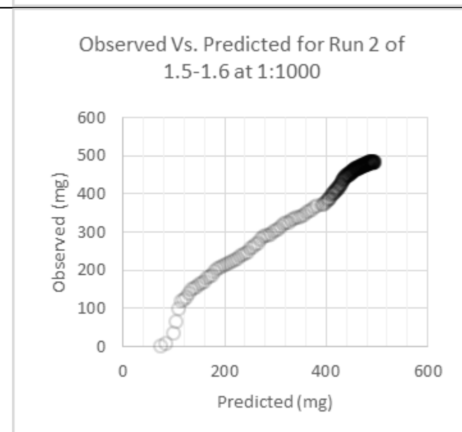

Table 28:A28 - Analysis of wetting rates obtained from the models from triplicate testing

Data used in Analysis:

Surfactant Dosage	Gravity Class		
	1.3-1.35	1.4-1.45	1.5-1.6
1:5000	0.110	0.075	0.435
	0.196	0.259	0.204
	0.172	0.215	0.374
1:3000	0.189	0.293	0.605
	0.187	0.241	0.610
	0.202	0.228	0.500
1:1000	0.569	0.849	1.512
	0.590	0.877	1.596
	0.646	0.723	2.524

Description of Data:

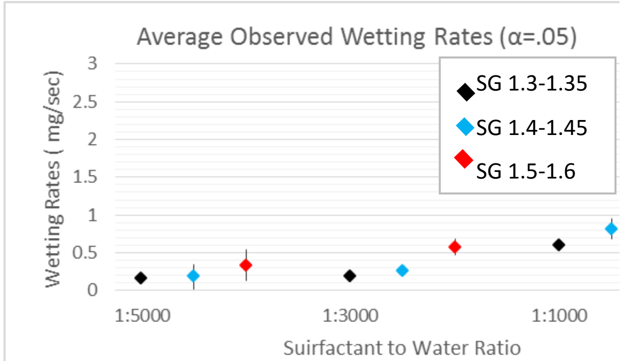

Coefficient of Determination of models

Surfactant Dosage	Gravity Class		
	1.3-1.35	1.4-1.45	1.5-1.6
1:5000	0.984	0.992	0.991
	0.987	0.994	0.972
	0.997	0.992	0.991
1:3000	0.981	0.963	0.987
	0.997	0.999	0.990
	0.986	0.994	0.979
1:1000	0.993	0.996	0.984
	0.993	0.999	0.963
	0.998	0.993	0.989

Analysis: ANOVA Two-Factor With Replication (α=0.05)

H_{0a}: There is no significant difference in the wetting rates correlated to the surfactant dosage ratio
H_{0b}: There is no significant difference in the wetting rates correlated to the gravity class
H_{0c}: There is no interaction between the variables mention in H_{0a} and H_{0b}

	SUMMARY	1.3-1.35	1.4-1.45	1.5-1.6	Total		
1:5000	Count	3	3	3	9		
	Sum	0.48	0.55	1.01	2.04		
	Average	0.16	0.18	0.34	0.23		
	Variance	0.00	0.01	0.01	0.01		
1:3000	Count	3	3	3	9		
	Sum	0.58	0.76	1.71	3.05		
	Average	0.19	0.25	0.57	0.34		
	Variance	0.00	0.00	0.00	0.03		
1:1000	Count	3	3	3	9		
	Sum	1.81	2.45	5.63	9.89		
	Average	0.60	0.82	1.88	1.10		
	Variance	0.00	0.01	0.32	0.43		
AVOVA	Source of Variation	SS	df	MS	F	P-value	F crit
	Surfactant Dosage	4.05	2.00	2.02	51.41	0.00	3.55
	Gravity Class	1.93	2.00	0.97	24.55	0.00	3.55
	Interaction	1.17	4.00	0.29	7.43	0.00	2.93
	Within	0.71	18	0.04			
	Total	7.86	26				

Results: H_{0a} is rejected, H_{0b} is rejected, and H_{0c} is rejected

Conclusion: There is a significant difference in the wetting rates which correlate with both the Surfactant dosage and the Gravity class. There is also, a less considerable, but still significant interaction between the two variables.

Table 29:A29 - Tabulated sink test using dust with gravity 1.3 float

Data and Model	Residuals	Observed Vs. Predicted
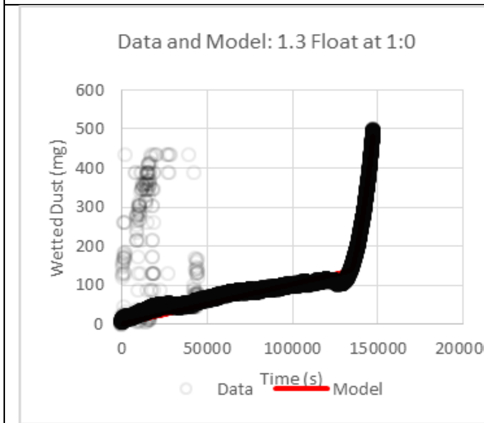	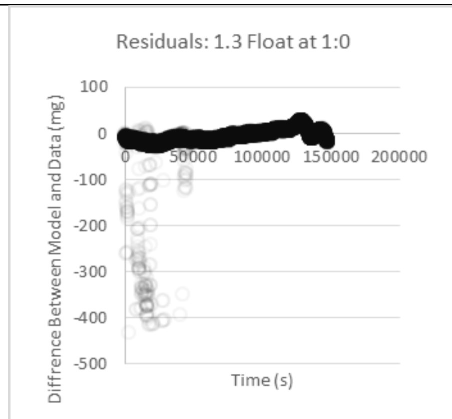	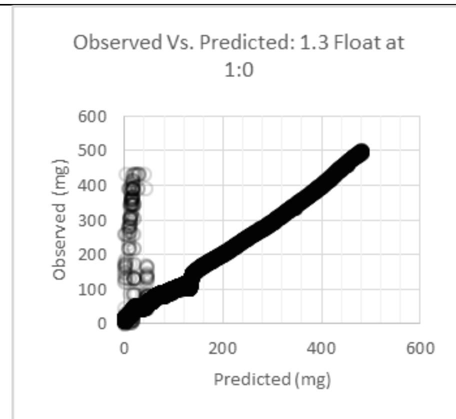
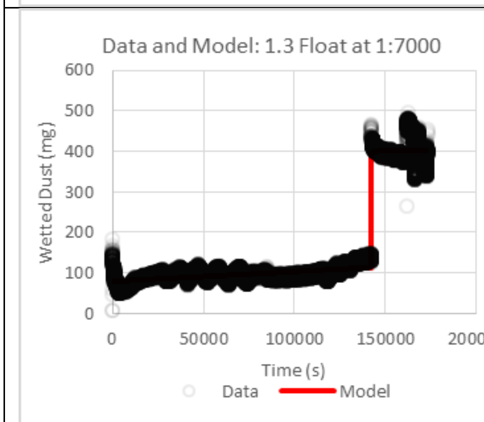	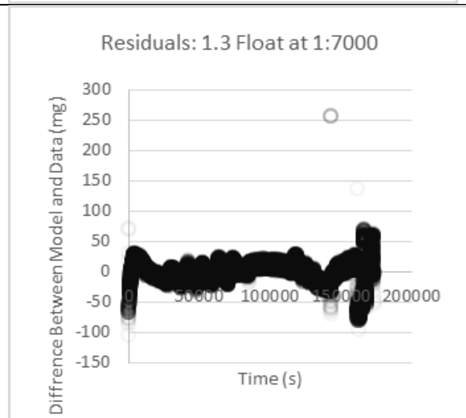	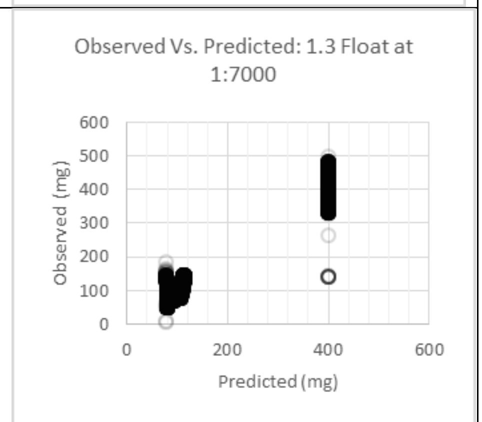
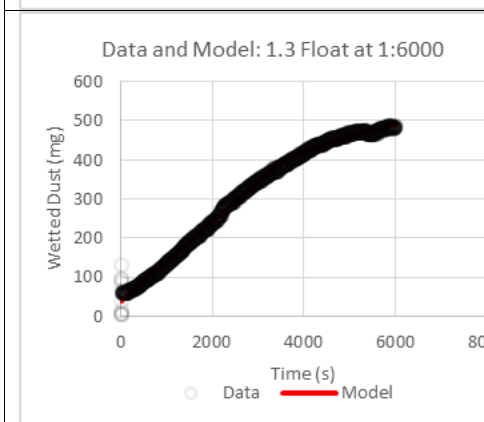	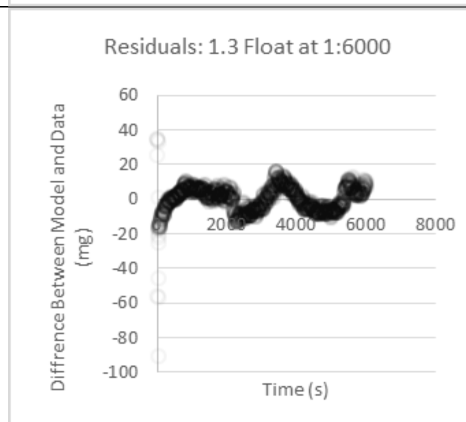	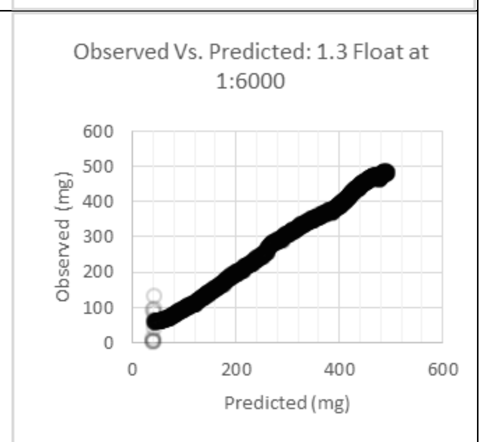

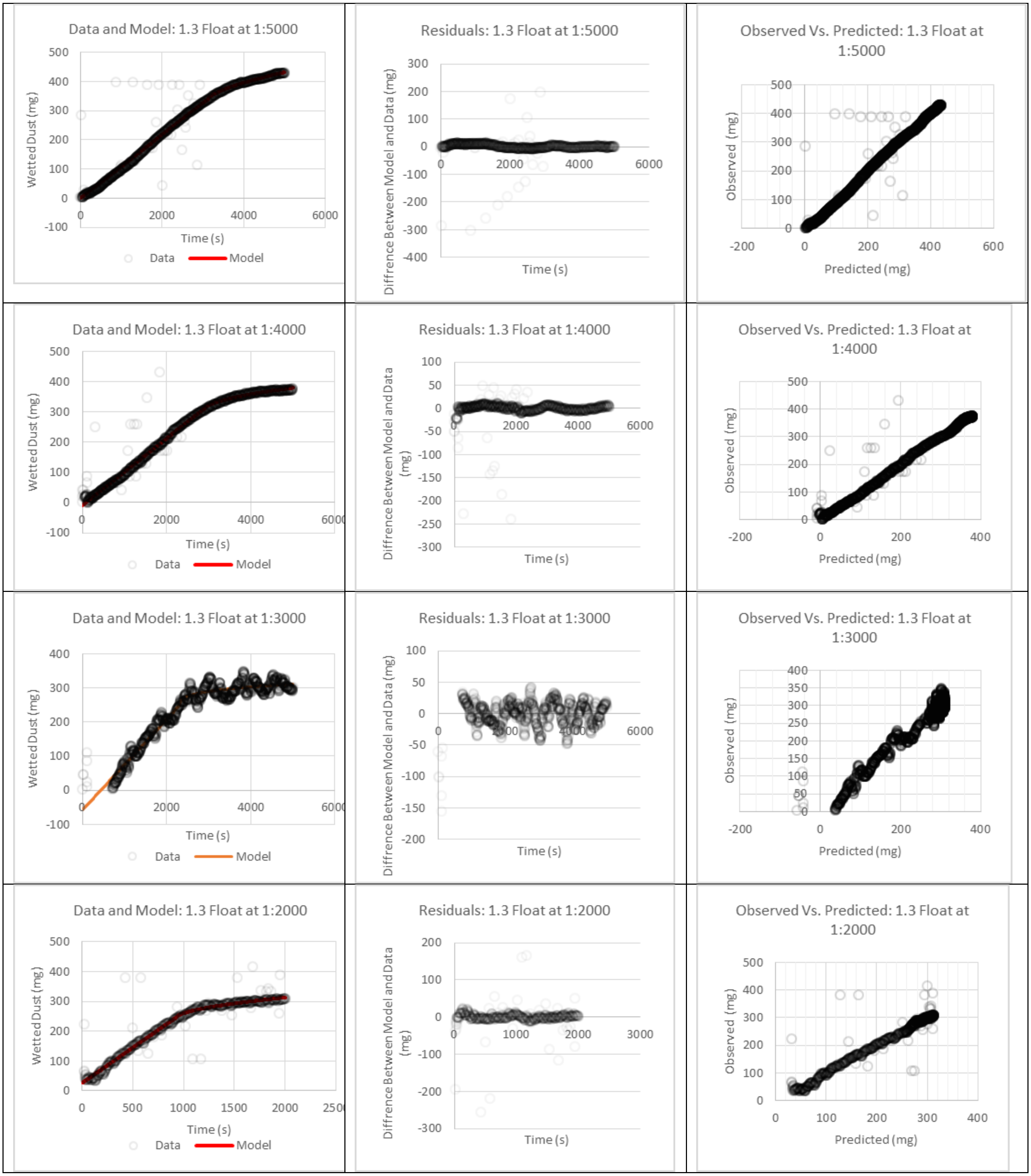

Data and Model: 1.3 Float at 1:5000
Wetted Dust (mg)
Time (s)
Data
Model
Residuals: 1.3 Float at 1:5000
Diffrence Between Model and Data (mg)
Time (s)
Observed Vs. Predicted: 1.3 Float at 1:5000
Observed (mg)
Predicted (mg)
Data and Model: 1.3 Float at 1:4000
Wetted Dust (mg)
Time (s)
Data
Model
Residuals: 1.3 Float at 1:4000
Diffrence Between Model and Data (mg)
Time (s)
Observed Vs. Predicted: 1.3 Float at 1:4000
Observed (mg)
Predicted (mg)
Data and Model: 1.3 Float at 1:3000
Wetted Dust (mg)
Time (s)
Data
Model
Residuals: 1.3 Float at 1:3000
Diffrence Between Model and Data (mg)
Time (s)
Observed Vs. Predicted: 1.3 Float at 1:3000
Observed (mg)
Predicted (mg)
Data and Model: 1.3 Float at 1:2000
Wetted Dust (mg)
Time (s)
Data
Model
Residuals: 1.3 Float at 1:2000
Diffrence Between Model and Data (mg)
Time (s)
Observed Vs. Predicted: 1.3 Float at 1:2000
Observed (mg)
Predicted (mg)

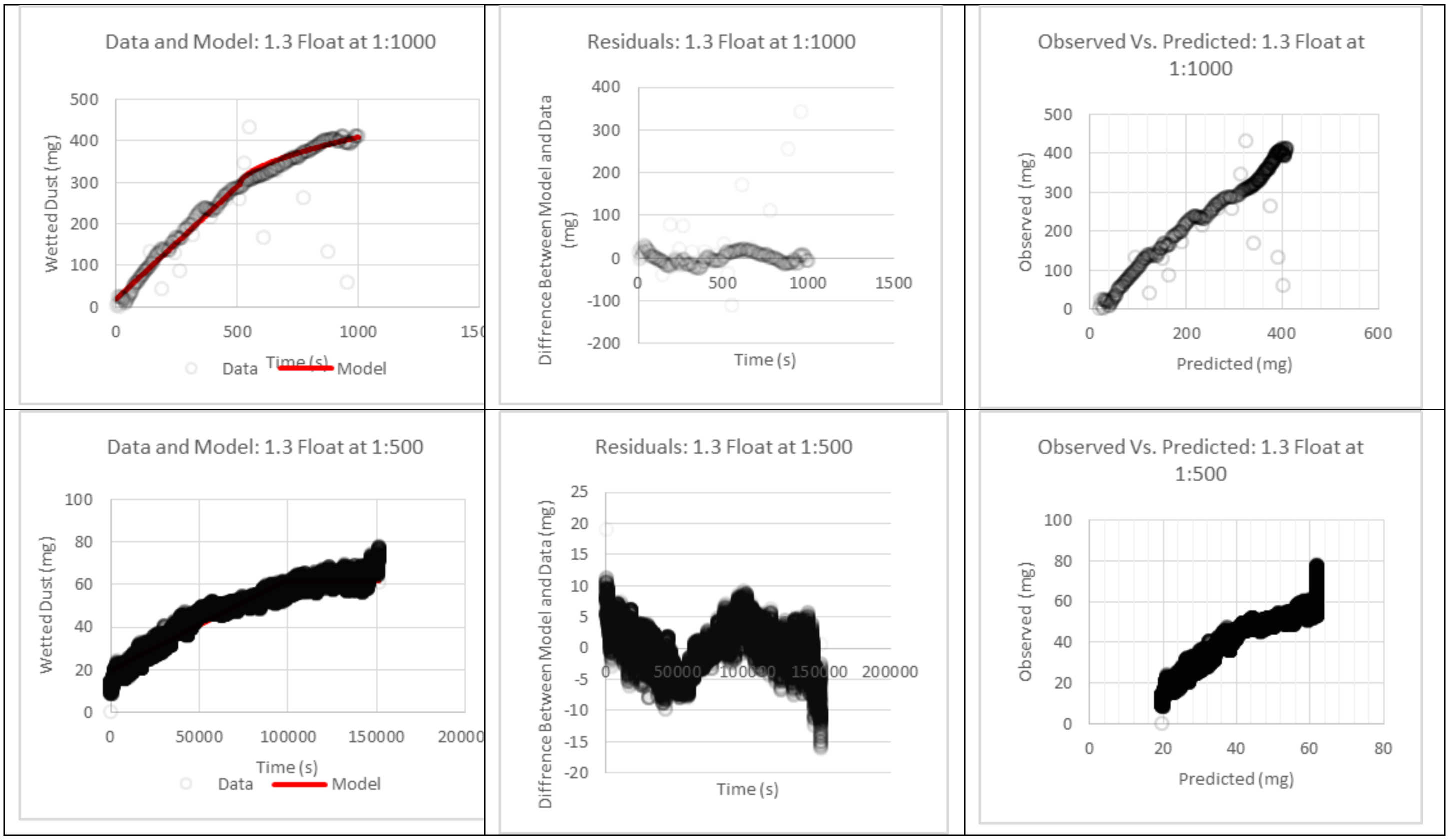
Data and Model: 1.3 Float at 1:1000
Wetted Dust (mg)
Time (s)
Data
Model
Residuals: 1.3 Float at 1:1000
Diffrence Between Model and Data (mg)
Time (s)
Observed Vs. Predicted: 1.3 Float at 1:1000
Observed (mg)
Predicted (mg)
Data and Model: 1.3 Float at 1:500
Wetted Dust (mg)
Time (s)
Data
Model
Residuals: 1.3 Float at 1:500
Diffrence Between Model and Data (mg)
Time (s)
Observed Vs. Predicted: 1.3 Float at 1:500
Observed (mg)
Predicted (mg)

Table 30:A30 - Tabulated sink test using dust with gravity 1.3-1.35

Data and Model	Residuals	Observed Vs. Predicted

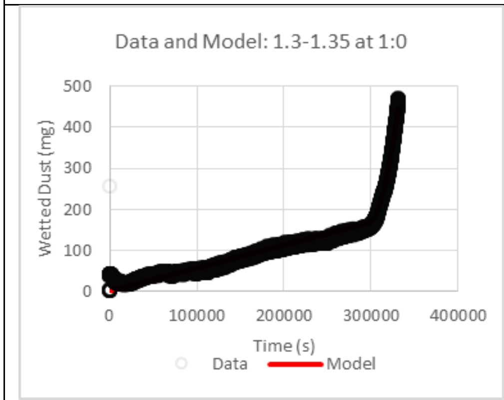

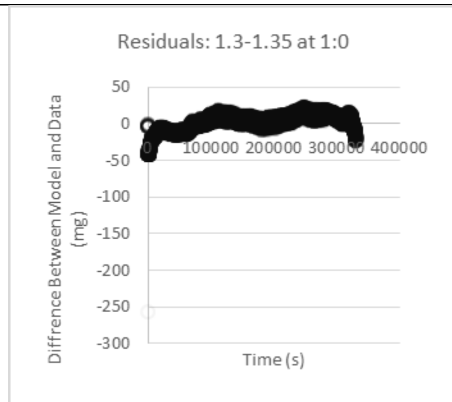

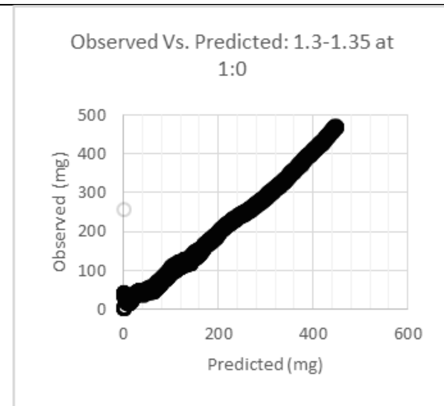

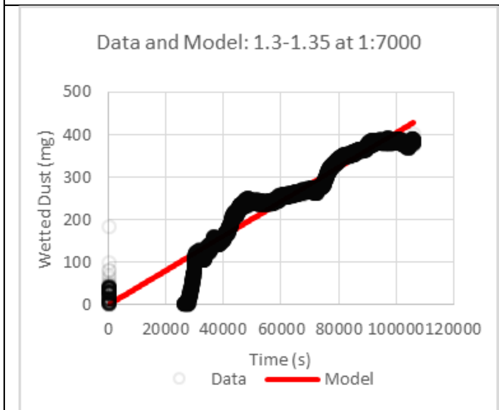

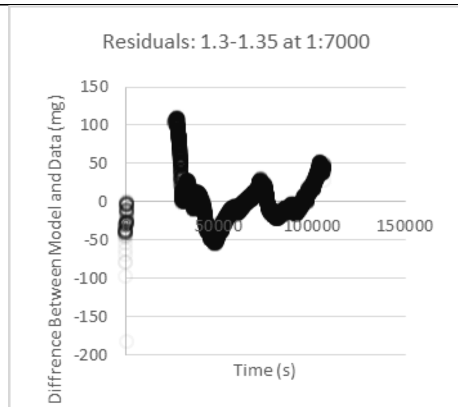

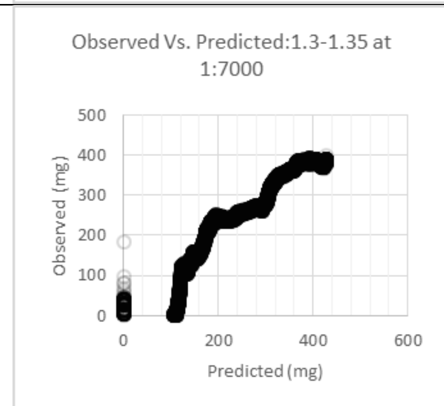

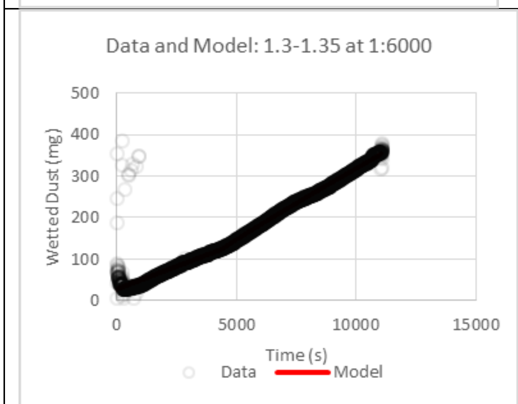

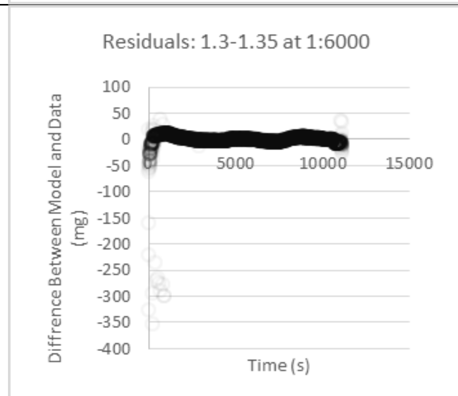

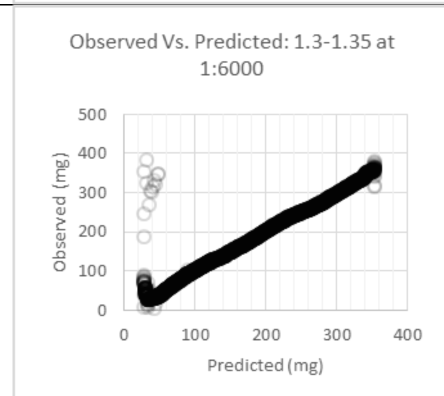

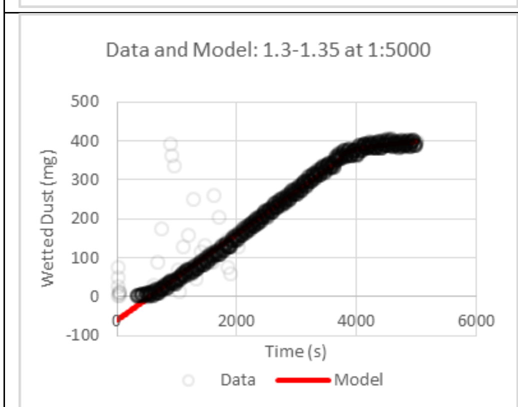

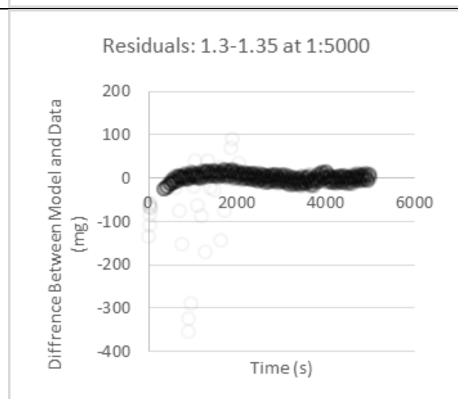

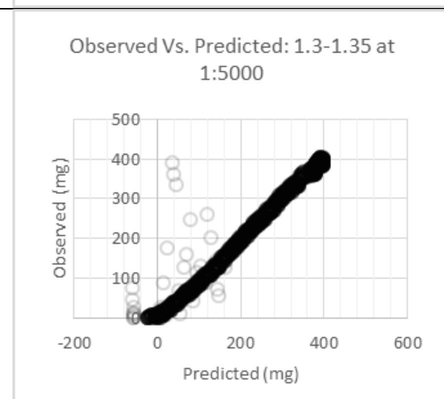

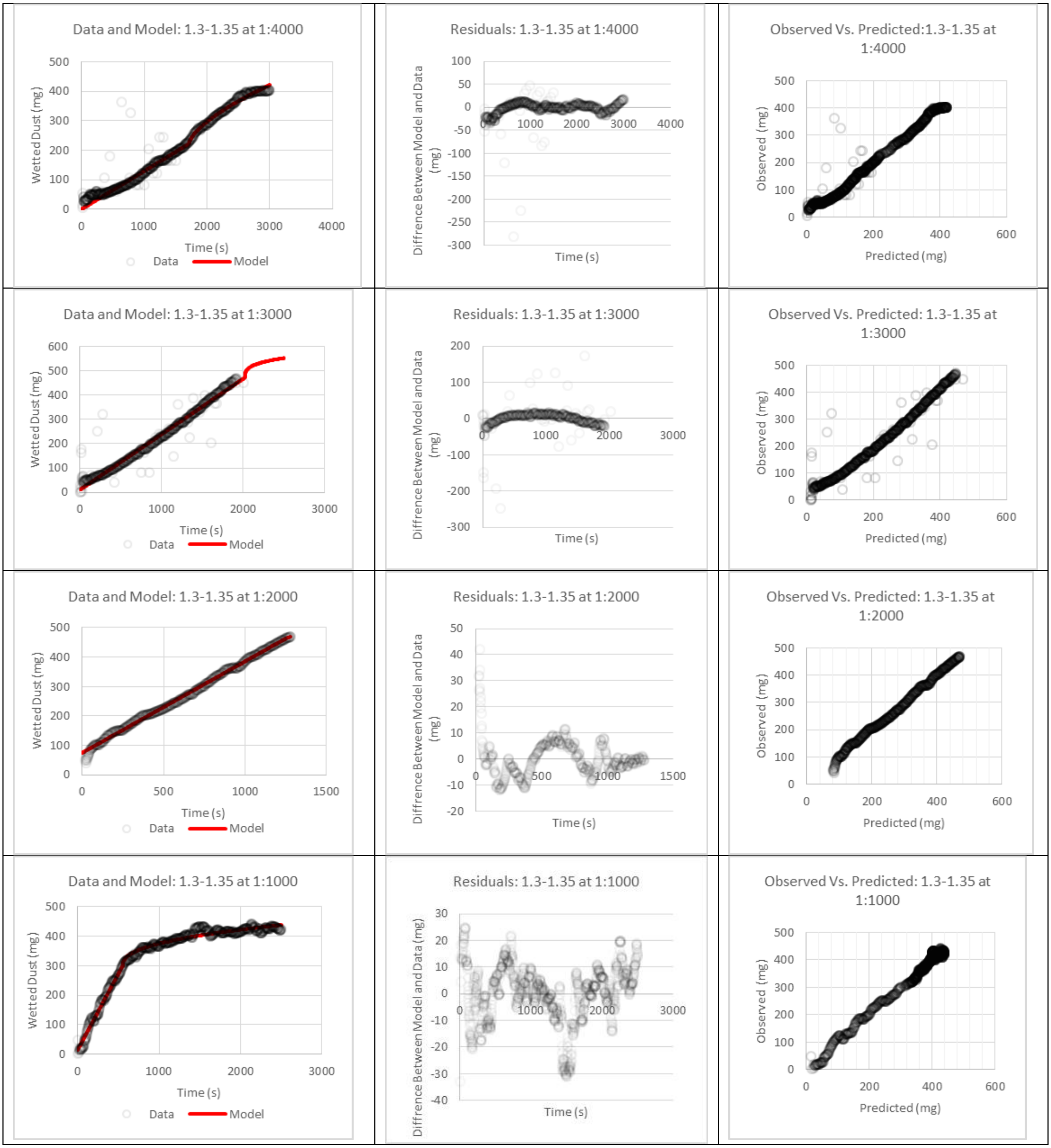
Data and Model: 1.3-1.35 at 1:4000
Wetted Dust (mg)
Time (s)
Data
Model
Residuals: 1.3-1.35 at 1:4000
Diffrence Between Model and Data (mg)
Time (s)
Observed Vs. Predicted:1.3-1.35 at 1:4000
Observed (mg)
Predicted (mg)
Data and Model: 1.3-1.35 at 1:3000
Wetted Dust (mg)
Time (s)
Data
Model
Residuals: 1.3-1.35 at 1:3000
Diffrence Between Model and Data (mg)
Time (s)
Observed Vs. Predicted: 1.3-1.35 at 1:3000
Observed (mg)
Predicted (mg)
Data and Model: 1.3-1.35 at 1:2000
Wetted Dust (mg)
Time (s)
Data
Model
Residuals: 1.3-1.35 at 1:2000
Diffrence Between Model and Data (mg)
Time (s)
Observed Vs. Predicted: 1.3-1.35 at 1:2000
Observed (mg)
Predicted (mg)
Data and Model: 1.3-1.35 at 1:1000
Wetted Dust (mg)
Time (s)
Data
Model
Residuals: 1.3-1.35 at 1:1000
Diffrence Between Model and Data (mg)
Time (s)
Observed Vs. Predicted: 1.3-1.35 at 1:1000
Observed (mg)
Predicted (mg)

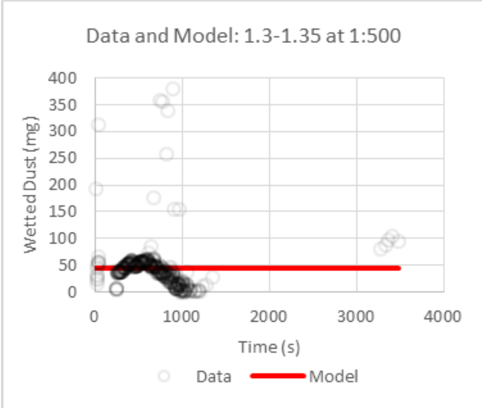
Data and Model: 1.3-1.35 at 1:500
Wetted Dust (mg)
400
350
300
250
200
150
100
50
0
0
1000
2000
3000
4000
Time (s)
Data
Model

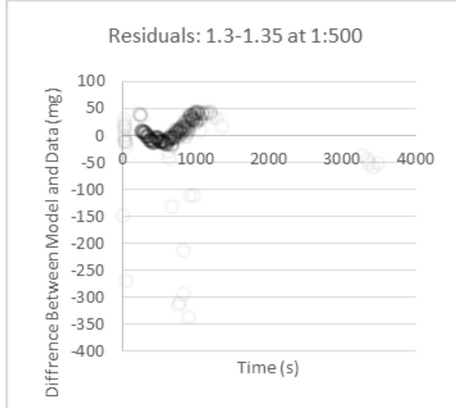
Residuals: 1.3-1.35 at 1:500
Diffrence Between Model and Data (mg)
100
50
0
-50
-100
-150
-200
-250
-300
-350
-400
0
1000
2000
3000
4000
Time (s)

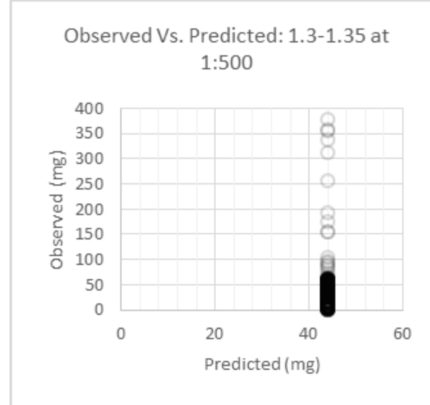
Observed Vs. Predicted: 1.3-1.35 at 1:500
Observed (mg)
400
350
300
250
200
150
100
50
0
0
20
40
60
Predicted (mg)

Table 31:A31 - Tabulated sink test using dust with gravity 1.35-1.4

Data and Model	Residuals	Observed Vs. Predicted

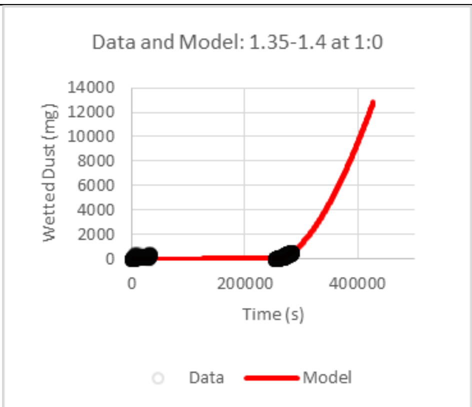

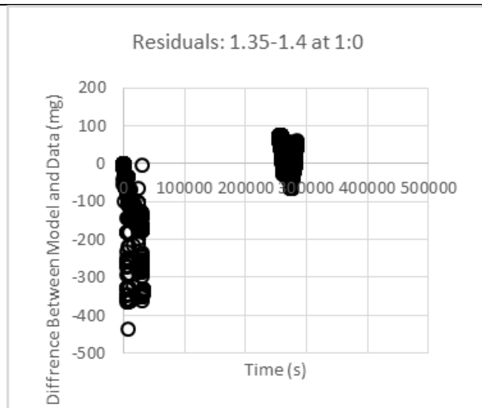

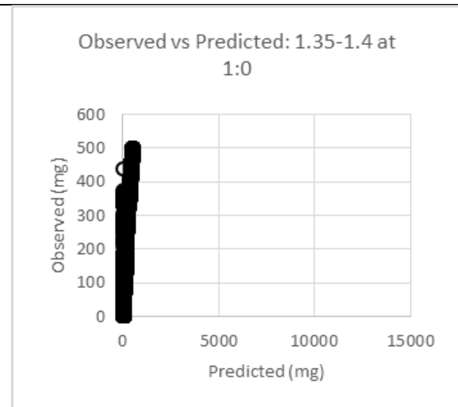

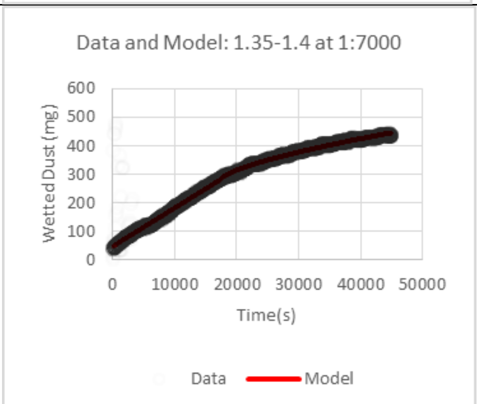

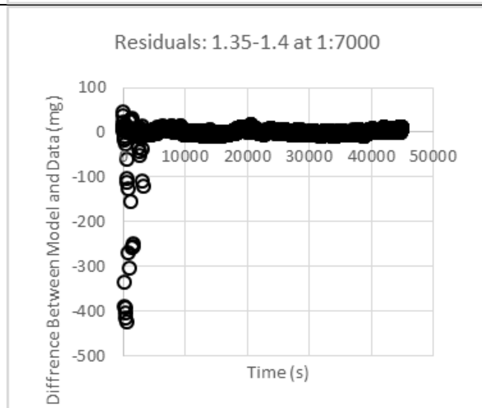

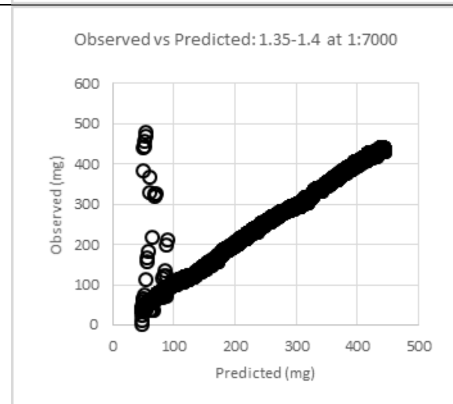

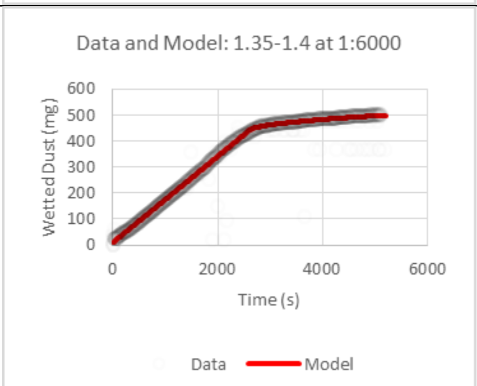

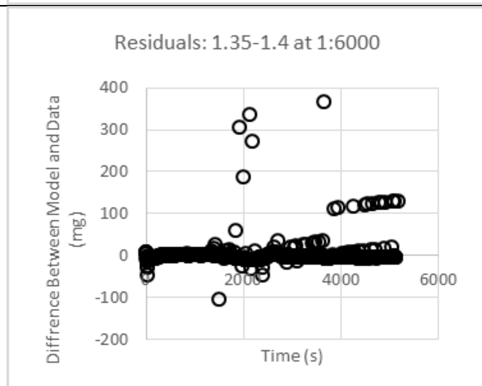

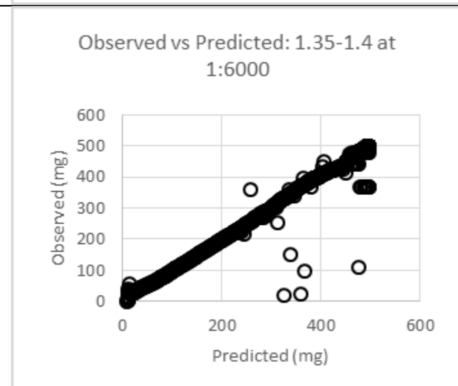

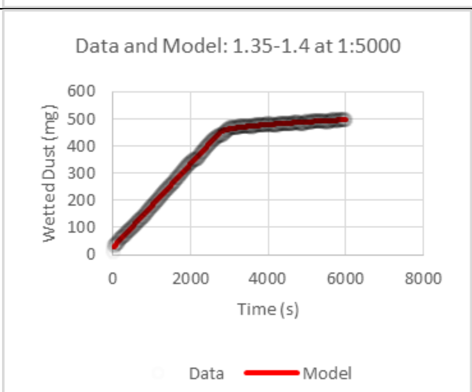

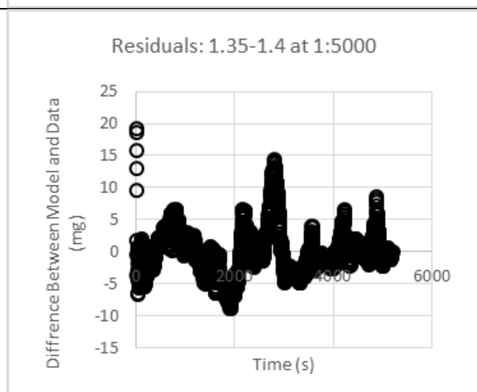

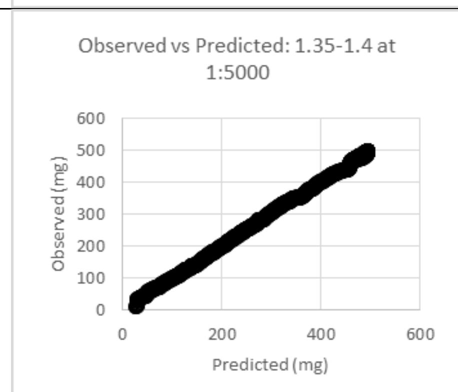

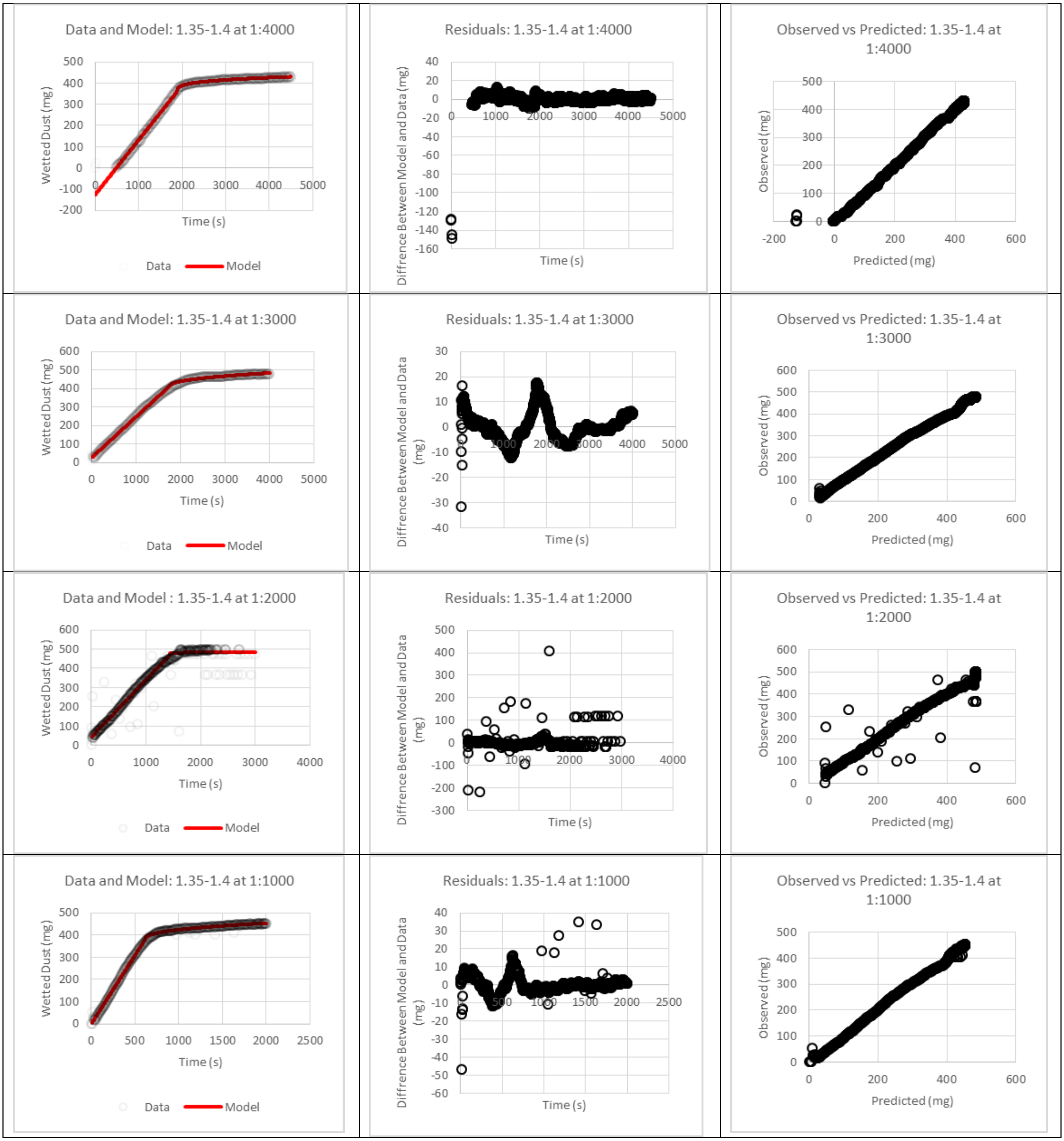
Data and Model: 1.35-1.4 at 1:4000
Wetted Dust (mg)
Time (s)
Data
Model
Residuals: 1.35-1.4 at 1:4000
Diffrence Between Model and Data (mg)
Time (s)
Observed vs Predicted: 1.35-1.4 at 1:4000
Observed (mg)
Predicted (mg)
Data and Model: 1.35-1.4 at 1:3000
Wetted Dust (mg)
Time (s)
Data
Model
Residuals: 1.35-1.4 at 1:3000
Diffrence Between Model and Data (mg)
Time (s)
Observed vs Predicted: 1.35-1.4 at 1:3000
Observed (mg)
Predicted (mg)
Data and Model : 1.35-1.4 at 1:2000
Wetted Dust (mg)
Time (s)
Data
Model
Residuals: 1.35-1.4 at 1:2000
Diffrence Between Model and Data (mg)
Time (s)
Observed vs Predicted: 1.35-1.4 at 1:2000
Observed (mg)
Predicted (mg)
Data and Model: 1.35-1.4 at 1:1000
Wetted Dust (mg)
Time (s)
Data
Model
Residuals: 1.35-1.4 at 1:1000
Diffrence Between Model and Data (mg)
Time (s)
Observed vs Predicted: 1.35-1.4 at 1:1000
Observed (mg)
Predicted (mg)

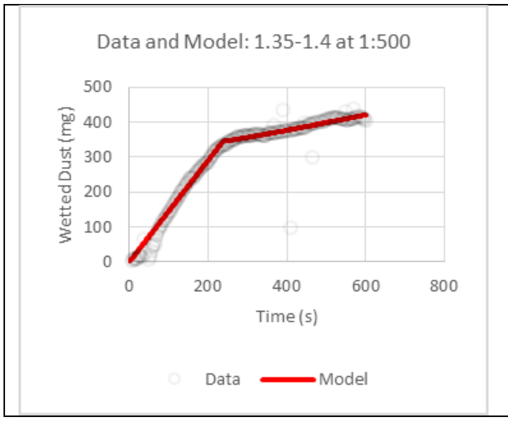
Data and Model: 1.35-1.4 at 1:500
Wetted Dust (mg)
500
400
300
200
100
0
0
200
400
600
800
Time (s)
Data
Model

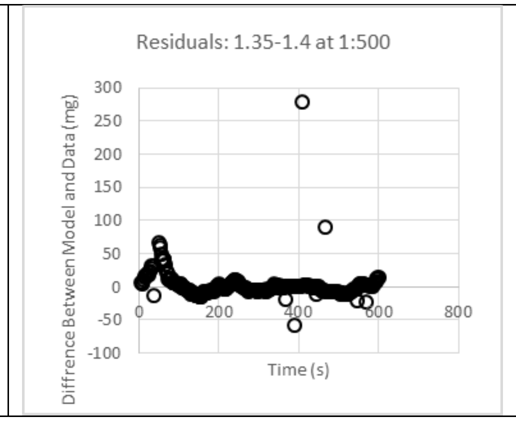
Residuals: 1.35-1.4 at 1:500
Diffrence Between Model and Data (mg)
300
250
200
150
100
50
0
-50
-100
0
200
400
600
800
Time (s)

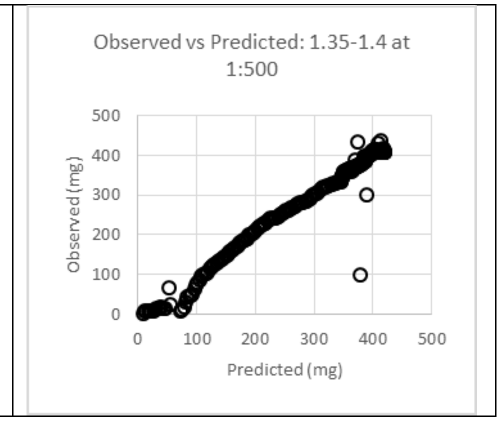
Observed vs Predicted: 1.35-1.4 at 1:500
Observed (mg)
500
400
300
200
100
0
0
100
200
300
400
500
Predicted (mg)

Table 32:A32 - Tabulated sink test using dust with gravity 1.4-1.45

<table>
<tr><th>Data and Model</th><th>Residuals</th><th>Observed Vs. Predicted</th></tr>
<tr>
<td>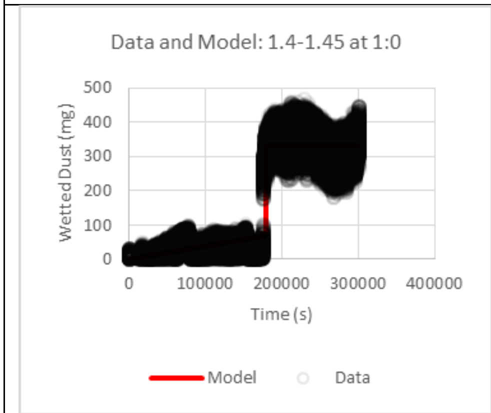
</td>
<td>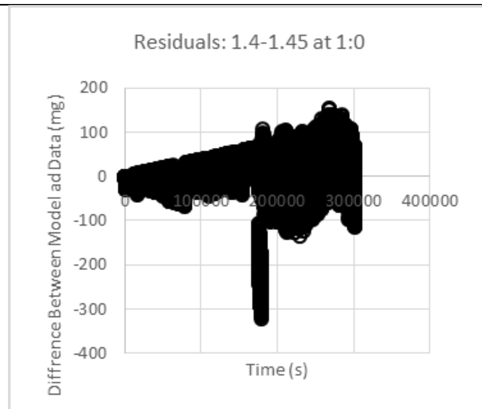
</td>
<td>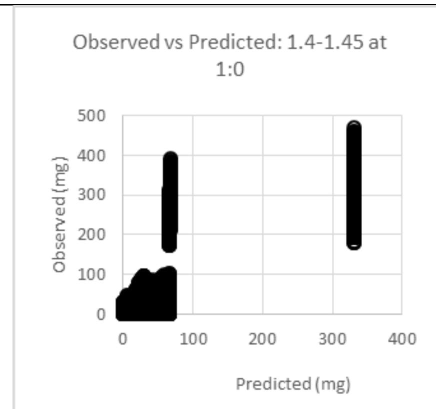
</td>
</tr>
<tr>
<td>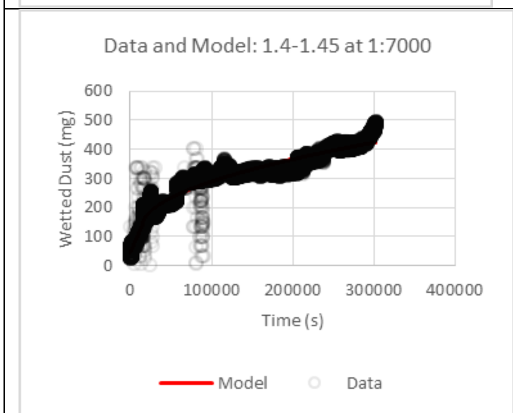
</td>
<td>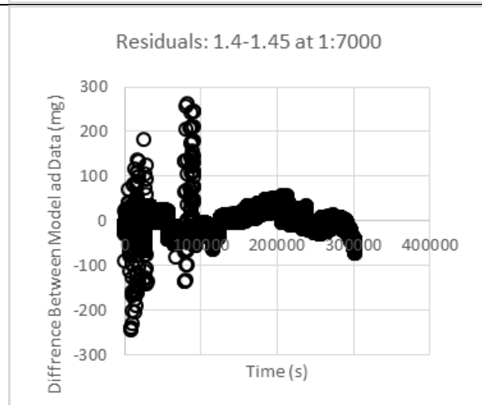
</td>
<td>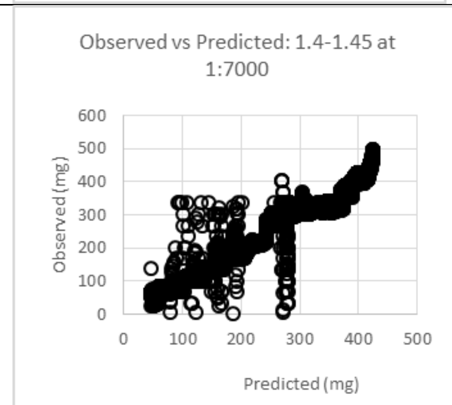
</td>
</tr>
<tr>
<td>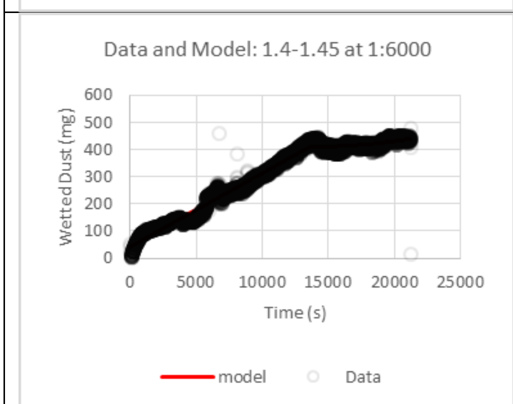
</td>
<td>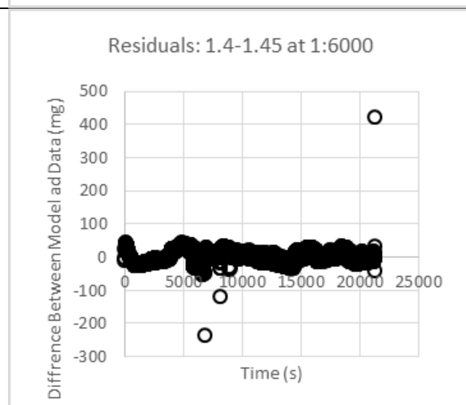
</td>
<td>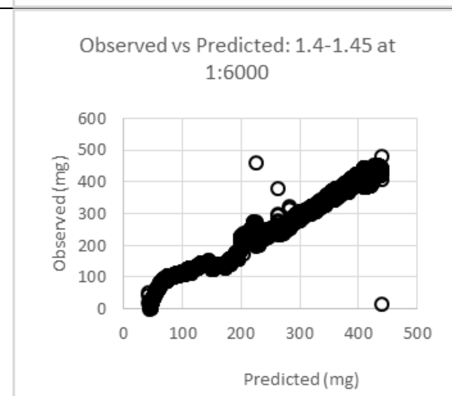
</td>
</tr>
</table>

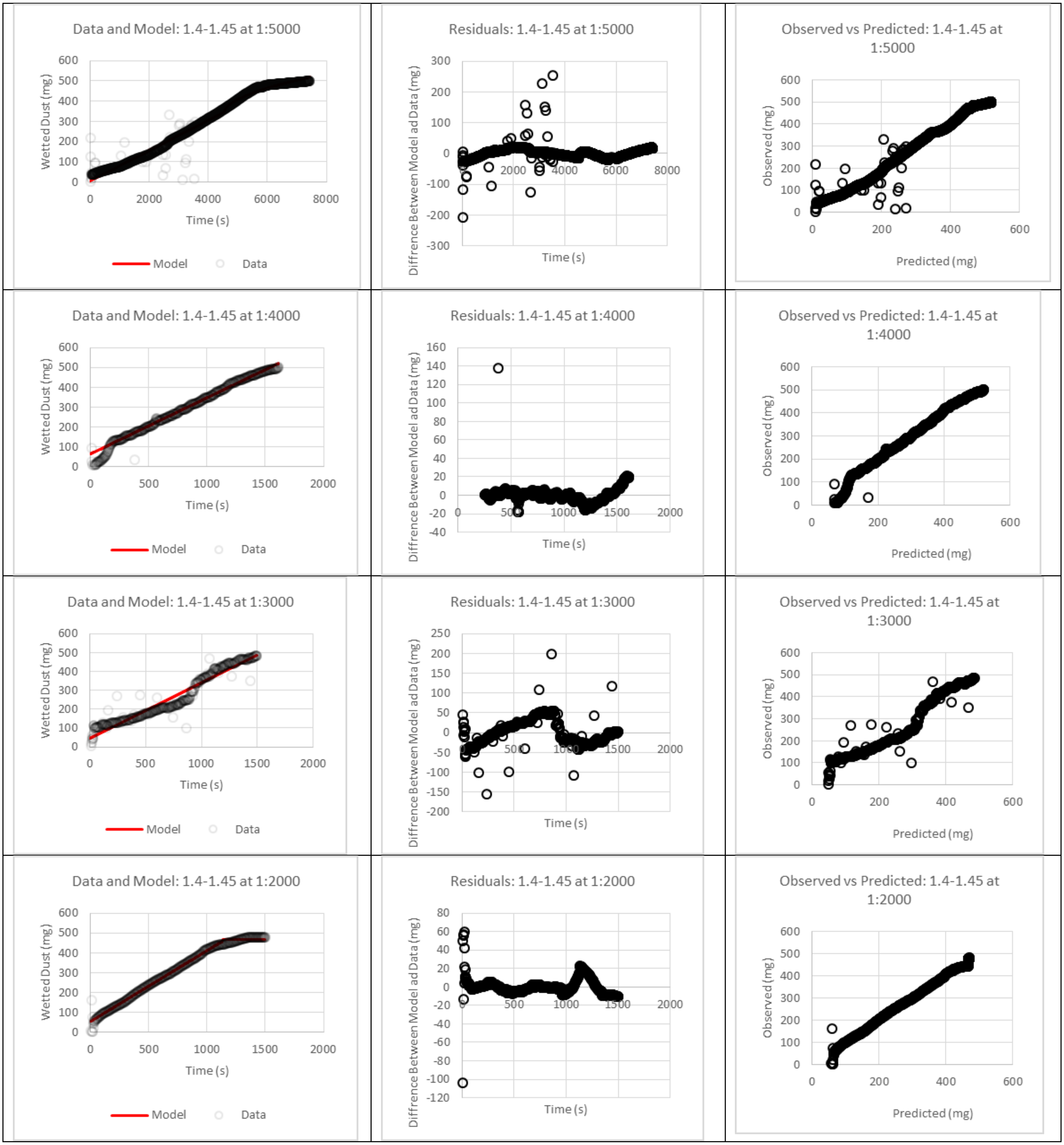

Data and Model: 1.4-1.45 at 1:5000
Wetted Dust (mg)
Time (s)
Model
Data
Residuals: 1.4-1.45 at 1:5000
Diffrence Between Model ad Data (mg)
Time (s)
Observed vs Predicted: 1.4-1.45 at 1:5000
Observed (mg)
Predicted (mg)
Data and Model: 1.4-1.45 at 1:4000
Wetted Dust (mg)
Time (s)
Model
Data
Residuals: 1.4-1.45 at 1:4000
Diffrence Between Model ad Data (mg)
Time (s)
Observed vs Predicted: 1.4-1.45 at 1:4000
Observed (mg)
Predicted (mg)
Data and Model: 1.4-1.45 at 1:3000
Wetted Dust (mg)
Time (s)
Model
Data
Residuals: 1.4-1.45 at 1:3000
Diffrence Between Model ad Data (mg)
Time (s)
Observed vs Predicted: 1.4-1.45 at 1:3000
Observed (mg)
Predicted (mg)
Data and Model: 1.4-1.45 at 1:2000
Wetted Dust (mg)
Time (s)
Model
Data
Residuals: 1.4-1.45 at 1:2000
Diffrence Between Model ad Data (mg)
Time (s)
Observed vs Predicted: 1.4-1.45 at 1:2000
Observed (mg)
Predicted (mg)

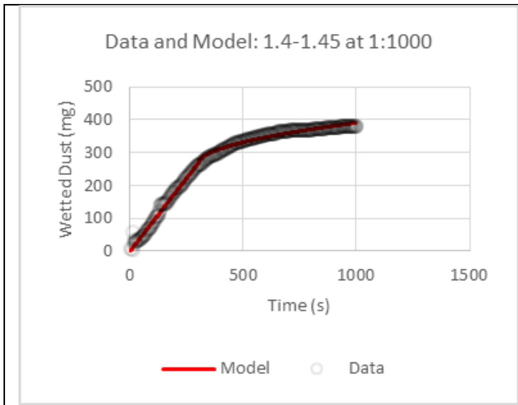
Data and Model: 1.4-1.45 at 1:1000
Wetted Dust (mg)
Time (s)
Model
Data

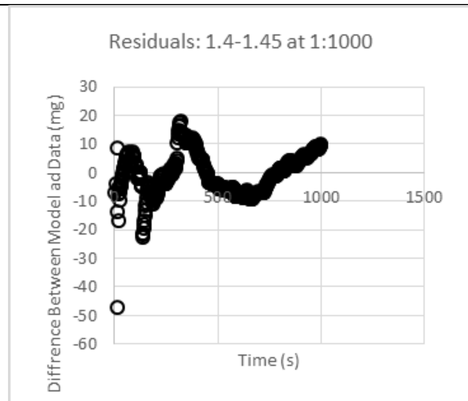
Residuals: 1.4-1.45 at 1:1000
Diffrence Between Model ad Data (mg)
Time (s)

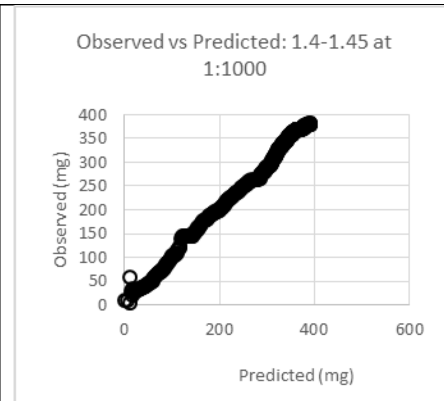
Observed vs Predicted: 1.4-1.45 at 1:1000
Observed (mg)
Predicted (mg)

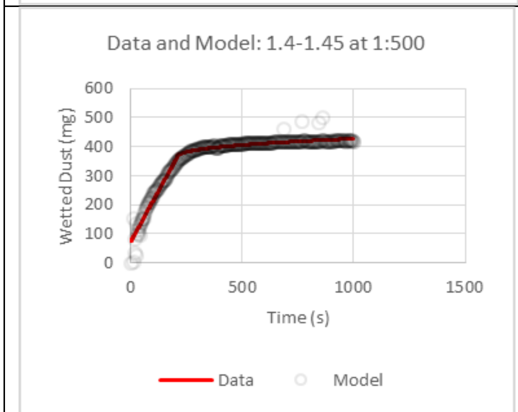
Data and Model: 1.4-1.45 at 1:500
Wetted Dust (mg)
Time (s)
Data
Model

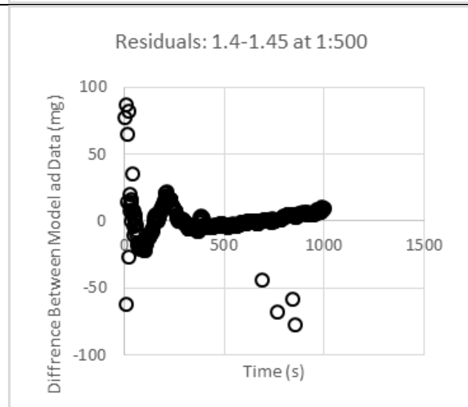
Residuals: 1.4-1.45 at 1:500
Diffrence Between Model ad Data (mg)
Time (s)

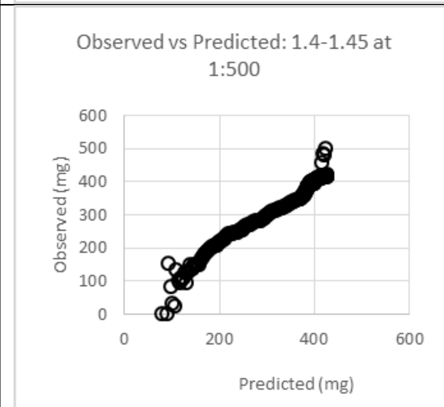
Observed vs Predicted: 1.4-1.45 at 1:500
Observed (mg)
Predicted (mg)

Table 33:A33 - Tabulated sink test using dust with gravity 1.45-1.5

Data and Model	Residuals	Observed Vs. Predicted
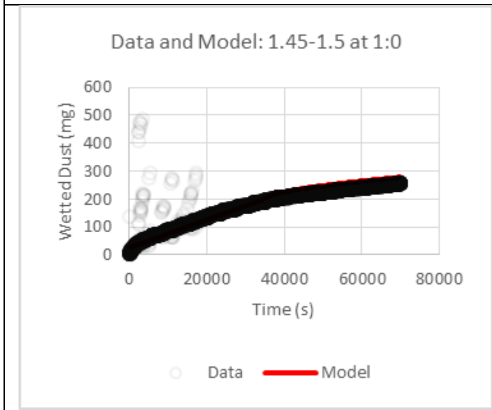	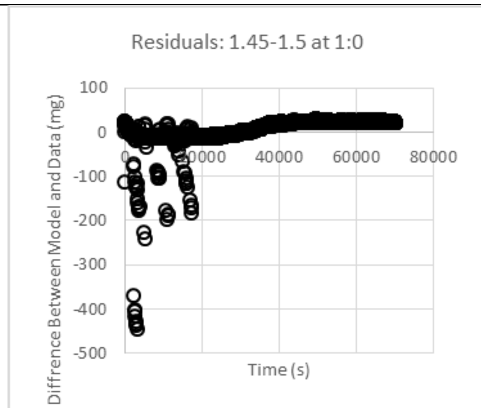	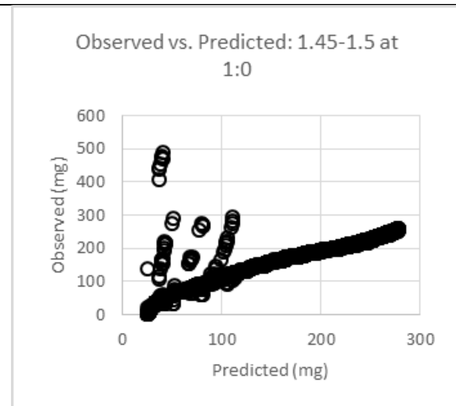
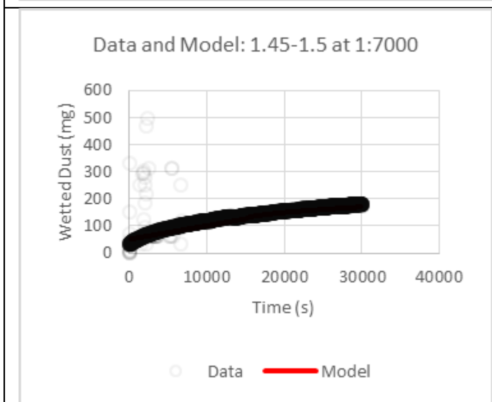	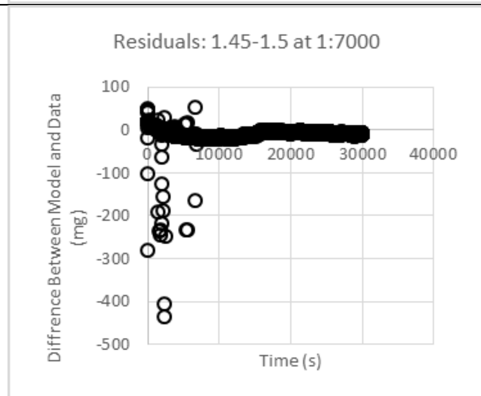	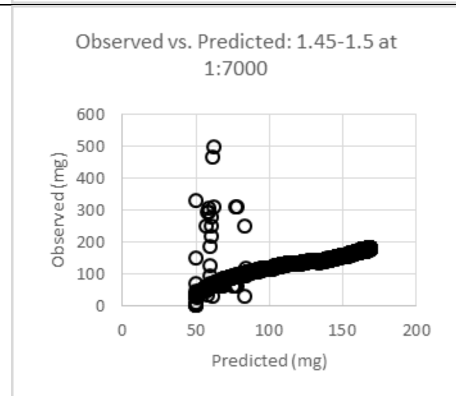
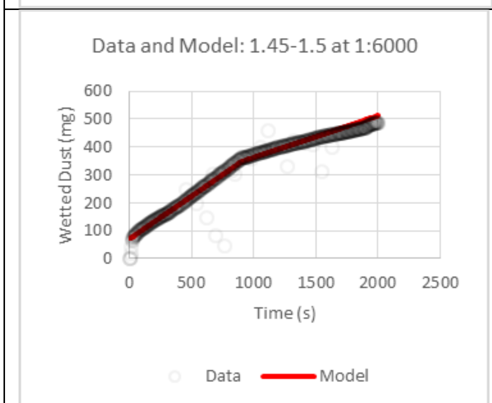	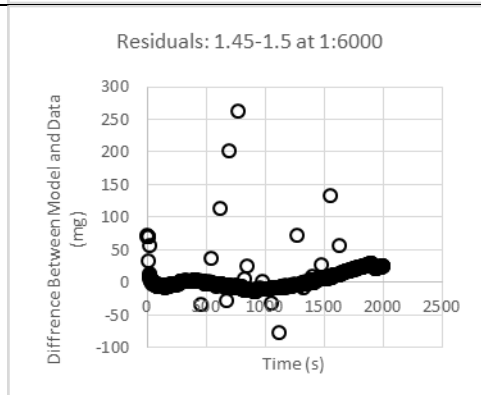	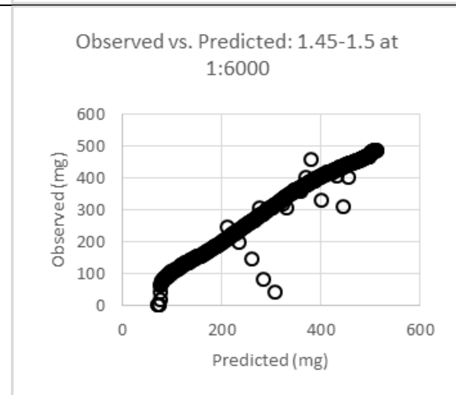
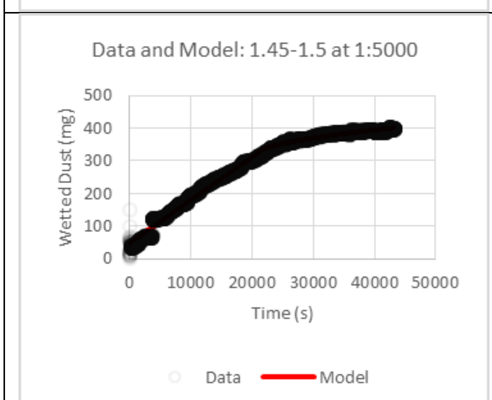	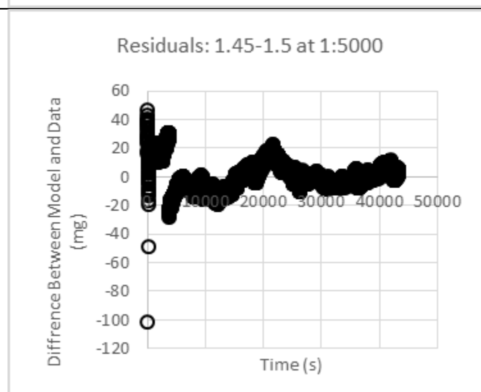	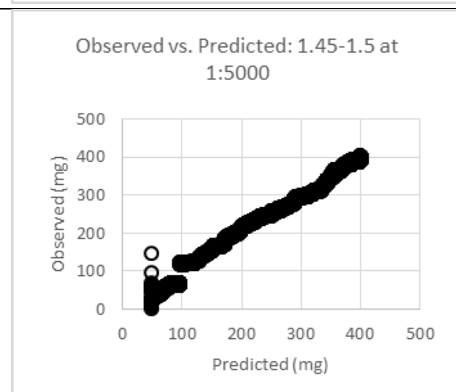

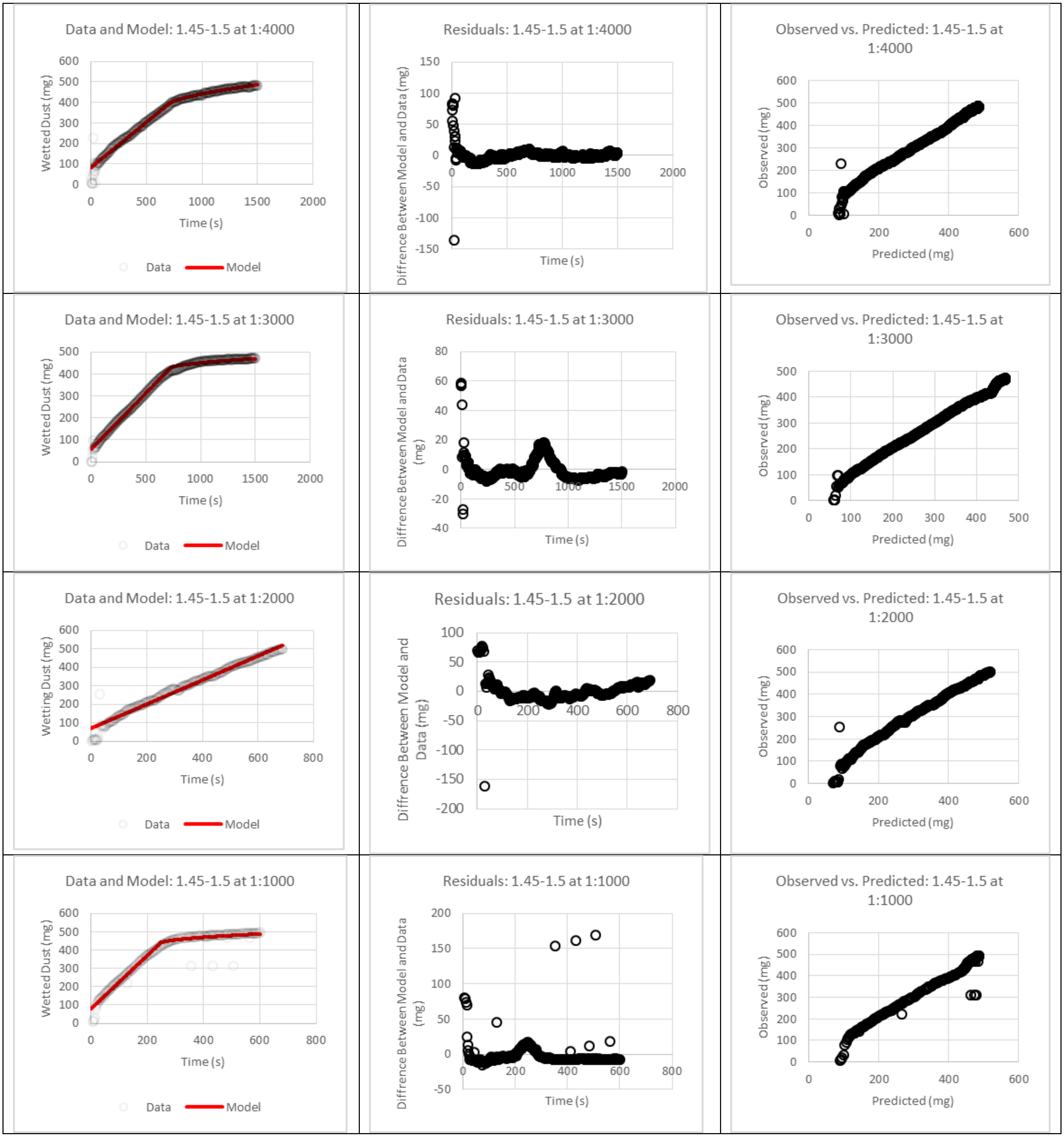
Data and Model: 1.45-1.5 at 1:4000
Wetted Dust (mg)
Time (s)
Data
Model
Residuals: 1.45-1.5 at 1:4000
Diffrence Between Model and Data (mg)
Time (s)
Observed vs. Predicted: 1.45-1.5 at 1:4000
Observed (mg)
Predicted (mg)
Data and Model: 1.45-1.5 at 1:3000
Wetted Dust (mg)
Time (s)
Data
Model
Residuals: 1.45-1.5 at 1:3000
Diffrence Between Model and Data (mg)
Time (s)
Observed vs. Predicted: 1.45-1.5 at 1:3000
Observed (mg)
Predicted (mg)
Data and Model: 1.45-1.5 at 1:2000
Wetting Dust (mg)
Time (s)
Data
Model
Residuals: 1.45-1.5 at 1:2000
Diffrence Between Model and Data (mg)
Time (s)
Observed vs. Predicted: 1.45-1.5 at 1:2000
Observed (mg)
Predicted (mg)
Data and Model: 1.45-1.5 at 1:1000
Wetted Dust (mg)
Time (s)
Data
Model
Residuals: 1.45-1.5 at 1:1000
Diffrence Between Model and Data (mg)
Time (s)
Observed vs. Predicted: 1.45-1.5 at 1:1000
Observed (mg)
Predicted (mg)

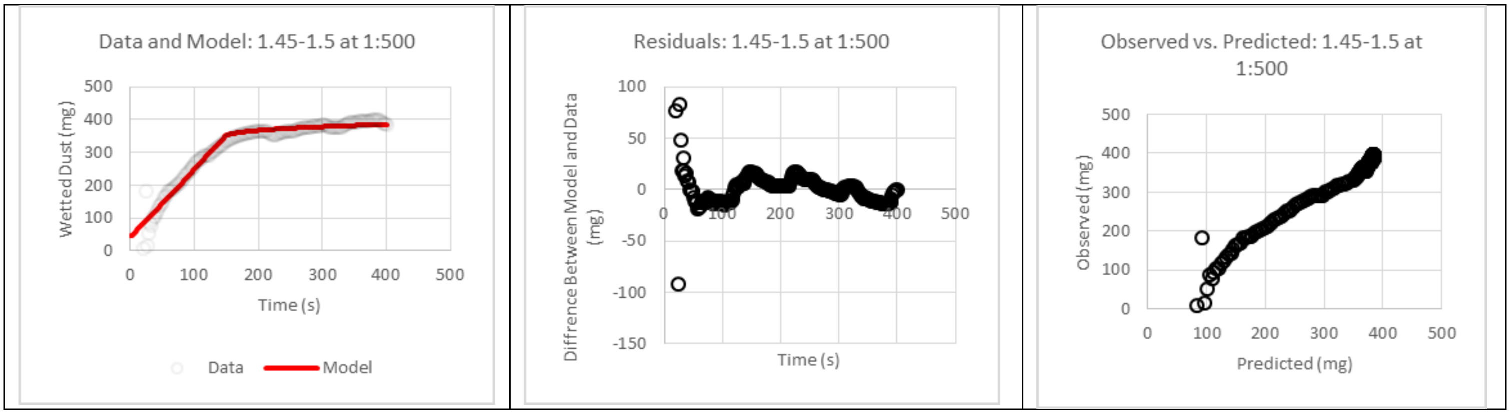
Data and Model: 1.45-1.5 at 1:500
Wetted Dust (mg)
Time (s)
Data
Model
Residuals: 1.45-1.5 at 1:500
Diffrence Between Model and Data (mg)
Time (s)
Observed vs. Predicted: 1.45-1.5 at 1:500
Observed (mg)
Predicted (mg)

Table 34:A34 - Tabulated sink test using dust with gravity 1.5-1.6

Data and Model	Residuals	Observed Vs. Predicted
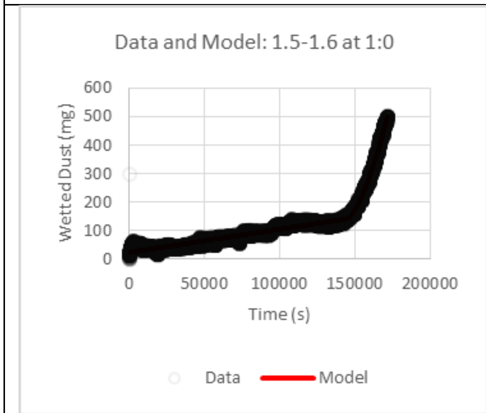	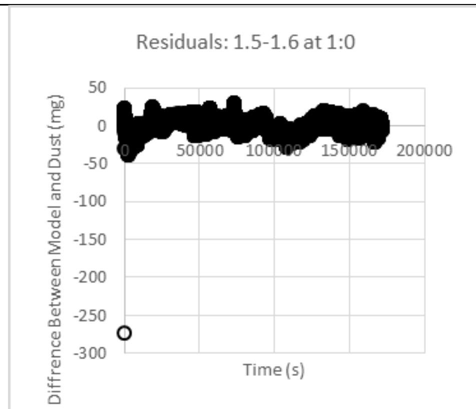	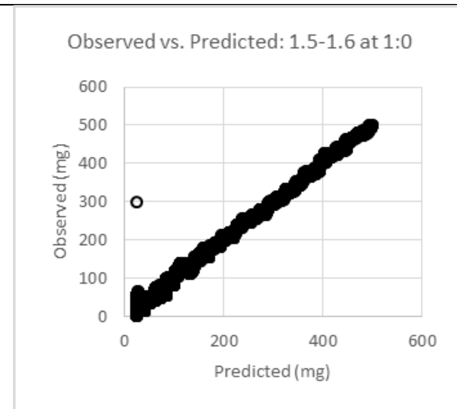
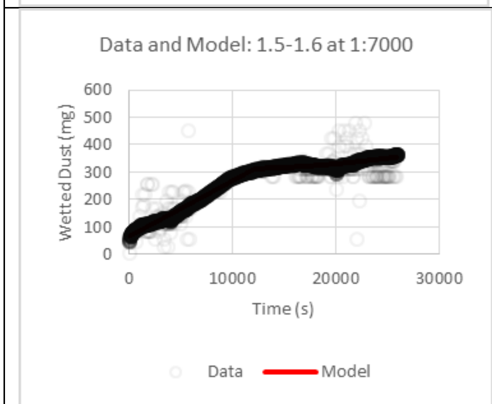	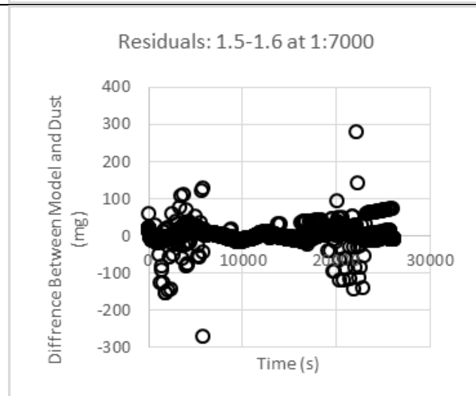	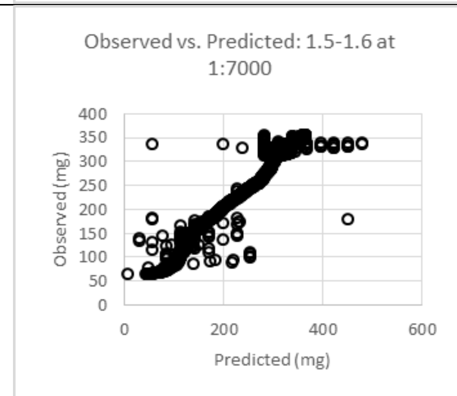
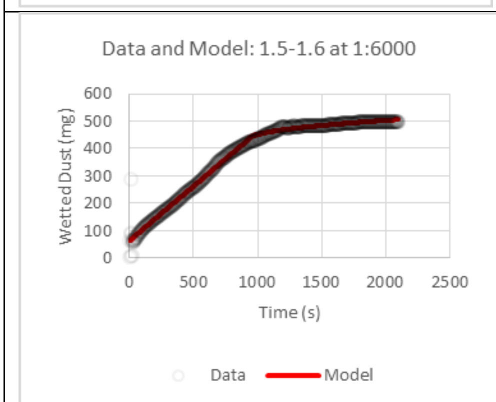	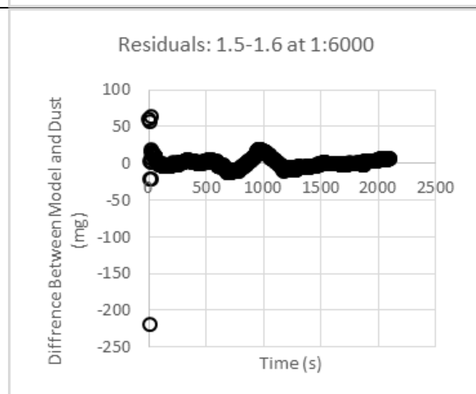	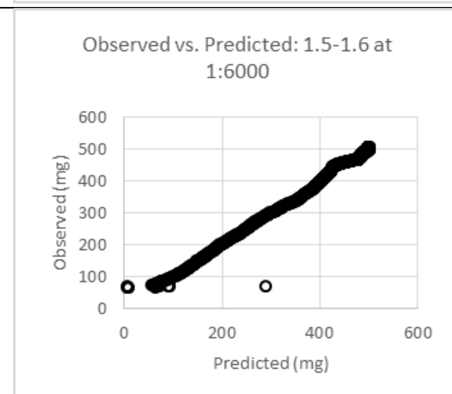
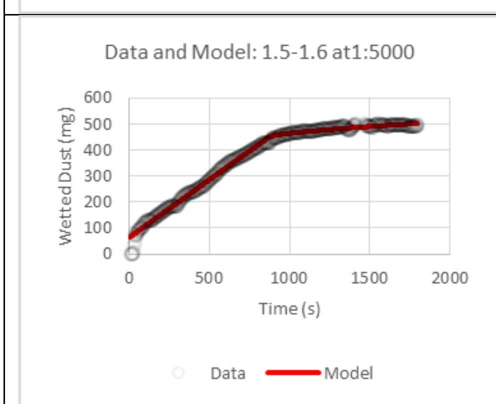	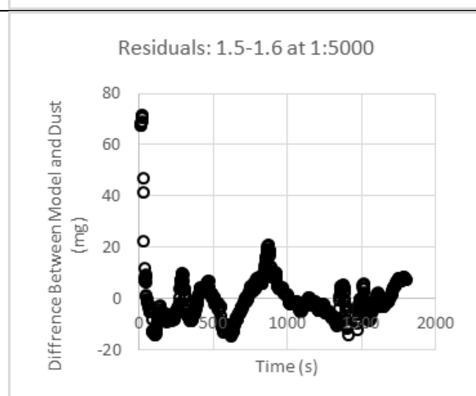	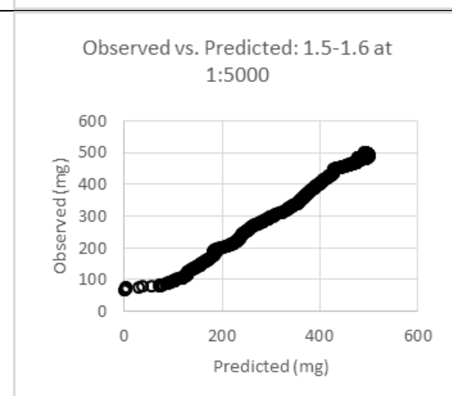

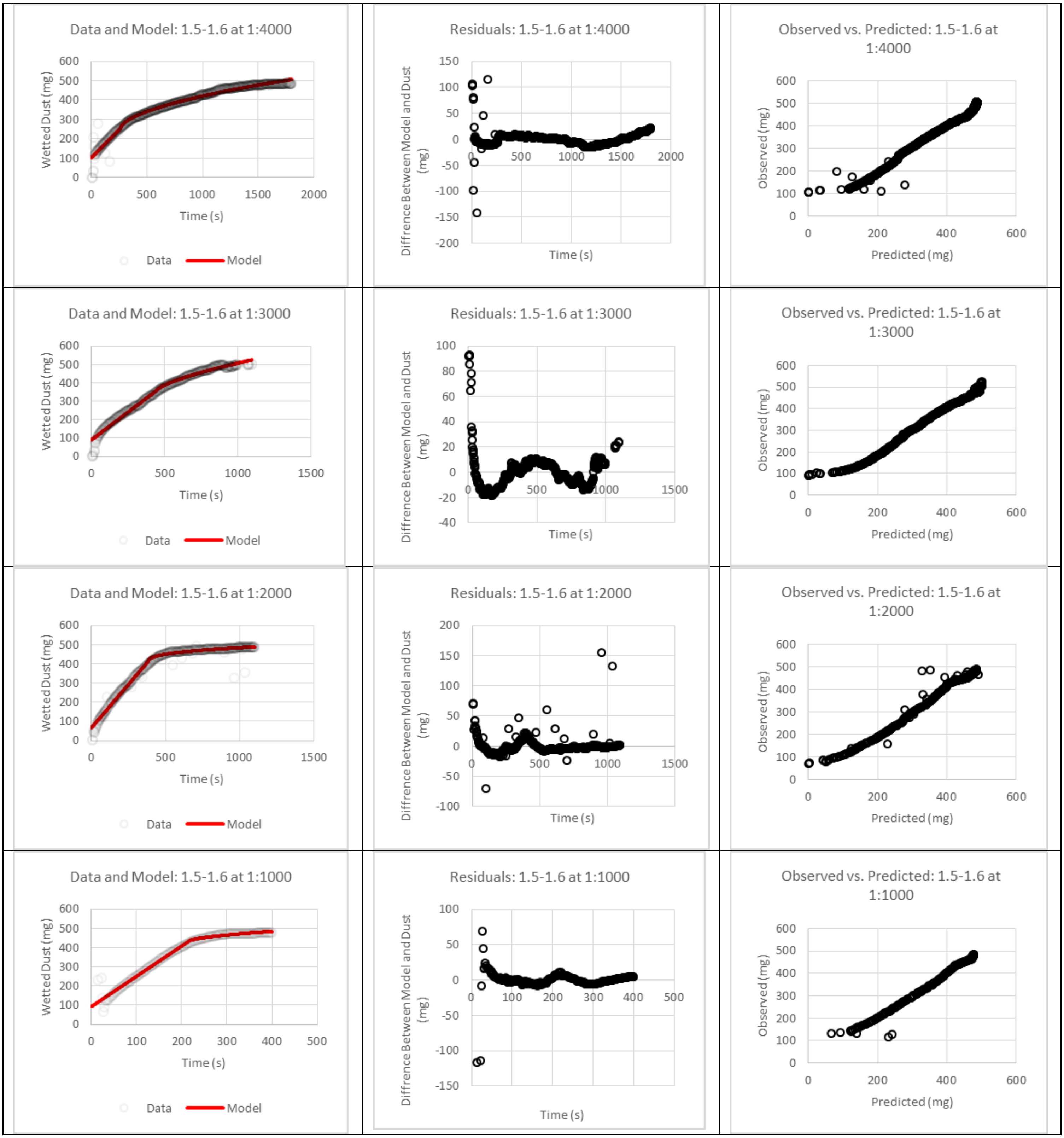
Data and Model: 1.5-1.6 at 1:4000
Wetted Dust (mg)
Time (s)
Data
Model
Residuals: 1.5-1.6 at 1:4000
Diffrence Between Model and Dust (mg)
Time (s)
Observed vs. Predicted: 1.5-1.6 at 1:4000
Observed (mg)
Predicted (mg)
Data and Model: 1.5-1.6 at 1:3000
Wetted Dust (mg)
Time (s)
Data
Model
Residuals: 1.5-1.6 at 1:3000
Diffrence Between Model and Dust (mg)
Time (s)
Observed vs. Predicted: 1.5-1.6 at 1:3000
Observed (mg)
Predicted (mg)
Data and Model: 1.5-1.6 at 1:2000
Wetted Dust (mg)
Time (s)
Data
Model
Residuals: 1.5-1.6 at 1:2000
Diffrence Between Model and Dust (mg)
Time (s)
Observed vs. Predicted: 1.5-1.6 at 1:2000
Observed (mg)
Predicted (mg)
Data and Model: 1.5-1.6 at 1:1000
Wetted Dust (mg)
Time (s)
Data
Model
Residuals: 1.5-1.6 at 1:1000
Diffrence Between Model and Dust (mg)
Time (s)
Observed vs. Predicted: 1.5-1.6 at 1:1000
Observed (mg)
Predicted (mg)

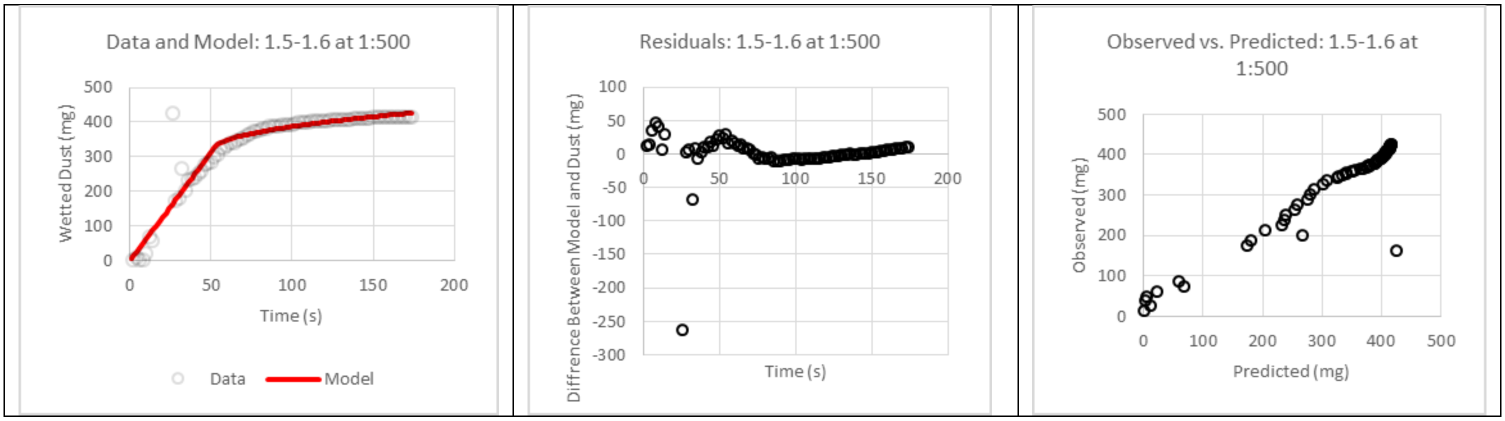
Data and Model: 1.5-1.6 at 1:500
Wetted Dust (mg)
Time (s)
Data
Model
Residuals: 1.5-1.6 at 1:500
Diffrence Between Model and Dust (mg)
Time (s)
Observed vs. Predicted: 1.5-1.6 at 1:500
Observed (mg)
Predicted (mg)

Table 35:A35 - Tabulated sink test using dust with gravity 1.6-1.7

Data and Model	Residuals	Observed Vs. Predicted

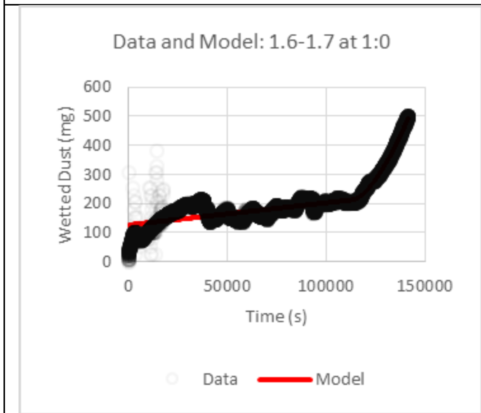

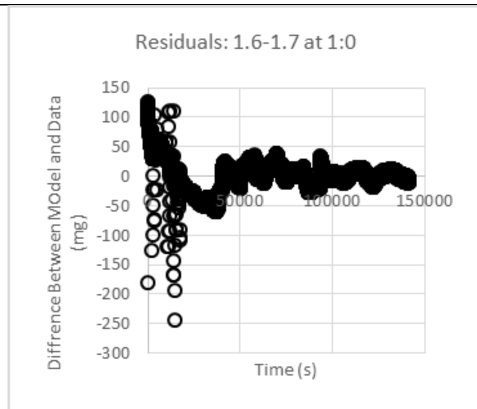

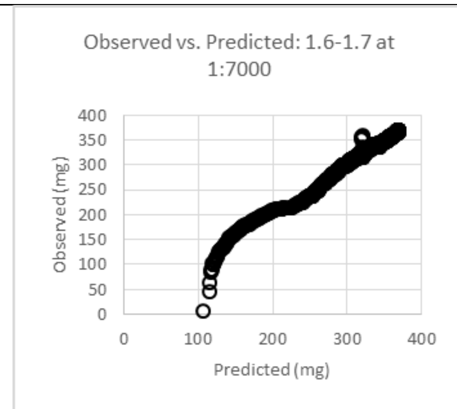

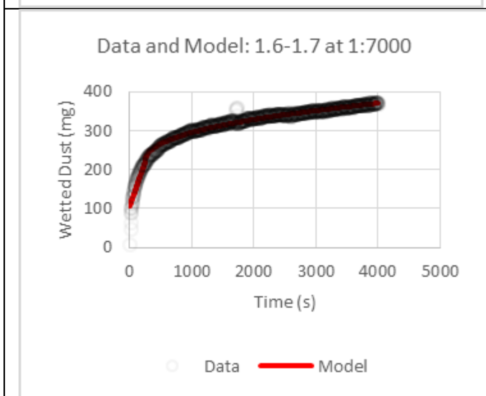

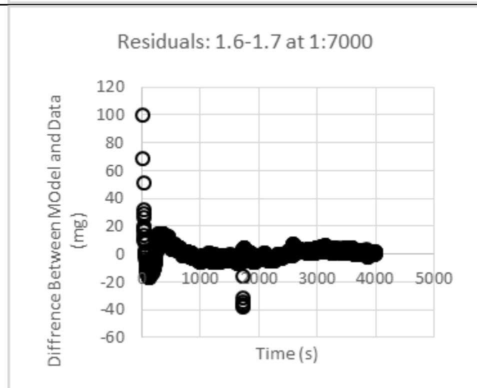

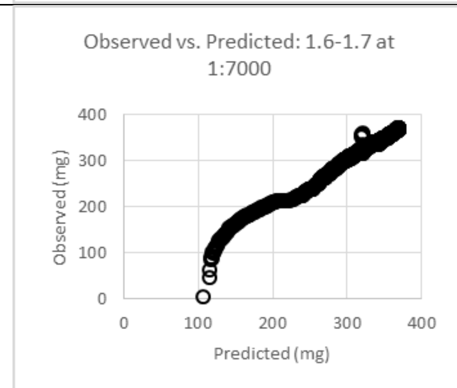

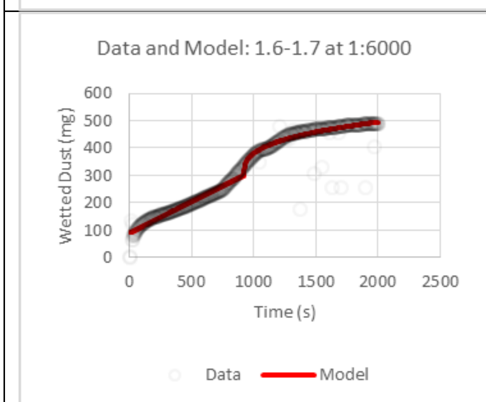

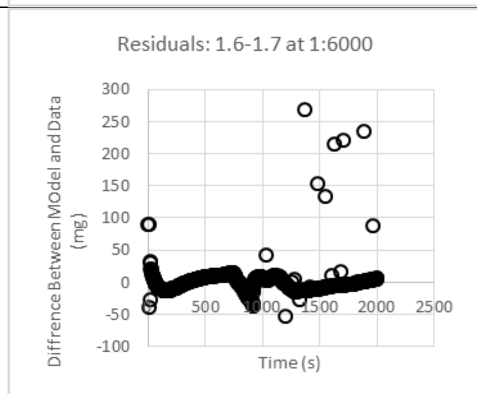

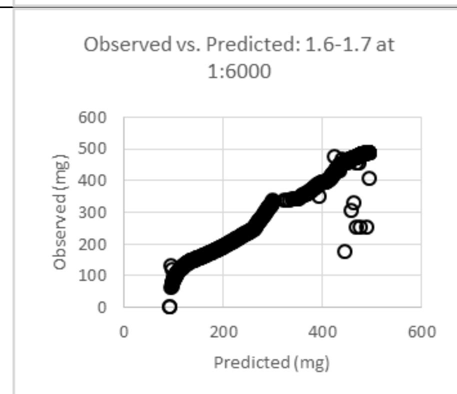

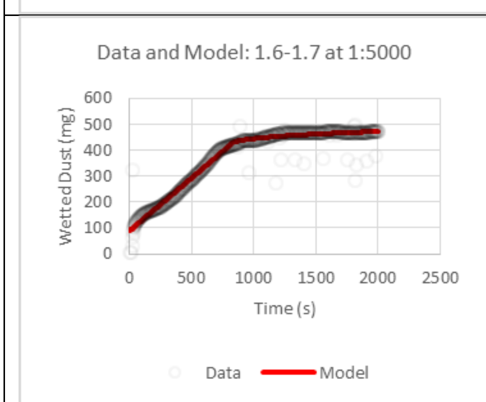

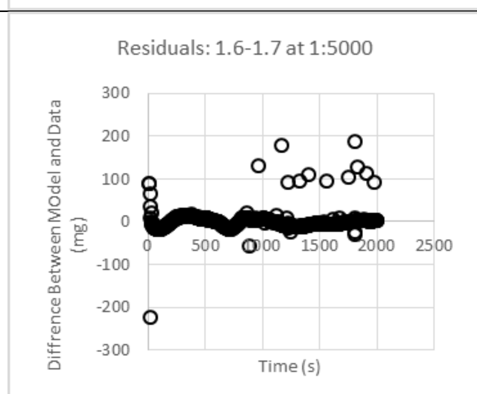

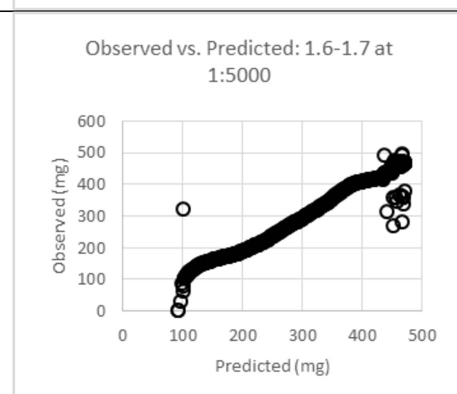

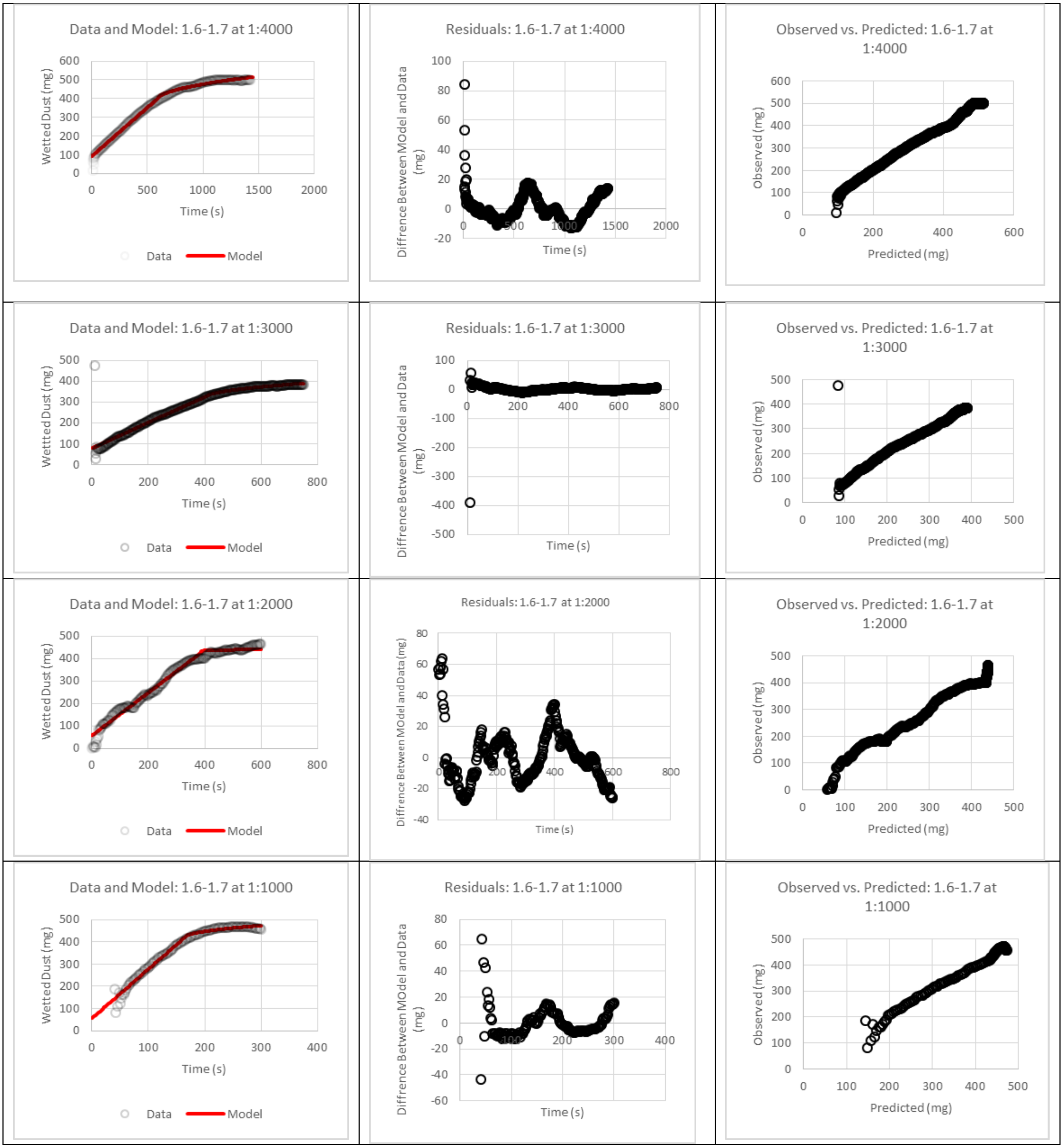
Data and Model: 1.6-1.7 at 1:4000
Wetted Dust (mg)
Time (s)
Data
Model
Residuals: 1.6-1.7 at 1:4000
Diffrence Between MOdel and Data (mg)
Time (s)
Observed vs. Predicted: 1.6-1.7 at 1:4000
Observed (mg)
Predicted (mg)
Data and Model: 1.6-1.7 at 1:3000
Wetted Dust (mg)
Time (s)
Data
Model
Residuals: 1.6-1.7 at 1:3000
Diffrence Between MOdel and Data (mg)
Time (s)
Observed vs. Predicted: 1.6-1.7 at 1:3000
Observed (mg)
Predicted (mg)
Data and Model: 1.6-1.7 at 1:2000
Wetted Dust (mg)
Time (s)
Data
Model
Residuals: 1.6-1.7 at 1:2000
Diffrence Between MOdel and Data (mg)
Time (s)
Observed vs. Predicted: 1.6-1.7 at 1:2000
Observed (mg)
Predicted (mg)
Data and Model: 1.6-1.7 at 1:1000
Wetted Dust (mg)
Time (s)
Data
Model
Residuals: 1.6-1.7 at 1:1000
Diffrence Between MOdel and Data (mg)
Time (s)
Observed vs. Predicted: 1.6-1.7 at 1:1000
Observed (mg)
Predicted (mg)

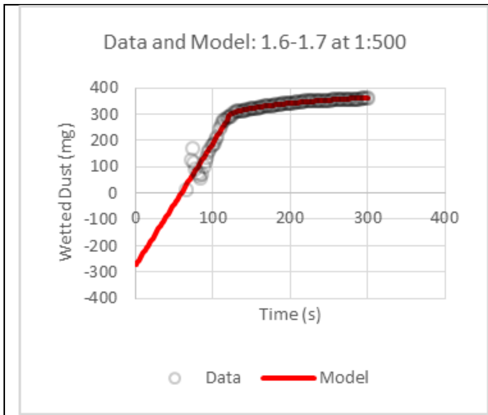
Data and Model: 1.6-1.7 at 1:500
Wetted Dust (mg)
400
300
200
100
0
-100
-200
-300
-400
0
100
200
300
400
Time (s)
Data
Model

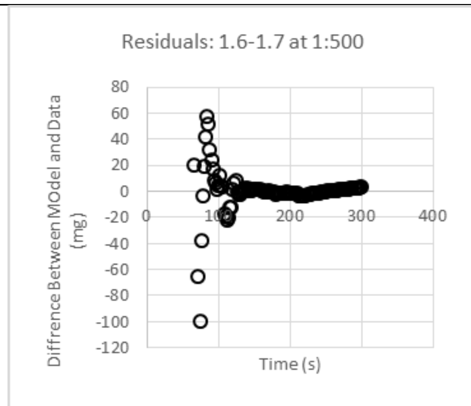
Residuals: 1.6-1.7 at 1:500
Diffrence Between MOdel and Data (mg)
80
60
40
20
0
-20
-40
-60
-80
-100
-120
0
100
200
300
400
Time (s)

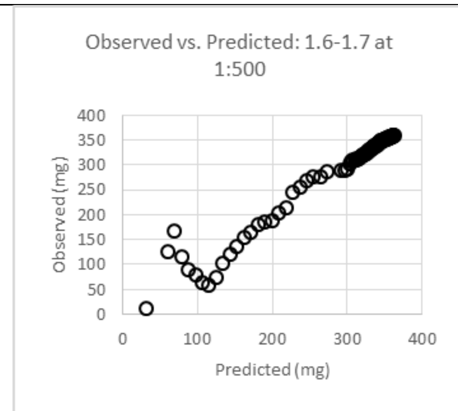
Observed vs. Predicted: 1.6-1.7 at 1:500
Observed (mg)
400
350
300
250
200
150
100
50
0
0
100
200
300
400
Predicted (mg)

Table 36:A36 - Tabulated sink test using dust with gravity 1.7-1.8

<table>
<tr><th>Data and Model</th><th>Residuals</th><th>Observed Vs. Predicted</th></tr>
<tr>
<td>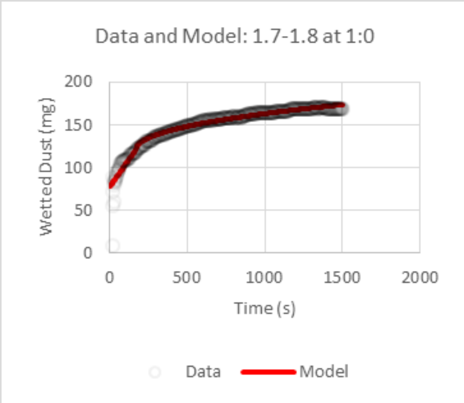
</td>
<td>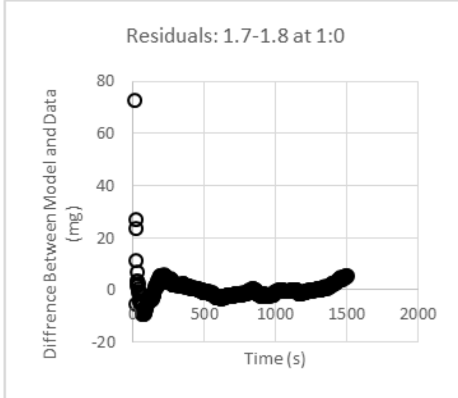
</td>
<td>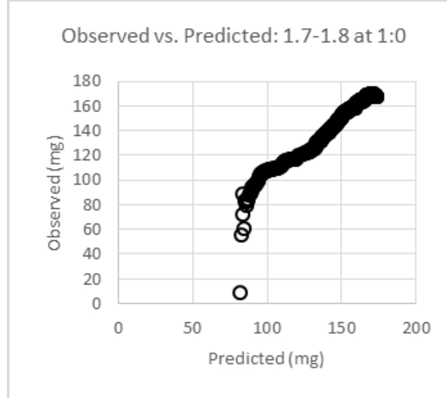
</td>
</tr>
<tr>
<td>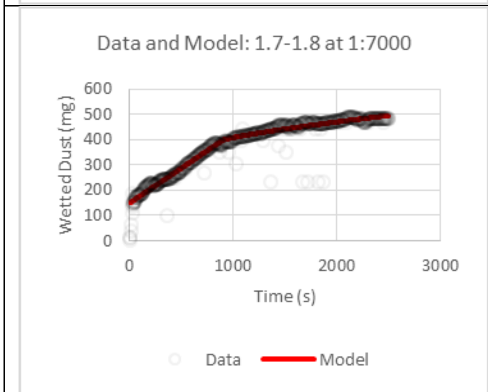
</td>
<td>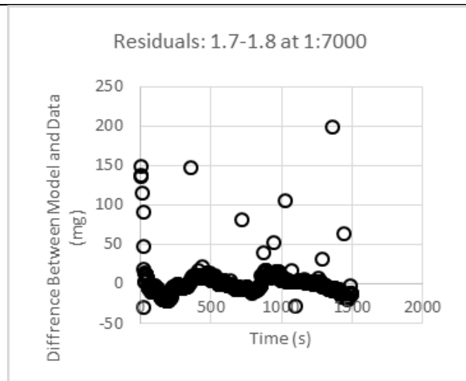
</td>
<td>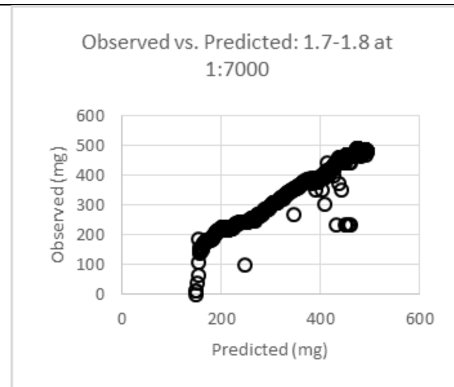
</td>
</tr>
<tr>
<td>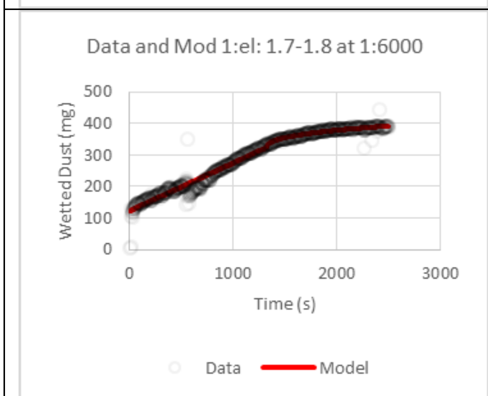
</td>
<td>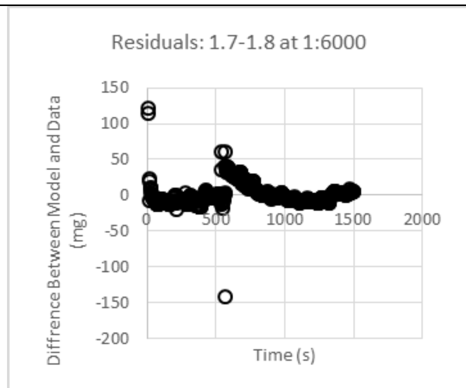
</td>
<td>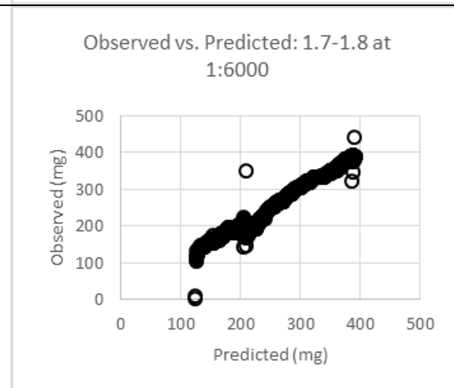
</td>
</tr>
<tr>
<td>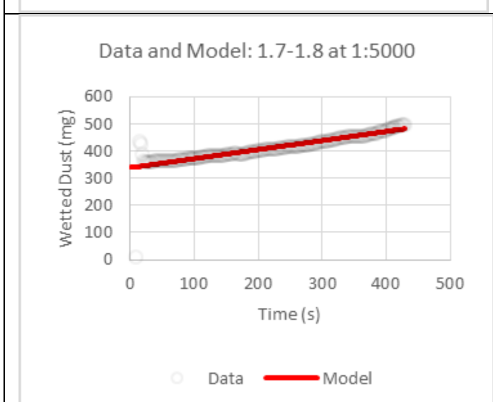
</td>
<td>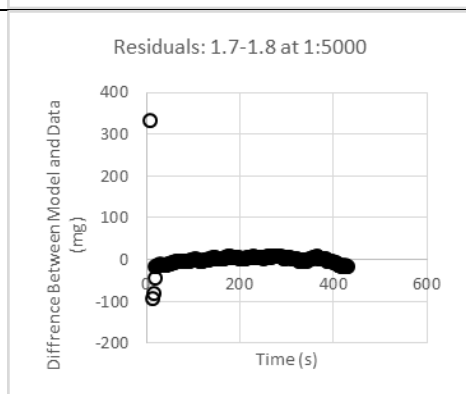
</td>
<td>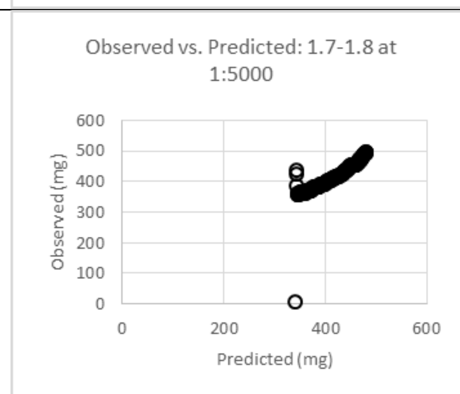
</td>
</tr>
</table>

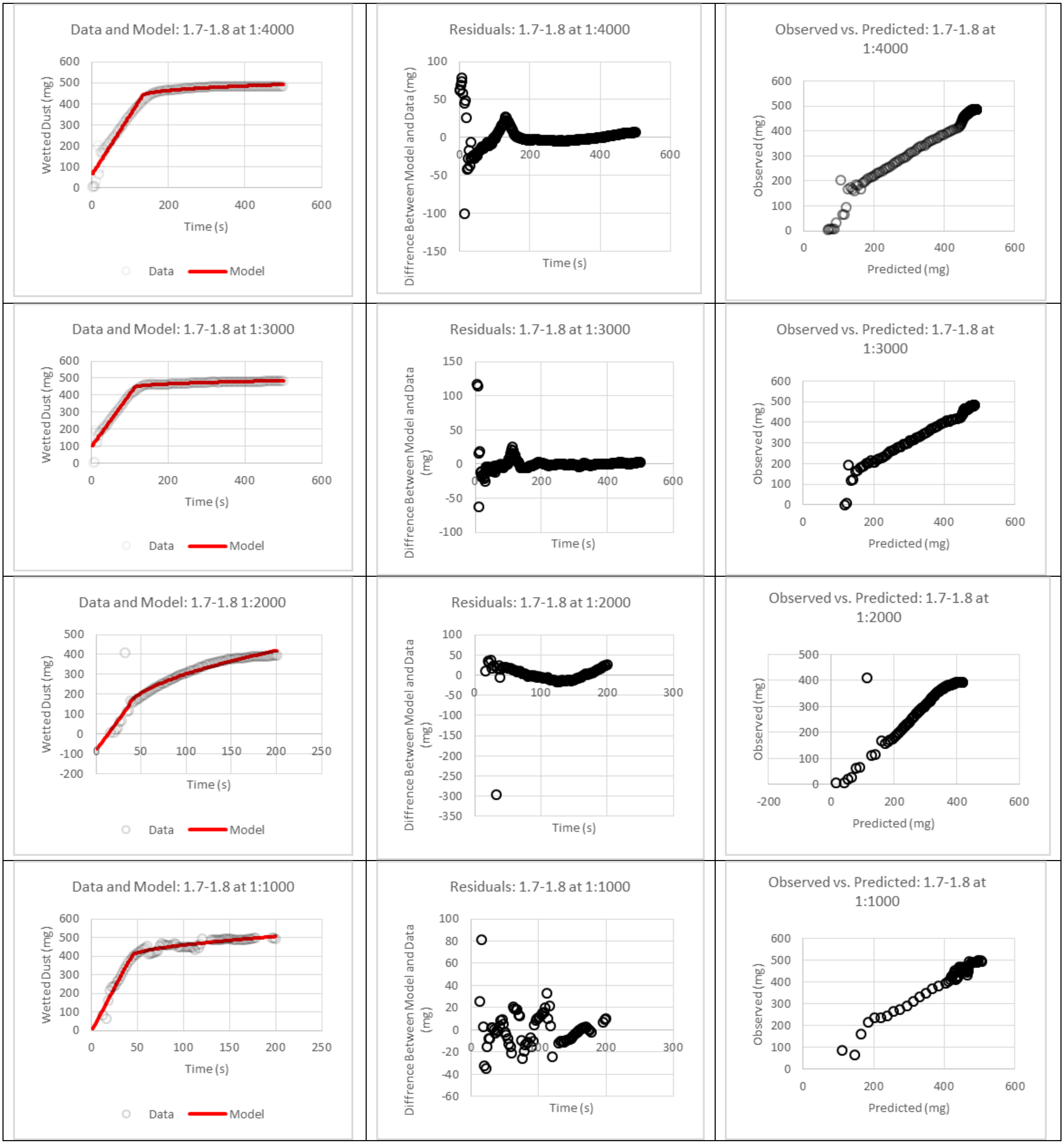
Data and Model: 1.7-1.8 at 1:4000
Wetted Dust (mg)
Time (s)
Data
Model
Residuals: 1.7-1.8 at 1:4000
Diffrence Between Model and Data (mg)
Time (s)
Observed vs. Predicted: 1.7-1.8 at 1:4000
Observed (mg)
Predicted (mg)
Data and Model: 1.7-1.8 at 1:3000
Wetted Dust (mg)
Time (s)
Data
Model
Residuals: 1.7-1.8 at 1:3000
Diffrence Between Model and Data (mg)
Time (s)
Observed vs. Predicted: 1.7-1.8 at 1:3000
Observed (mg)
Predicted (mg)
Data and Model: 1.7-1.8 1:2000
Wetted Dust (mg)
Time (s)
Data
Model
Residuals: 1.7-1.8 at 1:2000
Diffrence Between Model and Data (mg)
Time (s)
Observed vs. Predicted: 1.7-1.8 at 1:2000
Observed (mg)
Predicted (mg)
Data and Model: 1.7-1.8 at 1:1000
Wetted Dust (mg)
Time (s)
Data
Model
Residuals: 1.7-1.8 at 1:1000
Diffrence Between Model and Data (mg)
Time (s)
Observed vs. Predicted: 1.7-1.8 at 1:1000
Observed (mg)
Predicted (mg)

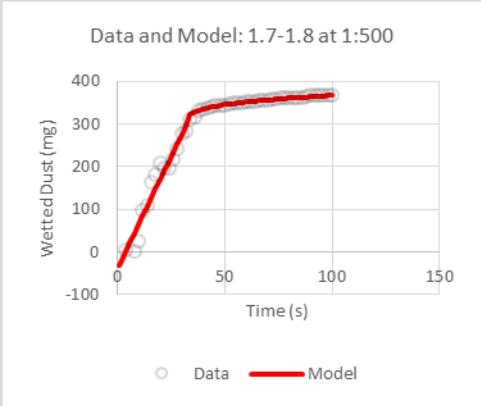
Data and Model: 1.7-1.8 at 1:500
Wetted Dust (mg)
400
300
200
100
0
-100
0
50
100
150
Time (s)
Data
Model

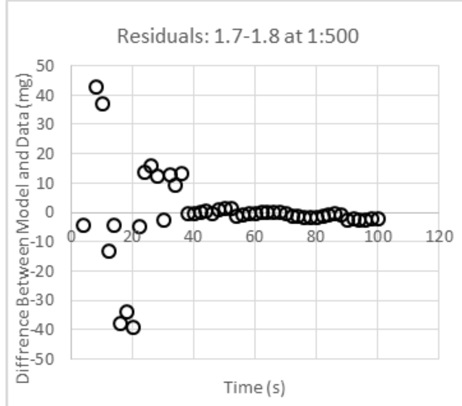
Residuals: 1.7-1.8 at 1:500
Diffrence Between Model and Data (mg)
50
40
30
20
10
0
-10
-20
-30
-40
-50
0
20
40
60
80
100
120
Time (s)

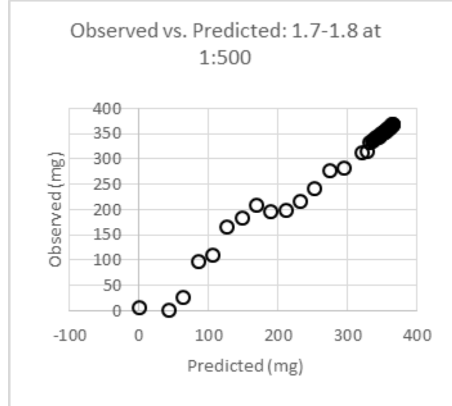
Observed vs. Predicted: 1.7-1.8 at 1:500
Observed (mg)
400
350
300
250
200
150
100
50
0
-100
0
100
200
300
400
Predicted (mg)

Table 37:A37 - Tabulated sink test using dust with gravity 1.8 sink

Data and Model	Residuals	Observed Vs. Predicted
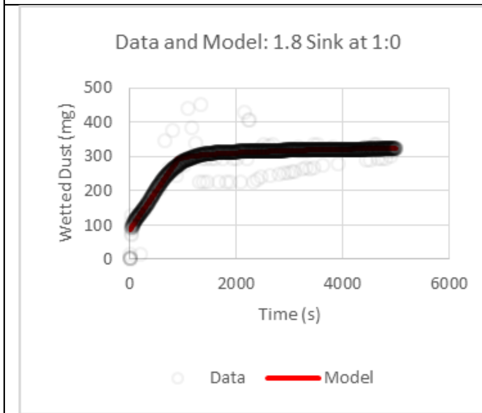	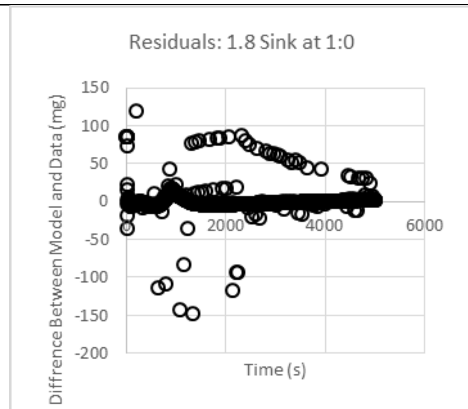	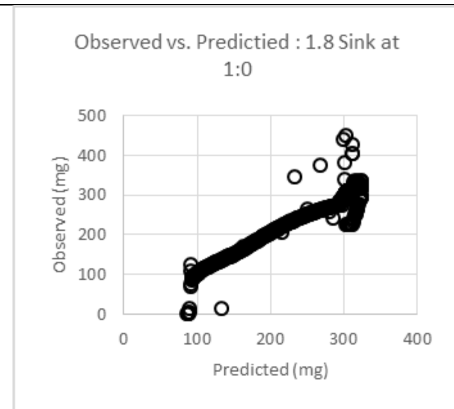
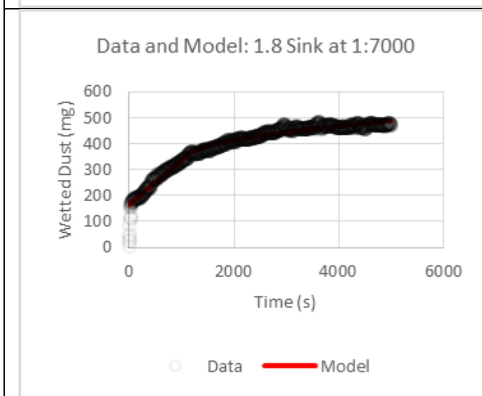	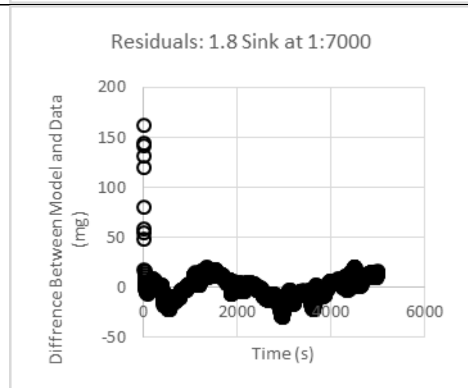	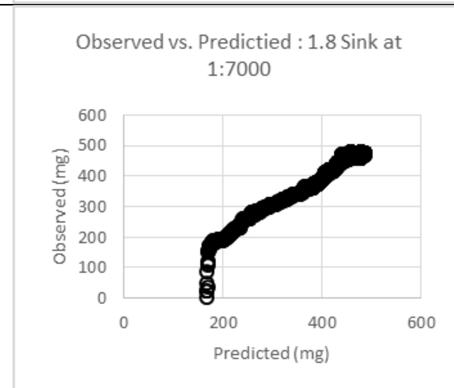
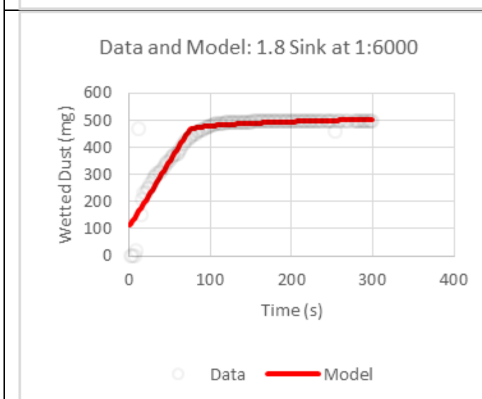	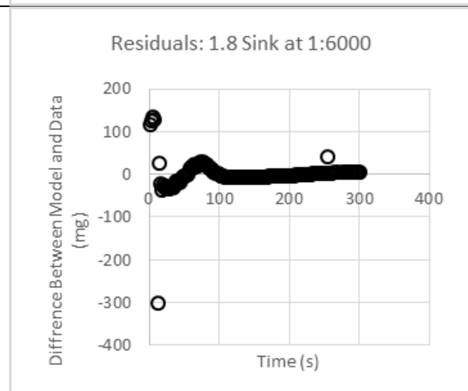	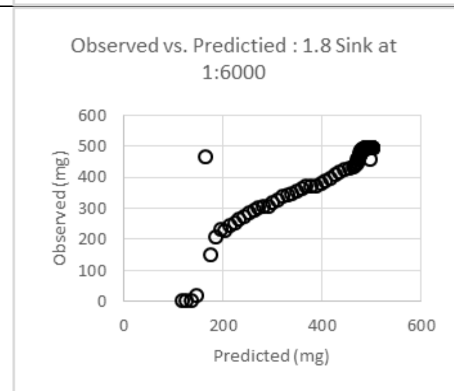
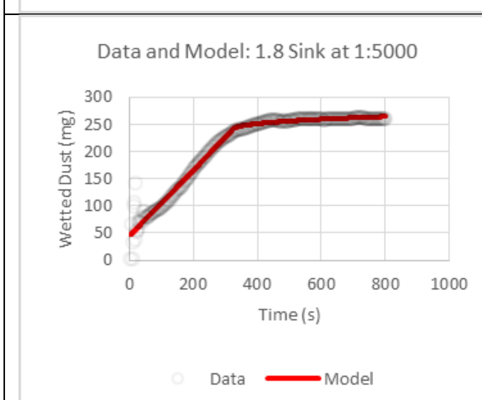	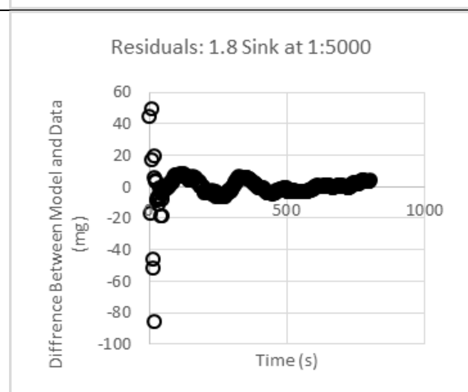	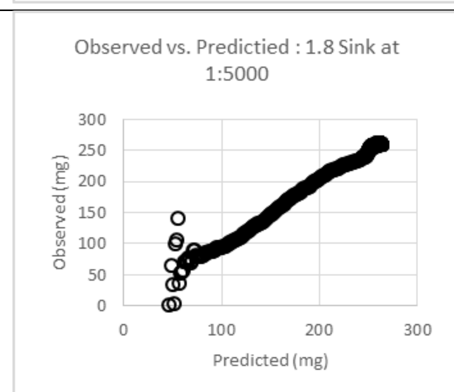

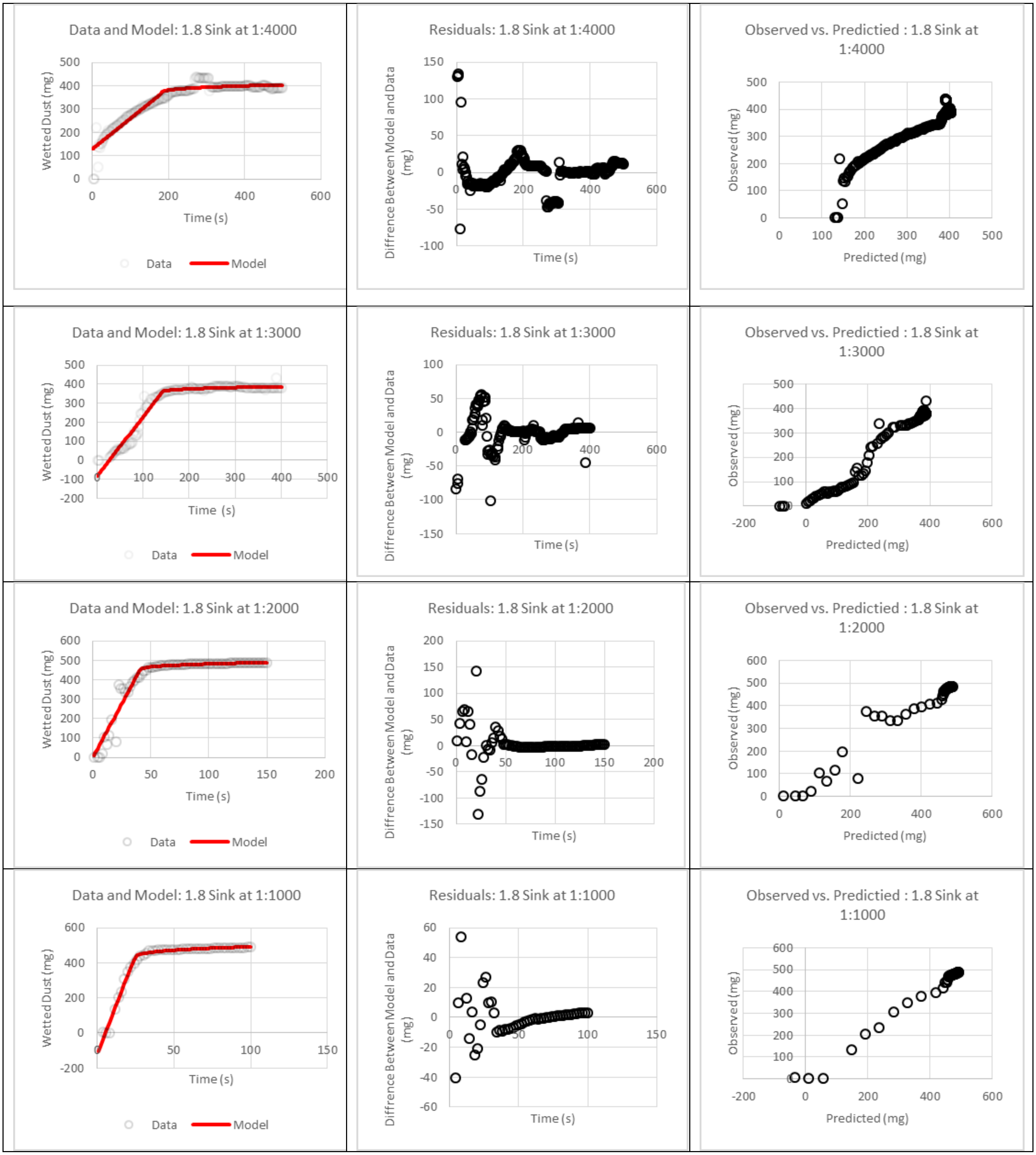

Data and Model: 1.8 Sink at 1:4000
Wetted Dust (mg)
Time (s)
Data
Model
Residuals: 1.8 Sink at 1:4000
Diffrence Between Model and Data (mg)
Time (s)
Observed vs. Predictied : 1.8 Sink at 1:4000
Observed (mg)
Predicted (mg)
Data and Model: 1.8 Sink at 1:3000
Wetted Dust (mg)
Time (s)
Data
Model
Residuals: 1.8 Sink at 1:3000
Diffrence Between Model and Data (mg)
Time (s)
Observed vs. Predictied : 1.8 Sink at 1:3000
Observed (mg)
Predicted (mg)
Data and Model: 1.8 Sink at 1:2000
Wetted Dust (mg)
Time (s)
Data
Model
Residuals: 1.8 Sink at 1:2000
Diffrence Between Model and Data (mg)
Time (s)
Observed vs. Predictied : 1.8 Sink at 1:2000
Observed (mg)
Predicted (mg)
Data and Model: 1.8 Sink at 1:1000
Wetted Dust (mg)
Time (s)
Data
Model
Residuals: 1.8 Sink at 1:1000
Diffrence Between Model and Data (mg)
Time (s)
Observed vs. Predictied : 1.8 Sink at 1:1000
Observed (mg)
Predicted (mg)

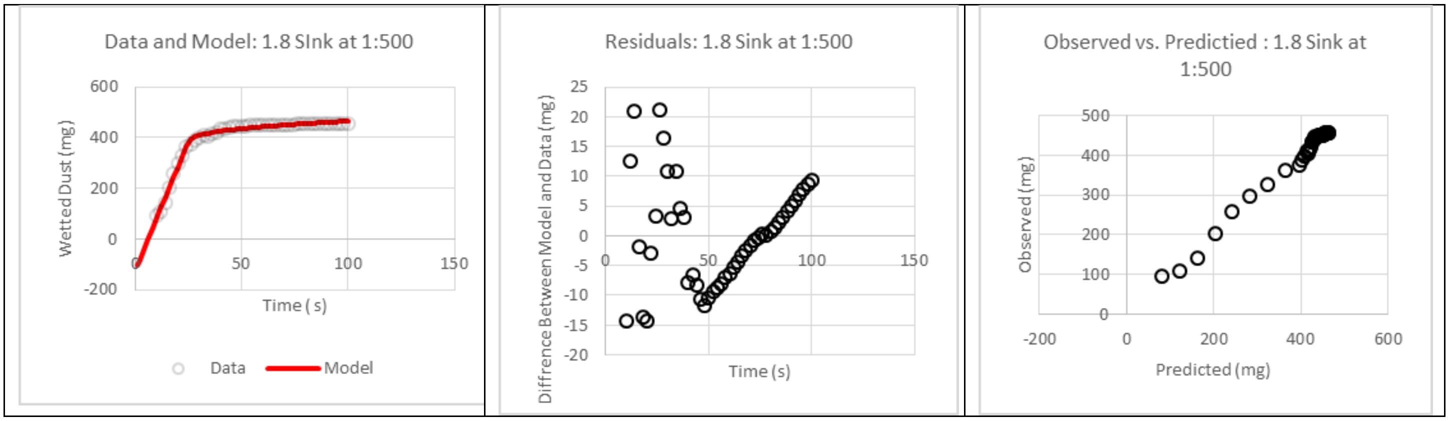
Data and Model: 1.8 SInk at 1:500
Wetted Dust (mg)
Time (s)
Data
Model
Residuals: 1.8 Sink at 1:500
Diffrence Between Model and Data (mg)
Time (s)
Observed vs. Predictied : 1.8 Sink at 1:500
Observed (mg)
Predicted (mg)

Table 38:A38 - Analysis of dosage level and gravity class on wetting rates with all data

	1.3 FL	1.3-1.35	1.35-1.4-	1.4-1.45	1.45-1.5	1.5-1.6	1.6-1.7	1.7-1.8	1.8 Sink
1:0	0.001	0.001	0.000	0.000	0.005	0.001	0.005	0.253	0.227
1:7000	0.000	0.004	0.013	0.006	0.006	0.020	0.455	0.276	0.169
1:6000	0.101	0.022	0.165	0.027	0.317	0.398	0.228	0.152	4.834
1:5000	0.109	0.110	0.153	0.075	0.013	0.441	0.407	0.333	0.601
1:4000	0.110	0.114	0.258	0.282	0.441	0.575	0.519	2.841	1.313
1:3000	0.133	0.228	0.220	0.294	0.508	0.603	0.616	3.087	3.166
1:2000	0.237	0.311	0.296	0.356	0.651	0.904	0.954	6.210	11.144
1:1000	0.542	0.535	0.622	0.886	1.453	1.577	2.213	9.162	22.636
1:500	0.000	0.000	1.625	2.120	2.048	6.262	4.657	10.516	20.332

* The data highlighted in the red was deemed as an inadequate model or run. This data was still used when conducting the ANOVA two-factor without replication test.

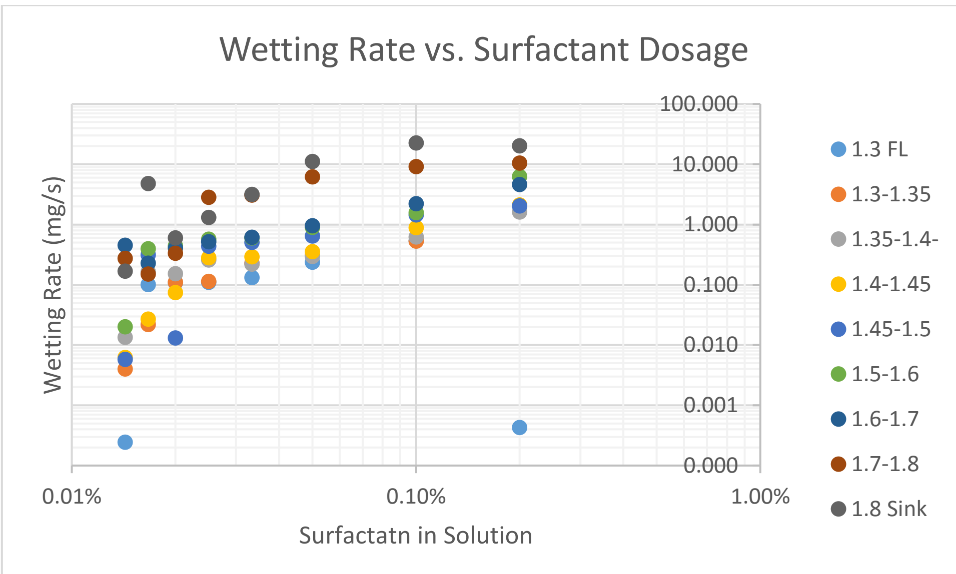

	1.3 FL	1.3-1.35	1.35-1.4	1.4-1.45	1.45-1.5	1.5-1.6	1.6-1.7	1.7-1.8	1.8 Sink
0.00%		0.001			0.005	0.001		0.253	0.227
0.01%			0.013			0.020	0.455	0.276	0.169
0.02%	0.101	0.022	0.165	0.027	0.317	0.398	0.228	0.152	
0.02%	0.109	0.110	0.153	0.075	0.013	0.441	0.407		0.601
0.03%	0.110	0.114	0.258	0.282	0.441	0.575	0.519	2.841	
0.03%	0.133	0.228	0.220		0.508	0.603	0.616	3.087	3.166
0.05%	0.237	0.311	0.296	0.356	0.651	0.904	0.954		11.144
0.10%	0.542	0.535	0.622	0.886	1.453	1.577	2.213	9.162	22.636
0.20%			1.625	2.120	2.048		4.657	10.516	20.332

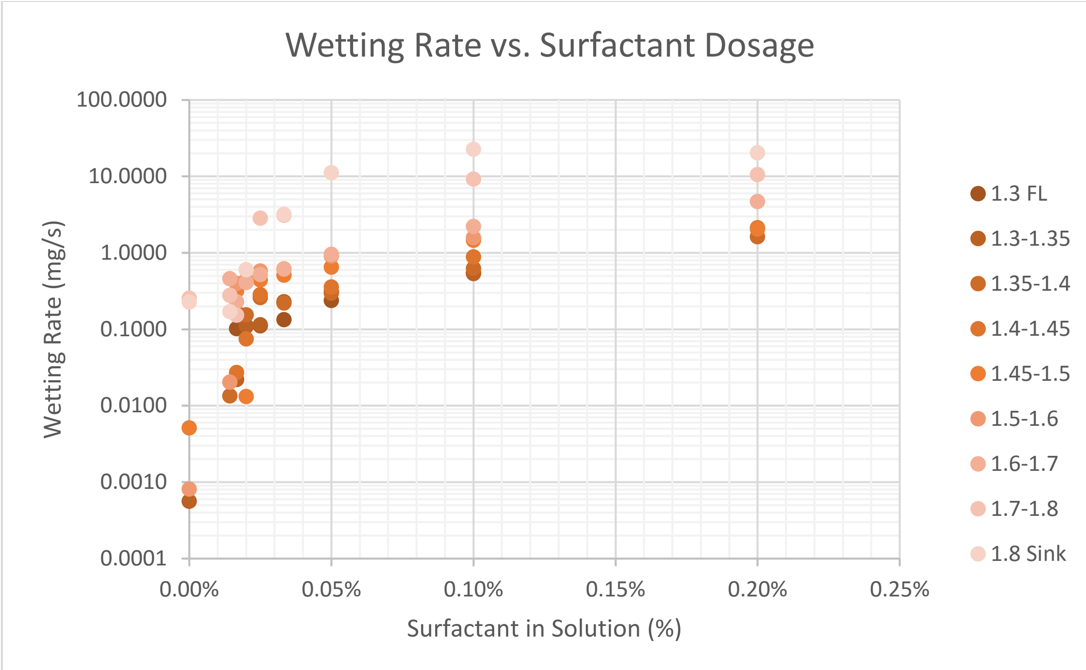
Wetting Rate vs. Surfactant Dosage
Wetting Rate (mg/s)
100.0000
10.0000
1.0000
0.1000
0.0100
0.0010
0.0001
0.00%
0.05%
0.10%
0.15%
0.20%
0.25%
Surfactant in Solution (%)
1.3 FL
1.3-1.35
1.35-1.4
1.4-1.45
1.45-1.5
1.5-1.6
1.6-1.7
1.7-1.8
1.8 Sink

Table 39:A39 - Analysis of gravity class on wetting rates with dropped data

Dosage Level	Gravity Class 1.3 FL	1.3-1.35	1.35-1.4	1.4-1.45	1.45-1.5	1.5-1.6	1.6-1.7	1.7-1.8	1.8 Sink
0					0.005	0.001			0.227
0.000143			0.013			0.020		0.276	0.169
0.000167	0.101	0.022	0.165	0.027	0.317	0.398			
0.0002	0.109	0.110	0.153	0.075	0.013	0.441	0.407		0.601
0.00025	0.110	0.114	0.258	0.282	0.441	0.575	0.519	2.841	1.313
0.000333	0.133	0.228	0.220		0.508	0.603	0.616	3.087	
0.0005	0.237	0.311	0.296	0.356	0.651	0.904	0.954	6.210	
0.001	0.542	0.535	0.618	0.886	1.453	1.577	2.213	9.162	22.636
0.002			1.448	1.551	2.048	6.262	4.657	10.516	20.332

The data that was deemed inadequate has been removed from the data set and the analysis was limited to ANOVA single factor

Analysis: ANOVA: Single Factor (α=0.05)

H_0: There is no significant difference in the wetting rates correlated with the gravity class of the dust

SUMMARY						
Groups	Count	Sum	Average	Variance		
1.3 FL	7	1.23	0.18	0.03		
1.3-1.35	7	1.32	0.19	0.04		
1.35-1.4	9	3.17	0.35	0.20		
1.4-1.45	7	3.18	0.45	0.33		
1.45-1.5	8	5.44	0.68	0.51		
1.5-1.6	9	10.78	1.20	3.83		
1.6-1.7	6	9.37	1.56	2.74		
1.7-1.8	6	32.09	5.35	15.82		
1.8 sink	6	45.28	7.55	117.25		
ANOVA						
Source of Variation	SS	df	MS	F	P-value	F crit
Between Groups	355.10	8	44.39	3.47	0.00	2.11
Within Groups	717.28	56	12.81			
Total	1072.38	64				

Results: H_0 is rejected

Conclusion: There is a significant difference in the wetting rates correlated with the different gravity classes of the dust.

Table 40:A40 - Analysis of dosage level on wetting rates with dropped data

Dosage Level	Gravity Class 1.3 FL	1.3-1.35	1.35-1.4	1.4-1.45	1.45-1.5	1.5-1.6	1.6-1.7	1.7-1.8	1.8 Sink
0					0.005	0.001			0.227
0.000143			0.013			0.020		0.276	0.169
0.000167	0.101	0.022	0.165	0.027	0.317	0.398			
0.0002	0.109	0.110	0.153	0.075	0.013	0.441	0.407		0.601
0.00025	0.110	0.114	0.258	0.282	0.441	0.575	0.519	2.841	1.313
0.000333	0.133	0.228	0.220		0.508	0.603	0.616	3.087	
0.0005	0.237	0.311	0.296	0.356	0.651	0.904	0.954	6.210	
0.001	0.542	0.535	0.618	0.886	1.453	1.577	2.213	9.162	22.636
0.002			1.448	1.551	2.048	6.262	4.657	10.516	20.332

The data that was deemed inadequate has been removed from the data set and the analysis was limited to ANOVA single factor

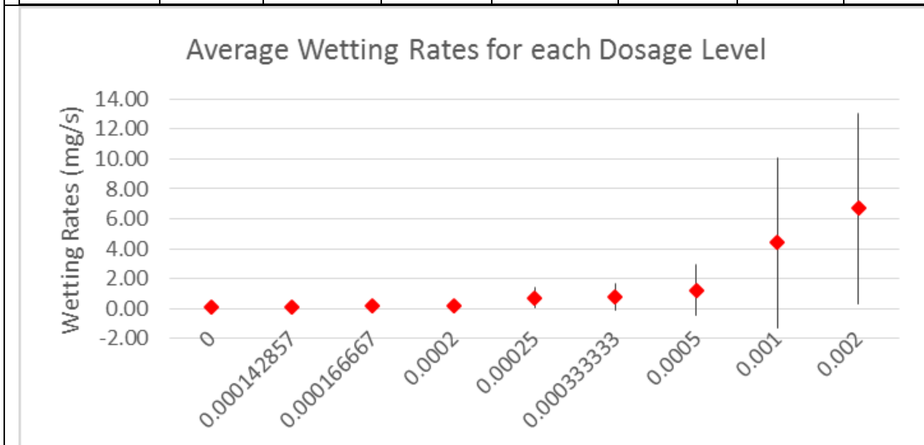

Analysis:

ANOVA: Single Factor (α=0.05)

H_0: There is no significant difference in the wetting rates correlated with the dosage level of the surfactant

SUMMARY						
Groups	Count	Sum	Average	Variance		
0	3	0.23	0.08	0.02		
0.000142857	4	0.48	0.12	0.02		
0.000166667	6	1.03	0.17	0.02		
0.0002	8	1.91	0.24	0.05		
0.00025	9	6.45	0.72	0.77		
0.000333333	7	5.40	0.77	1.08		
0.0005	8	9.92	1.24	4.11		
0.001	9	39.62	4.40	54.14		
0.002	7	46.81	6.69	46.75		
ANOVA						
Source of Variation	SS	df	MS	F	P-value	F crit
Between Groups	316.805	8	39.60	2.94	0.01	2.11
Within Groups	755.5746	56	13.49			
Total	1072.38	64				

Results: H_0 is rejected

Conclusion: There is a significant difference in the wetting rates correlated with the different dosage ratios of the surfactant.

APPENDIX B

Date		Leave Portal, hh:mm		Filter Number	Pump Number	Duration, min	Location
		Arrive Section, hh:mm					
Section		Leave Section, hh:mm					
Shift		Arrive Portal, hh:mm					
Water Pressure							
Left	CM, psi		Drum, psi				
Right	CM, psi		Drum, psi			Field Blank	
Notes and General Mine Condition:							

Cut, #		CM	L / R	Face, #		L / C / R	
Air (cfm)	Start depth	Start Time	Feet of Advance	Time Finished	Replaced bits. #	Total Feet of Advance from Previous Cuts	Total Feet of Advance
Notes:							

Cut, #		CM	L / R	Face, #		L / C / R	
Air (cfm)	Start depth	Start Time	Feet of Advance	Time Finished	Replaced bits. #	Total Feet of Advance from Previous Cuts	Total Feet of Advance
Notes:							

Figure 67. Sample of blank data sheet

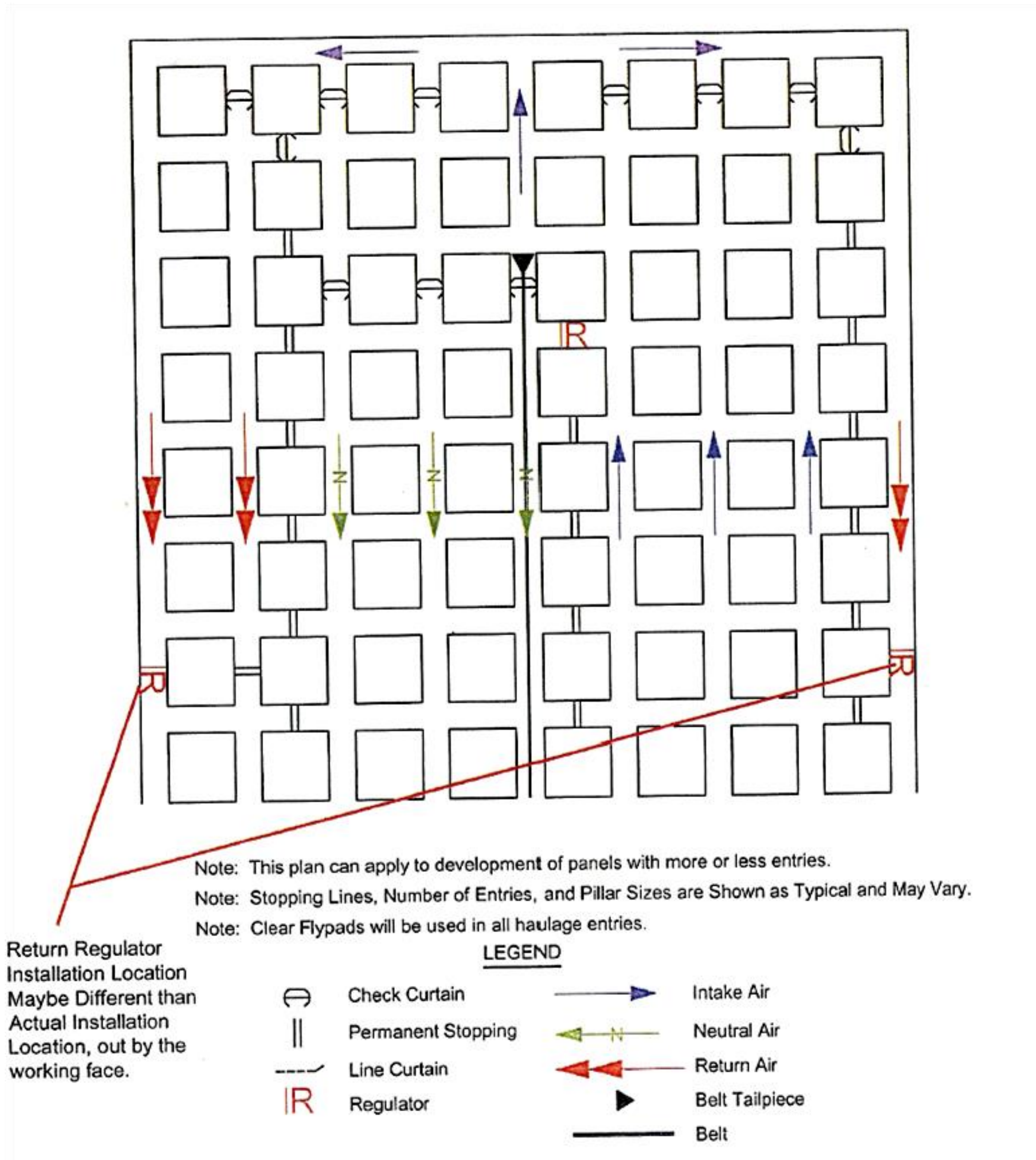

Figure 68: Ventilation schematic of coal mine supersection

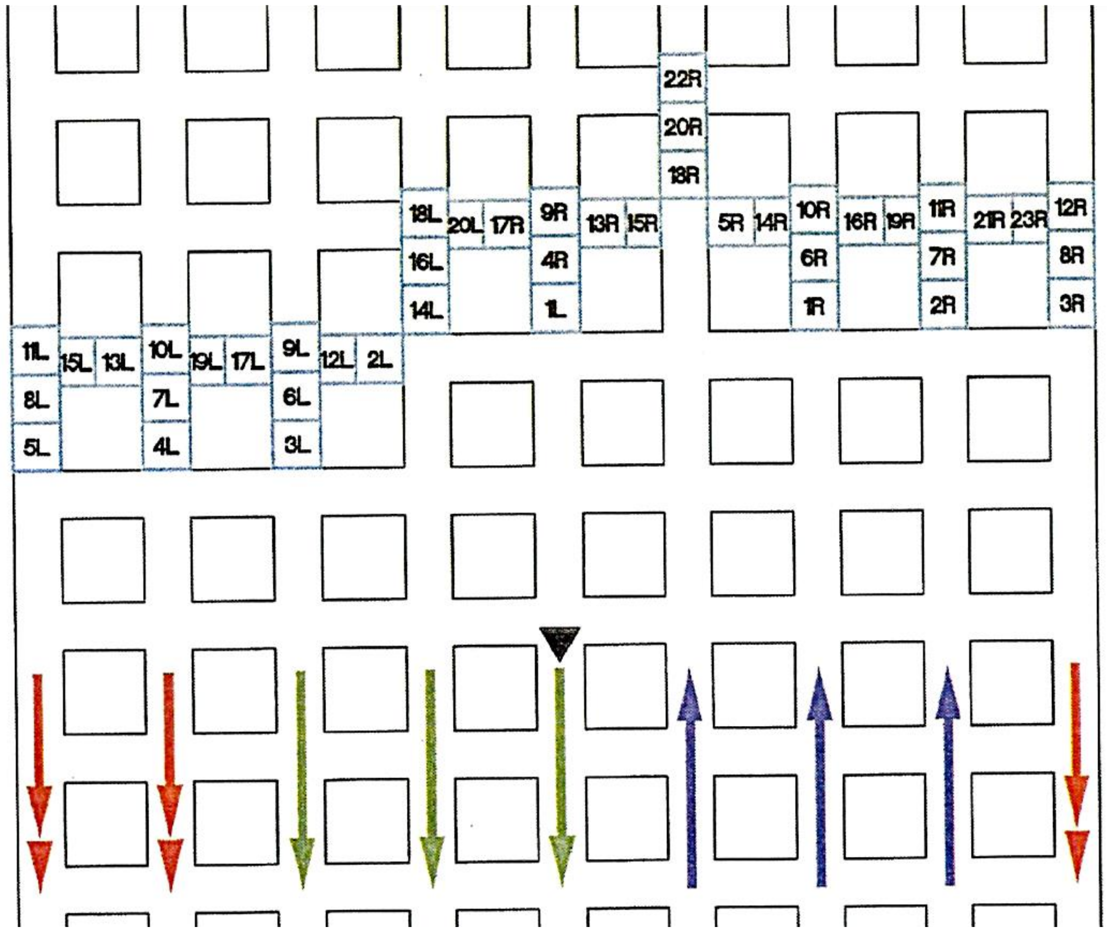

Figure 69: Typical cut cycle on coal mine supersection

Table 41:B1 Tabulation of surface tension analysis results

Dust Control Trial – (Underground water - 'Surface Tension Analysis')				
Date	Sample #	Description	Time taken	Surface tension, dyne/cm^2
7/14/2014	1	Miner (Left)	5:32	72.5
				72.6
				72.6
7/14/2014	2	Miner (Right)	6:06	74.1
				73.7
				72.6
7/14/2014	3	Miner (Left)	6:28	69.9
				70.4
				70.1
7/14/2014	4	Miner (Right)	7:05	71.2
				71.5
				71.3
7/14/2014	5	Miner (Left)	7:44	71.5
				71.5
				72.2
7/14/2014	6	Miner (Right)	9:26	63.8
				63.5
				67.6
7/15/2014	7	Miner (Right)	4:13	67.4
				66.9
				63.4
7/15/2014	8	Miner (Left)	4:36	70.8
				70.5
				70.6
7/15/2014	9	Miner (Right)	5:04	73.7
				73.5
				73.8
7/15/2014	10	Miner (Left)	6:35	71.5
				71.0
				71.0
7/15/2014	11	Miner (Left)	8:21	70.4
				70.7
				69.6
7/15/2014	12	Miner (Right)	9:45	70.1
				70.3
				70.1
7/16/2014	13	Miner (Right)	4:39	42.8
				42.7
				43.2
7/16/2014	14	Miner (Left)	5:13	45.0
				44.5
				45.0
7/16/2014	15	Miner (Left)	6:18	36.7
				37.3
				36.4
7/16/2014	16	Miner (Right)	6:36	35.7
				36.2
				36.4

7/16/2014	17	Miner (Right)	7:10	36.2
				36.1
				35.6
7/16/2014	18	Miner (Left)	7:57	36.0
				36.1
				35.9
7/16/2014	19	Miner (Left)	8:42	35.9
				36.0
				36.0
7/17/2014	20	Miner (Right)	4:06	35.5
				35.9
				35.7
7/17/2014	21	Miner (Left)	4:44	36.0
				35.9
				36.0
7/17/2014	22	Miner (Right)	5:09	35.9
				36.4
				35.7
7/17/2014	23	Miner (Left)	5:49	35.8
				35.6
				36.0
7/17/2014	24	Miner (Right)	6:20	35.0
				35.1
				35.0
7/21/2014	25	Miner (Left)	5:53	35.7
				35.9
				35.9
7/21/2014	26	Miner (Left)	4:16	45.8
				49.1
				49.3
7/21/2014	27	Miner (Right)	4:48	55.4
				56.1
				56.0
7/21/2014	28	Miner (Left)	6:31	58.2
				58.0
				58.4
7/21/2014	29	Miner (Right)	7:10	58.1
				58.3
				58.0
7/21/2014	30	Miner (Left)	7:41	58.0
				58.0
				58.3
7/21/2014	31	Miner (Right)	9:08	60.7
				61.0
				62.0
7/22/2014	32	Miner (Right)	3:50	67.4
				69.0
				70.1
7/22/2014	33	Miner (Left)	4:11	60.7
				60.9
				60.6
7/22/2014	34	Miner (Right)	5:06	59.3

				59.3
				59.3
7/22/2014	35	Miner (Left)	6:09	65.1
				64.9
				64.8
7/22/2014	36	Miner (Left)	7:31	73.9
				73.9
				74.0
7/23/2014	37	Miner (Left)	5:12	35.3
				35.4
				35.7
7/23/2014	38	Miner (Left)	6:12	35.0
				35.2
				35.2
7/23/2014	39	Miner (Right)	6:53	35.0
				35.0
				35.1
7/23/2014	40	Miner (Right)	8:41	36.0
				36.7
				36.5
7/23/2014	41	Miner (Left)	9:04	35.0
				34.6
				34.6
7/24/2014	42	Miner (Right)	4:41	34.2
				35.0
				34.5
7/24/2014	43	Miner (Left)	5:39	34.6
				34.5
				34.7
7/24/2014	44	Miner (Right)	7:24	35.0
				34.7
				35.0
7/24/2014	45	Miner (Left)	7:59	35.6
				35.5
				35.4
7/24/2014	46	Miner (Left)	9:08	34.9
				34.8
				34.4
7/24/2014	47	Miner (Right)	9:30	34.4
				34.3
				34.4

Table 42:B2 Tabulation of dust concentration data from NIOSH – PDS

	Location	Respirable dust (mg)	Sampling time (min)	Respirable dust concentration (mg/m³)	Sample	Silica mass Estimation (µg)	Silica Concentration Estimation (µg/m³)	% Silica Estimation
Day 1	LC	0.641	161	1.99	386	62.879	195.277	30.5%
	RC	0.767	179	2.14	414	70.621	197.264	25.7%
	LR	0.295	180	0.82	396	31.405	87.235	29.6%
	RR	0.381	184	1.04	402	38.970	105.898	27.8%
Day 2	LC	1.112	340	1.64	382	163.020	239.736	21.6%
	RC	1.317	301	2.19	385	255.869	425.031	32.3%
	LR	0.848	409	1.04	392	136.049	166.319	19.6%
	RR	0.217	52	2.09	400	39.101	375.970	173.3%
Day 3	LC	0.954	270	1.77	401	94.544	175.082	18.4%
	RC	0.755	221	1.71	399	84.088	190.245	25.2%
	LR	0.712	271	1.31	411	65.421	120.703	17.0%
	RR	0.260	227	0.57	394	29.917	65.896	25.3%
Day 4	LC	1.314	197	3.34	398	136.016	345.219	26.3%
	RC	0.937	175	2.68	395	88.467	252.764	27.0%
	LR	0.556	194	1.43	388	45.897	118.290	21.3%
	RR	0.206	180	0.57	390	44.784	124.401	60.4%
Day 5	LC	1.390	204	3.41	102391	225.540	552.795	39.8%
	RC	1.309	165	3.97	102389	149.292	452.401	34.6%
	LR	0.324	205	0.79	102384	106.077	258.723	79.9%
	RR	0.390	165	1.18	102406	45.735	138.592	35.5%
Day 6	LC	1.211	198	3.06	102412	166.401	420.205	34.7%
	RC	0.419	161	1.30	102417	31.762	98.639	23.5%
	LR	0.725	214	1.69	102413	98.829	230.910	31.8%
	RR	0.213	157	0.68	102404	9.654	30.746	14.4%
Day 7	LC	1.154	222	2.60	102403	118.776	267.514	23.2%
	RC	1.491	198	3.77	102408	139.500	352.273	23.6%
	LR	0.738	222	1.66	102416	119.088	268.217	36.3%
	RR	0.239	193	0.62	102415	20.498	53.102	22.2%
Day 8	LC	1.768	309	2.86	102440	254.564	411.916	23.3%
	RC	1.178	228	2.58	102409	118.005	258.783	22.0%
	LR	0.414	311	0.67	102445	69.724	112.096	27.1%
	RR	0.416	230	0.90	102407	51.170	111.240	26.7%

Table 43:B3 Tabulation of dust concentration data from CPDM's

	Location	Respirable dust (mg)	Sampling Time (min)	Respirable dust concentration (mg/m^3)
Day 1	LC	0.62	161	1.76
	RC	1.12	179	2.85
	LR	0.32	180	0.81
	RR	0.28	184	0.69
Day 2	LC	1.79	340	2.39
	RC	2.38	301	3.60
	LR	1.74	409	1.93
	RR	0.30	51	2.70
Day 3	LC	2.35	270	3.96
	RC	1.30	221	2.67
	LR	0.86	271	1.44
	RR	0.40	227	0.79
Day 4	LC	2.06	197	4.76
	RC	1.20	175	3.12
	LR	0.91	194	2.14
	RR	0.33	180	0.82
Day 5	LC	2.18	204	4.85
	RC	2.61	165	7.20
	LR	1.36	205	3.02
	RR	0.72	165	1.98
Day 6	LC	1.84	198	4.22
	RC	0.69	161	1.95
	LR	0.99	214	2.11
	RR	0.31	157	0.90
Day 7	LC	2.52	222	5.17
	RC	2.94	198	6.75
	LR	1.14	222	2.34
	RR	0.45	193	1.05
Day 8	LC	2.50	309	3.67
	RC	1.92	228	3.82
	LR	0.68	311	1.00
	RR	1.07	230	2.11

Table 44: Multivariate regression of variables during the collection of silica samples

Data:

Surfactant	CM location	Sample location	% silica
without / with	Left / Right	Curtain / Return	
w/o	L	C	9.81%
w/o	R	C	9.21%
w/o	L	R	10.65%
w/o	R	R	10.23%
w/o	L	C	14.66%
w/o	R	C	19.43%
w/o	L	R	16.04%
w/o	R	R	18.02%
w/	L	C	9.91%
w/	R	C	11.14%
w/	L	R	9.19%
w/	R	R	11.51%
w/	L	C	10.35%
w/	R	C	9.44%
w/	L	R	8.25%
w/	R	R	21.74%
w/o	L	C	16.23%
w/o	R	C	11.41%
w/o	L	R	32.74%
w/o	R	R	11.73%
w/o	L	C	13.74%
w/o	R	C	7.58%
w/o	L	R	13.63%
w/o	R	R	4.53%
w/	L	C	10.29%
w/	R	C	9.36%
w/	L	R	16.14%
w/	R	R	8.58%
w/	L	C	14.40%
w/	R	C	10.02%
w/	L	R	16.84%
w/	R	R	12.30%

Regression Statistics	
Multiple R	0.359172524
R Square	0.129004902
Adjusted R Square	0.035683999
Standard Error	0.051285467
Observations	32

ANOVA					
	df	SS	MS	F	Significance F
Regression	3	0.011	0.004	1.382	0.269
Residual	28	0.074	0.003		
Total	31	0.085			

	Coeff.	SE	P-value
Intercept	0.138	0.018	0.000
Surfactant (without to with)	-0.019	0.018	0.307
CM location (Left to Right)	-0.023	0.018	0.217
Sample location (Curtain to Return)	0.022	0.018	0.236

Table 45: Disruptive statistics of silica mass

Data:

Silica mass Estimation (µg)
62.879
70.621
31.405
38.97
163.02
255.869
136.049
39.101
94.544
84.088
65.421
29.917
136.016
88.467
45.897
44.784
225.54
149.292
106.077
45.735
166.401
31.762
98.829
9.654
118.776
139.5
119.088
20.498
254.564
118.005
69.724

Histogram of Silica Mass, µg

Low Bin	**High Bin**	**Average**	**Count**	**Ind. Frequency**	**Cum. Frequency**
0.00	35.00	17.50	5	16%	16%
35.00	70.00	52.50	9	28%	44%
70.00	105.00	87.50	5	16%	59%
105.00	140.00	122.50	7	22%	81%
140.00	175.00	157.50	3	9%	91%
175.00	210.00	192.50	0	0%	91%
210.00	245.00	227.50	1	3%	94%
245.00	280.00	262.50	2	6%	100%

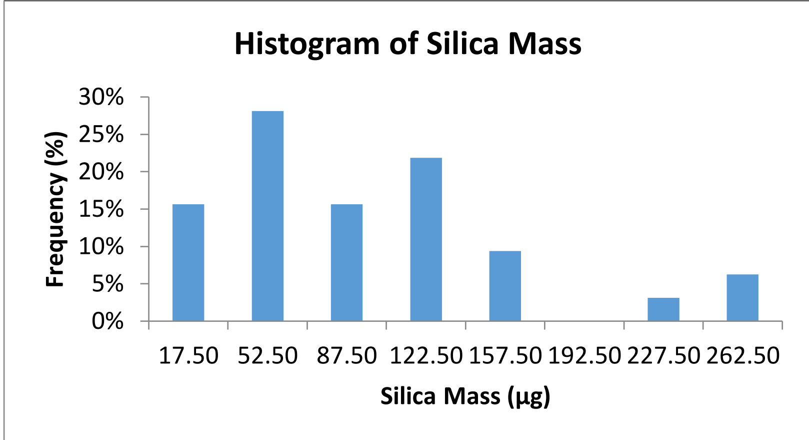

Silica mass Estimation (µg)	
Mean	97.23946875
Standard Error	11.53589587
Median	86.2775
Mode	#N/A
Standard Deviation	65.25688155
Sample Variance	4258.46059
Kurtosis	0.524813664
Skewness	0.985283839
Range	246.215
Minimum	9.654
Maximum	255.869
Sum	3111.663
Count	32
Confidence Level(95.0%)	23.52761473

Table 46: Descriptive statistics of estimated silica content

Data:

% Silica
9.81%
9.21%
10.65%
10.23%
14.66%
19.43%
16.04%
18.02%
9.91%
11.14%
9.19%
11.51%
10.35%
9.44%
8.25%
21.74%
16.23%
11.41%
32.74%
11.73%
13.74%
7.58%
13.63%
4.53%
10.29%
9.36%
16.14%
8.58%
14.40%
10.02%
16.84%
12.30%

Histogram of % Silica Estimation

Low Bin	High Bin	Average	Count	Ind. Frequency	Cum. Frequency
0%	5%	3%	1	3%	3%
5%	10%	8%	9	28%	31%
10%	15%	13%	14	44%	75%
15%	20%	18%	6	19%	94%
20%	25%	23%	1	3%	97%
25%	30%	28%	0	0%	97%
30%	35%	33%	1	3%	100%
35%	40%	38%	0	0%	100%

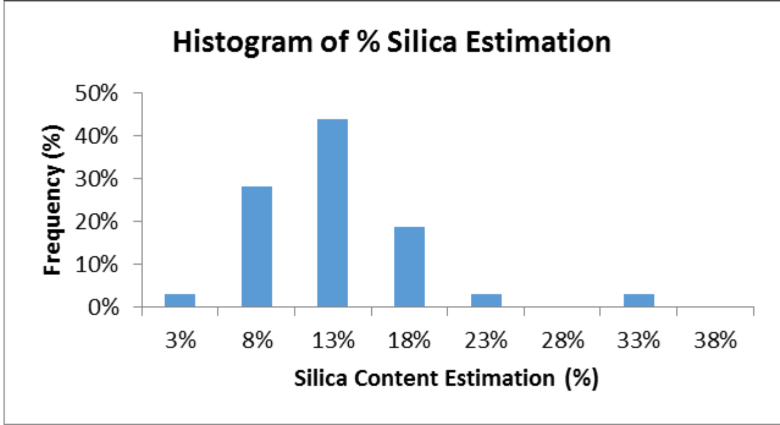

% Silica Estimation	
Mean	0.127836
Standard Error	0.009232
Median	0.112713
Mode	#N/A
Standard Deviation	0.052226
Sample Variance	0.002728
Kurtosis	5.921049
Skewness	1.960792
Range	0.282074
Minimum	0.045324
Maximum	0.327398
Sum	4.090744
Count	32
Confidence Level(95.0%)	0.018829

Table 47: Descriptive statistics of estimated silica content at the curtain and in the returns

Data:

% Silica Estimation at the Curtain	% Silica Estimation in the Returns
9.8%	10.6%
9.2%	10.2%
14.7%	16.0%
19.4%	18.0%
9.9%	9.2%
11.1%	11.5%
10.4%	8.3%
9.4%	21.7%
16.2%	32.7%
11.4%	11.7%
13.7%	13.6%
7.6%	4.5%
10.3%	16.1%
9.4%	8.6%
14.4%	16.8%
10.0%	12.3%

Histogram of % Silica Estimation at the Curtain

Low Bin	High Bin	Average	Count	Ind. Frequency	Cum. Frequency
0.040	0.050	0.045	0	0%	0%
0.050	0.060	0.055	0	0%	0%
0.060	0.110	0.085	9	56%	56%
0.110	0.160	0.135	5	31%	88%
0.160	0.210	0.185	2	13%	100%
0.210	0.260	0.235	0	0%	100%
0.260	0.310	0.285	0	0%	100%
0.310	0.360	0.335	0	0%	100%

Histogram of % Silica Estimation in the Return

Low Bin	High Bin	Average	Count	Ind. Frequency	Cum. Frequency
0%	5%	3%	1	6%	6%
5%	10%	8%	3	19%	25%
10%	15%	13%	6	38%	63%
15%	20%	18%	4	25%	88%
20%	25%	23%	1	6%	94%
25%	30%	28%	0	0%	94%
30%	35%	33%	1	6%	100%
35%	40%	38%	0	0%	100%

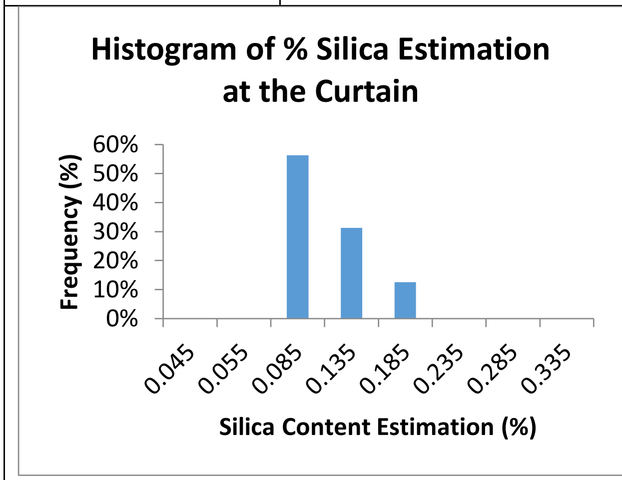

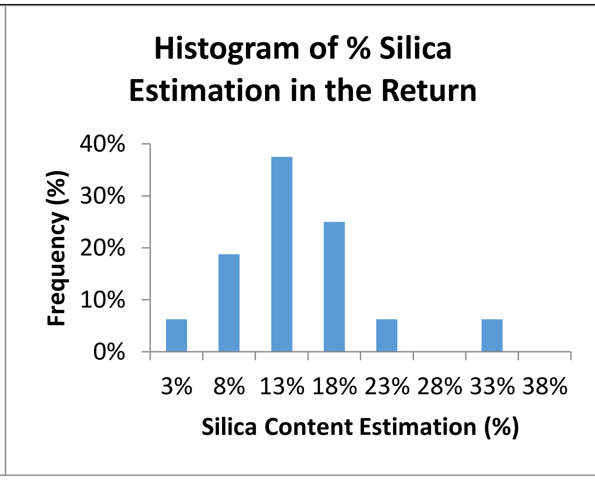

Data:

% Silica Estimation at the Curtain	*% Silica Estimation in the Returns*
9.8%	10.6%
9.2%	10.2%
14.7%	16.0%
19.4%	18.0%
9.9%	9.2%
11.1%	11.5%
10.4%	8.3%
9.4%	21.7%
16.2%	32.7%
11.4%	11.7%
13.7%	13.6%
7.6%	4.5%
10.3%	16.1%
9.4%	8.6%
14.4%	16.8%
10.0%	12.3%

	% Silica Estimation at the Curtain	*% Silica Estimation in the Returns*
Mean	0.117	0.139
Standard Error	0.008	0.017
Median	0.103	0.120
Mode	#N/A	#N/A
Standard Deviation	0.031	0.066
Sample Variance	0.001	0.004
Kurtosis	0.982	3.569
Skewness	1.186	1.557
Range	0.118	0.282
Minimum	0.076	0.045
Maximum	0.194	0.327
Sum	1.870	2.221
Count	16	16
Confidence Level(95.0%)	0.017	0.035

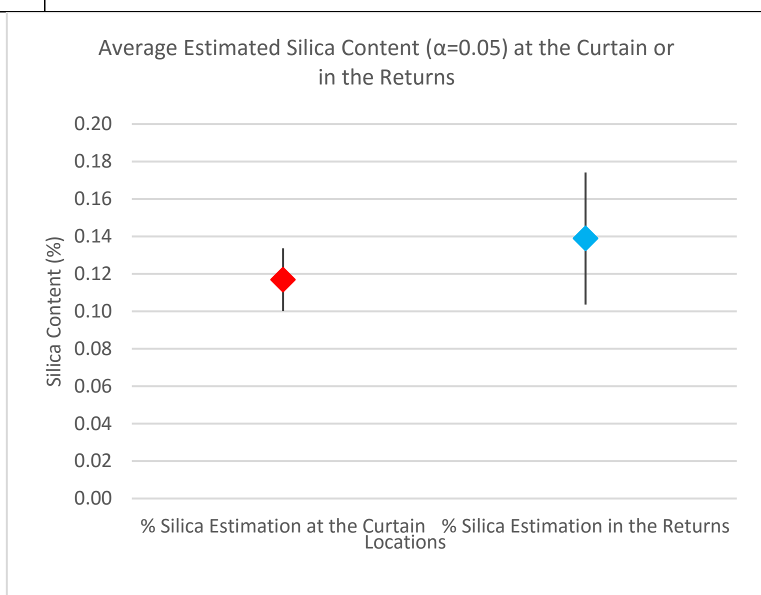

Table 48: Descriptive statistics of estimated silica content from the left and right CM

Data:

% Silica Estimation from Left CM	% Silica Estimation from Right CM
9.8%	9.2%
10.6%	10.2%
14.7%	19.4%
16.0%	18.0%
9.9%	11.1%
9.2%	11.5%
10.4%	9.4%
8.3%	21.7%
16.2%	11.4%
32.7%	11.7%
13.7%	7.6%
13.6%	4.5%
10.3%	9.4%
16.1%	8.6%
14.4%	10.0%
16.8%	12.3%

Histogram of % Silica Estimation from Left CM

Low Bin	High Bin	Average	Count	Ind. Frequency	Cum. Frequency
0%	5%	3%	0	0%	0%
5%	5%	5%	0	0%	0%
5%	10%	8%	4	25%	25%
10%	15%	13%	7	44%	69%
15%	20%	18%	4	25%	94%
20%	25%	23%	0	0%	94%
25%	30%	28%	0	0%	94%
30%	35%	33%	1	6%	100%

Histogram of % Silica Estimation from Right CM

Low Bin	High Bin	Average	Count	Ind. Frequency	Cum. Frequency
0%	5%	3%	1	6%	6%
5%	10%	8%	5	31%	38%
10%	15%	13%	7	44%	81%
15%	20%	18%	2	13%	94%
20%	25%	23%	1	6%	100%
25%	30%	28%	0	0%	100%
30%	35%	33%	0	0%	100%
35%	40%	38%	0	0%	100%

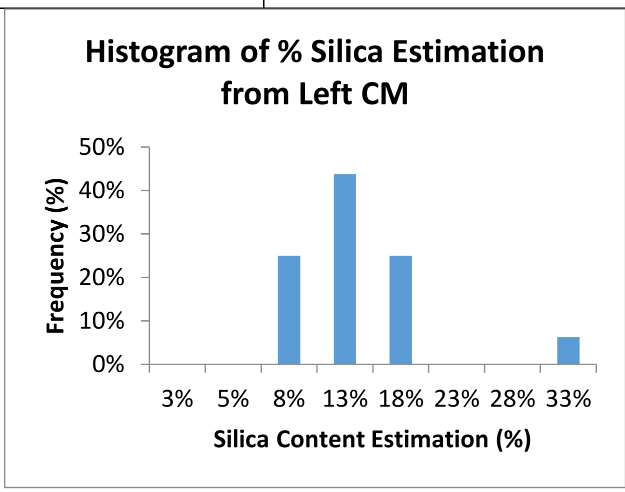

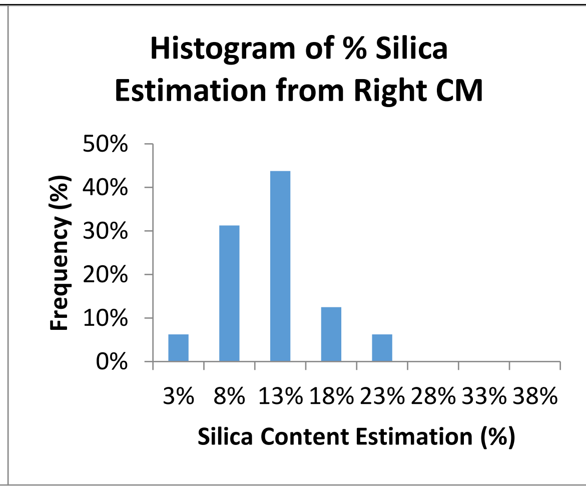

Data:

% Silica Estimation from Left CM	% Silica Estimation from Right CM
9.8%	9.2%
10.6%	10.2%
14.7%	19.4%
16.0%	18.0%
9.9%	11.1%
9.2%	11.5%
10.4%	9.4%
8.3%	21.7%
16.2%	11.4%
32.7%	11.7%
13.7%	7.6%
13.6%	4.5%
10.3%	9.4%
16.1%	8.6%
14.4%	10.0%
16.8%	12.3%

	% Silica Estimation from Left CM	*% Silica Estimation from Right CM*
Mean	0.139	0.116
Standard Error	0.014	0.011
Median	0.137	0.107
Mode	#N/A	#N/A
Standard Deviation	0.058	0.045
Sample Variance	0.003	0.002
Kurtosis	7.649	0.930
Skewness	2.421	1.072
Range	0.245	0.172
Minimum	0.083	0.045
Maximum	0.327	0.217
Sum	2.229	1.862
Count	16	16
Confidence Level(95.0%)	0.031	0.024

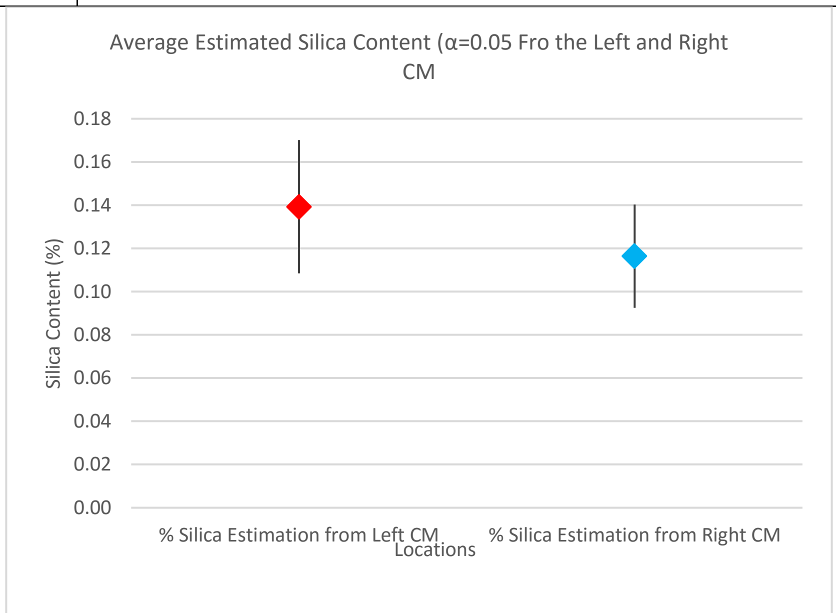

Table 49: Descriptive statistics of estimated silica content with and without surfactant

Data:

% Silica Estimation without Surfactant	% Silica Estimation with Surfactant
9.8%	9.9%
9.2%	11.1%
10.6%	9.2%
10.2%	11.5%
14.7%	10.4%
19.4%	9.4%
16.0%	8.3%
18.0%	21.7%
16.2%	10.3%
11.4%	9.4%
32.7%	16.1%
11.7%	8.6%
13.7%	14.4%
7.6%	10.0%
13.6%	16.8%
4.5%	12.3%

Histogram of% Silica Estimation without Surfactant

Low Bin	High Bin	Average	Count	Ind. Frequency	Cum. Frequency
0%	5%	3%	1	6%	6%
5%	5%	5%	0	0%	6%
5%	10%	8%	3	19%	25%
10%	15%	13%	7	44%	69%
15%	20%	18%	4	25%	94%
20%	25%	23%	0	0%	94%
25%	30%	28%	0	0%	94%
30%	35%	33%	1	6%	100%

Histogram of% Silica Estimation with Surfactant

Low Bin	High Bin	Average	Count	Ind. Frequency	Cum. Frequency
5%	7.00%	6%	0	0%	0%
7%	9%	8%	2	13%	13%
9%	11%	10%	7	44%	56%
11%	13%	12%	3	19%	75%
13%	15%	14%	1	6%	81%
15%	17%	16%	2	13%	94%
17%	19%	18%	0	0%	94%
19%	21%	20%	0	0%	94%

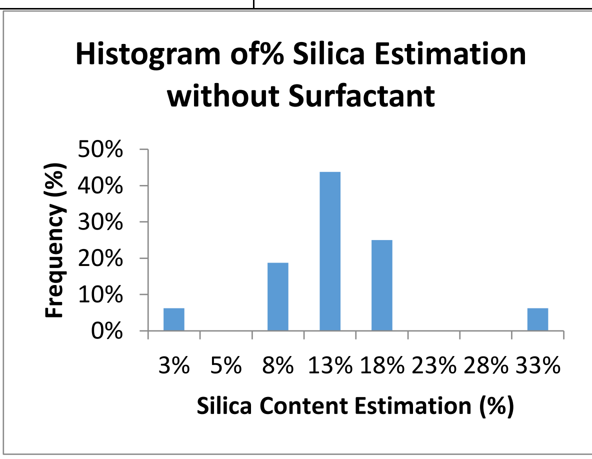

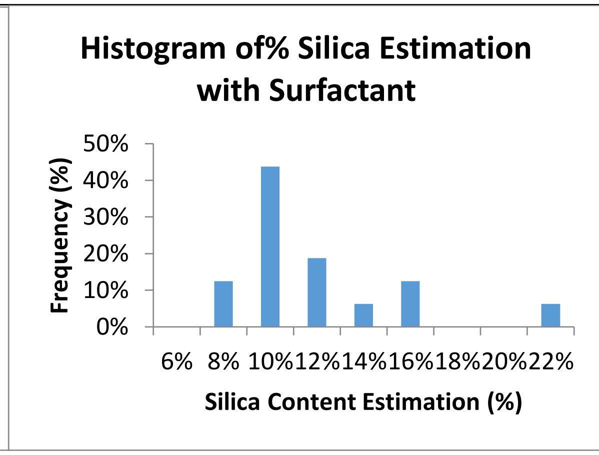

Data:

% Silica Estimation from Left CM	% Silica Estimation from Right CM
9.8%	9.2%
10.6%	10.2%
14.7%	19.4%
16.0%	18.0%
9.9%	11.1%
9.2%	11.5%
10.4%	9.4%
8.3%	21.7%
16.2%	11.4%
32.7%	11.7%
13.7%	7.6%
13.6%	4.5%
10.3%	9.4%
16.1%	8.6%
14.4%	10.0%
16.8%	12.3%

	% Silica Estimation from Left CM	*% Silica Estimation from Right CM*
Mean	0.139	0.116
Standard Error	0.014	0.011
Median	0.137	0.107
Mode	#N/A	#N/A
Standard Deviation	0.058	0.045
Sample Variance	0.003	0.002
Kurtosis	7.649	0.930
Skewness	2.421	1.072
Range	0.245	0.172
Minimum	0.083	0.045
Maximum	0.327	0.217
Sum	2.229	1.862
Count	16	16
Confidence Level(95.0%)	0.031	0.024

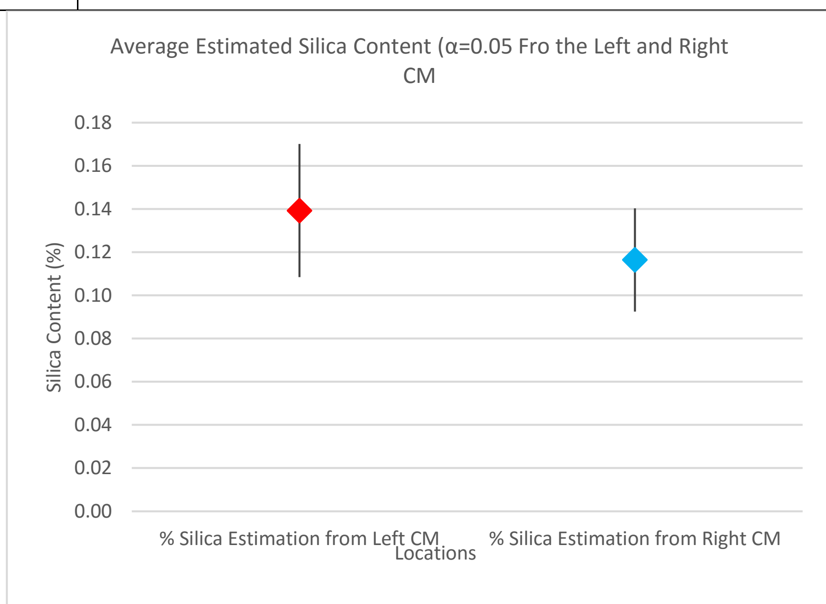

Table 50: Multivariate regression of variables during the collection of dust concentration

Data:

Surf.	CM location	Sample location	Sampling Device	Dust Conc.
without / with	Left / Right	Curtain / Return	PDS / CPDM	mg/ m3
w/o	L	C	PDS	1.99
w/o	R	C	PDS	2.14
w/o	L	R	PDS	0.82
w/o	R	R	PDS	1.04
w/o	L	C	PDS	1.64
w/o	R	C	PDS	2.19
w/o	L	R	PDS	1.04
w/o	R	R	PDS	2.09
w/	L	C	PDS	1.77
w/	R	C	PDS	1.71
w/	L	R	PDS	1.31
w/	R	R	PDS	0.57
w/	L	C	PDS	3.34
w/	R	C	PDS	2.68
w/	L	R	PDS	1.43
w/	R	R	PDS	0.57
w/o	L	C	PDS	3.41
w/o	R	C	PDS	3.97
w/o	L	R	PDS	0.79
w/o	R	R	PDS	1.18
w/o	L	C	PDS	3.06
w/o	R	C	PDS	1.3
w/o	L	R	PDS	1.69
w/o	R	R	PDS	0.68
w/	L	C	PDS	2.6
w/	R	C	PDS	3.77
w/	L	R	PDS	1.66
w/	R	R	PDS	0.62
w/	L	C	PDS	2.86
w/	R	C	PDS	2.58
w/	L	R	PDS	0.67
w/	R	R	PDS	0.9
w/o	L	C	CPDM	1.75
w/o	R	C	CPDM	2.84
w/o	L	R	CPDM	0.81
w/o	R	R	CPDM	0.69
w/o	L	C	CPDM	2.39
w/o	R	C	CPDM	2.67
w/o	L	R	CPDM	1.44
w/o	R	R	CPDM	0.80
w/	L	C	CPDM	4.75
w/	R	C	CPDM	3.12
w/	L	R	CPDM	2.13
w/	R	R	CPDM	0.83
w/	L	C	CPDM	4.86
w/	R	C	CPDM	7.19
w/	L	R	CPDM	3.02
w/	R	R	CPDM	1.98
w/o	L	C	CPDM	4.22
w/o	R	C	CPDM	1.95
w/o	L	R	CPDM	2.10

Regression Statistics	
Multiple R	0.740818
R Square	0.548812
Adjusted R Square	0.518223
Standard Error	1.007189
Observations	64

ANOVA					
	df	SS	MS	F	Significance F
Regression	3	72.801	18.200	17.941	0.000
Residual	28	59.851	1.014		
Total	31	132.653			

	Coeff.	SE	P-value
Intercept	2.7951	0.2815	0.0000
Surfactant (without to with)	0.0852	0.2518	0.7362
CM location (Left to Right)	-0.1445	0.2518	0.5681
Sample location (Curtain to Return)	-1.9015	0.2518	0.0000
Sampling Device (PDS to CPDM)	0.9520	0.2518	0.0004

w/o	R	R	CPDM	0.90
w/o	L	C	CPDM	5.16
w/o	R	C	CPDM	6.75
w/o	L	R	CPDM	2.33
w/o	R	R	CPDM	1.06
w/	L	C	CPDM	3.68
w/	R	C	CPDM	3.83
w/	L	R	CPDM	0.99
w/	R	R	CPDM	2.11
w/	L	C	CPDM	2.67
w/	R	C	CPDM	1.44
w/	L	R	CPDM	0.80
w/	R	R	CPDM	4.75

Table 51: Descriptive statistics of dust concentration between CPDM and PDS

Data:	
Dust Conc. From PDS (mg/m3)	*Dust Conc. From CPDM (mg/m3)*
1.99	1.75
2.14	2.84
0.82	0.81
1.04	0.69
1.64	2.39
2.19	3.59
1.04	1.93
2.09	2.67
1.77	3.96
1.71	2.67
1.31	1.44
0.57	0.80
3.34	4.75
2.68	3.12
1.43	2.13
0.57	0.83
3.41	4.86
3.97	7.19
0.79	3.02
1.18	1.98
3.06	4.22
1.3	1.95
1.69	2.10
0.68	0.90
2.6	5.16
3.77	6.75
1.66	2.33
0.62	1.06
2.86	3.68
2.58	3.83
0.67	0.99
0.9	2.11

Histogram of PDS Dust Concentrations

Low Bin	High Bin	Average	Count	Ind. Frequency	Cum. Frequency
0.00	0.50	0.25	0	0%	0%
0.50	1.00	0.75	8	25%	25%
1.00	1.50	1.25	6	19%	44%
1.50	2.00	1.75	6	19%	63%
2.00	2.50	2.25	3	9%	72%
2.50	3.00	2.75	4	13%	84%
3.00	3.50	3.25	3	9%	94%
3.50	4.00	3.75	2	6%	100%

Histogram of CPDM Dust Concentrations

Low Bin	High Bin	Average	Count	Ind. Frequency	Cum. Frequency
0.00	1.00	0.50	6	19%	19%
1.00	1.50	1.25	2	6%	25%
1.50	2.00	1.75	4	13%	38%
2.00	2.50	2.25	5	16%	53%
2.50	3.00	2.75	3	9%	63%
3.00	3.50	3.25	2	6%	69%
3.50	4.00	3.75	4	13%	81%
4.00	4.50	4.25	1	3%	84%

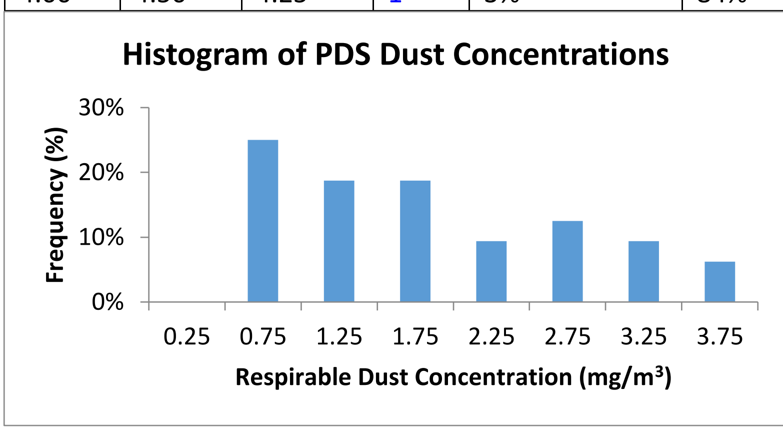

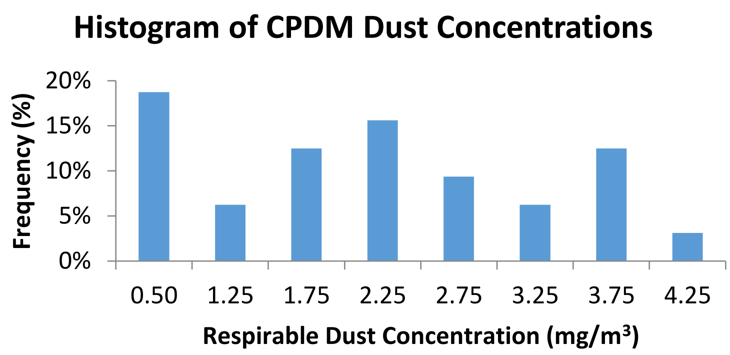

Data:

Dust Conc. From PDS (mg/m3)	*Dust Conc. From CPDM (mg/m3)*
1.99	1.75
2.14	2.84
0.82	0.81
1.04	0.69
1.64	2.39
2.19	3.59
1.04	1.93
2.09	2.67
1.77	3.96
1.71	2.67
1.31	1.44
0.57	0.80
3.34	4.75
2.68	3.12
1.43	2.13
0.57	0.83
3.41	4.86
3.97	7.19
0.79	3.02
1.18	1.98
3.06	4.22
1.3	1.95
1.69	2.10
0.68	0.90
2.6	5.16
3.77	6.75
1.66	2.33
0.62	1.06
2.86	3.68
2.58	3.83
0.67	0.99
0.9	2.11

	Dust Conc. From PDS (mg/m3)	*Dust Conc. From CPDM (mg/m3)*
Mean	1.815	2.767
Standard Error	0.176	0.297
Median	1.675	2.364
Mode	1.040	#N/A
Standard Deviation	0.994	1.680
Sample Variance	0.988	2.823
Kurtosis	-0.627	0.664
Skewness	0.595	0.968
Range	3.400	6.498
Minimum	0.570	0.692
Maximum	3.970	7.190
Sum	58.070	88.534
Count	32	32
Confidence Level(95.0%)	0.358	0.606

t-Test: Two-Sample Assuming Unequal Variances		
	PDS	CPDM
Mean	1.815	2.767
Variance	0.988	2.823
Observations	32	32
Hypothesized Mean Difference	0.000	
df	50.000	
t Stat	-2.758	
P(T<=t) one-tail	0.004	
t Critical one-tail	1.676	
P(T<=t) two-tail	0.008	
t Critical two-tail	2.009	

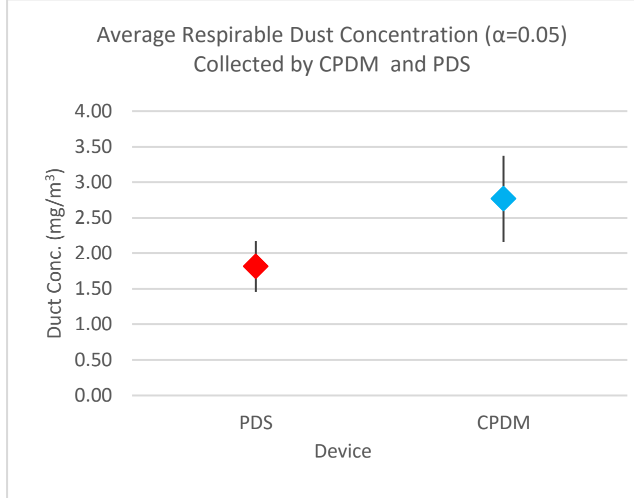

Table 52: Descriptive statistics of dust concentration between the curtain and the returns

Data:

Dust Conc. Curtains (mg/m³)	*Dust Conc. Returns (mg/m³)*
1.99	0.82
2.14	1.04
2.86	1.04
2.58	2.09
1.64	1.31
2.19	0.57
2.6	1.43
3.77	0.57
1.77	0.79
1.71	1.18
3.06	1.69
1.3	0.68
3.34	1.66
2.68	0.62
3.41	0.67
3.97	0.9
1.75	0.81
2.84	0.69
3.68	1.93
3.83	2.67
2.39	1.44
3.59	0.80
5.16	2.13
6.75	0.83
3.96	3.02
2.67	1.98
4.22	2.10
1.95	0.90
4.75	2.33

Histogram of Dust Concentrations at the Curtain

Low Bin	High Bin	Average	Count	Ind. Frequency	Cum. Frequency
0.00	1.00	0.50	0	0%	0%
1.00	2.00	1.50	7	22%	22%
2.00	3.00	2.50	9	28%	50%
3.00	4.00	3.50	10	31%	81%
4.00	5.00	4.50	3	9%	91%
5.00	6.00	5.50	1	3%	94%
6.00	7.00	6.50	1	3%	97%
7.00	8.00	7.50	1	3%	100%

Histogram of Dust Concentrations in the Returns

Low Bin	High Bin	Average	Count	Ind. Frequency	Cum. Frequency
0.00	0.35	0.18	0	0%	0%
0.35	0.70	0.53	6	19%	19%
0.70	1.05	0.88	10	31%	50%
1.05	1.40	1.23	3	9%	59%
1.40	1.75	1.58	4	13%	72%
1.75	2.10	1.93	3	9%	81%
2.10	2.45	2.28	4	13%	94%
2.45	2.80	2.63	1	3%	97%

3.12	1.06
4.86	0.99
7.19	2.11

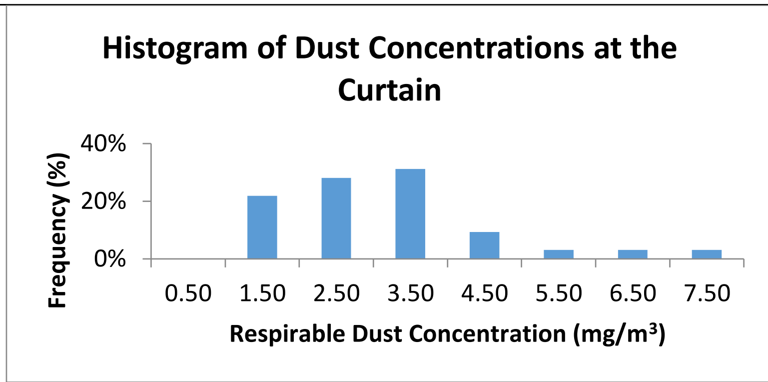

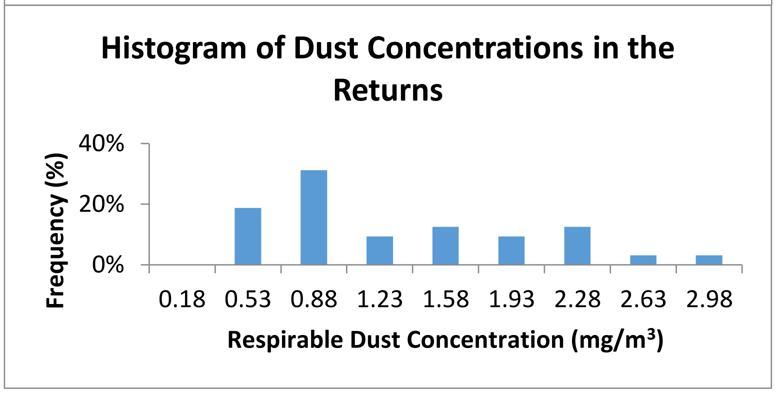

Data:

Dust Conc. Curtains (mg/m³)	*Dust Conc. Returns (mg/m³)*
1.99	0.82
2.14	1.04
2.86	1.04
2.58	2.09
1.64	1.31
2.19	0.57
2.6	1.43
3.77	0.57
1.77	0.79
1.71	1.18
3.06	1.69
1.3	0.68
3.34	1.66
2.68	0.62
3.41	0.67
3.97	0.9
1.75	0.81
2.84	0.69
3.68	1.93
3.83	2.67
2.39	1.44
3.59	0.80
5.16	2.13
6.75	0.83
3.96	3.02
2.67	1.98
4.22	2.10
1.95	0.90
4.75	2.33
3.12	1.06
4.86	0.99
7.19	2.11

	Dust Conc. Curtains (mg/m³)	*Dust Conc. Returns (mg/m³)*
Mean	3.241	1.340
Standard Error	0.247	0.119
Median	2.960	1.050
Mode	#N/A	1.040
Standard Deviation	1.399	0.676
Sample Variance	1.956	0.457
Kurtosis	1.463	-0.349
Skewness	1.155	0.809
Range	5.890	2.446
Minimum	1.300	0.570
Maximum	7.190	3.016
Sum	103.726	42.878
Count	32	32
Confidence Level(95.0%)	0.504	0.244

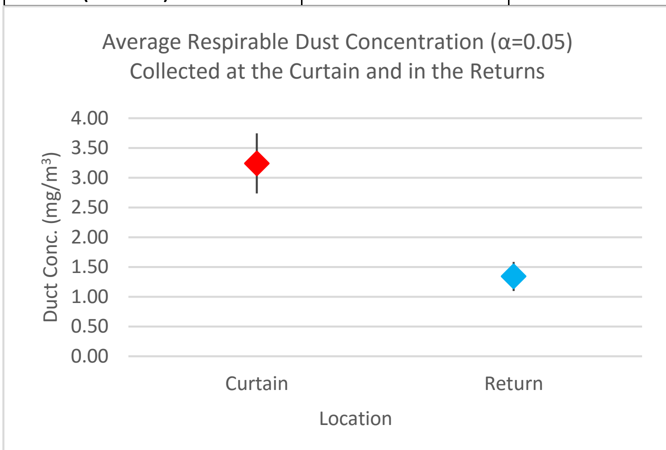

ANOVA						
Source of Variation	SS	df	MS	F	P-value	F crit
Between Groups	57.850	1	57.850	47.949	2.90389E-09	3.996
Within Groups	74.802	62	1.206			
Total	132.653	63				

Table 53: Descriptive statistics of dust concentration between left and right CM

Data:

Dust Conc. Left CM (mg/m3)	Dust Conc. Right CM (mg/m3)
1.99	2.14
2.86	2.58
1.64	2.19
2.6	3.77
1.77	1.71
3.06	1.3
3.34	2.68
3.41	3.97
1.75	2.84
3.68	3.83
2.39	3.59
5.16	6.75
3.96	2.67
4.22	1.95
4.75	3.12
4.86	7.19
0.82	1.04
1.04	2.09
1.31	0.57
1.43	0.57
0.79	1.18
1.69	0.68
1.66	0.62
0.67	0.9
0.81	0.69
1.93	2.67
1.44	0.80
2.13	0.83
3.02	1.98
2.10	0.90
2.33	1.06
0.99	2.11

Histogram of Dust Concentrations From the Left CM

Low Bin	High Bin	Average	Count	Ind. Frequency	Cum. Frequency
0.00	1.00	0.50	5	16%	16%
1.00	2.00	1.50	11	34%	50%
2.00	3.00	2.50	6	19%	69%
3.00	4.00	3.50	6	19%	88%
4.00	5.00	4.50	3	9%	97%
5.00	6.00	5.50	1	3%	100%
6.00	7.00	6.50	0	0%	100%
7.00	8.00	7.50	0	0%	100%

Histogram of Dust Concentrations From the Right CM

Low Bin	High Bin	Average	Count	Ind. Frequency	Cum. Frequency
0.00	1.00	0.50	9	28%	28%
1.00	2.00	1.50	7	22%	50%
2.00	3.00	2.50	9	28%	78%
3.00	4.00	3.50	5	16%	94%
4.00	5.00	4.50	0	0%	94%
5.00	6.00	5.50	0	0%	94%
6.00	7.00	6.50	1	3%	97%
7.00	8.00	7.50	1	3%	100%

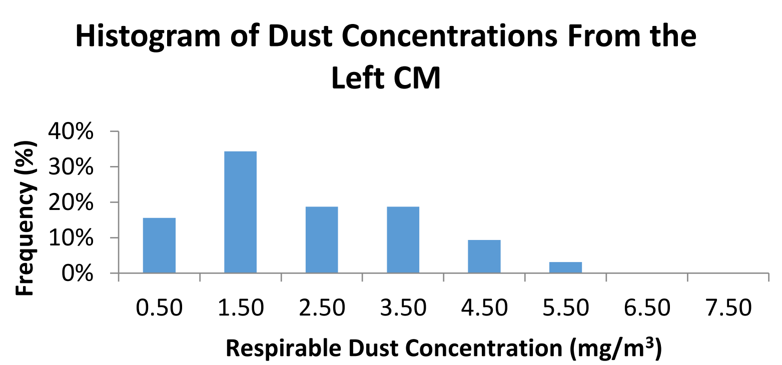

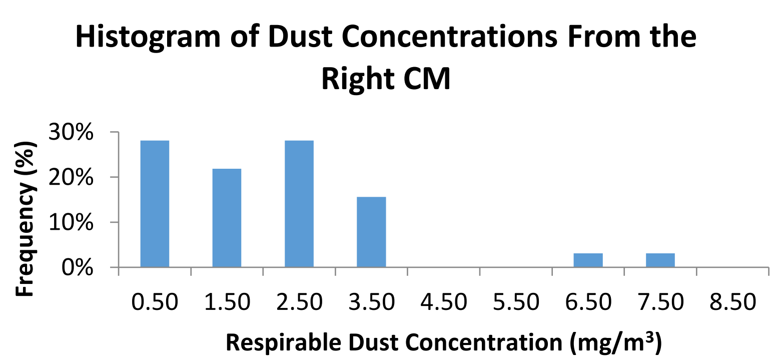

Data:

Dust Conc. Left CM (mg/m3)	Dust Conc. Right CM (mg/m3)
1.99	2.14
2.86	2.58
1.64	2.19
2.6	3.77
1.77	1.71
3.06	1.3
3.34	2.68
3.41	3.97
1.75	2.84
3.68	3.83
2.39	3.59
5.16	6.75
3.96	2.67
4.22	1.95
4.75	3.12
4.86	7.19
0.82	1.04
1.04	2.09
1.31	0.57
1.43	0.57
0.79	1.18
1.69	0.68
1.66	0.62
0.67	0.9
0.81	0.69
1.93	2.67
1.44	0.80
2.13	0.83
3.02	1.98
2.10	0.90
2.33	1.06
0.99	2.11

	Dust Conc. Left CM (mg/m3)	Dust Conc. Right CM (mg/m3)
Mean	2.362947711	2.21841432
Standard Error	0.224473663	0.288092173
Median	2.046401869	2.036735537
Mode	#N/A	0.57
Standard Deviation	1.269814792	1.62969543
Sample Variance	1.612429607	2.655907196
Kurtosis	-0.411218758	2.85116126
Skewness	0.69240795	1.569978017
Range	4.48970516	6.620082645
Minimum	0.67	0.57
Maximum	5.15970516	7.190082645
Sum	75.61432676	70.98925823
Count	32	32
Confidence Level (95.0%)	0.457817053	0.58756786

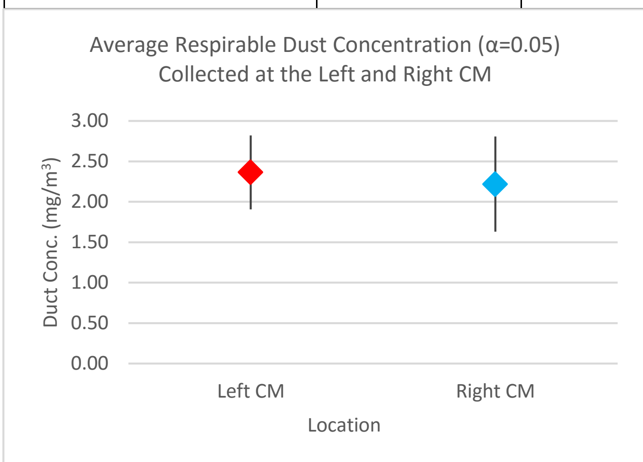

Table 54: Descriptive statistics of dust concentration with and without surfactant

Data:

Dust Conc. without Surfactant (mg/m3)	*Dust Conc. with Surfactant (mg/m3)*
1.99	1.77
2.14	1.71
0.82	1.31
1.04	0.57
1.64	3.34
2.19	2.68
1.04	1.43
2.09	0.57
3.41	2.6
3.97	3.77
0.79	1.66
1.18	0.62
3.06	2.86
1.3	2.58
1.69	0.67
0.68	0.9
1.75	3.96
2.84	2.67
0.81	1.44
0.69	0.80
2.39	4.75
3.59	3.12
1.93	2.13
2.67	0.83
4.86	5.16
7.19	6.75
3.02	2.33
1.98	1.06
4.22	3.68
1.95	3.83
2.10	0.99
0.90	2.11

Histogram of Dust Concentrations without Surfactant

Low Bin	**High Bin**	**Average**	**Count**	**Ind. Frequency**	**Cum. Frequency**
0.00	1.00	0.50	6	19%	19%
1.00	2.00	1.50	11	34%	53%
2.00	3.00	2.50	7	22%	75%
3.00	4.00	3.50	5	16%	91%
4.00	5.00	4.50	2	6%	97%
5.00	6.00	5.50	0	0%	97%
6.00	7.00	6.50	0	0%	97%
7.00	8.00	7.50	1	3%	100%

Histogram of Dust Concentrations with Surfactant

Low Bin	**High Bin**	**Average**	**Count**	**Ind. Frequency**	**Cum. Frequency**
0.00	1.00	0.50	8	25%	25%
1.00	2.00	1.50	7	22%	47%
2.00	3.00	2.50	8	25%	72%
3.00	4.00	3.50	6	19%	91%
4.00	5.00	4.50	1	3%	94%
5.00	6.00	5.50	1	3%	97%
6.00	7.00	6.50	1	3%	100%
7.00	8.00	7.50	0	0%	100%

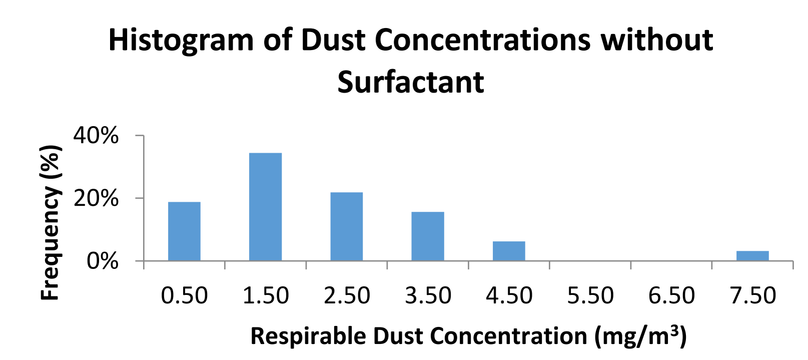

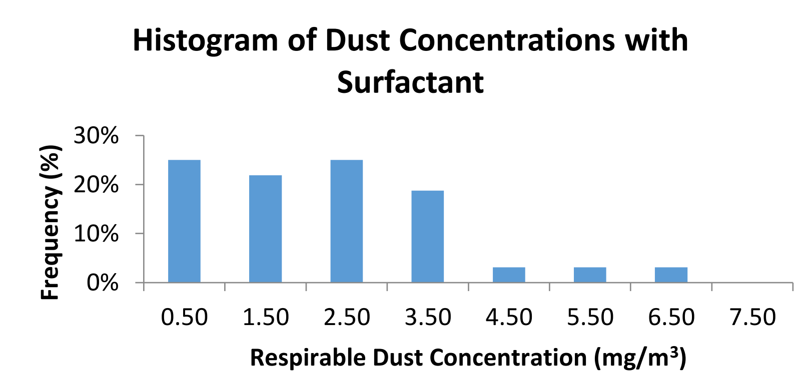

Data:

Dust Conc. without Surfactant (mg/m3)	*Dust Conc. with Surfactant (mg/m3)*
1.99	1.77
2.14	1.71
0.82	1.31
1.04	0.57
1.64	3.34
2.19	2.68
1.04	1.43
2.09	0.57
3.41	2.6
3.97	3.77
0.79	1.66
1.18	0.62
3.06	2.86
1.3	2.58
1.69	0.67
0.68	0.9
1.75	3.96
2.84	2.67
0.81	1.44
0.69	0.80
2.39	4.75
3.59	3.12
1.93	2.13
2.67	0.83
4.86	5.16
7.19	6.75
3.02	2.33
1.98	1.06
4.22	3.68
1.95	3.83
2.10	0.99
0.90	2.11

	Dust Conc. without Surfactant (mg/m3)	Dust Conc. with Surfactant (mg/m3)
Mean	2.248	2.333
Standard Error	0.251	0.266
Median	1.987	2.123
Mode	1.040	0.570
Standard Deviation	1.417	1.505
Sample Variance	2.009	2.266
Kurtosis	3.552	0.944
Skewness	1.586	1.003
Range	6.510	6.179
Minimum	0.680	0.570
Maximum	7.190	6.749
Sum	71.938	74.666
Count	32	32
Confidence Level (95.0%)	0.511	0.543

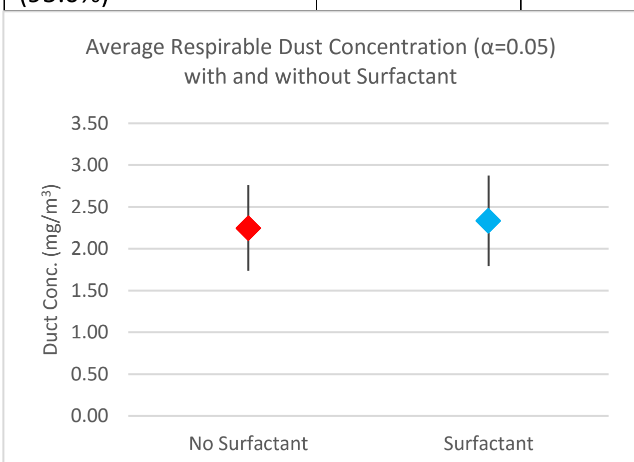

Table 55: Multivariate regression of variables during the collection of dust concentration on a cut by cut basis

Data:

Cut Depth (ft)	Starting Depth (ft)	Surf	Left/ Right CM	Curtain /Return	Number od Bits Changed (#)	Air Flow (CFM)	Dust Conc. for Cut (mg/m^3)
20	20	w/o	L	L	12	14904	2.88
20	20	w/o	L	R	12	14904	0.44
20	28	w/o	R	L	11	12690	1.60
20	28	w/o	R	R	11	12690	1.07
20	32	w/o	L	L	10	10458	3.23
20	32	w/o	L	R	10	10458	0.31
20	10	w/o	R	L	10	11088	3.63
20	10	w/o	R	R	10	11088	1.02
20	40	w/o	L	L	10	9261	4.51
20	40	w/o	L	R	10	9261	0.28
25	0	w/o	R	L	9	11016	5.29
25	0	w/o	R	R	9	11016	0.85
20	0	w/o	L	L	12	11795	5.04
20	0	w/o	L	R	12	11795	1.89
25	0	w/o	R	L	19	12587	8.77
25	0	w/o	L	R	10	13680	8.44
25	0	w/o	L	L	10	13680	6.76
25	33	w/o	R	R	0	11875	2.25
25	33	w/o	R	L	0	11875	1.07
15	0	w/o	R	R	18	12300	8.56
15	0	w/o	R	L	18	12300	2.76
15	20	w/o	L	R	12	9980	1.50
15	20	w/o	L	L	12	9980	5.90
20	20	w/	R	R	15	9643	2.72
20	20	w/	R	L	15	9643	0.61
20	0	w/	R	R	23	12690	5.67
20	0	w/	R	L	23	12690	1.40
25	55	w/	R	R	14	13797	4.82
25	55	w/	R	L	14	13797	2.63
25	0	w/	L	R	21	14960	13.63
25	0	w/	L	L	21	14960	5.62
20	46	w/	R	R	11	10260	4.03
20	46	w/	R	R	11	10260	1.62
20	25	w/	L	L	13	9010	3.52
20	25	w/	L	R	13	9010	1.41
30	54	w/	R	L	10	9324	7.19
30	54	w/	R	R	10	9324	0.14
10	25	w/	L	L	0	11178	4.89
10	25	w/	L	R	0	11178	1.92
20	0	w/o	L	L	24	18080	10.24
20	0	w/o	L	R	24	18080	7.14
15	20	w/o	R	L	11	9207	5.82
15	20	w/o	R	R	11	9207	4.33
20	30	w/o	L	L	4	11560	3.82
20	30	w/o	L	R	4	11560	1.61
15	50	w/o	R	L	6	10044	6.64
15	50	w/o	R	R	6	10044	0.69
15	20	w/o	L	L	9	11760	1.60
15	20	w/o	L	R	9	11760	7.26
30	20	w/o	R	L	12	9820	7.88

Regression Statistics	
Multiple R	0.617
R Square	0.380
Adjusted R Square	0.323
Standard Error	3.045
Observations	83

ANOVA					
	df	*SS*	*MS*	*F*	*Significance F*
Regression	7	427.123	61.018	6.579	4.6E-06
Residual	75	695.575	9.274		
Total	82	1122.698			

30	20	w/o	R	R	12	9820	2.85
10	0	w/o	L	L	9	15066	6.72
10	0	w/o	L	R	9	15066	1.71
30	65	w/o	R	L	20	12690	3.18
30	65	w/o	R	R	20	12690	1.66
35	0	w/o	L	L	18	14784	13.14
35	0	w/o	L	R	18	14784	4.70
30	87	w/o	R	L	7	11088	2.29
30	87	w/o	R	R	7	11088	1.31
15	36	w/o	L	L	0	15620	10.38
15	36	w/o	L	R	0	15620	2.09
30	0	w/	R	L	6	17388	7.21
30	0	w/	R	R	6	17388	1.64
30	0	w/	L	L	19	15302	9.35
30	0	w/	L	R	19	15302	1.90
10	0	w/	L	L	6	16855	21.38
10	0	w/	L	R	6	16855	6.39
35	0	w/	R	L	10	12852	10.14
35	0	w/	R	R	10	12852	0.56
35	0	w/	R	L	17	10792	5.47
35	0	w/	R	R	17	10792	3.39
10	30	w/	L	L	5	13008	4.71
10	30	w/	L	R	5	13008	1.58
20	37	w/	L	L	25	14769	11.97
20	37	w/	L	R	25	14769	1.97
10	0	w/	L	L	8	12600	7.19
10	0	w/	L	R	8	12600	3.16
25	20	w/	R	L	7	16870	9.03
25	20	w/	R	R	7	16870	3.86
10	40	w/	L	L	9	11576	3.10
10	40	w/	L	R	9	11576	1.19
10	47	w/	L	L	8	10240	3.86
10	47	w/	L	R	8	10240	1.94

	Coeff.	*SE*	P-value
Intercept	0.0399	2.2903	0.9862
Cut Depth (ft.)	0.0059	0.0553	0.9152
Starting Depth (ft.)	-0.0300	0.0173	0.0864
Surfactant	0.4341	0.6803	0.5253
Left to Right	-0.5798	0.7991	0.4703
Curtain to Return	-2.8198	0.6697	0.0001
Number of Bits Changed (#)	0.0482	0.0605	0.4284
Air Flow (CFM)	0.0005	0.0002	0.0035

Table 56: Descriptive statistics of dust concentration at the curtain and in the returns on a cut by cut basis

Data:

Dust Conc. for Cut at the Curtain (mg/m^3)	Dust Conc. for Cut in the Returns (mg/m^3)
2.88	0.44
1.60	1.07
3.23	0.31
3.63	1.02
4.51	0.28
5.29	0.85
5.04	1.89
8.77	6.76
8.44	1.07
2.25	2.76
8.56	5.90
1.50	1.44
1.45	1.40
5.67	0.99
6.87	1.80
5.20	4.98
17.60	0.61
2.72	3.24
6.17	2.63
4.82	5.62
13.63	1.62
4.03	1.41
3.52	0.14
7.19	1.92
4.89	7.14
10.24	4.33
5.82	1.61
3.82	0.69
6.64	7.26
1.60	2.85
7.88	1.71
6.72	1.66
3.18	4.70
13.14	1.31
2.29	2.09
10.38	1.28
2.51	4.46
1.39	1.64
7.21	1.90
9.35	6.39
21.38	0.56
10.14	3.39
5.47	1.58
4.71	1.97
11.97	3.16
7.19	3.86
9.03	1.19
3.10	1.94
3.86	

Histogram of Dust Concentrations per cut at the Curtain

Low Bin	High Bin	Average	Count	Ind. Frequency	Cum. Frequency
0.00	3.00	1.50	10	20%	20%
3.00	6.00	4.50	18	37%	57%
6.00	9.00	7.50	11	22%	80%
9.00	12.00	10.50	6	12%	92%
12.00	15.00	13.50	2	4%	96%
15.00	18.00	16.50	1	2%	98%
18.00	21.00	19.50	0	0%	98%
21.00	24.00	22.50	1	2%	100%

Histogram of Dust Concentrations per cut in the Return

Low Bin	High Bin	Average	Count	Ind. Frequency	Cum. Frequency
0.00	1.00	0.50	9	19%	19%
1.00	2.00	1.50	21	44%	63%
2.00	3.00	2.50	4	8%	71%
3.00	4.00	3.50	4	8%	79%
4.00	5.00	4.50	4	8%	88%
5.00	6.00	5.50	2	4%	92%
6.00	7.00	6.50	2	4%	96%
7.00	8.00	7.50	2	4%	100%

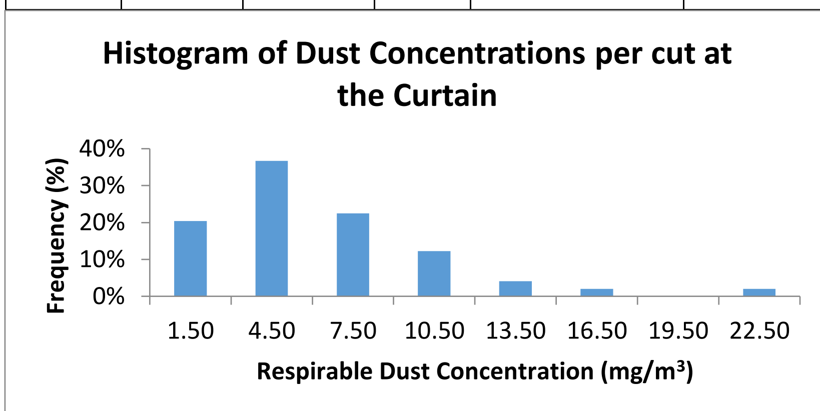

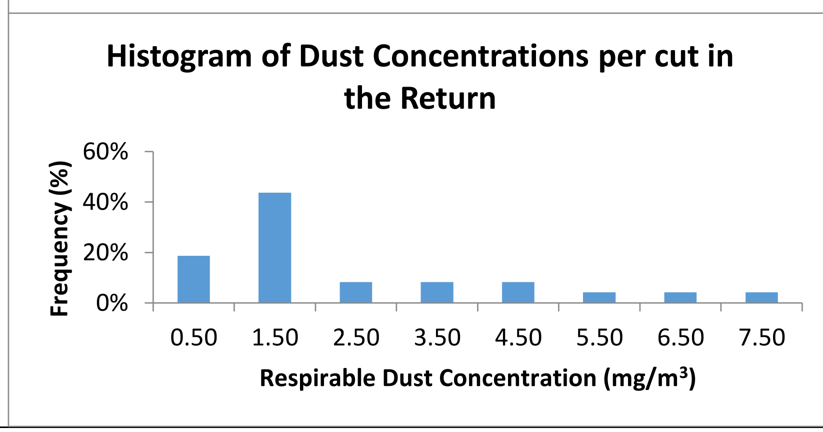

Data:	
Dust Conc. for Cut at the Curtain (mg/m^3)	Dust Conc. for Cut in the Returns (mg/m^3)
2.88	0.44
1.60	1.07
3.23	0.31
3.63	1.02
4.51	0.28
5.29	0.85
5.04	1.89
8.77	6.76
8.44	1.07
2.25	2.76
8.56	5.90
1.50	1.44
1.45	1.40
5.67	0.99
6.87	1.80
5.20	4.98
17.60	0.61
2.72	3.24
6.17	2.63
4.82	5.62
13.63	1.62
4.03	1.41
3.52	0.14
7.19	1.92
4.89	7.14
10.24	4.33
5.82	1.61
3.82	0.69
6.64	7.26
1.60	2.85
7.88	1.71
6.72	1.66
3.18	4.70
13.14	1.31
2.29	2.09
10.38	1.28
2.51	4.46
1.39	1.64
7.21	1.90
9.35	6.39
21.38	0.56
10.14	3.39
5.47	1.58
4.71	1.97
11.97	3.16
7.19	3.86
9.03	1.19
3.10	1.94
3.86	

	Dust Conc. for Cut at the Curtain (mg/m^3)	Dust Conc. for Cut in the Returns (mg/m^3)
Mean	6.296	2.425
Standard Error	0.596	0.279
Median	5.289	1.712
Mode	#N/A	#N/A
Standard Deviation	4.173	1.953
Sample Variance	17.414	3.815
Kurtosis	2.988	0.338
Skewness	1.507	1.130
Range	19.991	7.261
Minimum	1.392	0.000
Maximum	21.383	7.261
Sum	308.504	118.828
Count	49	49
Confidence Level (95.0%)	1.199	0.561

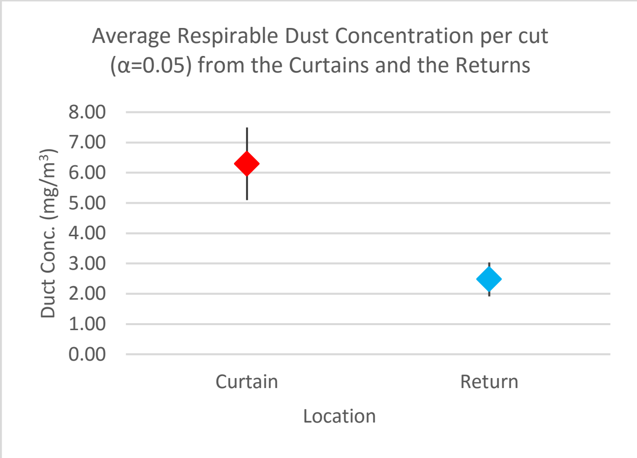

t-Test: Two-Sample Assuming Unequal Variances	Curtain	Return
Mean	6.296	2.476
Variance	17.414	3.769
Observations	49	48
Hypothesized Mean Difference	0	
df	68	
t Stat	5.800	
P(T<=t) one-tail	0.000	
t Critical one-tail	1.668	
P(T<=t) two-tail	0.000	
t Critical two-tail	1.995	

Table 57: Descriptive statistics of dust concentration at the left and right CM on a cut by cut basis

Data:

Dust Conc. per cut from Left CM (mg/m^3)	Dust Conc. per cut from Right CM (mg/m^3)
2.88	1.60
0.44	1.07
3.23	3.63
0.31	1.02
4.51	5.29
0.28	0.85
5.04	8.77
1.89	2.25
8.44	1.07
6.76	8.56
1.50	2.76
5.90	5.67
1.45	1.40
1.44	5.20
6.87	1.80
0.99	2.72
17.60	0.61
4.98	4.82
6.17	2.63
3.24	4.03
13.63	1.62
5.62	7.19
3.52	0.14
1.41	5.82
4.89	4.33
1.92	6.64
10.24	0.69
7.14	7.88
3.82	2.85
1.61	3.18
1.60	1.66
7.26	2.29
6.72	1.31
1.71	7.21
13.14	1.64
4.70	10.14
10.38	0.56
2.09	5.47
2.51	3.39
1.28	9.03
1.39	3.86
4.46	
9.35	
1.90	
21.38	
6.39	
4.71	
1.58	
11.97	
1.97	

Histogram of Dust Concentrations per cut from Left CM

Low Bin	High Bin	Average	Count	Ind. Frequency	Cum. Frequency
0.00	3.00	1.50	23	41%	41%
3.00	6.00	4.50	16	29%	70%
6.00	9.00	7.50	9	16%	86%
9.00	12.00	10.50	4	7%	93%
12.00	15.00	13.50	2	4%	96%
15.00	18.00	16.50	1	2%	98%
18.00	21.00	19.50	0	0%	98%
21.00	24.00	22.50	1	2%	100%

Histogram of Dust Concentrations per cut from Right CM

Low Bin	High Bin	Average	Count	Ind. Frequency	Cum. Frequency
0.00	1.50	0.75	10	24%	24%
1.50	3.00	2.25	11	27%	51%
3.00	4.50	3.75	6	15%	66%
4.50	6.00	5.25	6	15%	80%
6.00	7.50	6.75	3	7%	88%
7.50	9.00	8.25	3	7%	95%
9.00	10.50	9.75	2	5%	100%
10.50	12.00	11.25	0	0%	100%

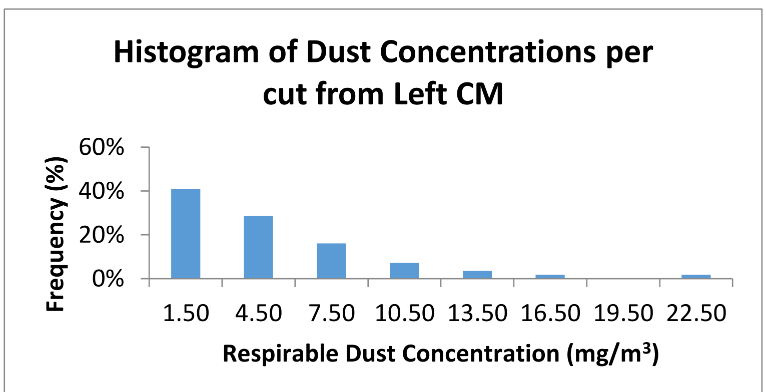

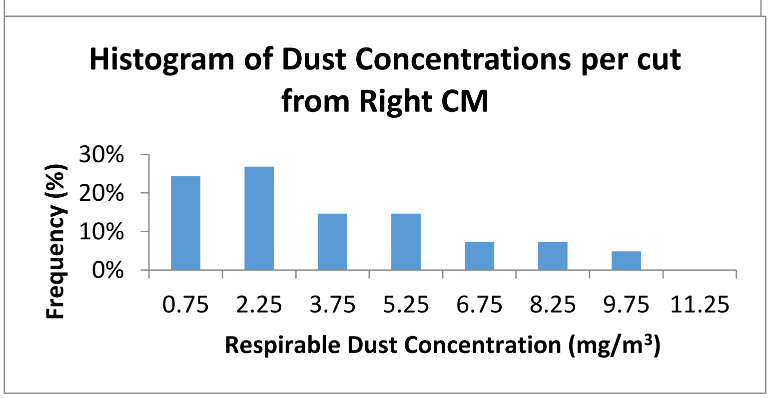

7.19	
3.16	
3.10	
1.19	
3.86	
1.94	

Data:

Dust Conc. for Cut at the Curtain (mg/m^3)	Dust Conc. for Cut in the Returns (mg/m^3)
2.88	0.44
1.60	1.07
3.23	0.31
3.63	1.02
4.51	0.28
5.29	0.85
5.04	1.89
8.77	6.76
8.44	1.07
2.25	2.76
8.56	5.90
1.50	1.44
1.45	1.40
5.67	0.99
6.87	1.80
5.20	4.98
17.60	0.61
2.72	3.24
6.17	2.63
4.82	5.62
13.63	1.62
4.03	1.41
3.52	0.14
7.19	1.92
4.89	7.14
10.24	4.33
5.82	1.61
3.82	0.69
6.64	7.26
1.60	2.85
7.88	1.71
6.72	1.66
3.18	4.70
13.14	1.31
2.29	2.09
10.38	1.28
2.51	4.46
1.39	1.64
7.21	1.90
9.35	6.39
21.38	0.56
10.14	3.39
5.47	1.58
4.71	1.97

	Dust Conc. per cut from Left CM (mg/m^3)	Dust Conc. per cut from Right CM (mg/m^3)
Mean	4.905	3.724
Standard Error	0.580	0.426
Median	3.672	2.847
Mode	#N/A	#N/A
Standard Deviation	4.340	2.730
Sample Variance	18.833	7.452
Kurtosis	3.612	-0.502
Skewness	1.757	0.735
Range	21.102	9.998
Minimum	0.281	0.140
Maximum	21.383	10.137
Sum	274.669	152.664
Count	56	41
Confidence Level(95.0%)	1.162	0.862

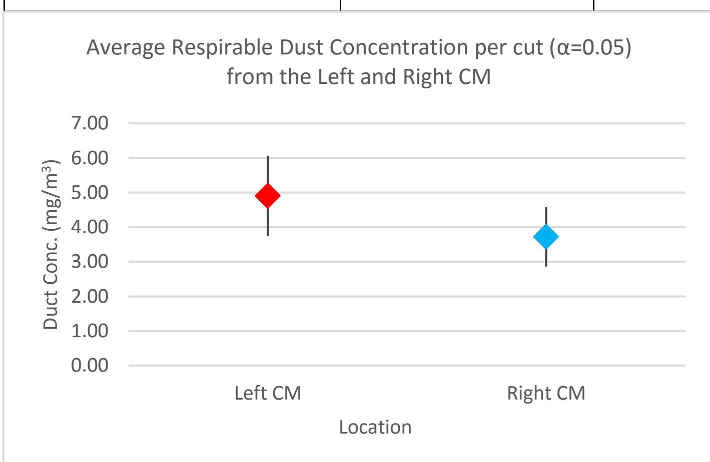

11.97	3.16	
7.19	3.86	
9.03	1.19	
3.10	1.94	
3.86		

Table 58: Descriptive statistics of dust concentration with and without surfactant on a cut by cut basis

Data:

Dust Conc. per cut without Surfactant (mg/m^3)	Dust Conc. per cut with Surfactant (mg/m^3)
2.88	1.45
0.44	1.44
1.60	5.67
1.07	1.40
3.23	6.87
0.31	0.99
3.63	5.20
1.02	1.80
4.51	17.60
0.28	4.98
5.29	2.72
0.85	0.61
5.04	6.17
1.89	3.24
8.77	4.82
8.44	2.63
6.76	13.63
2.25	5.62
1.07	4.03
8.56	1.62
2.76	3.52
1.50	1.41
5.90	7.19
10.24	0.14
7.14	4.89
5.82	1.92
4.33	1.39
3.82	4.46
1.61	7.21
6.64	1.64
0.69	9.35
1.60	1.90
7.26	21.38
7.88	6.39
2.85	10.14
6.72	0.56
1.71	5.47
3.18	3.39
1.66	4.71
13.14	1.58
4.70	11.97
2.29	1.97
1.31	7.19
10.38	3.16
2.09	9.03
2.51	3.86
1.28	3.10
	1.19
	3.86
	1.94

Histogram of Dust Concentrations per cut without Surfactant

Low Bin	High Bin	Average	Count	Ind. Frequency	Cum. Frequency
0.00	2.00	1.00	17	36%	36%
2.00	4.00	3.00	11	23%	60%
4.00	6.00	5.00	7	15%	74%
6.00	8.00	7.00	6	13%	87%
8.00	10.00	9.00	3	6%	94%
10.00	12.00	11.00	2	4%	98%
12.00	14.00	13.00	1	2%	100%
14.00	16.00	15.00	0	0%	100%

Histogram of Dust Concentrations per cut with Surfactant

Low Bin	High Bin	Average	Count	Ind. Frequency	Cum. Frequency
0.00	3.00	1.50	20	40%	40%
3.00	6.00	4.50	17	34%	74%
6.00	9.00	7.50	6	12%	86%
9.00	12.00	10.50	4	8%	94%
12.00	15.00	13.50	1	2%	96%
15.00	18.00	16.50	1	2%	98%
18.00	21.00	19.50	0	0%	98%
21.00	24.00	22.50	1	2%	100%

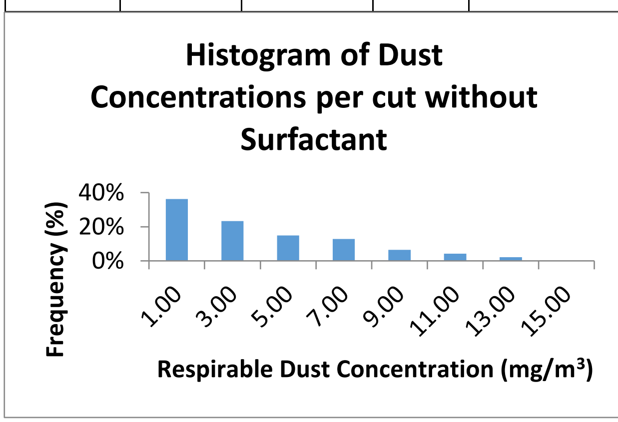

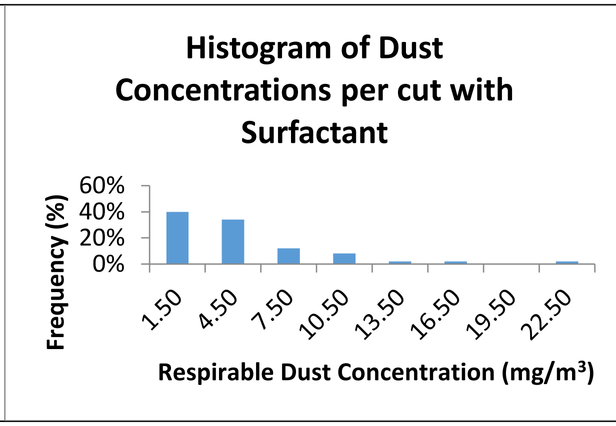

Data:

Dust Conc. per cut without Surfactant (mg/m^3)	Dust Conc. per cut with Surfactant (mg/m^3)
2.88	1.45
0.44	1.44
1.60	5.67
1.07	1.40
3.23	6.87
0.31	0.99
3.63	5.20
1.02	1.80
4.51	17.60
0.28	4.98
5.29	2.72
0.85	0.61
5.04	6.17
1.89	3.24
8.77	4.82
8.44	2.63
6.76	13.63
2.25	5.62
1.07	4.03
8.56	1.62
2.76	3.52
1.50	1.41
5.90	7.19
10.24	0.14
7.14	4.89
5.82	1.92
4.33	1.39
3.82	4.46
1.61	7.21
6.64	1.64
0.69	9.35
1.60	1.90
7.26	21.38
7.88	6.39
2.85	10.14
6.72	0.56
1.71	5.47
3.18	3.39

	Dust Conc. per cut without Surfactant (mg/m^3)	Dust Conc. per cut with Surfactant (mg/m^3)
Mean	4.019	4.769
Standard Error	0.457	0.606
Median	2.876	3.689
Mode	#N/A	#N/A
Standard Deviation	3.136	4.288
Sample Variance	9.836	18.385
Kurtosis	0.221	4.771
Skewness	0.945	1.989
Range	12.864	21.243
Minimum	0.281	0.140
Maximum	13.145	21.383
Sum	188.901	238.432
Count	47	50
Confidence Level (95.0%)	0.921	1.219

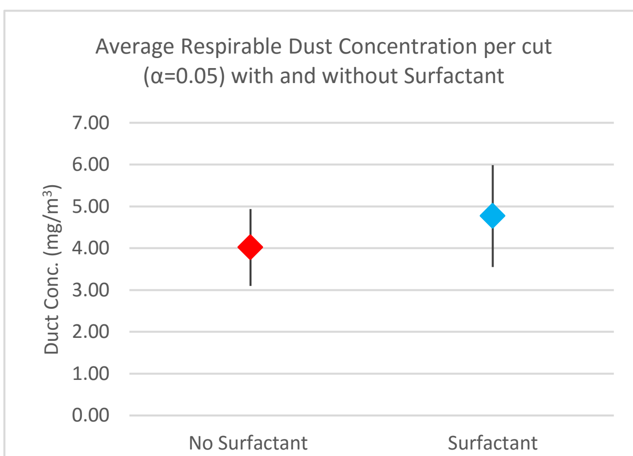

1.66	4.71
13.14	1.58
4.70	11.97
2.29	1.97
1.31	7.19
10.38	3.16
2.09	9.03
2.51	3.86
1.28	3.10
	1.19
	3.86
	1.94

Table 59: Descriptive statistics of dust concentration with regards to the number of bits changed per cut

Data:

Dust Conc. per cut with 0-9 bits changed (mg/m^3)	Dust Conc. per cut with 10-19 bits changed (mg/m^3)	Dust Conc. per cut with 20+ bits changed (mg/m^3)
5.29	2.88	5.67
0.85	0.44	1.40
2.25	1.60	13.63
1.07	1.07	5.62
1.45	3.23	10.24
1.44	0.31	7.14
5.20	3.63	3.18
1.80	1.02	1.66
17.60	4.51	1.39
4.98	0.28	4.46
6.17	5.04	11.97
3.24	1.89	1.97
4.89	8.77	
1.92	8.44	
3.82	6.76	
1.61	8.56	
6.64	2.76	
0.69	1.50	
1.60	5.90	
7.26	6.87	
6.72	0.99	
1.71	2.72	
2.29	0.61	
1.31	4.82	
10.38	2.63	
2.09	4.03	
7.21	1.62	
1.64	3.52	
21.38	1.41	
6.39	7.19	
4.71	0.14	
1.58	5.82	
7.19	4.33	
3.16	7.88	

Histogram of Dust Concentrations per cut with 0-9 bits changed

Low Bin	High Bin	Average	Count	Ind. Frequency	Cum. Frequency
0.00	3.00	1.50	18	46%	46%
3.00	6.00	4.50	11	28%	74%
6.00	8.00	7.00	7	18%	92%
8.00	10.00	9.00	1	3%	95%
10.00	12.00	11.00	1	3%	97%
12.00	14.00	13.00	0	0%	97%
14.00	16.00	15.00	0	0%	97%
16.00	18.00	17.00	1	3%	100%

Histogram of Dust Concentrations per cut with 10-19 bits changed

Low Bin	High Bin	Average	Count	Ind. Frequency	Cum. Frequency
0.00	2.00	1.00	16	36%	36%
2.00	4.00	3.00	10	22%	58%
4.00	6.00	5.00	9	20%	78%
6.00	8.00	7.00	4	9%	87%
8.00	10.00	9.00	4	9%	96%
10.00	12.00	11.00	1	2%	98%
12.00	14.00	13.00	1	2%	100%
14.00	16.00	15.00	0	0%	100%

Histogram of Dust Concentrations per cut with 20+ bits changed

Low Bin	High Bin	Average	Count	Ind. Frequency	Cum. Frequency
0.00	2.00	1.00	4	33%	33%
2.00	4.00	3.00	1	8%	42%
4.00	6.00	5.00	3	25%	67%
6.00	8.00	7.00	1	8%	75%
8.00	10.00	9.00	0	0%	75%
10.00	12.00	11.00	2	17%	92%
12.00	14.00	13.00	1	8%	100%

9.03	2.85	
3.86	13.14	
3.10	4.70	
1.19	2.51	
3.86	1.28	
1.94	9.35	
	1.90	
	10.14	
	0.56	
	5.47	
	3.39	

14.00	16.00	15.00	0	0%	100%

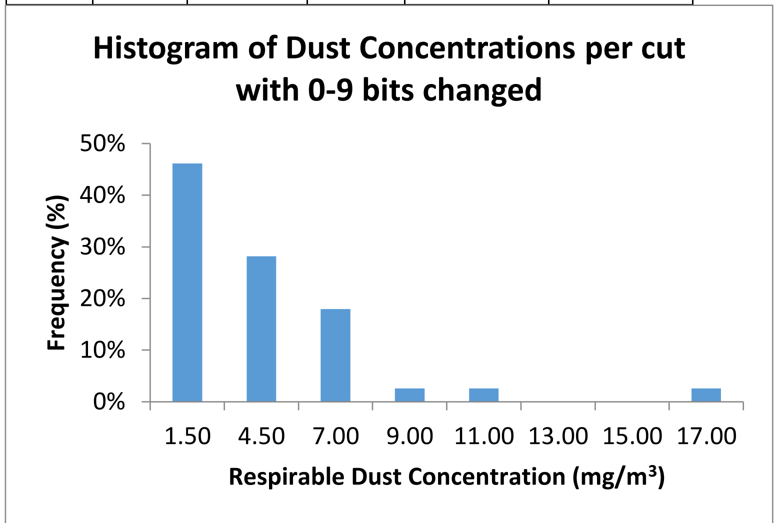

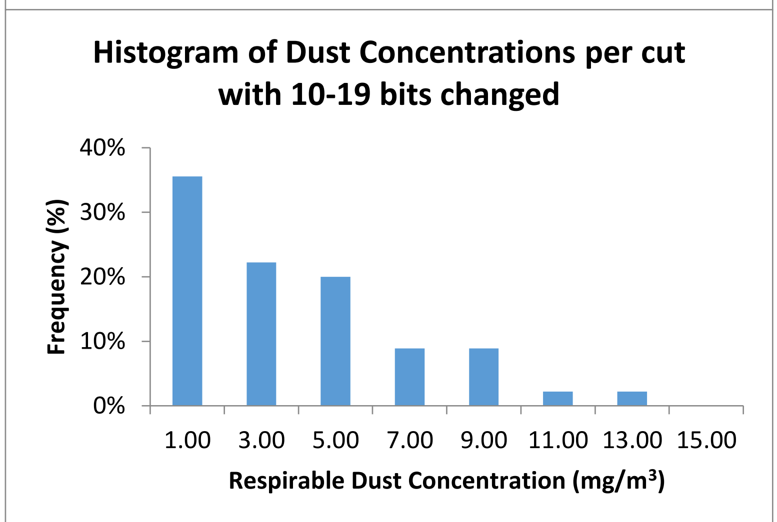

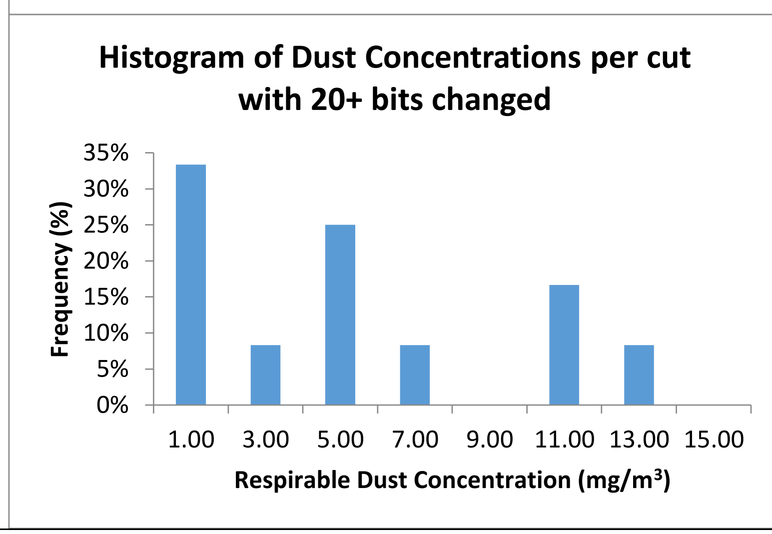

Data:

Dust Conc. per cut with 0-9 bits changed (mg/m^3)	Dust Conc. per cut with 10-19 bits changed (mg/m^3)	Dust Conc. per cut with 20+ bits changed (mg/m^3)
5.29	2.88	5.67
0.85	0.44	1.40
2.25	1.60	13.63
1.07	1.07	5.62
1.45	3.23	10.24
1.44	0.31	7.14
5.20	3.63	3.18
1.80	1.02	1.66
17.60	4.51	1.39
4.98	0.28	4.46
6.17	5.04	11.97
3.24	1.89	1.97
4.89	8.77	
1.92	8.44	
3.82	6.76	
1.61	8.56	
6.64	2.76	
0.69	1.50	
1.60	5.90	
7.26	6.87	
6.72	0.99	
1.71	2.72	
2.29	0.61	
1.31	4.82	
10.38	2.63	
2.09	4.03	
7.21	1.62	
1.64	3.52	
21.38	1.41	
6.39	7.19	
4.71	0.14	
1.58	5.82	
7.19	4.33	
3.16	7.88	
9.03	2.85	
3.86	13.14	
3.10	4.70	
1.19	2.51	
3.86	1.28	
1.94	9.35	
	1.90	
	10.14	
	0.56	
	5.47	
	3.39	

	Dust Conc. per cut with 0-9 bits changed (mg/m^3)	Dust Conc. per cut with 10-19 bits changed (mg/m^3)	Dust Conc. per cut with 20+ bits changed (mg/m^3)
Mean	4.513	3.966	5.695
Standard Error	0.677	0.462	1.231
Median	3.199	3.233	5.038
Mode	#N/A	#N/A	#N/A
Standard Deviation	4.282	3.099	4.265
Sample Variance	18.334	9.605	18.193
Kurtosis	6.871	0.381	-0.636
Skewness	2.385	0.928	0.774
Range	20.695	13.005	12.241
Minimum	0.687	0.140	1.392
Maximum	21.383	13.145	13.633
Sum	180.507	178.481	68.345
Count	40	45	12
Confidence Level(95.0%)	1.369	0.931	2.710

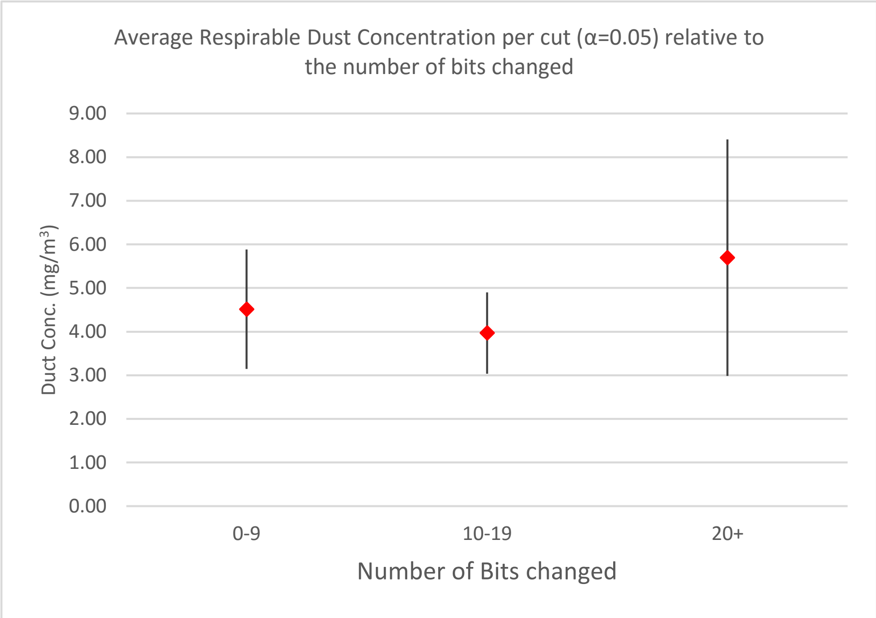

Table 60: Descriptive statistics of dust concentration with regards to the volumetric airflow

Dust Conc. per cut with air flow in the range of 9000-9999 cfm (mg/m^3)	Dust Conc. per cut with air flow in the range of 10000-10999 cfm (mg/m^3)	Dust Conc. per cut with air flow in the range of 11000-11999 cfm (mg/m^3)	Dust Conc. per cut with air flow in the range of 12000-12999 cfm (mg/m^3)	Dust Conc. per cut with air flow in the range of 13000-13999 cfm (mg/m^3)	Dust Conc. per cut with air flow in the range of 14000-14999 cfm (mg/m^3)	Dust Conc. per cut with air flow in the range of 15000+ cfm (mg/m^3)
4.51	3.23	3.63	1.60	8.44	2.88	1.45
0.28	0.31	1.02	1.07	6.76	0.44	1.44
1.50	4.03	5.29	8.77	4.82	13.63	17.60
5.90	1.62	0.85	8.56	2.63	5.62	4.98
5.20	6.64	5.04	2.76	2.51	13.14	10.24
1.80	0.69	1.89	5.67	1.28	4.70	7.14
2.72	5.47	2.25	1.40	4.71	11.97	6.72
0.61	3.39	1.07	6.87	1.58	1.97	1.71
3.52	3.86	6.17	0.99			10.38
1.41	1.94	3.24	3.18			2.09
7.19		4.89	1.66			7.21
0.14		1.92	1.39			1.64
5.82		3.82	4.46			9.35
4.33		1.61	10.14			1.90
7.88		1.60	0.56			21.38
2.85		7.26	7.19			6.39
		2.29	3.16			9.03
		1.31				3.86
		3.10				
		1.19				

Histogram of Dust Concentrations per cut with air flow in the range of 9000-9999 cfm

Low Bin	High Bin	Average	Count	Ind. Frequency	Cum. Frequency
0.00	2.00	1.00	6	38%	38%
2.00	4.00	3.00	3	19%	56%
4.00	6.00	5.00	5	31%	88%
6.00	8.00	7.00	2	13%	100%
8.00	10.00	9.00	0	0%	100%
10.00	12.00	11.00	0	0%	100%
12.00	14.00	13.00	0	0%	100%
14.00	16.00	15.00	0	0%	100%

Histogram of Dust Concentrations per cut with air flow in the range of 10000-10999 cfm

Low Bin	High Bin	Average	Count	Ind. Frequency	Cum. Frequency
0.00	2.00	1.00	4	40%	40%
2.00	4.00	3.00	3	30%	70%
4.00	6.00	5.00	2	20%	90%

6.00	8.00	7.00	1	10%	100%
8.00	10.00	9.00	0	0%	100%
10.00	12.00	11.00	0	0%	100%
12.00	14.00	13.00	0	0%	100%
14.00	16.00	15.00	0	0%	100%

Histogram of Dust Concentrations per cut with air flow in the range of 11000-11999 cfm

Low Bin	High Bin	Average	Count	Ind. Frequency	Cum. Frequency
0.00	1.50	0.75	5	25%	25%
1.50	3.00	2.25	6	30%	55%
3.00	4.50	3.75	4	20%	75%
4.50	6.00	5.25	3	15%	90%
6.00	7.50	6.75	2	10%	100%
7.50	9.00	8.25	0	0%	100%
9.00	10.50	9.75	0	0%	100%
10.50	12.00	11.25	0	0%	100%

Histogram of Dust Concentrations per cut with air flow in the range of 12000-12999 cfm

Low Bin	High Bin	Average	Count	Ind. Frequency	Cum. Frequency
0.00	2.00	1.00	7	41%	41%
2.00	4.00	3.00	3	18%	59%
4.00	6.00	5.00	2	12%	71%
6.00	8.00	7.00	2	12%	82%
8.00	10.00	9.00	2	12%	94%
10.00	12.00	11.00	1	6%	100%
12.00	14.00	13.00	0	0%	100%
14.00	16.00	15.00	0	0%	100%

Histogram of Dust Concentrations per cut with air flow in the range of 13000-13999 cfm

Low Bin	High Bin	Average	Count	Ind. Frequency	Cum. Frequency
0.00	2.00	1.00	2	25%	25%
2.00	4.00	2.50	2	25%	50%
4.00	6.00	5.00	2	25%	75%
6.00	8.00	7.00	1	13%	88%
8.00	10.00	9.00	1	13%	100%
10.00	12.00	11.00	0	0%	100%
12.00	14.00	13.00	0	0%	100%

14.00	16.00	15.00	0	0%	100%
Histogram of Dust Concentrations per cut with air flow in the range of 14000-14999 cfm					
Low Bin	**High Bin**	**Average**	**Count**	**Ind. Frequency**	**Cum. Frequency**
0.00	4.00	2.00	3	38%	38%
4.00	6.00	5.00	2	25%	63%
6.00	8.00	7.00	0	0%	63%
8.00	10.00	9.00	0	0%	63%
10.00	12.00	11.00	1	13%	75%
12.00	14.00	13.00	2	25%	100%
14.00	16.00	15.00	0	0%	100%
16.00	18.00	17.00	0	0%	100%
Histogram of Dust Concentrations per cut with air flow in the range of 15000+ cfm					
Low Bin	**High Bin**	**Average**	**Count**	**Ind. Frequency**	**Cum. Frequency**
0.00	4.00	2.00	7	39%	39%
4.00	8.00	6.00	5	28%	67%
8.00	12.00	10.00	4	22%	89%
12.00	16.00	14.00	0	0%	89%
16.00	20.00	18.00	1	6%	94%
20.00	24.00	22.00	1	6%	100%
24.00	28.00	26.00	0	0%	100%
28.00	32.00	30.00	0	0%	100%

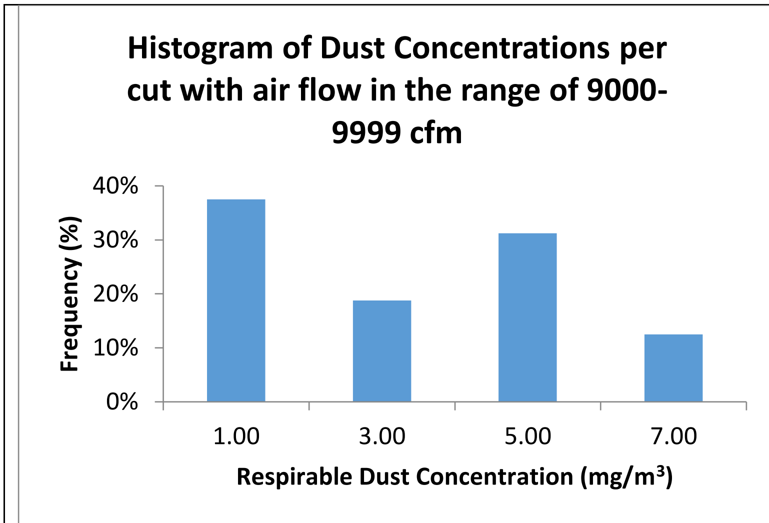
Histogram of Dust Concentrations per cut with air flow in the range of 9000-9999 cfm
Frequency (%)
40%
30%
20%
10%
0%
1.00
3.00
5.00
7.00
Respirable Dust Concentration (mg/m³)

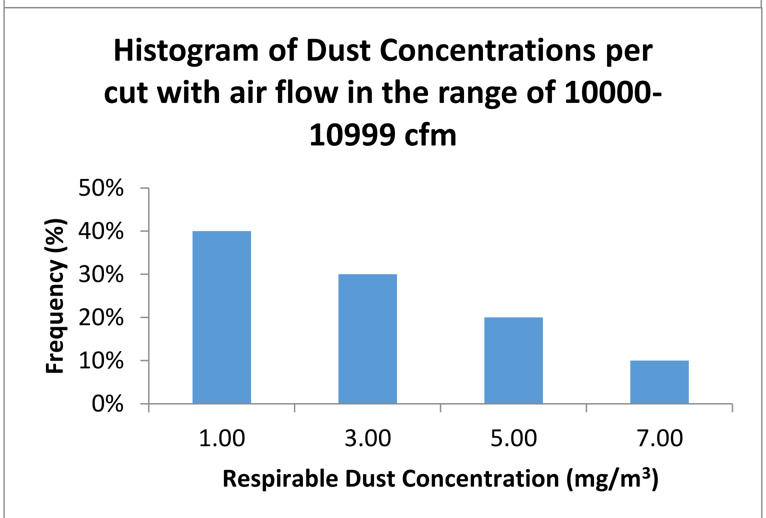
Histogram of Dust Concentrations per cut with air flow in the range of 10000-10999 cfm
Frequency (%)
50%
40%
30%
20%
10%
0%
1.00
3.00
5.00
7.00
Respirable Dust Concentration (mg/m³)

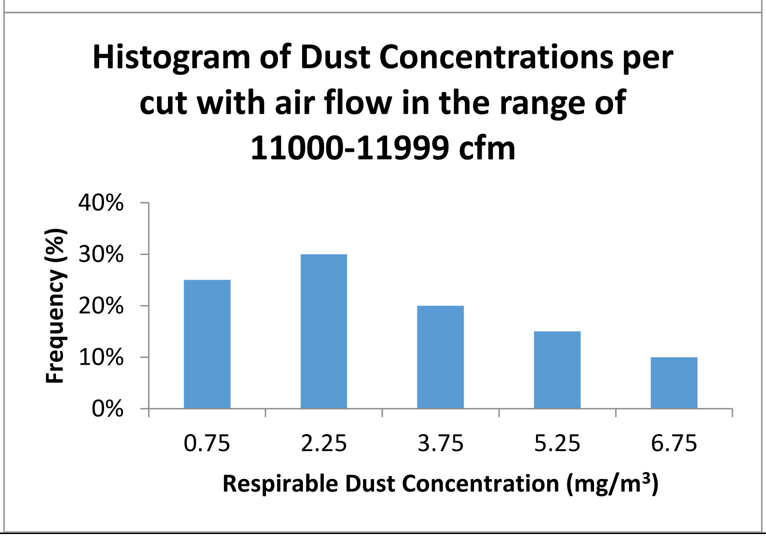
Histogram of Dust Concentrations per cut with air flow in the range of 11000-11999 cfm
Frequency (%)
40%
30%
20%
10%
0%
0.75
2.25
3.75
5.25
6.75
Respirable Dust Concentration (mg/m³)

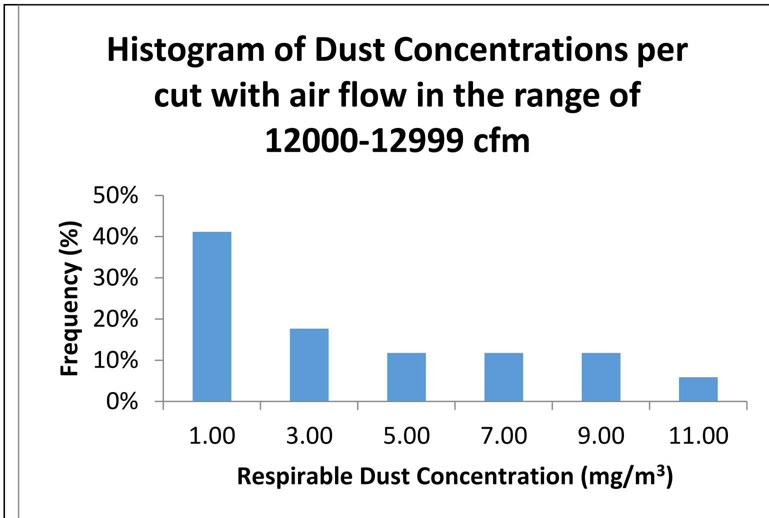
Histogram of Dust Concentrations per cut with air flow in the range of 12000-12999 cfm
Frequency (%)
50%
40%
30%
20%
10%
0%
1.00
3.00
5.00
7.00
9.00
11.00
Respirable Dust Concentration (mg/m³)

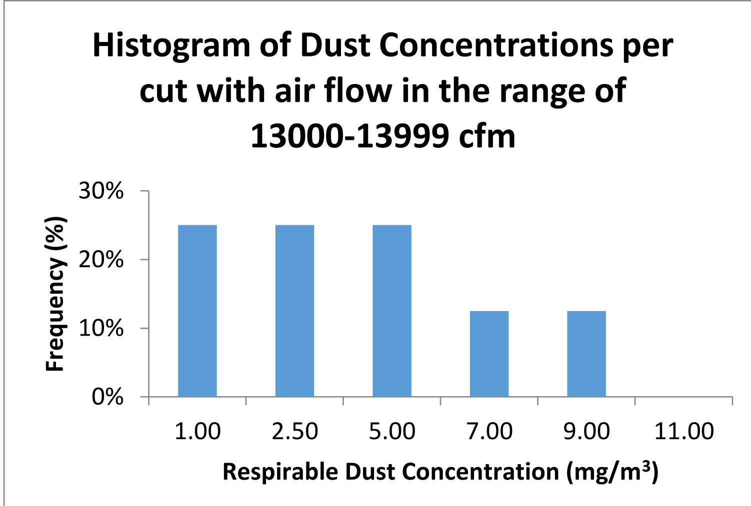
Histogram of Dust Concentrations per cut with air flow in the range of 13000-13999 cfm
Frequency (%)
30%
20%
10%
0%
1.00
2.50
5.00
7.00
9.00
11.00
Respirable Dust Concentration (mg/m³)

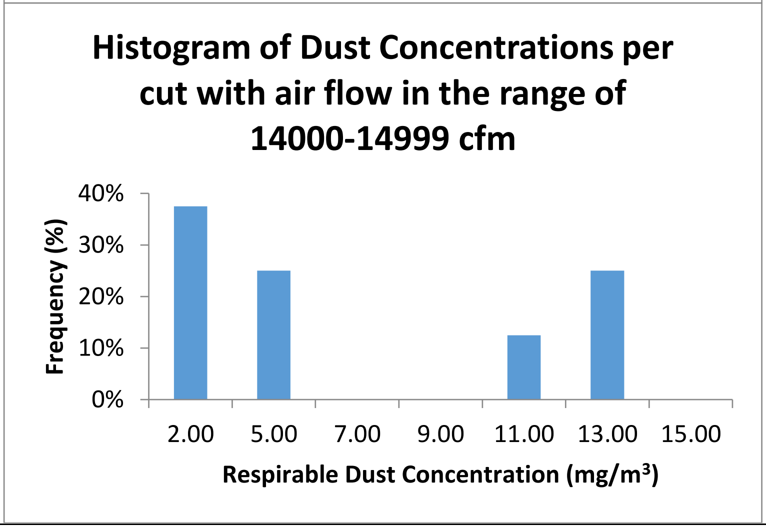
Histogram of Dust Concentrations per cut with air flow in the range of 14000-14999 cfm
Frequency (%)
40%
30%
20%
10%
0%
2.00
5.00
7.00
9.00
11.00
13.00
15.00
Respirable Dust Concentration (mg/m³)

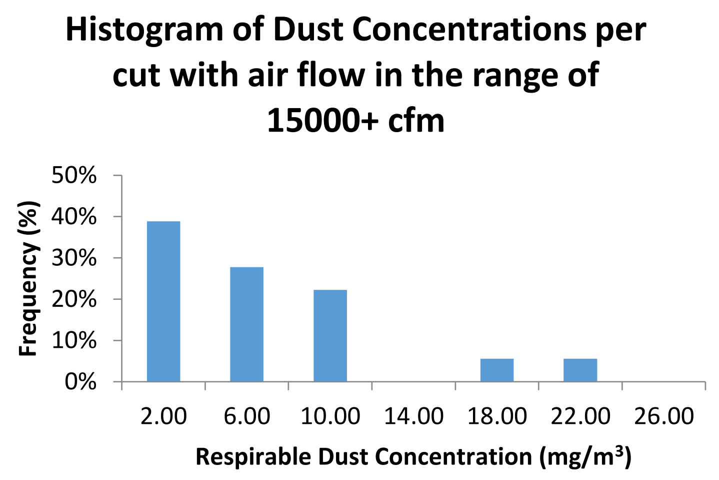

	Dust Conc. per cut with air flow in the range of 9000-9999 cfm (mg/m^3)	Dust Conc. per cut with air flow in the range of 10000-10999 cfm (mg/m^3)	Dust Conc. per cut with air flow in the range of 11000-11999 cfm (mg/m^3)	Dust Conc. per cut with air flow in the range of 12000-12999 cfm (mg/m^3)	Dust Conc. per cut with air flow in the range of 13000-13999 cfm (mg/m^3)	Dust Conc. per cut with air flow in the range of 14000-14999 cfm (mg/m^3)	Dust Conc. per cut with air flow in the range of 15000+ cfm (mg/m^3)
Mean	3.478	3.119	2.971	4.085	4.091	6.795	6.918
Standard Error	0.615	0.640	0.423	0.766	0.905	1.884	1.321
Median	3.185	3.313	2.271	3.160	3.669	5.160	6.555
Mode	#N/A	#N/A	#N/A	#N/A	#N/A	#N/A	#N/A
Standard Deviation	2.461	2.022	1.893	3.158	2.559	5.328	5.603
Sample Variance	6.058	4.090	3.585	9.976	6.549	28.384	31.390
Kurtosis	-1.050	-0.570	-0.273	-1.010	-0.715	-1.937	1.636
Skewness	0.280	0.275	0.850	0.667	0.647	0.346	1.301
Range	7.744	6.324	6.410	9.574	7.167	13.194	19.942
Minimum	0.140	0.314	0.851	0.564	1.277	0.439	1.441
Maximum	7.884	6.638	7.261	10.137	8.444	13.633	21.383
Sum	55.649	31.187	59.429	69.449	32.729	54.358	124.532
Count	16	10	20	17	8	8	18
Confidence Level(95.0%)	1.312	1.447	0.886	1.624	2.139	4.454	2.786

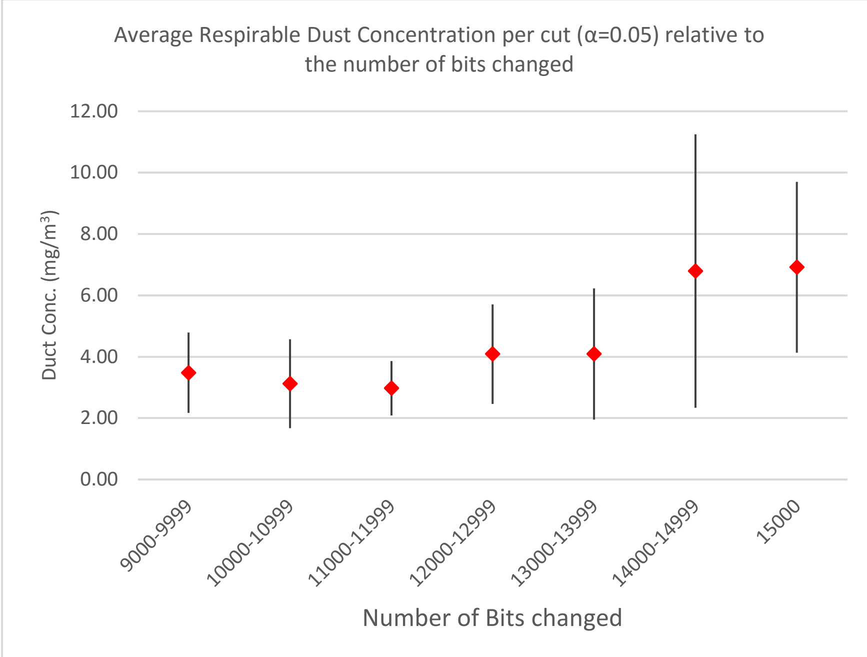

ANOVA						
Source of Variation	*SS*	*df*	*MS*	*F*	*P-value*	*F crit*
Between Groups	233.3223	6	38.88705	3.087454	0.008538	2.201056
Within Groups	1133.566	90	12.59518			
Total	1366.889	96				

Table 61: Descriptive statistics of dust concentration with regards to the starting cut depth

Dust Conc. per cut with Start Depth of -10 ft. (mg/m^3)	Dust Conc. per cut with Start Depth of -11-20 ft. (mg/m^3)	Dust Conc. per cut with air flow in the range of 21-30 ft. (mg/m^3)	Dust Conc. per cut with air flow in the range of 31-40 ft. (mg/m^3)	Dust Conc. per cut with air flow in the range of 40+ ft. (mg/m^3)
3.63	2.88	1.60	3.23	4.82
1.02	0.44	1.07	0.31	2.63
5.29	1.50	3.52	4.51	4.03
0.85	5.90	1.41	0.28	1.62
5.04	2.72	4.89	2.25	7.19
1.89	0.61	1.92	1.07	0.14
8.77	5.82	3.82	10.38	6.64
8.44	4.33	1.61	2.09	0.69
6.76	1.60	4.71	11.97	3.18
8.56	7.26	1.58	1.97	1.66
2.76	7.88		3.10	2.29
5.67	2.85		1.19	1.31
1.40	9.03			3.86
13.63	3.86			1.94
5.62				
10.24				
7.14				
6.72				

1.71				
13.14				
4.70				
7.21				
1.64				
9.35				
1.90				
21.38				
6.39				
10.14				
0.56				
5.47				
3.39				
7.19				
3.16				

Histogram of Dust Concentrations per cut with Start Depth of -10 ft.

Low Bin	High Bin	Average	Count	Ind. Frequency	Cum. Frequency
0.00	4.00	2.00	12	38%	38%
4.00	8.00	6.00	12	38%	75%
8.00	10.00	9.00	4	13%	88%
10.00	12.00	11.00	2	6%	94%
12.00	14.00	13.00	2	6%	100%
14.00	16.00	15.00	0	0%	100%
16.00	18.00	17.00	0	0%	100%
18.00	20.00	19.00	0	0%	100%
20.00	22.00	21.00	1	3%	103%

Histogram of Dust Concentrations per cut with Start Depth of 11-20 ft.

Low Bin	High Bin	Average	Count	Ind. Frequency	Cum. Frequency
0.00	2.00	1.00	4	29%	29%
2.00	4.00	3.00	4	29%	57%
4.00	6.00	5.00	3	21%	79%
6.00	8.00	7.00	2	14%	93%
8.00	10.00	9.00	1	7%	100%
10.00	12.00	11.00	0	0%	100%
12.00	14.00	13.00	0	0%	100%
14.00	16.00	15.00	0	0%	100%

Histogram of Dust Concentrations per cut with Start Depth of 21-30 ft.					
Low Bin	**High Bin**	**Average**	**Count**	**Ind. Frequency**	**Cum. Frequency**
0.00	1.00	0.50	0	0%	0%
1.00	2.00	1.50	6	60%	60%
2.00	3.00	2.50	0	0%	60%
3.00	4.00	3.50	2	20%	80%
4.00	5.00	4.50	2	20%	100%
5.00	6.00	5.50	0	0%	100%
6.00	7.00	6.50	0	0%	100%
7.00	8.00	7.50	0	0%	100%

Histogram of Dust Concentrations per cut with Start Depth of 31-40 ft.					
Low Bin	**High Bin**	**Average**	**Count**	**Ind. Frequency**	**Cum. Frequency**
0.00	3.00	1.50	7	58%	58%
3.00	5.00	4.00	3	25%	83%
5.00	7.00	6.00	0	0%	83%
7.00	9.00	8.00	0	0%	83%
9.00	11.00	10.00	1	8%	92%
11.00	13.00	12.00	1	8%	100%
13.00	15.00	14.00	0	0%	100%
15.00	17.00	16.00	0	0%	100%

Histogram of Dust Concentrations per cut with Start Depth of 40+ ft.					
Low Bin	**High Bin**	**Average**	**Count**	**Ind. Frequency**	**Cum. Frequency**
0.00	2.00	1.00	6	43%	43%
2.00	4.00	2.00	4	29%	71%
4.00	6.00	5.00	2	14%	86%
6.00	8.00	7.00	2	14%	100%
8.00	10.00	9.00	0	0%	100%
10.00	12.00	11.00	0	0%	100%
12.00	14.00	13.00	0	0%	100%
14.00	16.00	15.00	0	0%	100%

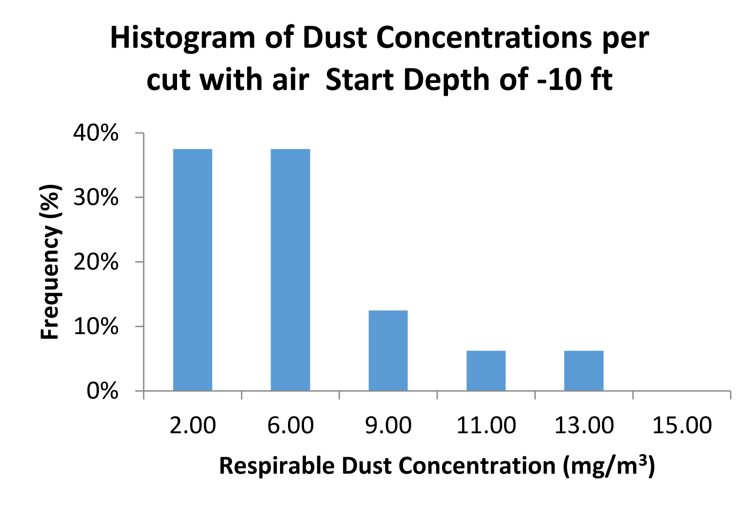
Histogram of Dust Concentrations per cut with air Start Depth of -10 ft
Frequency (%)
40%
30%
20%
10%
0%
2.00
6.00
9.00
11.00
13.00
15.00
Respirable Dust Concentration (mg/m3)

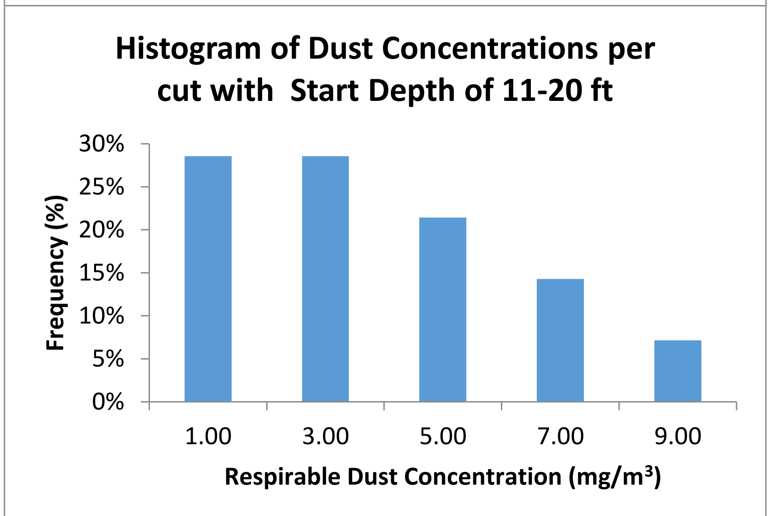
Histogram of Dust Concentrations per cut with Start Depth of 11-20 ft
Frequency (%)
30%
25%
20%
15%
10%
5%
0%
1.00
3.00
5.00
7.00
9.00
Respirable Dust Concentration (mg/m3)

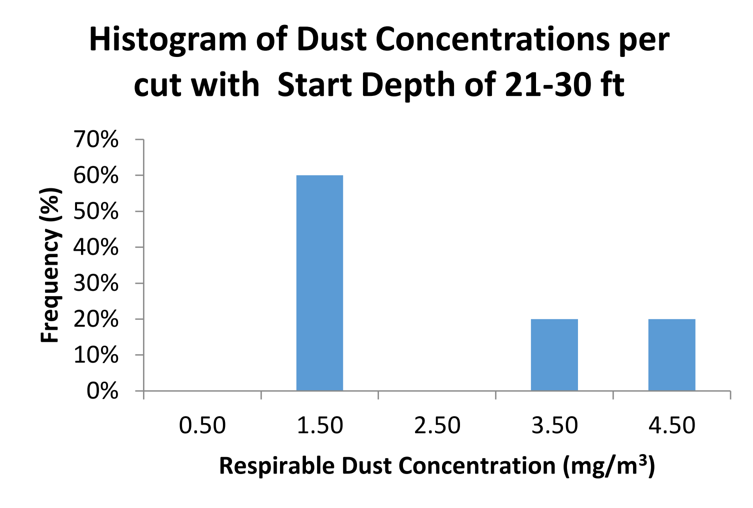

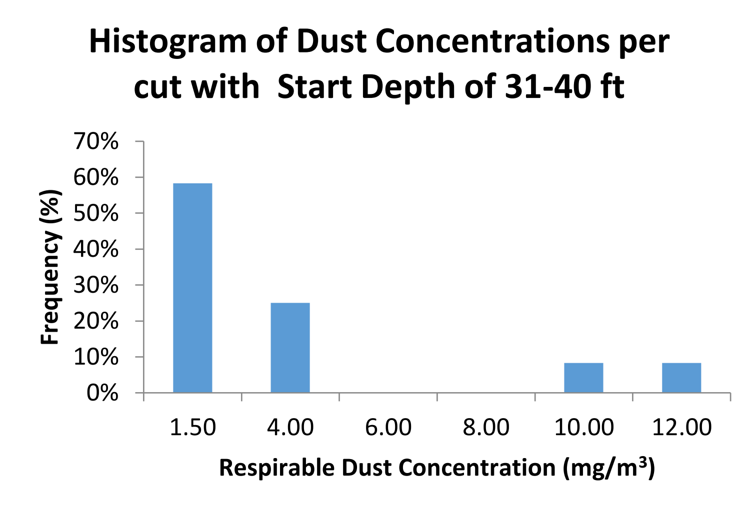

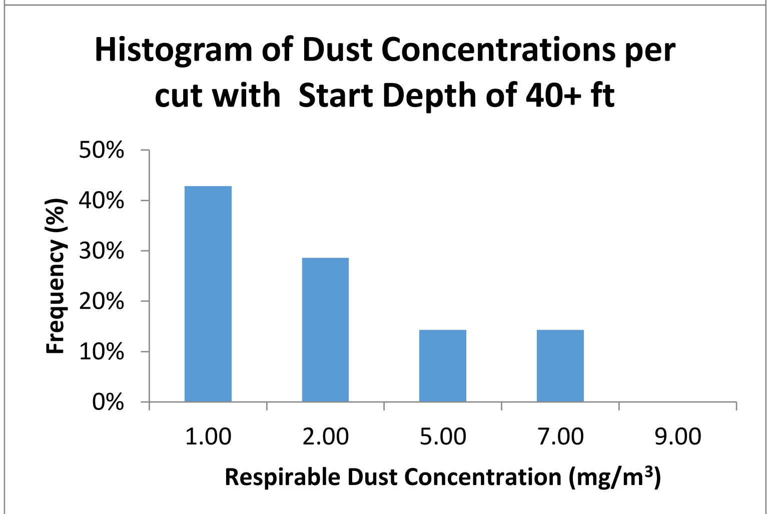

	Dust Conc. per cut with Start Depth of -10 ft. (mg/m^3)	Dust Conc. per cut with Start Depth of -11-20 ft. (mg/m^3)	Dust Conc. per cut with air flow in the range of 21-30 ft. (mg/m^3)	Dust Conc. per cut with air flow in the range of 31-40 ft. (mg/m^3)	Dust Conc. per cut with air flow in the range of 40+ ft. (mg/m^3)

Mean	6.084	4.048	2.614	3.530	2.999
Standard Error	0.770	0.736	0.462	1.094	0.563
Median	5.616	3.369	1.767	2.170	2.461
Mode	#N/A	#N/A	#N/A	#N/A	#N/A
Standard Deviation	4.421	2.753	1.462	3.791	2.108
Sample Variance	19.544	7.577	2.137	14.370	4.443
Kurtosis	3.191	-0.950	-1.477	1.756	-0.077
Skewness	1.395	0.433	0.647	1.643	0.787
Range	20.819	8.592	3.814	11.693	7.046
Minimum	0.564	0.439	1.074	0.281	0.140
Maximum	21.383	9.031	4.888	11.974	7.186
Sum	200.787	56.668	26.140	42.358	41.992
Count	33	14	10	12	14
Confidence Level(95.0%)	1.568	1.589	1.046	2.409	1.217

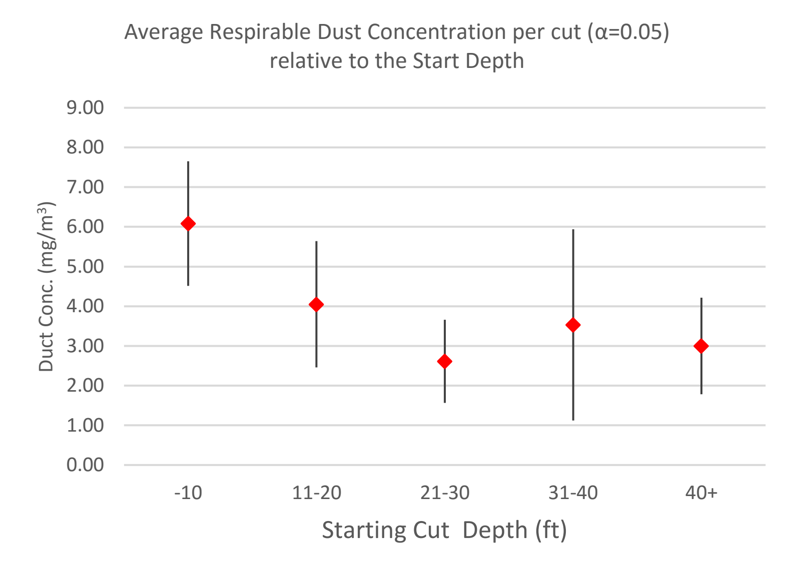

ANOVA						
Source of Variation	*SS*	*df*	*MS*	*F*	*P-value*	*F crit*
Between Groups	92.3503	1	92.3503	7.473868	0.007784	3.96676
Within Groups	939.0884	76	12.35643			
Total	1031.439	77				

Table 62: Descriptive statistics of dust concentration with regards to the scrubber activation

Dust Conc. per cut without Scrubber (mg/m^3)	Dust Conc. per cut with Scrubber (mg/m^3)
5.04	2.88
1.89	0.44
8.56	1.60
2.76	1.07
5.67	3.23
1.40	0.31
10.24	4.51
7.14	0.28
6.72	2.25
1.71	1.07
21.38	1.50
6.39	5.90
7.19	1.45
3.16	1.44
	6.87
	0.99
	5.20
	1.80
	17.60
	4.98
	2.72
	0.61
	6.17
	3.24
	4.82
	2.63
	4.03
	1.62
	3.52
	1.41
	7.19
	0.14
	4.89
	1.92
	5.82
	4.33
	3.82
	1.61
	6.64
	0.69

	1.60
	7.26
	7.88
	2.85
	3.18
	1.66
	2.29
	1.31
	10.38
	2.09
	2.51
	1.28
	1.39
	4.46
	4.71
	1.58
	11.97
	1.97
	9.03
	3.86
	3.10
	1.19
	3.86
	1.94

Histogram of Dust Concentrations per cut without Scrubber

Low Bin	High Bin	Average	Count	Ind. Frequency	Cum. Frequency
0.00	3.00	1.50	4	29%	29%
3.00	6.00	4.50	3	21%	50%
6.00	9.00	7.50	5	36%	86%
9.00	12.00	10.50	1	7%	93%
12.00	15.00	13.50	0	0%	93%
15.00	18.00	16.50	0	0%	93%
18.00	21.00	19.50	0	0%	93%
21.00	24.00	22.50	1	7%	100%

Histogram of Dust Concentrations per cut with Scrubber

Low Bin	High Bin	Average	Count	Ind. Frequency	Cum. Frequency
0.00	2.50	1.25	30	47%	47%
2.50	5.00	3.75	21	33%	80%
5.00	7.50	6.25	8	13%	92%

7.50	10.00	8.75	2	3%	95%
10.00	12.50	11.25	2	3%	98%
12.50	15.00	13.75	0	0%	98%
15.00	17.50	16.25	0	0%	98%
17.50	20.00	18.75	1	2%	100%

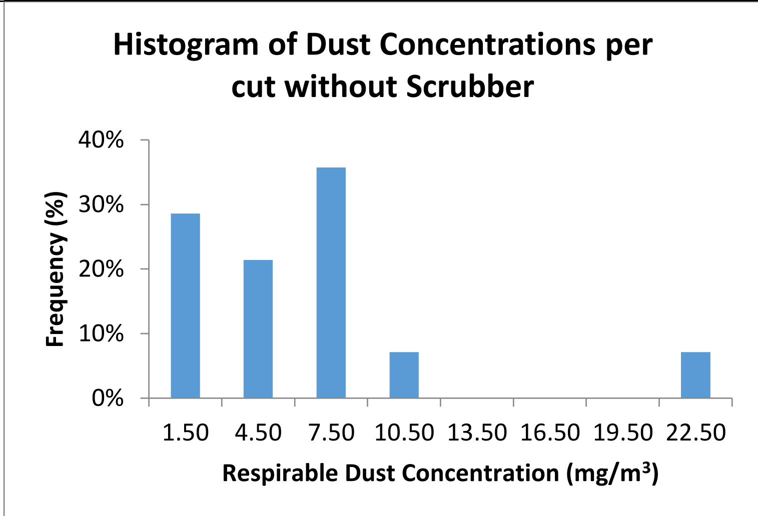

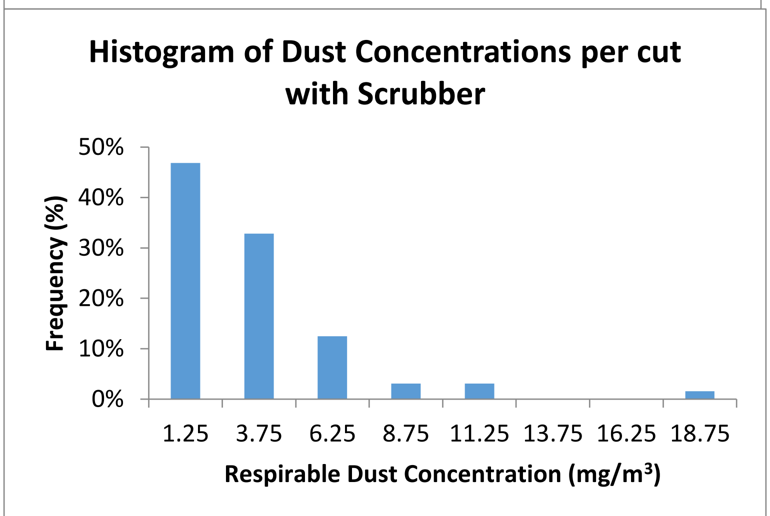

Mean	6.375	3.540
Standard Error	1.364	0.386
Median	6.031	2.675
Mode	#N/A	#N/A
Standard Deviation	5.104	3.087
Sample Variance	26.046	9.532
Kurtosis	5.674	6.331
Skewness	2.060	2.110
Range	19.980	17.461
Minimum	1.403	0.140
Maximum	21.383	17.601
Sum	89.252	226.546

Count	14	64
Confidence Level(95.0%)	2.947	0.771

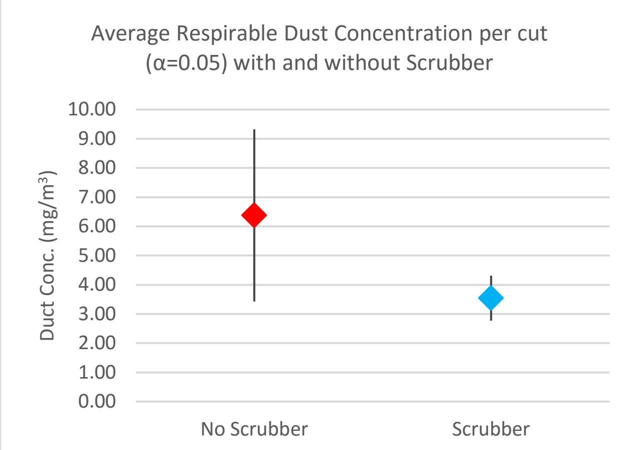

ANOVA						
Source of Variation	*SS*	*df*	*MS*	*F*	*P-value*	*F crit*
Between Groups	92.3503	1	92.3503	7.473868	0.007784	3.96676
Within Groups	939.0884	76	12.35643			
Total	1031.439	77				